1-1-2013

Phenotypic Characteristics of Mucosally Transmitted HIV-1

Nicholas F. Parrish
University of Pennsylvania, nparrish@upenn.edu

Phenotypic Characteristics of Mucosally Transmitted HIV-1

Abstract
Mucosal transmission accounts for the majority of new human immunodeficiency virus type 1 (HIV-1) infections and results in a genetically and phenotypically homogenous founder virus population in 60-80 percent of cases. Biological properties common to these transmitted and founder (T/F) viruses but not chronic control (CC) viruses would define key targets for microbicides and vaccines. To identify such properties, we tested 45 T/F and 52 CC envelope glycoproteins (Envs) from the best studied and most prevalent HIV-1 subtypes (B and C, respectively) in various pseudotype assays to determine their receptor and coreceptor interaction, tropism for primary CD4+ T cell subsets, and sensitivity to neutralizing antibodies. T/F Envs were unable to mediate entry into cells expressing low amounts of CD4, thus macrophages and other CD4low cells likely do not support their replication during mucosal transmission. In contrast, T/F Env pseudoviruses efficiently infected primary memory CD4+ T cells with a preference for the effector rather than central memory subset, as did CC pseudoviruses. There was a trend towards increased sensitivity of T/F viruses to neutralization by antibodies targeting the CD4 binding site. All T/F Envs were able to use the coreceptor CCR5 for cell entry, whereas some CC Envs used CXCR4 alone. However, one bona fide T/F virus entered and replicated very poorly in CCR5+ cells in vitro, so efficient use of CCR5 as tested is not absolutely required for transmission. To extend these studies beyond intrinsic Env functions, we characterized the Env content, infectivity, dendritic cell interaction, and interferon alpha (IFN-α) sensitivity of 27 T/F and 14 CC infectious molecular clones from subtypes B and C. T/F viruses contained more Env and were more infectious than CC viruses. T/F viruses also readily attached to DCs and were effectively transferred to CD4+ T cells. T/F viruses were more resistant to the inhibitory effect of IFN-α on virus spread than CC viruses, suggesting that selective pressure imposed by the innate immune response may in part mediate the bottleneck associated with mucosal transmission. Future work is needed to define the mechanistic basis of these phenomena in order to target them to prevent HIV-1 transmission.

Degree Type
Dissertation

Degree Name
Doctor of Philosophy (PhD)

Graduate Group
Cell & Molecular Biology

First Advisor
Beatrice H. Hahn

Subject Categories
Molecular Biology | Virology

PHENOTYPIC CHARACTERISTICS OF MUCOSALLY TRANSMITTED HIV-1

Nicholas F. Parrish

A DISSERTATION

in

Cell and Molecular Biology

Presented to the Faculties of the University of Pennsylvania

in

Partial Fulfillment of the Requirements for the

Degree of Doctor of Philosophy

2013

Supervisor of Dissertation

_____

Beatrice H. Hahn

Professor of Medicine and Microbiology

Graduate Group Chairperson

_____

Daniel S. Kessler, Associate Professor, Department of Cell and Developemental Biology

Dissertation Committee:

Robert W. Doms, Chair and Pathologist-in-Chief, Children's Hospital of Philadelphia

James A. Hoxie, Professor of Medicine

Ronald G. Collman, Professor of Medicine

Scott E. Hensley, Assistant Professor, The Wistar Institute

DEDICATION

This dissertation is dedicated to the memory of Matthias H. Kraus, M.D., an artisan of molecular biology. He discovered ERBB3, which is the topic of over 1000 peer-reviewed publications and the target of monoclonal antibodies under clinical development as cancer therapeutics. His tutelage was a provident gift. It is solely to his credit if I lack any of the bad habits of a retrovirologist.

ACKNOWLEDGMENT

I thank my mentor Dr. Beatrice Hahn. It has been an honor to sit at the feet of such an accomplished scientist. She directed me to important problems and made sure I stayed focused on them, somehow without limiting my perceived creativity and freedom. She has encouraged me when I needed encouragement and challenged me when I needed to be challenged. The support she has provided seemed limitless. Most critically, her desire for me to improve as a scientist has been unrelenting; I sincerely hope that will continue.

Dr. George Shaw has done more than anyone other than Dr. Hahn to improve the environment of my training. His perspective on HIV, especially that from “5,000 feet,” is unparalleled. I have also gained an undeserved benefactor in Dr. Robert Doms. In the same way that Dr. Shaw is the master of defining the big question, Dr. Doms is the ultimate authority on the proper manner(s) of addressing the question.

I would not have withstood the challenges of the endeavor this dissertation represents without the careful sculpting of my undergraduate mentor, Dr. Bruce Levin. I am honored to share what I do of his approach and hermeneutics.

I had the pleasure of receiving training and airing ideas in several external labs. The six weeks I spent at Penn in Dr. Doms’ lab prior to our move were easily the most productive of my entire four years in terms of data generation. Dr. Craig Wilen, my closest collaborator and friend, had more to do with that than I did. Dr. Nina Bhardwaj at NYU, along with Dr. Meagan O’Brien, hosted me for my first trip to dendritic cell mecca and taught me tissue culture techniques important for this work. Dr. Feng Gao allowed me to train with his group at Duke and was a critical collaborator entrusting me with many reagents his lab spent countless hours generating. Dr. Ben Greenbaum and Dr. Arnold Levine at the Institute for Advanced Studies listened to my speculation with the interest normally reserved for data, helping refine some of the hypotheses tested here.

Committee members Dr. James Hoxie, Dr. Ronald Collman, and Dr. Scott Hensley provided exponentially more useful guidance than would be predicted based on the number of our meetings.

Those to whom I am sincerely grateful for direct guidance and assistance include: Dr. Jesus Salazar-Gonzalez, a yeoman with whom I shared many late evenings in Birmingham, and Maria Salazar. Dr. Brandon Keele, who has thought more and more clearly on this topic than anyone except Dr. Hahn and Dr. Shaw. Dr. Hui Li, Dr. Fredric Bibollet-Ruche, Julie Decker, Juliet Easlick, Dr. Yingying Li, and Dr. Weimin Liu, each true professionals who patiently suffered through teaching an amateur their techniques. Fellow students in Dr. Hahn's, Dr. Shaw's, and Dr. Doms' labs including Dr. Rebecca Rudicell, Dr. Rui Kong, Dr. Joshua Baalwa, Michael Lopker, Mark Stoddard, Shilpa Iyer, Dr. Jason Wojcechowskyj, Josiah Peterson, Chuka Didigu, Sesh Sundararaman, and Hannah Barbian provided helpful discussions.

I especially thank my parents, who nurtured my scientific leaning from an early age and along with my in-laws continue to support my long training. I am especially proud of my dad's blessing to pursue research and my mom's unconditional conviction that I am great at it. Because of my passion to answer the questions raised in this work, my lifestyle over the past four years has been distinct from what I would have imagined, and with foresight and self-control, perhaps even chosen. Thus my wife Erica's steadfast commitment to me, extending even to the same scientific pursuit, warrants gratitude and accolades for which this is not the venue. I cannot imagine a better colleague.

ABSTRACT

PHENOTYPIC CHARACTERISTICS OF MUCOSALLY TRANSMITTED HIV-1

Nicholas F. Parrish

Beatrice H. Hahn

Mucosal transmission accounts for the majority of new human immunodeficiency virus type 1 (HIV-1) infections and results in a genetically and phenotypically homogenous founder virus population in 60-80 percent of cases. Biological properties common to these transmitted and founder (T/F) viruses but not chronic control (CC) viruses would define key targets for microbicides and vaccines. To identify such properties, we tested 45 T/F and 52 CC envelope glycoproteins (Envs) from the best studied and most prevalent HIV-1 subtypes (B and C, respectively) in various pseudotype assays to determine their receptor and coreceptor interaction, tropism for primary CD4+ T cell subsets, and sensitivity to neutralizing antibodies. T/F Envs were unable to mediate entry into cells expressing low amounts of CD4, thus macrophages and other $CD4^{low}$ cells likely do not support their replication during mucosal transmission. In contrast, T/F Env pseudoviruses efficiently infected primary memory CD4+ T cells with a preference for the effector rather than central memory subset, as did CC pseudoviruses. There was a trend towards increased sensitivity of T/F viruses to neutralization by antibodies targeting the CD4 binding site. All T/F Envs were able to use the coreceptor CCR5 for cell entry, whereas some CC Envs used CXCR4 alone. However, one *bona fide* T/F virus entered and replicated very poorly in CCR5+ cells *in vitro*, so efficient use of CCR5 as tested is not absolutely required for transmission. To extend these studies beyond intrinsic Env functions, we characterized the Env content, infectivity, dendritic cell interaction, and interferon alpha (IFN-α) sensitivity of 27 T/F and 14 CC infectious molecular clones from subtypes B and C. T/F viruses contained more Env and were more infectious than CC viruses. T/F viruses also readily attached to DCs and were effectively transferred to CD4+ T cells. T/F viruses were more resistant to the inhibitory effect of IFN-α on virus spread than CC viruses, suggesting that selective pressure imposed by the innate immune

response may in part mediate the bottleneck associated with mucosal transmission. Future work is needed to define the mechanistic basis of these phenomena in order to target them to prevent HIV-1 transmission.

TABLE OF CONTENTS

LIST OF TABLES

LIST OF ILLUSTRATIONS

CHAPTER 1

Introduction to Mucosal HIV-1 Transmission

Nicholas F. Parrish

Department of Medicine and Microbiology, Perlman School of Medicine at the University of Pennsylvania

Abstract

The majority of new human immunodeficiency virus type 1 (HIV-1) infections result from mucosal virus exposure. Vaccines or microbicides must interfere with the processes that occur after a mucosal surface is exposed to virus but before life-long clinical HIV-1 infection is established. Here I review current models of these events, developed through a combination of simian immunodeficiency virus (SIV) and human explant challenge experiments, as well as the earliest immune responses to infection. These responses, which may guide immunization attempts, have been demonstrated to be effective based on the selective pressure they place on the transmitted virus population. By extension, I argue that characterizing the biological function of transmitted viruses prior to the onset of immune pressures is a complementary approach to refine current models of mucosal HIV-1 transmission and define vaccine targets. Previously defined genotypic traits of transmitted viruses have led to a number of hypotheses about phenotypic differences between transmitted viruses and their chronic counterparts. Technical and conceptual advances now allow us to define the exact nucleotide sequence of transmitted/founder genes and entire viruses, biologically characterize the encoded gene product(s), and thereby test these hypotheses.

Mucosal Transmission and Early Immune Responses

Human immunodeficiency virus is a lentivirus that causes Acquired Immunodeficiency Syndrome (AIDS) in humans. Since entering the human population via chimpanzees infected with simian immunodeficiency virus (SIV) (121), the main group of human immunodeficiency virus type 1 (HIV-1) has become a global pandemic, leading to over 25 million deaths. The pandemic main group (M) of HIV-1 is one of four HIV-1 groups (M, N, O and P), each representing independent SIV zoonoses (329), and is further divided into subtypes A-K along with circulating recombinant forms (122). Subtype C accounts for about half of all HIV-1 infections, and is prevalent in Southern Africa and India (154). Subtype B is prevalent in Western Europe and North America and is the most thoroughly studied of the subtypes. HIV-1 is transmitted predominantly by mucosal contact, especially in sub-Saharan Africa where most infected individuals reside (2) (82). While several types of interventions have recently been shown to reduce transmission through this route (265), a broadly effective vaccine holds promise as a cost-effective and cross-validated means to stop the epidemic (155, 244). Developing such a vaccine is thought to require a more detailed understanding of the biology of HIV-1 transmission (1).

At the most basic level, HIV-1 transmission requires virus entry into human target cells (reviewed in (373)). HIV-1 enters target cells following the interaction of viral envelope glycoprotein (Env) spikes, formed by three gp120/gp41 heterodimers, with the cellular receptor CD4 and a coreceptor. Gp120 and gp41 are translated as a single polypeptide, gp160, which is subsequently cleaved by cellular proteases (149). The surface subunit of Env, gp120, contains a signal peptide, five relatively conserved core domains, and five variable regions (V1-V5) with extraordinary diversity across different strains. The transmembrane subunit, gp41, contains external helical domains involved in membrane fusion, a transmembrane region, and a cytoplasmic domain. The CD4 binding site (CD4bs) of gp120 is formed predominantly via core domains (193), while both core region domains and the third variable region form the coreceptor-binding sites (301). HIV primarily uses chemokine receptors CCR5 (R5) and CXCR4 (X4) as

coreceptors. Use of X4 evolves during chronic infection in some individuals (318), but during acute infection most viruses use R5 (75).

A molecular perspective on viral entry is foundational but incomplete because HIV-1 transmission occurs in the context of tissues and organ systems. Our current understanding of HIV-1 transmission at this level of analysis is built largely by extension from SIV transmission, which can be studied directly and experimentally. For example, thoroughly rinsing the vaginal vault with a virus-inactivating solution prevents transmission if performed 15 minutes after exposure, but not if delayed for 60 minutes (163). Therefore it can be inferred that virus(es) sufficient to confer productive infection traverse the vaginal lumen within 60 minutes. Several mechanisms have been proposed to account for this movement, including diffusion between cells forming an otherwise intact barrier (159), active transcytosis through epithelial cells (37), or movement through breaks in the epithelial barrier due to microabrasions (254). Both cell-free and cell-associated (174) forms of SIV are capable of initiating infection after mucosal exposure, but most experiments are performed using a cell-free challenge. The endocervix, the transitional zone from the endocervix to the ectocervix, the ectocervix, and the vaginal epithelium have all been proposed as sites through which virus can be transmitted (reviewed in (158). Radically hysterectomized macaques are fully susceptible to intravaginal challenge (237), thus the vaginal epithelium is sufficient for transmission. SIV RNA derived from infected cells can be detected as soon as 2 hours after infection (238), yet the identity of these initial target cells in SIV and HIV-1 infection is controversial.

Early studies implicated macrophages and dendritic cells as the initial cellular targets of SIV and HIV. For SIV, histological data has been presented to suggest that macrophages (153, 236), intraepithelial dendritic cells (DCs) (163, 341) and Langerhan's cells (240) are productively infected days to weeks after exposure. Several studies have reported that HIV isolated from acutely infected subjects did not induce syncytia formation in MT2 cells (326) (303) or was macrophage tropic (399), (359). Notably, these reports pre-date the discovery of R5 as a coreceptor (95). Since the discovery of R5, the phenotypic dichotomies previously defined as

macrophage vs. T cell tropism or non-syncytia-inducing vs. syncytia-inducing has often been shown to correspond to R5 tropism vs. X4 or R5/X4 dual-tropism (197). Indeed, challenge experiments with a number of phenotypically characterized SIV strains suggested that macrophage tropism *per se* may not be required for mucosal transmission (239). Correspondingly, more recent studies of HIV isolated from acutely infected individuals have shown predominant use of R5 as a coreceptor but not necessarily robust virus production in macrophages (75). Nonetheless, this has been interpreted as indirect support for the hypothesis that myeloid lineage cells are initial targets cells: mucosal DCs express R5 but not much X4, thus implicating them as a potential "gatekeeper" for R5-using viruses (389). On the other hand, almost all CD4+ T cells express X4 while only a subset express R5 (35). A key aspect of models in which DCs or macrophages represent the initial productively-infected cells is that these cells, whether they stay in the mucosa or migrate to regional lymph nodes, eventually disseminate virus to CD4+ T cells.

A second model of mucosal transmission envisions CD4+ T cells as the critical first target cell. Evidence for this comes from similar histological methods as support the DC-first model. Ashley Haase and collaborators have been the major contributors to this work (209, 238, 395), which shows clusters of SIV RNA+ cells that express T cell receptors and CD4, but not conventional markers of cellular activation. Studies using human vaginal explants have shown that CD4+ T cells are more readily infected than DCs in these tissues (160). A concern in interpreting these studies is the super-physiologically high virus challenge used. Resting CD4+ T cells are proposed to be the initial target cells not solely due to ease of infection but by nature of their abundance relative to other susceptible cells (396). Because resting CD4+ T cells express more X4 than R5 (35), and generally less of both than activated cells (377), this model does not readily account for the predominance of R5-tropic viruses in acute HIV-1 infection. Moreover, resting CD4+ T cells are poorly infected by HIV-1 *in vitro* (340, 345). Unlike HIV-1, SIV encodes a Vpx protein capable of degrading SAMHD-1 (196), which is a restriction factor known to limit

HIV-1 infection of resting CD4+ T cells (17). Thus it is unclear if the tropism of SIV is representative of HIV-1 in this context.

Still another model of mucosal transmission proposes that viruses interact with both DCs and CD4+ T cells shortly after entering the mucosa. Specifically, it has been proposed that DCs can interact with HIV-1 and transfer infectious virus to CD4+ T-cells without being productively infecting themselves (123). This concept is supported by *in vitro* and *ex vivo* work. Early studies from Ralph Steinman and colleagues showed that DCs from skin pulsed with virus can interact with CD4+ T cells to facilitate infection and high-titer replication (283, 284). Virus replication within DC/CD4+ T-cell conjugates is extremely efficient, and the phenomenon of *trans*-infection, whereby a DC-associated virus infects a CD4+ T cell but not the original DC, is well described (376). The identity of the first infected cell has important practical implications. For example, it has been suggested that antibody-neutralized HIV is capable of being transmitted by DCs to CD4+ T cells (119, 358). If DCs are critically involved in the transmission event, inhibiting their glycan-dependent binding to HIV could be pursued (39, 249). On the other hand, if CD4+ T cells are the initial target, inhibiting their recruitment by chemokine-secreting cells may be an option (209).

Cells not directly targeted by SIV and HIV-1 are also involved in mucosal transmission. After exposure to an SIV inoculum, epithelial cells in the endocervix produce CCL20 (29), which leads to the recruitment of of plasmacytoid DCs (pDCs) (209). The specific triggers involved in these signaling events have not been explained, and pDC recruitment has also been reported in response to mild, non-specific tissue damage (120). It remains to be determined if pDC recruitment follows physiological HIV-1 exposure. However, pDCs are capable of secreting significant amounts of various cytokines; in the case of type I interferons, they produce 100-1000 times more than any other cell type (337). Thus even small numbers of pDCs may play a disproportionately important role in downstream events relevant to transmission. For example, by secreting beta-chemokines such as CCL4 they have been proposed to promote trafficking of additional CCR5+ CD4+ T cells to sites of exposure (209). Indeed, clusters of 40-50 infected

resting and activated CD4+ T cells are detectable in mucosal tissues three to four days after infection, whereas similar groupings of cells are not present in these tissues prior to exposure (209, 238). CCL4 can also occupy CCR5 and prevent its use as a viral coreceptor (69). However, the net effect of this and other innate immune responses by pDCs, including interferon alpha (IFN-α) and beta (IFN-β) secretion, has been interpreted as negative, because interfering with pDC recruitment and cytokine release prevents transmission after high-dose exposure (209). Furthermore, pre-treating animals with toll-like receptor agonists (CpG oligonucleotides and imiquimod) that induce IFN-α and other antiviral cytokines did protect from infection after high-dose challenge (364), leading authors to conclude "induction of mucosal innate immunity including an IFN-α response is not sufficient to prevent sexual transmission of human immunodeficiency virus."

After establishment of initial clusters of infection in mucosal tissues, virus spreads to regional lymph nodes (147). Around this time, as early as five to seven days prior to detectable plasma viral RNA, evidence of the first systemic antiviral immune response is detectable in the form of elevated acute phase serum amyloid A and a fragment of alpha-1-antitrypsin (190). Virus is detectable in the plasma seven days after SIV exposure (238) and approximately 10 days following HIV-1 exposure (225). In both cases the predominant site of viral replication is the gut-associated lymphoid tissues (139, 208, 360), which harbor the majority of activated CD4+ T cells under normal conditions (282). By the time virus is detectable in the plasma, many soluble innate immune factors are also detectable in both SIV and HIV-1 infection (118). To characterize this response for HIV-1, Borrow and colleagues measured levels of 30 cytokines in serial plasma samples from seroconverting plasma donors (343). They describe a storm of cytokine and chemokine production including rapid elevations of IFN-α and interleukin 15 (IL-15) and delayed production of the more anti-inflammatory IL-10. These investigators interpreted that "the intense early cytokine storm in acute HIV-1 infection may have immunopathological consequences, promoting immune activation, viral replication, and CD4+ T-cell loss."

In contrast to the seemingly ineffective innate immune responses to acute HIV-1infection, the first documented adaptive responses to HIV-1 are associated with decline of viremia and resolution of acute infection. HIV-1-specific major histocompatibility complex (MHC) class I-restricted cytotoxic lymphocytes (CTLs) become detectable a few days prior to peak viremia, some two to three weeks after exposure (114). The effectiveness of this response is evidenced by the strong selective pressure it places on the virus; as virus load begins to decrease towards set-point, mutations that mediate escape from CTLs become fixed in the viral population, completely replacing the wild-type strain (129). Mathematical modeling of the kinetics of this replacement suggests that CTLs contribute directly to decline of viral load (129). The specificity of these CTLs for transmitted viruses has been confirmed *in vitro* using ELISPOT (129) and replication inhibition assays (116); on the other hand, “escaped” peptides and viruses are not targeted. Thus by indirect, retrospective analysis the *in vivo* effectiveness of this immune response has been definitively shown for HIV-1. In accordance with this observation, depleting CD8+ cells in acutely simian/human immunodeficiency virus (SHIV)-infected macaques leads to a sustained peak of viral replication and rapid disease progression (222). CTLs also have a role in chronic infection, since depletion is associated with increased viral replication at these time points as well (321). Additionally, the genetic loci most closely associated with HIV disease progression encode MHC class I (273), thus determining the range of viral proteins that may be targeted in this response (187).

The humoral response to HIV-1 begins slightly after the CTL response and is initially comprised by antibodies (Abs) that bind to gp41 but are incapable of neutralization (353). Because these Abs also frequently bind to host proteins or bacteria in the normal gut flora, it is thought they arise from B cells that were activated prior to infection but cross-react with HIV, thus explaining their rapid ontogeny (210). While these and gp120-binding Abs are capable of mediating Ab dependent cell-mediated cytotoxicity (ADCC), their importance *in vivo* is uncertain because there are conflicting reports regarding whether or not mutations that prevent binding of such antibodies arise *in vivo* (11, 61). However, if Env-binding Abs exert selective pressure on

HIV-1, one mechanism of escape may be to avoid these Abs (for example, by limiting Env expression at the cell surface (317)) rather than mutate the epitopes involved.

Neutralizing antibodies (nAbs) develop as early as two weeks after the first binding antibodies and, like CTLs, are known to be effective because they drive replacement of the infecting strain with escape mutants (22). Notably, they impose this selective pressure at titers at which neutralization cannot be readily detected *in vitro* (22). As with CTLs, the specificity of these responses for the transmitted but not escape variants can be demonstrated through *in vitro* neutralization and adsorption studies. These Abs are focused on variable regions of gp120 (22, 247), and Therefore they are effective only against the autologous or very closely related strains, and only later in infection do nAbs target more conserved viral epitopes (135, 216). Abs can also limit viral replication in chronic HIV-1 infection, as has been directly demonstrated by therapeutic B cell depletion (165).

Despite the range of known immune responses during chronic HIV-1 infection, there are no known cases in which natural immunity has lead to sterile cure. Indeed, some contend that established infection with one strain of HIV-1 provides little or no protection from subsequent infection with another strain of HIV-1 (189, 275, 293). Some reasons for this may be disruption of normal CD4+ T cell helper functions needed to develop functional adaptive immunity (175, 245), a large viral effective population size and rapid mutation rate that ensures pre-existence of immune escape (and similarly, drug resistance variants) at any single loci (368), or the large reservoir of latently infected cells that is established during acute infection (113). Thus the virus may be most susceptible to interventions at the earliest stages of infection when the viral population is small and less genetically diverse, prior to massive CD4+ T cell depletion and establishment of the reservoir.

However, all experimental systems currently available to study the earliest events in HIV-1 transmission have key deficiencies. Direct SIV challenge experiments can provide information about the first hours and days after exposure, but the cell tropism of these viruses may not be

representative and high inoculums must be used to ensure infection in a reasonable timeframe. This is in contrast to HIV-1, to which individuals may be exposed hundreds or thousands of times prior to productive infection (166, 287). Human tissue explant experiments can be informative about the tropism and initial target cells of HIV-1, but not about cells recruited after exposure, such as pDCs or activated CCR5+ CD4+ T cells. In contrast, indirect yet definitive evidence regarding the effectiveness of early immune responses to HIV-1 has been gained by studying the record they leave in sequences of the evolving viral population (22, 129). These studies have been enabled by very early samples that are difficult to acquire. In the earliest of these samples, the virus population is unchanged by selective pressure from immune responses, and thus is representative of the virus(es) that are transmitted (176, 201). These samples therefore provide the basis for an additional strategy to study mucosal HIV-1 transmission: characterizing the biological functions of the virus proteins or complete viruses directly responsible for HIV-1 transmission. By inference, the biological functions of these viruses are sufficient for transmission. For example, if these viruses are unable to replicate in epithelial cells *in vitro* it is highly unlikely that viruses must do so *in vivo* in order to be transmitted. Some of these functions are likely to be strictly necessary while others may be accessory, so studying large groups of these viruses may allow us to define the functions required for transmission. Finally, some properties may be more common in transmitted viruses than representative chronic control viruses, and such properties would be good vaccine targets. For example, if all transmitted viruses are able to use a certain coreceptor while only half of viruses from chronic infection use this coreceptor, the role of this coreceptor in transmission should be investigated and viruses that use this coreceptor should preferentially be evaluated as vaccine immunogens.

Genotypic and Phenotypic Characterization of Transmitted Viruses

The initial step in characterizing transmitted viruses to gain insights into HIV-1 transmission is identifying transmitted variants in comparison to non-transmitted control viruses by sequencing. The first report of genotypic differences between such viruses came from cases of vertical transmission. A potential N-linked glycosylation site (PNLG) was absent in sequences from three infants, yet was present in sequences from each of their mothers (375). Next, it was reported that sequences of the third variable region of gp120 were strikingly homogenous across six acutely infected individuals despite no epidemiological linkage between these individuals (393). *Env* sequences from individuals acutely infected with subtype C have been shown to have significantly shorter variable loops and fewer N-linked glycosylation sites than those from their partners (88) or *envs* from randomly chosen chronically infected individuals (207). Shorter V1 and V2 variable regions and fewer PNLGs were also observed in individuals acutely infected with subtype A compared to all subtype A sequences in the Los Alamos National Laboratory HIV sequence database; however, this same analysis did not result in significance for sequences from individuals infected with subtype B viruses (59). Longer V2 regions of have been reported for transmitted subtype B viruses in Trinidad (72). Subtype A and recombinant Envs transmitted from mother-to-child have also been reported to have fewer PNLGs than average Envs in the mother (378). Comparing recipient to donor sequences in 10 subtype A and three subtype D transmission pairs detected several signature amino acids, mostly following the V3 loop (309). A shorter V1-V5 region and lower V3 charge were also observed in the transmitted viruses. Several genetic signatures of acute viruses were found by analyzing thousands of subtype B *env* sequences, including a number in the cytoplasmic tail of gp41 and the signal peptide (126). Recent work has shown that T/F viruses often come from a minor population of the donor's plasma virus (36). Moreover, it has been concluded that this minor transmitted population is genetically closer to strains from earlier time points than those circulating in the plasma at the time of transmission (292).

Several mechanisms might explain the observed sequence differences between acute and chronic viral sequences or sequence differences between donors and recipients in epidemiologically linked pairs. The most trivial is that these differences reflect population-level sampling bias. It has been estimated that acutely infected individuals contribute to as many as 40-50% of new HIV-1 transmissions (42, 286, 365). Thus genetic changes that develop after years of chronic infection, as has been suggested for increased PNLGs or variable region length (79, 310), may be underrepresented in acute samples. Another potential interpretation is that the virus population in the genital track is compartmentalized and thus individuals are exposed to viruses that differ from those sampled from the plasma. Machine learning algorithms have been trained to predict with 90% accuracy whether a given sequence was derived from the semen or plasma, suggesting that some compartmentalization may exist (277). Other groups have shown that depending on the subject there may be almost complete compartmentalization or no evidence of compartmentalization (6, 76, 178, 400). Thus compartmentalization may play some role in the genetic differences observed between acute and chronic plasma sequences.

Another hypothesis is that these sequence differences correspond to phenotypic characteristics that confer an increased likelihood of transmission. A number of phenotypic characteristics of transmitted viruses have been proposed (143). The most robust is the observation that viruses from acute infection frequently use R5 (75), whereas X4-using strains are often found during chronic infection. Additionally, those who lack functional R5 are highly resistant to infection (212). However, this resistance is not absolute as 12 case reports of such individuals being infected with X4-using strains (260, 334). Several reviews have been dedicated to hypothesizing “gatekeepers” responsible for selective transmission of R5-using variants (137, 220). However, others have recently contended that transmission is stochastic with respect to coreceptor tropism, arguing that when dual-tropic or X4-using variants are present in the transmitting partner, they are found in virus recipients based on their proportion in the donor (51, 83, 152). Thus it is of ongoing interest to determine if the preponderance of R5-using virus in acute infection is due to a selective bottleneck requiring or favoring R5 use at transmission.

One hypothesis about the phenotype of transmitted viruses pertains to their sensitivity or resistance to nAbs. The transmitted virus population replicates during acute infection for at least one month , and more routinely ~80 days (71), prior to development of autologous neutralizing antibodies. Does this allow for reversion of mutations that mediated escape from the previous host's nAb? Are neutralization-sensitive Envs inherently more fit for transmission? Acute Envs from transmission pairs were shown to be more sensitive to neutralization by donor plasma than randomly chosen donor Envs taken at time points close to transmission (88). However, it is unclear if this is a generalizable phenomenon because subsequent studies have observed a similar difference (307, 390), no difference (182, 308), or a difference in the opposite direction (90, 290, 378) in sensitivity of viruses from acute infection to nAb.

Another hypothesized property of transmitted viruses pertains to their efficiency of receptor or coreceptor use. Since macrophages, proposed to be an initial target cell (359, 399) have little CD4 on their plasma membrane, successfully transmitted viruses might use CD4 very efficiently. Additionally, increased CCR5-use efficiency might allow some viruses to gain a foothold in early infection (104, 167). Transmitted viruses might interact better than chronic viruses with the integrin pair α4β7, which is present on CD4+ T cells homing to the gut (250). The most statistically robust genotypic signature found after analyzing the largest set of acute *env* sequences to date was shown to increase steady-state Env expression, which may have a number of biological effects that could promote transmission (11). Cheng-Mayer and colleagues found mutations in SHIV gp120 that increased dendritic cell-specific intercellular adhesion molecule-3-grabbing non-integrin (DC-SIGN) binding as well as mucosal transmissibility (162, 215), suggesting that attachment to dendritic cells could be important for transmission. Finally, while innate immune responses may be harmful once foci of infection are established, viruses better able to overcome these responses may have an advantage in establishing productive clinical infection.

The approach taken here to test these hypotheses was enabled by a single-genome amplification technique that allows proportional sampling and sequencing of viral variants without

PCR recombination or other *in vitro* artifacts (312). Using this technique, Keele and colleagues analyzed the plasma of patients early in acute HIV infection and discovered that the sequences were often homogenous (176). In fact, mathematical modeling of random evolution of HIV sequences showed that the consensus of these homogenous sequences likely represented the very virus or infected cell that crossed the mucosa and gave rise to infection (201). Experimental SIV challenges with genetically defined stocks showed that sequence of the virus inferred to be transmitted was often identical to a sequence from the challenge stock (177). When the sequences inferred in this manner were cloned or synthesized, they invariably encoded Envs functional for entry (176) or replication-competent viruses (313). Thus it is possible to define the exact nucleotide identity of the virus or viruses that are transmitted and found clinical infection. These have been termed transmitted/founder (T/F) viruses; the properties of T/F viruses are precisely those relevant for mucosal HIV-1 transmission.

CHAPTER 2

Phenotypic and Immunologic Comparison of Subtype B Transmitted/Founder and Chronic HIV-1 Envelope Glycoproteins

Nicholas F. Parrish[1,2#], Craig B. Wilen[1#], Jennifer M. Pfaff[1], Julie M. Decker[3], Elizabeth A. Henning[1], Hillel Haim[34], Josiah E. Petersen[1], Jason A. Wojcechowskyj[1], Joseph Sodroski[4], Barton F. Haynes[5], David C. Montefiori[5], John C. Tilton[6], George M. Shaw[1,2], Beatrice H. Hahn[1,2], and Robert W. Doms[1,7*]

Department of [1]Microbiology and [2]Medicine, Perlman School of Medicine at the University of Pennsylvania, Philadelphia, PA, 19104, [3]Departments of Medicine and Microbiology, University of Alabama at Birmingham, Birmingham, AL 35294, [4]Department of Cancer Immunology and AIDS, Dana-Farber Cancer Institute, Harvard Medical School, Boston, MA, [5]Duke Human Vaccine Institute, Duke University Medical Center, Durham, NC 27710, [6]Department of General Medical Sciences, Center for Proteomics, Case Western Reserve University School of Medicine, Cleveland, OH 44106, [7]Department of Pathology and Laboratory Medicine, Children's Hospital of Philadelphia, Philadelphia, PA, 19104

#These authors contributed equally.

Originally published in Journal of Virology 85(17):8514-27. Published ahead of print June 29, 2011.

Abstract

Sexual transmission of human immunodeficiency virus type 1 (HIV-1) across mucosal barriers is responsible for the vast majority of new infections. This relatively inefficient process results in the transmission of a single transmitted/founder (T/F) virus - from a diverse viral swarm in the donor - in approximately 80% of cases. Here we compared the biological activity of 24 subtype B T/F envelopes (Envs) with that of 17 chronic controls (CC) to determine whether the genetic bottleneck that occurs during transmission is linked to a particular Env phenotype. To maximize the likelihood of an intact mucosal barrier in the recipients and to enhance the sensitivity of detecting phenotypic differences, only T/F Envs from individuals infected with a single T/F variant were selected. Using pseudotyping to assess Env function in single round infectivity assays, we compared coreceptor tropism, CCR5 utilization efficiency, primary CD4+ T cell subset tropism, dendritic cell *trans*-infection, fusion kinetics, and neutralization sensitivity. T/F and CC Envs were phenotypically equivalent in most assays; however, T/F Envs were modestly more sensitive to CD4 binding site antibodies b12 and VRC01, as well as pooled immunoglobulin from HIV-1-infected subjects (HIVIG). This finding was independently validated with a panel of 14 additional CC HIV-1 Envs controls. Moreover, the enhanced neutralization sensitivity was associated with more efficient binding of b12 and VRC01 to T/F Env trimers. These data suggest that there are subtle but significant structural differences between T/F and CC subtype B Envs that may have implications for HIV-1 transmission and the design of effective vaccines.

Introduction

Sexual transmission of HIV-1 across mucosal barriers is a relatively inefficient process and is most often due to the transmission of a single transmitted/founder (T/F) virus from the swarm of viral variants present in the donor, resulting in a profound genetic bottleneck (88, 176, 267, 285, 374, 375, 393, 399). A question of central importance is whether T/F viruses have particular phenotypic properties, which favor their transmission. If so, viruses with these properties should logically be targets of vaccination and microbicide efforts. The viral envelope (Env) protein is a likely candidate for transmission-related signatures. For example, viruses expressing Envs that utilize the CCR5 coreceptor (R5-tropic) are transmitted far more frequently than those expressing Envs that utilize CXCR4 (X4-tropic) (176, 303, 326, 399). Variations in Env have also been linked to differences in the utilization of CD4 and coreceptor, the rate and efficiency of membrane fusion, as well as binding to C-type lectins such as DC-SIGN that are expressed on dendritic cells (DCs) and can function as virus attachment factors (123, 288, 294, 351).

Studies to characterize the properties of transmitted HIV-1 strains face several challenges. First, it is difficult to identify individuals during the acute phase of HIV-1 infection, particularly before the onset of immune responses (that is, at early Fiebig stages (112)), thus limiting sample sizes. Second, individual viruses cloned from the peripheral blood or plasma of acutely infected individuals within weeks of transmission may have already evolved away from the actual T/F virus and may thus have acquired phenotypic changes (40). Third, in the absence of extensive sampling of the early viral quasispecies by single genome amplification (SGA), it is impossible to know if one or more virus strains established the clinical infection, making it difficult to assess the integrity of the mucosal barrier (176). Infection with multiple T/F viruses may reflect a different mechanism of transmission, with these T/F Envs likely facing different or reduced transmission selection pressure (145, 204). Nonetheless, small numbers of Envs cloned from acutely infected individuals have been obtained and compared to Envs cloned from corresponding donors or from other chronically infected individuals. Derdeyn et al. examined subtype C Envs from eight heterosexual transmission pairs and concluded that transmitted Envs

have fewer putative N-linked glycosylation sites (PNGs), more compact variable loops, and enhanced neutralization sensitivity to donor plasma (88), although subsequent phenotypic studies of a subset of viruses bearing these Envs did not reveal functional differences (5, 167). Analysis of subtype A and D transmission pairs also identified shorter recipient Envs with a lower V3 charge, although no differences in the number of PNGs were noted (309). For subtype B Envs, initial studies suggested that transmission was independent of variable loop length and PNGs (59, 79, 117); however, more recent comparisons of thousands of subtype B T/F and chronic *env* sequences confirmed significantly fewer total PNGs and a trend towards fewer in the V1/V2 loops of transmitted Envs (126). Finally, several studies have investigated neutralization sensitivities of acute or T/F Envs compared to CC Envs, but reported conflicting results (117, 176, 307, 327). These discrepancies may have resulted from differences in sample size, demographics of acutely infected individuals and CCs, cloning strategy, and whether the Envs under investigation represented true T/F viruses.

The use of SGA of plasma viral RNA during the earliest stages of infection has allowed the inference of the nucleotide sequence of T/F viruses from an increasingly large number of individuals (3, 176, 312, 313). Recent analyses of a large number of subtype B T/F Env sequences led to the identification of transmission signatures in the CCR5 binding site, certain PNGs, and sites in the signal peptide and gp41 cytoplasmic domain that could affect Env processing and localization (126). These results suggested that T/F Envs might differ in some phenotypic properties from chronic Envs. To examine this, we conducted a comprehensive phenotypic analysis of T/F and CC subtype B HIV-1 Envs in the context of viral pseudotypes. Specifically, we assessed coreceptor tropism, CCR5 utilization efficiency, CD4+ T cell subset tropism, DC-mediated *trans*-infection efficiency of T cells, and membrane fusion kinetics. In addition, we examined the sensitivity T/F and CC Envs to neutralization by purified immunoglobulin from infected subjects (HIVIG) and a panel of broadly neutralizing monoclonal antibodies (MAbs) and assessed the binding efficiencies of these MAbs to trimeric Env on the cell surface. Our results failed to identify a major transmission phenotype, but uncovered subtle functional differences between T/F and CC Envs that may be of biological significance.

Materials and Methods

Pseudovirus production. Pseudotyped virus was produced by calcium phosphate co-transfection of 6 μg of pcDNA3.1+ containing *env* with 10 μg of HIV-1 core (pNL43-ΔEnv-vpr+-luc+ or pNL43- ΔEnv -vpr+-eGFP) into 293T17 cells. Virus was harvested 72 hours post-transfection, filtered through a 0.45 μm filter, aliquoted, and stored at -80°C. For the primary CD4+ T cell infection, pseudovius was concentrated by ultracentrifugation through a 20% sucrose cushion. Pelleted pseudovirus was then resuspended in PBS. All luciferase-encoding pseudoviral stocks were serial diluted and used to infect NP2 cells to define the linear range of the assay. A viral dilution was chosen in the middle of the five-fold linear range of the assay to maximize sensitivity.

***Env* cloning and sequence analysis.** The derivation of most T/F Env clones used in this study has been described (176). THRO.F4.2026, SUMAd5.B2.1713, 9010-09.A1.4924, and PRB959-02.A7.4345 were cloned from SGA amplicons known to contain the nucleotide sequence of the corresponding T/F *env* sequence into pcDNA3.1 according to manufacturer's instructions (Invitrogen). The AD17.1 *env* gene was subcloned from a full-length infectious molecular T/F clone described elsewhere (204). Chronic Envs HEMA.A4.2125 and HEMA.A23.2143 were also cloned in pcDNA3.1; briefly, viral RNA was extracted from plasma of chronically infected patients and amplified using SGA methods. Individual *env* genes were then either cloned at random, or selected, to maximize within-patient *env* sequence diversity. Env clones were sequenced to confirm that they did not contain *Taq* polymerase errors, but represented *env* genes of viruses circulating in the patient. The nucleotide sequences of all T/F and CC Envs have previously been reported (105). PNGs were determined with N-glycosite (hiv.lanl.org) (394). To assess lengths of the V1/2, V3, V4, V5, and V1-4 regions, sequences were aligned to HXB2, then boundaries were identified for each region and non-gap residues were counted.

Coreceptor tropism testing and cell line infections. NP2 cells stably expressing CD4 and either CCR5 (NP2/CD4/CCR5) or CXCR4 (NP2/CD4/CXCR4) were infected with HIV-1 pseudoviruses expressing luciferase by spinoculating in 96-well plates at 450 g for 90 minutes at 25°C. Cells were lysed with Brite-Glo (Promega) 72 hours post-infection and analyzed on a

Luminoskan Ascent luminometer. Coreceptor tropism was arbitrarily defined by mean relative light units (RLUs) greater than 1 (approximately 100-fold over background). To assess sensitivity to coreceptor inhibitors, NP2/CD4/CCR5 or NP2/CD4/CXCR4 cells were pre-incubated for 30 minutes with saturating concentrations of the CCR5 inhibitor maraviroc (1 μM), the CXCR4 inhibitor AMD3100 (2 μM), or the fusion inhibitor enfuvirtide (10 μ/ml) prior to infection. To assess sensitivity to broadly neutralizing MAbs, viral pseudotypes were pre-incubated with 10 μg/ml of antibody for 30 minutes at 37°C. Virus and antibody mixes were then used to infect NP2/CD4/CCR5 or NP2/CD4/CXCR4 cells. All NP2 cell line infections were done in at least triplicate in at least three independent experiments using R5-tropic JRFL as a positive control and Env-deficient pseudotypes as a negative control.

The following reagents were obtained through the NIH AIDS Research and Reference Reagent Program, Division of AIDS, NIAID, NIH: pNL4-3-deltaE-eGFP (Cat# 11100) from Drs. Haili Zhang, Yan Zhou, and Robert Siliciano (391), bicyclam JM-2987 (hydrobromide salt of AMD-3100; Cat# 8128) (43, 81, 156), maraviroc (Cat #11580) (34, 103, 344), and HIV-1 gp120 MAb IgG1 b12 (Cat# 2640) from Dr. Dennis Burton and Carlos Barbas (23, 46, 47, 302).

Primary human CD4+ T cell tropism assay. Primary human CD4+ T cells, purified by negative selection, were obtained from the University of Pennsylvania's Human Immunology Core. $2x10^6$ cells per virus were stimulated with plate-bound anti-CD3 (clone OKT3) (eBiosciences) and anti-CD28 (clone 28.2, BD biosciences) and 20 units (U)/ml recombinant IL-2 in RPMI containing 10% FBS. Three days post-stimulation cells were transferred to 96-well V-bottom plates prior to infection. Five μl/well of concentrated HIV-GFP was used to infect cells in triplicate. Plates were then spinoculated at 1200 g for 2 hrs. Cells were then transferred to new 24-well plates and new media containing 20 U/ml IL-2 was added. Three days post-infection, cells were stained for flow cytometry.

Determination of alternative coreceptor use. Primary human CD4+ T cells from two different *ccr5Δ32* homozygous donors were obtained and purified as previously described. Prior to infection, cells were pre-incubated with 50 μM AMD3100 for 30 min. Cells were infected as previously described. Two hours after spinfection, enfuvirtide (1 μg/ml final concentration) was

added to all samples to prevent additional fusion prior to transferring cells to a 24-well plate for further incubation. Samples were stained and analyzed as previously described.

Flow cytometry. 1-2x10^6 cells were stained per tube for flow cytometry. All incubations were done at RT and in Facs Wash Buffer (PBS, 2.5% FBS, 2mM EDTA), and all antibodies were from BD Biosciences, unless otherwise noted. To stain CD4+ T cells, cells were first washed in PBS. Then, live/dead Aqua (Invitrogen) was added and incubated for 10 min. Next, anti-CCR7 IgM in Facs Wash Buffer was added and incubated for 30 min. Cells were then washed in Facs Wash Buffer before staining with anti-CD3 Qdot 655 (Invitrogen), anti-CD4 Alexa Fluor 700, anti-CD45RO PE-Texas Red (Beckman Coulter), and anti-IgM PE (Invitrogen) for 30 min. Cells were then washed in Facs Wash Buffer and resuspended in 1% PFA. Samples were run on a LSRII (BD) and analyzed with FlowJo 8.8.6 (Treestar). Cells were gated as follows: singlets (FSC-A by FSC-H), then live cells (SSC-A by live/dead), then lymphocytes (SSC-A by FSC-A), then CD3+ cells (SSC-A by CD3), then by memory markers (CCR7 by CD45RO).

DC *trans*-infection assay. To differentiate DCs, freshly isolated monocytes from the University of Pennsylvania's Human Immunology core were treated with 50 ng/ml GM-CSF (R&D systems) and 100 ng/ml IL-4 (R&D systems) in AIM V serum free media (Invitrogen). New media containing GM-CSF and IL-4 was added on day 3. Six days post-stimulation DCs were washed and plated at 3x10^4 cells per well in a V-bottom 96 well plate. 3x10^4 CD4+ T cells alone, three days post-stimulation with plate-bound anti-CD3/anti-CD28 were used as a negative control. Viral stocks were first titered by RLUs on NP2/CD4/CCR5 or CXCR4 cells. Virus sufficient to generate 80 RLUs was added to DCs or a CD4+ T cell control and allowed to bind for two hours at 37°C. Cells were washed three times with fresh media to remove cell-free virus. Then, 3x10^5 stimulated heterologous CD4+ T cells were added to each well containing 3x10^4 HIV-bound DCs or CD4+ T cells. As an additional control, and equal amount of virus was added to 3x10^5 stimulated CD4+ T cells to ensure there was no differential infection of CD4+ T cells. For CD4+ T cell luciferase infection, cells were spinoculated at 450 g for 90 minutes and then incubated without washing off virus. Cells were then transferred to a flat bottom 96-well plate for three days

prior to take down with Brite Glo. Each condition was done in triplicate and each viral pseudotype was used in at least three independent experiments with cells from different healthy donors.

Enfuvirtide time-of-addition assay. To assess entry kinetics of T/F and CC Envs, NL43vpr+luc+ pseudotypes were chilled to 4°C and added to NP2/CD4/CCR5 (or NP2/CD4/CXCR4 for the one X4-tropic Env) cells on metal blocks embedded in ice covered by a moist towel. Cells were then spinoculated at 1300 rpm for 90 minutes at 4°C to enhance viral binding. Immediately post-spinoculation, cold supernatant was aspirated off and all wells were flooded with 270 µl of pre-warmed 37°C media and transferred to a 37°C incubator. 30 µl of 10 µg/ml enfuvirtide (final concentration of 1µg/ml) was then added at 0, 5, 10, 20, 40, 80, or 160 minutes post-warming. A no drug control was also included to normalize percent infection. Cells were then incubated for 72 hours and assessed for RLUs. At least three wells per virus per time point were included in each experiment, and all Envs were examined in at least three independent experiments. Data was analyzed with Prism 4.0 (GraphPad Software, Inc.) by fitting a best-fit sigmoidal line to each independent experiment prior to averaging the Hill slopes and time to half-max fusion.

Neutralization sensitivity. Neutralization assays were performed using both NP2 and TZM-bl cells in two independent laboratories. To assess sensitivity to MAbs b12, VRC01, PG9, and PG16, viral pseudotypes were pre-incubated with 10 µg/ml of antibody for one hour prior to infection of NP2 cells. To assess sensitivity to HIVIG, pseudotypes were pre-incubated with two-fold serial dilutions of subtype B HIVIG from 1500-23 µg/ml. This mix was then added to NP2 cells and spinoculated as described previously. For MAbs, neutralization was assessed by determining the maximum percent inhibition (MPI) compared to a no antibody control. Subtype B HIVIG (lot 12 100158) was obtained from the AIDS Repository.

Neutralization sensitivity was assessed on TZM-bl cells as previously described (84, 367). Briefly, 8 x 10^3 TZM-bl cells were plated overnight. Five-fold dilutions of MAbs (b12, VRC01, PG9, PG16, and subtype B HIVIG) were incubated in the presence of 40 µg/ml DEAE-Dextran and 2000 infectious units (as measured on TZM-bl cells) of pseudovirius for one hour at 37°C. After media was removed from TZM-bl cells, the virus/MAb dilutions were added to the

cells and incubated for 48 hours before being analyzed for luciferase expression (Promega). The highest concentration tested for b12, VRC01, PG19 and P16 was 10 μg/ml. The highest concentraion of subtype B HIVIG was 1500 μg/ml. Samples were tested in duplicate with all experiments repeated at least two times. IC_{50} values were calculated as described previously (84).

Cell-Based Enzyme-Linked Immunosorbent Assay (CELISA). The binding of MAbs to HIV-1 Env trimers expressed on cells was measured using a cell-based ELISA system, as previously described (148). Briefly, COS-1 cells were seeded in 96-well plates (1.8×10^4 cells/well) and transfected the next day with 0.1 μg of a plasmid expressing Env and 0.02 μg of a Rev-expressing plasmid per well using Effectene transfection reagent. Three days later, cells were incubated with the indicated MAb suspended in blocking buffer (35 mg/ml BSA, 10 mg/ml non-fat dry milk, 1.8 mM $CaCl_2$, 1 mM $MgCl_2$, 25 mM Tris, pH 7.5 and 140 mM NaCl) for one hour at room temperature. Cells were then washed four times with blocking buffer and four times with washing buffer (140 mM NaCl, 1.8 mM $CaCl_2$, 1 mM $MgCl_2$ and 20 mM Tris, pH 7.5). A horseradish peroxidase-conjugated antibody specific for the Fc region of human IgG was then incubated with the samples for 45 minutes at room temperature. Cells were washed five times with blocking buffer and five times with washing buffer. HRP enzyme activity was determined after the addition of 33 μl per well of a 1:1 mix of Western Lightning oxidizing and luminol reagents (Perkin Elmer Life Sciences) supplemented with 150 mM NaCl. Light emission was measured with a Mithras LB 940 luminometer (Berthold Technologies). To correct for the level of cell surface expression of each envelope glycoprotein, binding of the antibodies is expressed as percent binding of the CD4-Ig probe at saturating concentrations (5 mg/ml). We decided a priori to exclude all envelope glycoproteins that bound CD4-Ig at less than 20% of the binding measured for the SC05.8H2.3243 control isolate. Five of the 57 Envs were thus not analyzed, including three T/F and two CC Envs. Measurements of antibody binding and neutralization were performed under code to prevent potential bias.

Statistical analyses. T/F and CC Envs were compared with Mann-Whitney tests and correlations were assessed by Spearman tests. P-values less than 0.05 were considered significant. Data was analyzed with Prism 4.0 software.

Ethics Statement. All human cells used in this study were from normal healthy donors who provided written informed consent after approval by the University of Pennsylvania's institutional review board.

Results

Panels of T/F and CC Envs. To determine if there are functional differences between T/F Envs and those that predominate during chronic infection, we assembled a panel of 24 subtype B T/F Envs previously inferred and cloned from plasma viral RNA of 24 individuals with acute HIV-1 infection as defined by the Fiebig staging system, in which patients are classified from Stage I (viral RNA positive, antibody and antigen negative) to Stage VI (ELISA and western blot positive with multiple bands) (21, 176, 204) (Table 1). Twelve individuals were sampled during Fiebig stage II, five during Fiebig stage III, two during in Fiebig stage IV, and five during Fiebig stage V. Acutely infected individuals were predominantly males (22 of 24) from the southeastern United States (18 of 24) with a variety of sexual risk factors, all denying intravenous drug use (IDU). All T/F Envs were inferred from SGA-derived sequences, which are devoid of PCR-induced errors and cloning bias (176). Env clones identical to this inferred T/F sequence were then chosen for phenotypic analysis. Importantly, all T/F Envs were selected from subjects with single variant transmissions. This was done to increase the likelihood that the viruses encoding these Envs were transmitted across an intact mucosal barrier, thereby maximizing our chances of observing properties required for this process (145, 204).

To generate chronic subtype B control Envs, we used SGA to amplify *env* genes from plasma viral RNA of two groups of anti-retroviral therapy naïve individuals. The first group consisted of 11 individuals sampled 14-83 months post-infection (mean 42 months). A test set of CC 17 Env clones was derived from this group consisting predominantly of males (8 of 11) from the southeastern United States (10 of 11) all denying IDU (Table 2-1). An additional 14 subtype B control Envs were SGA amplified and cloned from six chronically infected individuals residing in the northwestern United States. This second group of CC Envs served as a validation set to confirm differences in neutralization sensitivity observed with the first test set. A phylogenetic tree of the 31 CC Envs is depicted in Figure 2-1 along with the 24 T/F Envs. None of the Envs were from epidemiologically linked infections.

Table 1. Description of T/F and CC Envs

Env type	Subject	*env* Clone name	Fiebig Stage, or minimal time since infection	Viral load (copies/ml)	Gender	Risk behavior[c]	Geographic location	Sampling date	CoR[d]
T/F	REJO4541	REJO.D12.1972	V	722,349	M	HSX	Alabama	9/28/01	R5
	RHPA4259	RHPA.A19.2000	V	1,458,354	F	HSX	Alabama	12/5/00	R5
	SUMA0874	SUMAd5.82.1713	II	939,260	M	MSM	Alabama	5/13/91	R5
	THRO4156	THRO.F4.2026	V	5,413,140	M	MSM	Alabama	8/1/00	R5
	WEAU0575	WEAUd15.410.5017	II	216,415	M	MSM	Alabama	5/30/90	R5X4
	WITO4160	WITO.B10.2062	II	325,064	M	HSX	Alabama	8/4/00	R5
	700010040	CH40.C9.4520	V	298,026	M	MSM	North Carolina	7/27/06	R5
	700010058	CH58.A4.4375	III	394,649	M	Unknown	North Carolina	9/8/06	R5
	700010077	CH77.SA2.6559	V	144,145	M	Unknown	North Carolina	9/31/06	R5X4
	1006-11	1006-11.C3.1601	III	1,600,000	M	SPD	North Carolina	6/5/97	R5
	1018-10	1018-10.A5.1732	III	270,000	M	SPD	South Carolina	6/20/97	R5
	1053-07	1053-07.B15.1648	III	1,400,000	M	SPD	South Carolina	12/3/97	R5
	1056-10	1056-10.TA11.1826	II	140,000	M	SPD	South Carolina	1/14/98	R5
	1058-11	1058-11.B11.1550	IV	550,000	M	SPD	South Carolina	3/18/98	R5X4
	9010-09	9010-09.A1.4924	II	146,954	F	SPD	South Carolina	11/25/97	R5
	9015-07	9015-07.A1.4729	II	500,000	M	SPD	South Carolina	12/27/97	R5
	9021-14	9021-14.B2.4571	II	143,379	M	SPD	California	6/10/98	R5
	9032-08	9032-08.A1.4685	III	40,815	M	SPD	Alabama	7/30/98	R5
	PRB956-04	PRB956-04.B22.4267	II	600,000		SPD	Virginia	8/19/97	R5
	AD17	AD17.1	II	47,600,000	M	MSM	New York	6/14/99	R5
	PRB959-02	PRB959-02.A7.4345	II	>2,000,000		SPD	South Carolina	11/17/99	R5
	TT35P	TT35P.11H8.2874	II	1,849,301	M	HSX	Trinidad	1/26/99	R5
	SC20	SC20.8A8.2437	IV	2,789,313	M	HSX	Trinidad	2/18/98	R5
CC 1[a]	SC05	SC05.8C11.2344	II	9,980,952	M	HSX	Trinidad	6/28/93	R5
		SC05.A10.2362	5 y 5 m	19,514				12/9/98	R5
		SC05.8H2.3243							R5
		SC05.8A11.2363							R5
	SHKE4761	SHKE.A26.4112	1 y 2 m	544,000	M	MSM	Alabama	8/2/06	R5
		SHKE.A7.2118							R5
		SHKE.A4.2116							R5
	HEMA4284	HEMA.A4.2125	1 y 10 m	49,755	M	MSM	Alabama	10/2/02	R5
		HEMA.A23.2143							R5
	WICU4248	WICU.B4.2973	5 y 11 m	8,424	M	MSM	Alabama	10/6/05	R5
		WICU.C1.2992							R5
	CRPE4571	CRPE.B28.4072	2 y	21,917	F	HSX	Alabama	11/30/01	R5X4
	JOTO5278	JOTO.TA1.2247	1 y 6 m	404,180	M	HSX	Alabama	2/13/04	X4
	OLLA4645	OLLA.A14.1923	2 y 1 m	382,000	F	HSX	Alabama	2/22/02	R5
	SAMI4303	SAMI.A8.1863	3 y 11 m	116,000	M	MSM	Alabama	8/5/04	R5
	SMRE4166	SMRE.A13.4127	1 y 4 m	135,858	F	HSX	Alabama	11/16/01	R5
	TALA4022	TALA.A2.1780	6 y 11 m	228,200	M	MSM	Alabama	12/9/03	R5
	YOMI4024	YOMI.F2.4137	6 y 1 m	14,178	M	MSM	Alabama	2/15/06	R5
CC 2[b]	1632	1632.TA9	2 y 5 m	97,800	M	MSM	Washington	9/14/05	R5
		1632.A17							R5
		1632.A6							R5
		1632.TA1							R5
		1632.A7							R5
		1632.A23							R5
	1451	1451.D17	20 y 3 m	532,000	M	MSM	Washington	3/1/05	R5
		1451.C16							R5
		1451.D1							R5
		1451.C8							R5
	1588	1588.TA7	7 y 2 m	99,600	M	MSM/ID	Washington	7/6/05	R5
	1470	1470.D27	4 y 3 m	492,200	M	MSM/ID	Washington	3/15/05	R5
	1599	1599.B11	6 y 7 m	112,000	M-F	IDU	Washington	7/26/05	R5
	1444	1444.A21	7 y	86,300	M	MSM	Washington	2/22/05	R5

[a]Original panel of chronic control Envs

[b]Chronic control Envs from Washington state assessed only in neutralization assays

[c]Heterosexual (HSX); Men who have sex with men (MSM); Serial plasma donor (SPD); Intravenous drug user (IDU)

[d]Coreceptor tropism was assessed on NP2 cells for T/F and CC 1 Envs; tropism of CC 2 Envs was assessed on TZM-bl cells.

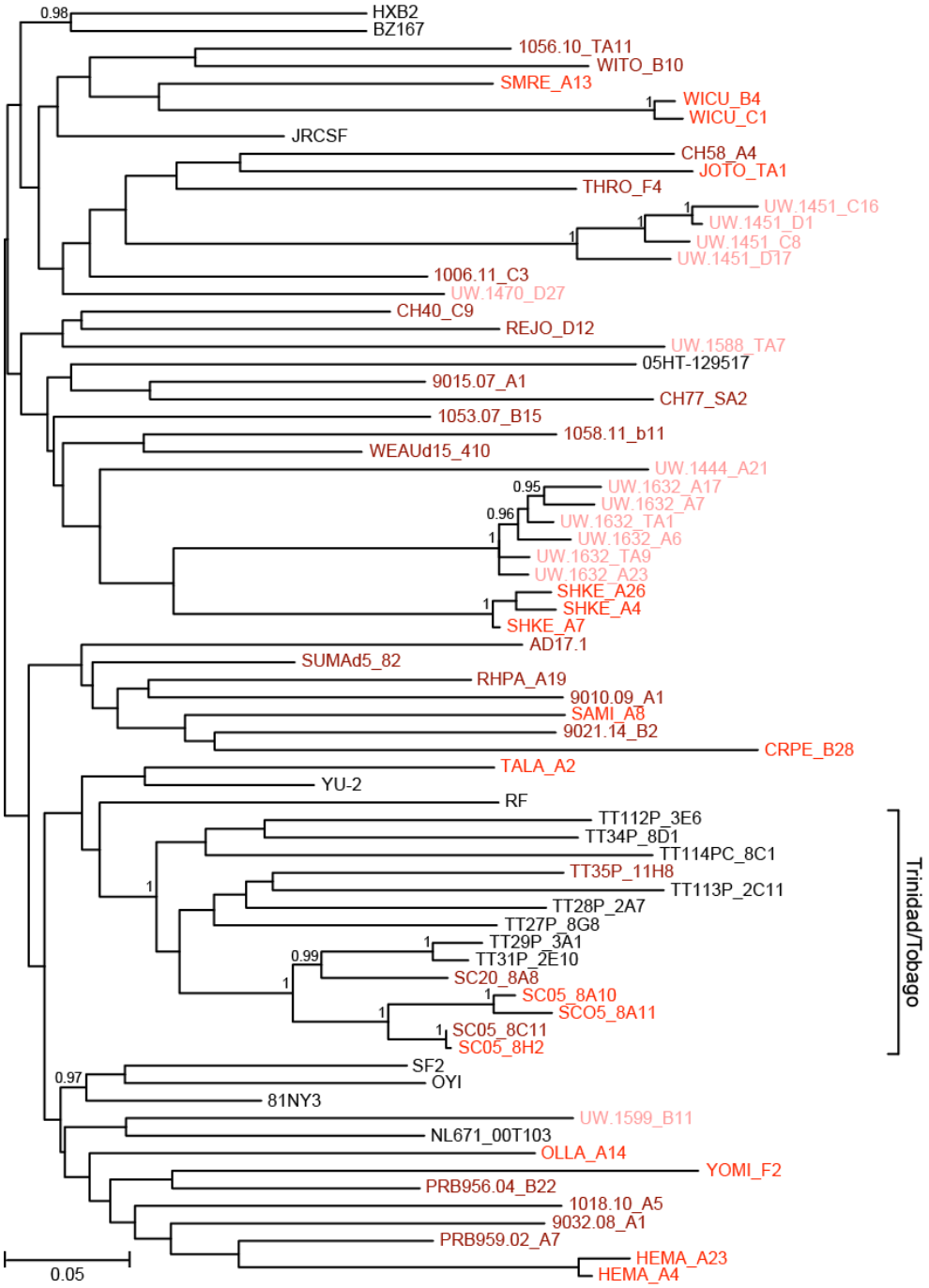

Figure 2-1. Phylogenetic relationships of T/F and chronic Envs selected for phenotypic analyses. The tree was constructed from Env amino acid sequences of T/F (dark red), original CC (red), and Washington state CC (pink) viruses. Subtype B reference sequences from the database are shown in black). All sequences were derived by SGA methods; Env sequences from the same individuals form discrete subclusters. A bracket indicates epidemiologically linked

infections from Trinidad and Tobago (68). The tree was inferred using maximum likelihood methods (141); Numbers on nodes indicate posterior probabilities (only values above 0.95 are shown). The scale bar represents 0.05 amino acid substitutions per site.

Previous studies noticed fewer PNGs in the gp120 region of T/F compared to CC Envs (207) (105). To determine whether our selected subset of T/F and CC Envs differed from this much larger group, we compared variable loop length as well as the number and distribution of putative PNGs. There were no differences in V1/2, V3, V4, V1-4 lengths between T/F and chronic subtype B Envs. Further, the median gp120 PNGs in T/F Envs was 26.0 compared to 27.0 for the CCs (p=0.16) and 26.0 for subtype B Envs in general (391). Thus, the panel of T/F Envs selected for our functional analyses exhibited no statistically significant differences in patient demographics, virus phylogeny, variable loop length, or PNGs relative to the panel of chronic Envs we assembled or to subtype B Envs in general.

Determination of coreceptor tropism. R5-tropic viruses represent the vast majority of transmitted viruses, with dual (R5X4)-tropic viruses being transmitted less frequently (176, 303, 326, 399). On rare occasions, X4-tropic viruses can be transmitted (20, 255, 348). To determine the coreceptor usage in our panel, we characterized the CCR5 and CXCR4 utilization of the 24 T/F and 17 CC Envs by producing viral pseudotypes and using these to infect NP2 cell lines expressing CD4 and either CCR5 (NP2/CD4/CCR5) or CXCR4 (NP2/CD4/CXCR4), as well as primary human CD4+ T cells. NP2 cells were selected because they provide a 5-6 log linear range of infection, approximately 2-3 logs greater than that of the TZM-bl assay. We found that of the 24 T/F Envs, 21 were R5-tropic and three were R5X4-tropic, while of the 17 CC Envs, 15 were R5-tropic, one was R5X4-tropic, and one was X4-tropic (Table 2-1). This is consistent with previous results with the exception of T/F Envs 1058-11.B11.1550 and CH77.SA2.6559, which were R5X4-tropic on NP2 cells and R5-tropic on TZM-bl cells (176) (105). This discrepancy is likely due to differences in CXCR4 expression, as the NP2 cells used stably express high levels of CXCR4 compared to the HeLa-derived TZM-bl cells, which express lower endogenous CXCR4 levels. All four R5X4-tropic Envs utilized CCR5 and CXCR4 with approximately equivalent efficiency as assessed by a less than two-fold difference in RLUs between the NP2/CD4/CCR5 and NP2/CD4/CXCR4 cells. To assess coreceptor use on human CD4+ T cells, we infected *ccr5Δ32* or *ccr5wt* CD4+ T cells in the presence or absence of saturating concentrations of the

CXCR4 inhibitor AMD3100. The results paralleled those obtained with the NP2 cell lines. R5-tropic Envs mediated infection of *ccr5wt* but not *ccr5Δ32* CD4+ T cells, while R5X4 Envs mediated infection of both cell types. Infection of *ccr5*Δ32 CD4+ T cells by three of the R5X4 Envs was completely inhibited by AMD3100, while Env CRPE.B28.4072 could infect *ccr5Δ32* cells in the presence of AMD3100, though with reduced efficiency (data not shown). However, we found that AMD3100 inhibited infection of NP2/CD4/CXCR4 cells by viruses bearing the CRPE.B28.4072 Env by only 50%. In addition, this Env was unable to infect NP2 cells expressing CD4 alone or in combination with any of 17 different putative alternative coreceptors, indicating that this Env can utilize the drug-bound conformation of CXCR4 (data not shown). Several other HIV-1 Env proteins have been shown to exhibit this property (151). In summary, all T/F Envs utilized CCR5, while three were R5X4-tropic. Thus, there were no differences in coreceptor tropism between the T/F and CC Envs with the exception of the one X4-tropic CC Env, and there was no evidence for utilization of coreceptors other than CCR5 or CXCR4 to infect human CD4+ T cells.

Sensitivity to coreceptor antagonists and CCR5 utilization efficiency. Mucosal transmission of HIV-1 is dependent upon CCR5. Hypothesizing that the ability to use low levels of CCR5 may confer selective advantage to viruses at the moment of transmission, we determined the sensitivity of each Env to the CCR5 inhibitor maraviroc (MVC) as a surrogate for CCR5 utilization efficiency. High MVC IC_{50} values indicate that an Env can mediate infection at low levels of CCR5, while low IC_{50} values suggest an Env requires high CCR5 expression for viral entry. We found no significant difference in median MVC IC_{50} values between the T/F (2.4 nM) and CC Envs (2.3 nM) ($p=0.79$; Mann-Whitney) (Figure 2-2A). In addition, we determined the maximal percent inhibition (MPI) of infection by MVC. While uncommon, several *in vivo* derived MVC-resistant R5-tropic viruses have been identified that can utilize the drug-bound form of CCR5 (352, 371). Such viruses engage the coreceptor differently, relying predominantly upon the N-terminus for entry whereas most viruses require the N-terminus as well as the extracellular loops of CCR5. Furthermore, determining the MVC sensitivity of T/F viruses has implications for microbicides and pre-exposure prophylaxis. All 41 Envs examined had MPIs greater than 85%,

with the vast majority greater than 95%. There were no significant differences (p=0.17 Mann-Whitney) between the T/F (median=99.1%) and CC Envs (median=98.3; Figure 2B). Together, these data indicate that the HIV-1 transmission bottleneck does not impose a selection pressure for viruses capable of using low concentrations of CCR5.

Primary CD4+ T cell tropism. CD4+ T cells, the major target and source of HIV-1 *in vivo* (183, 395), can be broadly divided into four subsets: naïve (CCR7+CD45RO-), central memory (T_{CM}) (CCR7+CD45RO+), effector memory (T_{EM}) (CCR7-CD45RO+), and CD45RA+ effector memory (T_{EMRA}) (CCR7-CD45RO-) (316). These subsets are differentially infected due in part to variation in coreceptor expression (274), cellular activation (124), and tissue localization (130). T_{EM} and T_{EMRA} cells are found predominantly in effector sites including the rectal and cervicovaginal mucosa, while naïve and T_{CM} cells are most abundant in the lymph nodes. T_{EM} cells, the most abundant subset in mucosal effector sites, are preferentially infected and massively depleted during acute infection (reviewed in (228)). Since potential target cells in the mucosa may be limiting during transmission, we hypothesized that T/F Envs may infect T_{EM} and T_{EMRA} cells preferentially relative to the matched CC controls.

Peripheral blood CD4+ T cells from three normal uninfected donors were purified by negative selection and stimulated with anti-CD3/anti-CD28 and IL-2 for three days prior to infection with HIV-1 pseudotypes expressing a GFP reporter. Three days post-infection, viability and expression of CD3, CD4, CCR7, CD45RO, and GFP was assessed by FACS analysis. Productively infected cells were defined as CD3+ GFP+ since CD4 was down-regulated in the majority of infected cells (80). The gating strategy is shown in Figure 3A. In all three donors, infected cells were predominantly T_{EM} (~65%), followed by T_{CM} (~30%), T_{EMRA} (~3%), and naïve (~2%) cells (Figure 2-3B). As X4-tropic viruses have been previously reported to readily infect naïve CD4+ T cells compared to R5-tropic viruses (99, 253, 263), this assay contains an important internal validation: the five viruses that could utilize CXCR4 for entry (one X4-tropic Env shown in

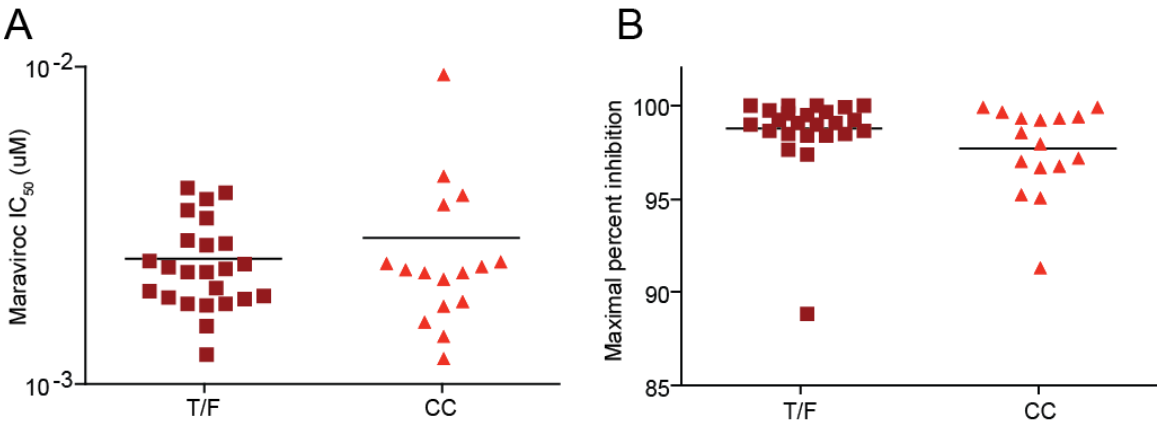

Figure 2-2. CCR5 utilization efficiency. **(A)** Viral pseudotypes were used to infect NP2/CD4/CCR5 cells in the presence of serial dilutions of the CCR5 antagonist maraviroc (MVC). Higher IC_{50} values correspond to Envs that can utilize CCR5 more efficiently, and vice versa. T/F and CC subtype B Envs have similar MVC IC_{50} values (p=0.79) suggesting they engage CCR5 comparably. **(B)** Since some Envs can utilize the MVC-bound conformation of CCR5 and since MVC is a candidate microbicide, we assessed the maximal percent inhibition (MPI) of MVC for each Env. All Envs were sensitive to MVC and there was no difference in MPI between the T/F and CC Envs (p=0.17). All infections were done in at least triplicate in each of at least three independent experiments. Data was analyzed by a Mann-Whitney test.

cyan; four R5X4-tropic Envs shown in red) preferentially infected naïve cells. With the exception of these five Envs, no other pseudotypes were reproducibly outliers in their ability to mediate entry into any of the subsets, and there were no statistically significant differences or trends between the T/F and CC Envs for any of the four cell subsets in any of the three donors examined (Figure 2-3B). In addition, there was no statistically significant difference in overall infectivity between the T/F and CC Env pseudotypes in any of the three donors examined suggesting comparable Env fitness in peripheral CD4+ T cells (Figure 2-3C). Together, this suggests that transmission and early expansion is not due to differential infection of CD4+T cells or their subsets between T/F and chronic Envs.

DC-mediated *trans*-infection. DCs can enhance HIV-1 infection in *trans* by efficiently capturing virus particles and presenting them to CD4+ T cells. *In vitro*, co-culture of monocyte-derived DCs with CD4+ T cells results in enhanced virus infection, particularly at low virus inocula (reviewed in (276)). To assess whether DCs preferentially bind and transfer T/F compared to chronic Env pseudoviruses, we performed DC:CD4+ T cell co-culture experiments. Viral pseudotype stocks were normalized for infectivity on NP2 cells to control for differences in viral titer. A relatively limiting amount of virus (80 RLUs on NP2 cells) was bound to DCs, which were then washed to remove cell-free virus and co-cultured with CD4+ T cells. All Envs were assessed in at least three independent experiments, each time using DCs and CD4+ T cells from different normal donors. Adding this amount of virus to $3x10^4$ CD4+ T cells, then washing as with the DCs, resulted in infection at background levels. However, adding virus associated with DCs markedly increased infection. Nonetheless, the magnitude of DC:CD4+ T cell *trans*-infection was not different between T/F and CC Envs (Figure 2-4; p=0.44 Mann-Whitney). In addition, there was no difference in CD4+ T cell infectivity in the absence of DCs and there was no detectable infection of DC control cultures in the absence of CD4+ T cells (data not shown). The absence of any difference between T/F and CC pseudoviruses in this *trans*-infection assay suggests that, at least when presented with an equal amount of infectious pseudovirus, DCs bind and transfer T/F and CC Env pseudotypes similarly.

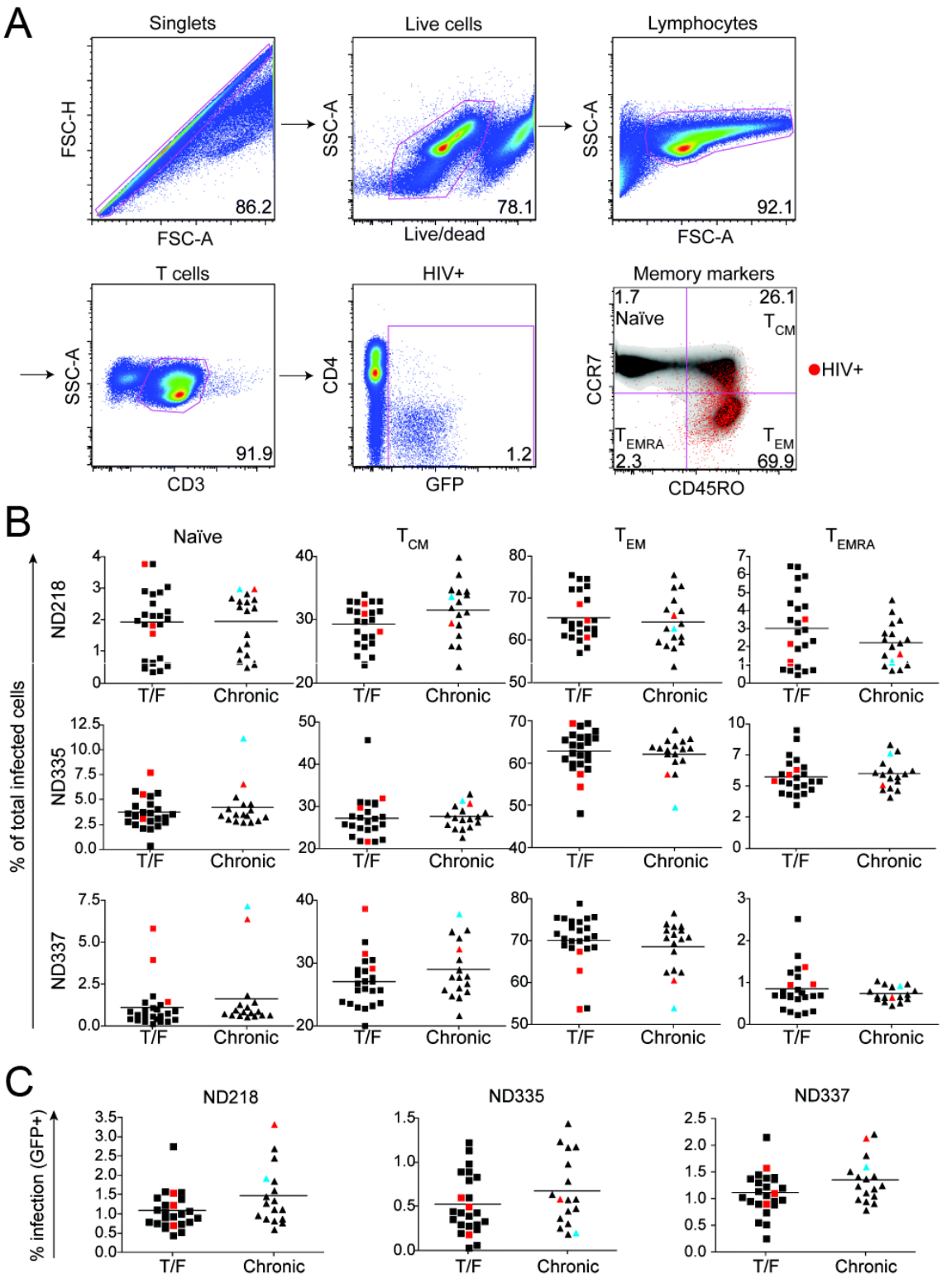
A
Singlets
FSC-H
FSC-A
86.2
Live cells
SSC-A
Live/dead
78.1
Lymphocytes
SSC-A
FSC-A
92.1
T cells
SSC-A
CD3
91.9
HIV+
CD4
GFP
1.2
Memory markers
1.7
Naïve
26.1
T CM
T EMRA
2.3
T EM
69.9
CCR7
CD45RO
HIV+
B
Naïve
T CM
T EM
T EMRA
ND218
ND335
ND337
% of total infected cells
T/F
Chronic
C
ND218
ND335
ND337
% infection (GFP+)
T/F
Chronic

Figure 2-3. CD4+ T cell subset tropism. To assess human CD4+ T subset tropism of the T/F and CC Envs, cells were infected with Env pseudotypes expressing GFP and then stained and analyzed by flow cytometry. **(A)** Cells were gated as shown. Infected cells (GFP+) were then back-gated on the memory markers CCR7 and CD45RO to evaluate differential subset infection. Naïve (CCR7+CD45RO-); central memory (T_{CM}) (CCR7+CD45RO+); effector memory (T_{EM}) (CCR7-CD45RO+), effector memory RA (T_{EMRA}) (CCR7-CD45RO-). **(B)** T/F and chronic Envs infected all four CD4+ T cell subsets comparably. T_{EM} and T_{CM} cells were infected most readily followed by naïve and T_{EMRA} cells. As expected, Envs that could utilize CXCR4 preferentially infected naïve cells compared to Envs that used exclusively CCR5. **(C)** T/F and CC Env pseudotypes have comparable overall CD4+ T cell infection frequency in each of the three donors examined. R5X4-tropic Envs are shown in red and the one X4-tropic Env is shown in cyan. R5X4-tropic Envs are shown in red and the one X4-tropic Env is shown in cyan. Tropism was assessed in cells obtained from three different, uninfected normal donors as indicated (ND218, ND335, and ND337). The horizontal lines indicate the mean value for each group of Envs.

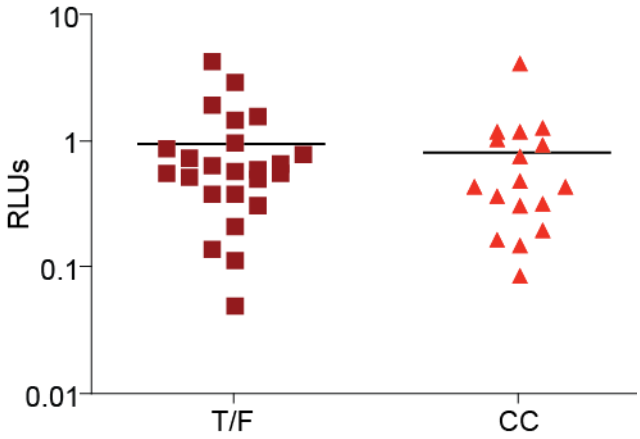

Figure 2-4. Dendritic cell (DC) *trans*-infection. To assess differential DC-binding and CD4+ T cell *trans*-infection of T/F and CC Envs, we pulsed DCs with luciferase expressing Env pseudotypes and then washed off unbound virus and added CD4+ T cells. Relative light units (RLUs) were then measured as a surrogate for infection. DC *trans*-infection efficiency was comparable between the T/F and CC Envs (p=0.44). Viral input was normalized based upon infectivity on NP2 cell lines. Data shown is from one of at least three independent experiments with cells from different donors, each done in at least triplicate. Data was analyzed by a Mann-Whitney test.

Entry kinetics and enfuvirtide sensitivity. Productive entry of HIV-1 into cells may occur following internalization and delivery to endosomes, albeit in a pH-independent manner (241). If so, then the rate at which a virus is internalized, fuses, and enters cells could impact viral tropism. In addition, the rate at which a virus fuses is a measure of how well it productively engages CD4 and coreceptor. Hypothesizing that faster-fusing viruses may preferentially overcome mucosal barriers to transmission, we indirectly assessed the entry kinetics of the T/F and CC pseudoviruses using a time-of-addition experiment with the fusion inhibitor enfuvirtide. As enfuvirtide is not membrane permeable, time to enfuvirtide escape may reflect the rate of viral endocytosis, fusion, or some combination thereof. HIV-1 pseudotypes were added to NP2 cells on ice. Cells were spinoculated at 4°C to facilitate HIV-1 binding and then cold media was removed and replaced immediately with pre-warmed media. Saturating concentrations of enfuvirtide were then added at 0, 5, 10, 20, 40, 80, and 160 minutes post-warming, and then infectivity was normalized to a no-drug control. To control for experimental variation, the prototypic R5-tropic virus JRFL was included in all experiments. There was no significant difference or trend in the rate at which T/F and CC Env pseudotypes productively entered NP2 cells, thus becoming resistant to enfuvirtide addition. The median time to half maximal resistance (t ½ max) post-warming was 32.5 minutes for the T/F and 31.4 minutes for the CC Envs (p=0.55 Mann-Whitney). Interestingly, JRFL became resistant to enfuvirtide significantly faster (t ½ max= 15.9 minutes) than all 41 T/F and chronic Envs (Figure 2-5A). In addition, we assessed enfuvirtide potency, a measure of pre-hairpin bundle exposure that also reflects kinetics of CD4/coreceptor engagement and endocytosis (242). There was no difference between T/F and CC Env sensitivity to enfuvirtide (mean IC_{50} 0.10 vs 0.13 μg/ml; p=0.53; Figure 2-5B). Together this suggests that the kinetics of viral entry/endocytosis are comparable between T/F and chronic Envs.

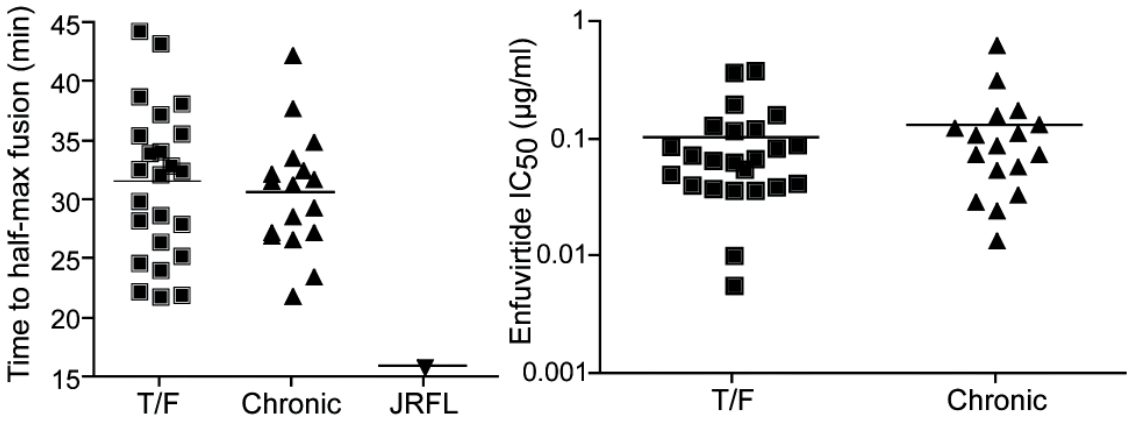

Figure 2-5. Entry kinetics and enfuvirtide sensitivity. (A) To examine differences in T/F and chronic Env endocytosis/fusion kinetics, we employed an indirect assay in which viral pseudotypes were bound to NP2 cells in the cold prior to the addition of pre-warmed media. A saturating concentration of enfuvirtide was added at various times post-warming. The time to half-maximal resistance to enfuvirtide (t ½ max) was then calculated. The T/F and CC Envs became resistant to enfuvirtide at equal rates (p=0.55), with all of the Envs acquiring resistance to enfuvirtide more slowly than a prototypic R5-tropic HIV-1 control, JRFL. **(B)** Enfuvirtide potency, a compound measure of fusion kinetics and affinity, was assessed for all T/F and CC Envs. There was no difference in enfuvirtide IC50 between the T/F and CC Envs (p=0.53) further suggesting there is no difference in endocytosis/fusion rates between T/F and chronic Envs. Each infection condition was done in triplicate (A) or duplicate (B) for each Env in each of at least three independent experiments. Data was analyzed by a Mann-Whitney test.

Sensitivity to broadly neutralizing antibodies and HIVIG. It has previously been reported that Envs derived from acutely infected individuals may exhibit enhanced sensitivity to antibody-mediated neutralization because of changes in glycosylation and/or variable loop length (88). This finding raised the possibility that such Envs might be able to bind to CD4 and coreceptor more efficiently. To examine this, we measured the sensitivity of the T/F and CC Envs to four broadly neutralizing MAbs. MAbs b12 (47) and VRC01 (397) neutralize Env by engaging the CD4 binding site (CD4bs), while the epitopes for PG9 and PG16 (363), distinct germ-line variants from the same individual, are glycosylation-dependent and include parts of the V1/2 and V3 loops (93). To assess neutralization sensitivity, pseudoviruses were pre-incubated with a single concentration (10 μg/ml) of each MAb for 60 minutes prior to infection of NP2 cells. Maximal percent inhibition was then determined by normalizing to a control without antibody. Interestingly, T/F Envs were more sensitive than CC Envs to both b12 (mean MPI 66% vs. 17%; p=0.0003; Figure 2-6A) and VRC01 (mean MPI 89% vs. 50%; p=0.0077; Figure 2-6B compare T/F to CC 1). There was also a trend towards enhanced sensitivity to neutralization by PG9 (Figure 2-6C) and PG16 (Figure 2-6D). To confirm these differences, the neutralization sensitivity of T/F Envs was independently examined using a different backbone (SG3) and HIV-1 reporter cell line (TZM-bl), with both MPI and IC_{50} values being determined. The results confirmed the NP2 cell data in that the T/F Envs were more sensitive to neutralization by b12 (Figure 6E) and VRC01 (Figure 6F). In addition, the T/F Envs exhibited a trend towards increased neutralization sensitivity to both PG9 (Figure 2-6G) and PG16 (Figure 2-6H). While this did not reach statistical significance, it is consistent with a more neutralization sensitive phenotype of T/F compared to chronic Envs.

To assess whether the neutralization sensitive phenotype of our T/F Envs depended on the particular panel of CC Envs used, we examined the neutralization sensitivity of 14 subtype B control Envs derived from six additional chronically infected individuals (Chronic 2 in Figure 2-6A-D). Similar to the initial test set of CC Envs (Chonic 1 in Figure 2-6A-D), this validation set exhibited increased resistance to b12 compared to T/F Envs (p=0.0001 Mann-Whitney). However, unlike the initial CC Env panel, the validation Envs were similar to the T/F Envs in their

sensitivity to VRC01 (p=0.14 Mann-Whitney). Finally, there were no differences in PG9 and PG16 sensitivity between the T/F and the validation Envs (Figure 2-6C, D).

While broadly neutralizing MAbs are useful tools in examining neutralization sensitivity, they are rare in HIV-1-infected individuals and thus may give a biased view of HIV-1 neutralization. Thus, we examined neutralization sensitivity of the T/F and CC Envs to pooled sera from patients infected with subtype B HIV-1 strains (subtype B HIVIG). The T/F Envs (median IC_{50} 741 µg/ml) were approximately two-fold more neutralization sensitive than the CC test panel (median IC_{50}= 1179 µg/ml p=0.062), the CC validation panel (median IC_{50} =1500 µg/ml p=0.0095), and the combined subtype B CC panel (median IC_{50} 1324 µg/ml p=0.0078; Figure 6I).

To examine the basis for the enhanced b12 and VRC01 neutralization sensitivity of T/F Envs, we measured the binding of the two MAbs to both T/F and CC Envs. Binding to the trimeric form of the Env expressed on the surface of cells was measured using a cell-based ELISA system (148). To obtain an accurate measure of antibody binding affinity, we corrected binding measurements for the level of cell surface expression of the different Envs. For this purpose, the binding efficiency of b12 and VRC01 was expressed as a fraction of the binding of a CD4-Ig probe added at saturating concentrations. CD4-Ig is a fusion protein that consists of two copies of the two N-terminal domains of CD4 that are linked to the Fc region of human IgG1.

For the entire group of Envs (i.e., T/F and both CC Envs groups combined), a very strong correlation was observed between the binding of the MAbs to the trimeric Envs and their sensitivity to inhibition. Spearman rank-order correlation coefficients of 0.62 ($p<0.0001$) and 0.77 ($p<0.0001$) were obtained for b12 and VRC01, respectively (Figure 7A and B). Comparison of MAb binding to the T/F and CC Envs showed clear differences between the two groups for both b12 and VRC01. Binding of b12 to the T/F Envs was significantly increased relative to both groups of CC Envs (Figure 7C). Binding of VRC01 to the T/F Envs was increased relative to

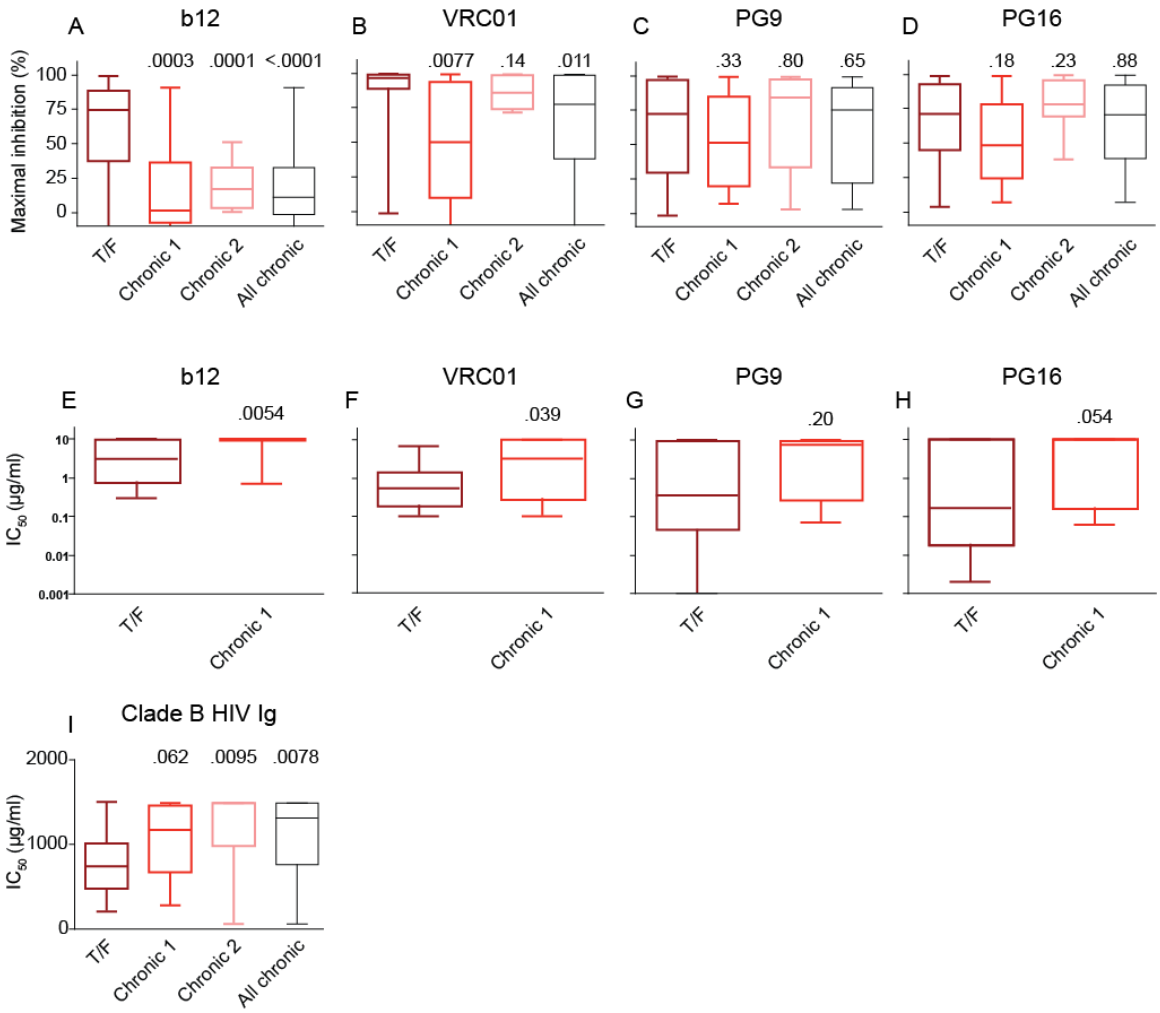

Figure 2-6. Neutralization sensitivity. The sensitivity to monoclonal antibodies b12, VRC01, PG9, and PG16 was assessed on both NP2 cells **(A-D)** and TZM-bl cells **(E-H)**. Neutralization sensitivity on NP2 cells was assessed by determining the maximal percent inhibition (MPI) to 10µg/ml of the indicated MAb. IC_{50} values were determined in the TZM-bl assay. Subtype B T/F Envs (dark red) were more sensitive to b12 and VRC01 compared to the geographically-matched panel of CC Envs (CC 1, light red). To confirm this finding, we assessed an independent panel of subtype B chronic Envs from Washington state (CC 2, pink). "All chronic" includes subtype B chronic panels 1 and 2 and is shown in black. **(I)** Subtype B T/F Envs are also more sensitive to subtype B HIVIG on NP2 cells as measured by IC_{50}. P-values shown are from Mann-Whitney tests with the corresponding T/F Envs. NP2 and TZM-bl experiments were performed in at least three and two independent experiments, respectively.

the original group of CC Envs (p=0.004; Figure 7D). The differential formation/exposure of these epitopes suggests the existence of at least modest structural differences within or near the CD4-binding site of T/F and chronic Envs. No significant differences were observed between VRC01 binding to the T/F and the Washington Envs (p= 0.21).

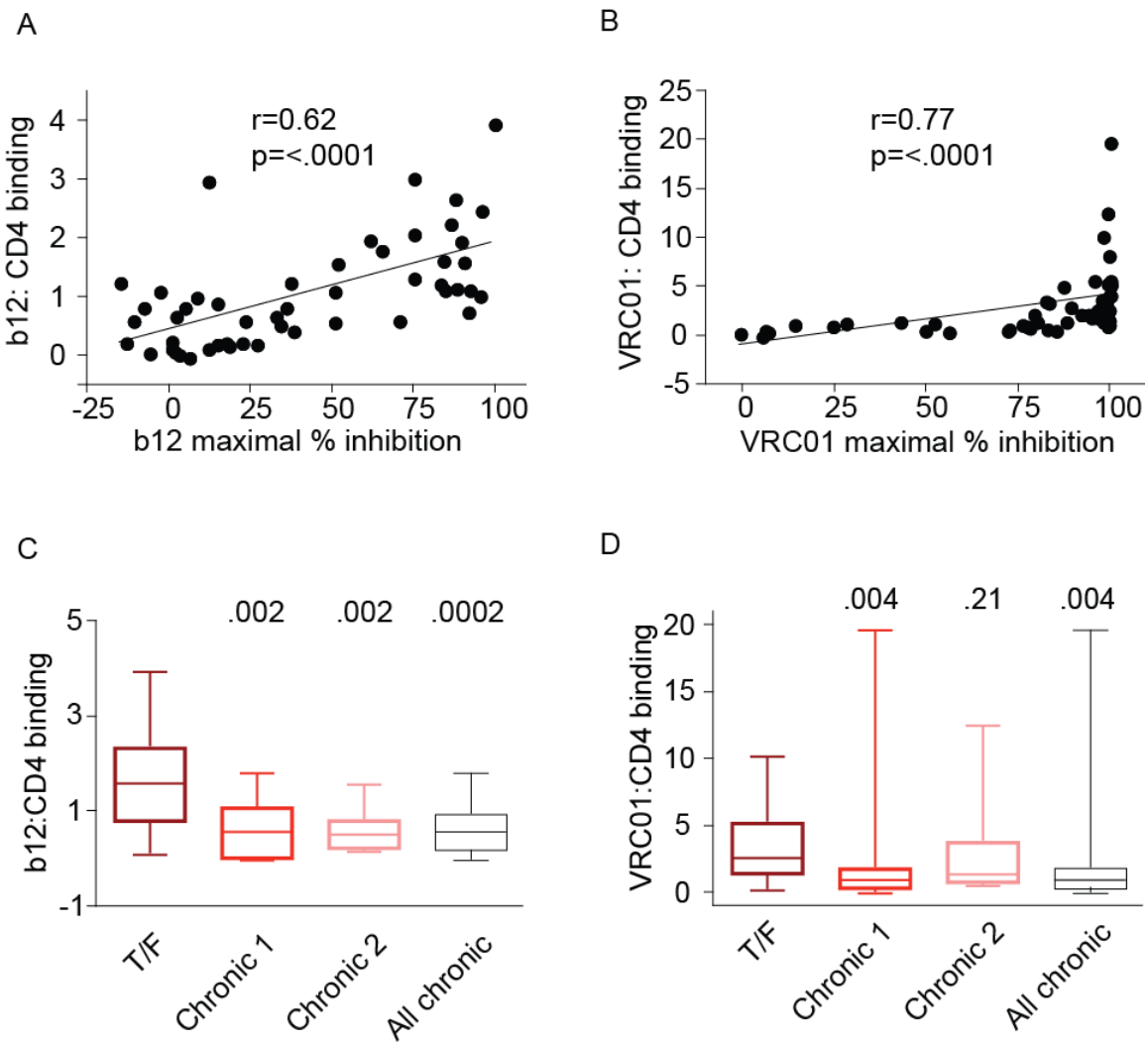

Figure 2-7. Correlation between MAb binding and neutralization. Env was expressed on the surface of cells and then binding to b12 (A) and VRC01 (B) was assessed relative to a CD4 control by ELISA. There is a strong positive correlation between binding and Env pseudotype neutralization sensitivity for both b12 and VRC01 for the T/F and both panels of CC Envs serving to validate the assay. To assess the mechanism of enhanced neutralization sensitivity, we compared b12 (C) and VRC01 (D) binding between T/F (dark red) and CC Envs (light red and pink for CC 1 and 2, respectively). This suggests that differences in MAb binding explain neutralization differences between T/F and CC Envs. Data shown is the mean of two independent experiments.

Discussion

The genetic bottleneck that occurs during mucosal transmission of HIV-1 is the result of a single founder virus that is successfully transmitted from amongst a diverse swarm of viruses present in the donor (176). It is evident that a significant degree of selection is manifest at this step since transmission of R5-tropic virus strains is far more efficient than that of X4-tropic and even R5X4-tropic viruses (318, 399). Whether there is selection for additional viral phenotypes beyond coreceptor use or whether viral transmission is essentially a stochastic process, in which any reasonably fit R5-tropic HIV-1 strain can be transmitted, has not yet been determined. Addressing this question is of practical importance since properties associated with preferential viral transmission could potentially be exploited by vaccine or other antiviral approaches.

Genetic, immunologic, and phenotypic signatures associated with transmitted HIV-1 Envs have been sought in a number of previous studies, most entailing Envs obtained from early infections (acute Envs) (5, 59, 88, 167, 307, 375, 399) as opposed to true T/F Envs obtained by SGA analyses (176, 204, 313). Several studies concluded that T/F and acute Envs have on average shorter variable loops and fewer PNGs than Envs derived from chronically infected individuals (88, 375). While such differences have been noted for Envs from multiple HIV-1 subtypes, they are relatively subtle, variable in location and far from predictive, with some being evident only when larger numbers of sequences are compared. The 24 T/F Envs examined here, for example, exhibited no consistent genetic differences from the CCs. Nonetheless, a much larger sequence comparison that included all but one of the *envs* examined here identified a small number of sequence signatures associated with transmission, including specific sites in the signal sequence and gp41 cytoplasmic domain that could affect Env processing, localization, and incorporation into virus particles as well as changes in the receptor binding regions in gp120 and in N-linked glycosylation sites (126). Thus, existing evidence points to an array of genetic features that may be associated with enhanced HIV-1 transmission across mucosal surfaces by unknown mechanisms.

The identification of genetic motifs in *env* that are enriched in T/F viruses is consistent with the possibility that specific phenotypic properties can be identified that might provide a

selective advantage to transmitted viruses. This is clearly the case at a global level, in that T/F Envs are almost invariably R5-tropic and replicate well in CD4+ T cells but poorly in monocyte-derived macrophages (with the exception of subtype D viruses, G.M. Shaw and J. Baalwa, unpublished data) (313). More detailed phenotypic studies of recently transmitted viruses are generally lacking, although donor and recipient Envs from eight transmission pairs exhibited no differences in CD4 or CCR5 utilization, while a second study using some of these same Envs did not find consistent differences in primary cell infection or use of receptors other than CCR5 and CXCR4 (5, 167). As genetic signatures associated with transmission can be both variable and subtle, we employed a more detailed series of functional assays to seek differences between viral pseudotypes bearing the T/F Envs and those expressing Envs from CCs. We found no phenotypic differences between the T/F and CC Envs examined here in assays designed to probe the efficiency and rate of membrane fusion, the efficiency of coreceptor use, the ability to infect primary CD4+ T cell subsets from different donors, and the ability of virus to be captured by DCs and transferred to adjoining CD4+ T cells. One could ask whether the assays we employed are sufficiently sensitive to detect functional differences between viruses bearing different Env glycoproteins. We feel that they are, as we and others have used these and similar assays to identify significant functional differences between Envs at the level of primary CD4+ T cell tropism, membrane fusion kinetics, the efficiency of CD4 and co-receptor utilization, and attachment to C-type lectins such as DC-SIGN (123, 288, 294, 351). Even single amino changes in Env can impact these properties to extents that can be easily detected. The CD4+ T cell subset tropism assay that we have developed, which can determine the efficiency with which a given virus infects T_{CM}, T_{EM}, T_{EMRA} and naïve T cells, is a particularly sensitive measure of CD4 and coreceptor use, as these receptors are expressed differently on various CD4+ T cell subsets (35, 138, 199, 243, 274). The fact that that 24 T/F Envs here were functionally equivalent to the chronic Env controls in all of the assays employed argues that any phenotypic differences between these and chronic Env controls are apt to be slight in magnitude.

A second consideration regarding the presence or absence of phenotypic traits associated with enhanced virus transmission is whether the assays we employed effectively

recapitulate the key events during the earliest stages of HIV-1 transmission (reviewed in (146)). Following mucosal transmission of HIV-1, virus is not detected in the circulation for about 10 days, a period termed the eclipse phase (reviewed in (190)). Detailed studies in the macaque model show that after vaginal exposure small clusters of infected cells are found in the endocervical region, which is lined by a single layer of epithelial cells (395). The recruitment of plasmacytoid DCs, T cells, and macrophages over several days transforms the initial focus of infection into a CD4+ T cell-rich environment. Similar studies have not yet been conducted assessing penile or rectal transmission in the rhesus model, the likely mode of transmission in the predominantly male cohort assessed in this study. Conceivably, Env properties that promote entry into resting and activated CD4+ T cells in the submucosa as well as transmission between cells could increase the possibility that an initial focus of infection will successfully propagate and eventually lead to dissemination to regional lymph nodes and a systemic infection. The CD4+ T cell subset tropism assay we employed, while more detailed and sensitive than bulk CD4+ T cell infection assays, may not produce CD4+ T cells with properties identical to those found in the rectal or cervicovaginal mucosa. In addition, the DC:CD4+ T cell transmission assay we used is but a surrogate for the likely more complex cell-cell interactions found in the initial foci of infection. It is important to keep in mind that since virus appears to replicate locally for a period of at least a few days to a week, even a relatively subtle change in an Env property that might enhance infection could result in a significant selective advantage over the course of multiple rounds of infection. The single-cycle assays we employed, while sensitive and well-validated, cannot capture the impact of more subtle differences in Env fitness over time. Future studies employing T/F infectious molecular clones in both primary cell and tissue explant cultures might be better suited for the identification of early fitness differences associated with T/F viruses.

In addition to genetic signatures, differences at the level of sensitivity to antibody-mediated neutralization have been found in some studies of recently transmitted viruses (88, 176). We found that the panel of subtype B T/F Envs was more sensitive to the CD4 binding site MAbs b12 and VRC01 as well as subtype B HIVIG, but not to the broadly neutralizing antibodies PG9 and PG16. These differences were approximately two-fold in magnitude and partially

dependent upon the control group employed. Specifically, when a second panel of CC Envs was used as a control, enhanced sensitivity to VRC01 was not observed, though MAb b12 and subtype B HIVIG continued to neutralize the T/F Envs more efficiently. The relatively modest differences that were observed, along with the fact that enhanced neutralization was not seen between all study groups raises several important questions: do T/F Envs exhibit features that generally enhance their sensitivity to certain types of neutralizing antibodies, and if so, what is the basis for these differences and what are the implications for virus transmission?

One limitation of this study is the selection of CC Envs. Ideally, CC Envs would be selected from longitudinal samples or confirmed transmission pairs; however, such samples are difficult to find in sufficient numbers, especially since the great majority of acute subtype B infections are treated with anti-retroviral therapy. It would also be preferable to obtain chronic Envs from semen or genital secretions, the likely source of the viral inoculum, but again such samples are exceedingly scarce. In addition, the majority of Envs used in this study were from males who likely acquired HIV by penile or rectal transmission. Thus, further work is needed to characterize the transmission bottleneck that occurs during vaginal transmission. Our results emphasize the importance of selecting appropriate matched controls since the chronic test and validation sets differed in their neutralization profiles to VRC01 (though not to MAb b12 and subtype B HIVIG) despite no obvious differences in length of infection, transmission risk factor, patient demographics, or phylogenetic relationships to the T/F Envs. Of course, since we are unable to reliably predict neutralization sensitivity from sequence information alone, a control group could by chance differ immunologically from the T/F Envs despite being otherwise well-matched. To mitigate this, selecting CC Envs from geographically-matched individuals may be important. For example, we previously reported that subtype B T/F Envs are more resistant than chronic Envs to b12 and the membrane proximal external region (MPER) antibodies 2F5 and 4E10 (176), seemingly in contradiction with our current findings. However, re-examination of the data in Keele et al. showed that this was due to the predominance of neutralization-sensitive Envs derived from chronically-infected individuals in Trinidad. These Trinidad Envs form a subcluster within the other subtype B Envs used in this study (Figure 2-1), have a Thr deletion in

the V3 loop compared to the subtype B consensus, were over-represented in the CCs and were more sensitive to neutralization by MAbs b12, 2F5 and 4E10 (68). Thus, the previous 2F5 and 4E10 neutralization difference between T/F and chronic Envs was due to bias resulting from disproportionate representation of Envs from Trinidad in the controls.

Several other studies that have assessed neutralization sensitivity of subtype B Envs did not use geographically-matched CCs, raising the possibility that the results from theses studies could be complicated by genotypic differences linked to geographic location (327, 363, 379). In addition to the location, it may also be important to match the time of sample collection when developing well-matched chronic control groups. For example, Bunnik et al. reported that HIV-1 has become more neutralization resistant over the course of the epidemic and thus patient sampling times may bias comparisons between T/F and chronic Envs (45). Here, the chronic Envs were sampled four calendar years before the T/F Envs on average. However, this difference is significantly shorter than the 14-21 year time-span between contemporary and historic Envs assessed in Bunnik et al. In addition, we detected no correlation between sampling time and neutralization sensitivity, and thus this cannot account for the neutralization differences between the T/F Envs and the chronic controls. It is also of note that multiple chronic Envs from the same individual were treated as independent events in this study. Reanalyzing the data to include only one CC Env value (mean of the multiple Envs) per individual did not change the magnitude of the neutralization difference, though it did decrease the p-values above the level of significance for VRC01 and HIVIG, but not b12, likely due to decreased sample size. In summary, more detailed studies involving larger numbers of T/F Envs with appropriately matched CC Envs, including Envs derived from the same individuals over time, and a greater number of broadly neutralizing MAbs and human sera, will be needed to draw definitive conclusions about the neutralization sensitivity of transmitted virus strains.

When our data are considered along with other published studies on T/F and acute Envs, several conclusions can be drawn. First, we believe that HIV-1 transmission is in part stochastic, with any reasonably fit R5-tropic virus being capable of initiating an infection (176, 303, 326, 399). With a now relatively large number of T/F and acute Envs having been examined, it is evident

that no single major genetic, phenotypic or immunologic signature is required for transmission beyond the use of CCR5. Second, an array of genetic traits including but not limited to shorter variable loops and reduced numbers of N-linked glycosylation sites are associated with enhanced virus transmission. The structural implications of these signatures are not well understood, and it is not yet clear if these or as yet unidentified other genetic traits are responsible for the modestly enhanced sensitivity to antibody-mediated neutralization that is characteristic of some T/F and acute Envs. Third, the presence of genetic signatures linked to transmission implies some impact on function that enhances transmission. If so, then the functional impact is apt to be modest given the variable nature of the genetic signatures and the fact that neither we, nor others, have observed clear differences between T/F and acute Envs with CCs. However, the possibility exists that relatively subtle alterations of Env function, perhaps in the context of full-length T/F viral genomes, could provide a sufficiently robust selective advantage during the eclipse phase of HIV-1 transmission to result in preferential transmission of viruses with specific properties. The growing application of SGA technology coupled with increasingly sophisticated cell-to-cell and *ex vivo* tissue systems will make it possible to more rigorously identify immunologic and phenotypic traits associated with HIV-1 transmission.

Acknowledgements

We would like to thank the University of Pennsylvania's Center for AIDS Research (CFAR) Immunology Core for human CD4+ T cells and monocytes; the University of Washington's CFAR HIV Specimen Repository for plasma; Dennis Burton and John Mascola for generously providing PG9/16 and VRC01, respectively; Gerald Learn for phylogenetic expertise; Peter Hraber for determining variable loop lengths of T/F Envs, Drew Weissman, Truman Grayson, Chuanxi Sun, James A. Hoxie, Yanji Yi, and Ronald G. Collman for technical expertise and helpful discussions. This work was funded by the Center for HIV/AIDS Vaccine Immunology, National Institutes of Health grants (AI67854, AI27767, AI40880), the Bill and Melinda Gates Foundation grants 37874 and 38619, and the International AIDS Vaccine Initiative. CBW and NFP were supported by T32 AI000632 and T32 GM008361, respectively.

CHAPTER 3

Transmitted/Founder and Chronic Subtype C HIV-1 Use CD4 and CCR5 Receptors with Equal Efficiency and Are Not Inhibited by Blocking the Integrin α4β7

Nicholas F. Parrish[1,2]#, Craig B. Wilen[1,2]#, Lauren B. Banks[1,2], Shilpa S. Iyer[1,2], Jennifer M. Pfaff[1], Jesus F. Salazar-Gonzalez[3], Maria G. Salazar[3], Julie M. Decker[3], Erica H. Parrish[1,2], Anna Berg[4], Jennifer Hopper[4], Bhavna Hora[4], Amit Kumar[4], Tatenda Mahlokozera[4], Sally Yuan[1], Charl Coleman[5], Marion Vermeulen[5], Haitao Ding[3], Christina Ochsenbauer[3], John C. Tilton[6], Sallie R. Permar[4,7], John C. Kappes[3], Michael R. Betts[1], Michael P. Busch[8], Feng Gao[4,9], David Montefiori[10], Barton F. Haynes[4,9,11], George M. Shaw[1,2], Beatrice H. Hahn[1,2] and Robert W. Doms[1]

Departments of Microbiology[1] and Medicine[2], Perelman School of Medicine at the University of Pennsylvania, Philadelphia, Pennsylvania, [3]Department of Medicine, University of Alabama at Birmingham, Birmingham, Alabama, [4]Duke Human Vaccine Institute, Duke University School of Medicine, Durham, North Carolina, United States of America, [5]Donation Testing Department, South African National Blood Service, Roodepoort, Gauteng, South Africa, [6]Department of General Medical Sciences, Center for Proteomics, Case Western Reserve University School of Medicine, Cleveland, Ohio, [7]Department of Pediatrics, Duke University School of Medicine, Durham, North Carolina, [8]Blood Systems Research Institute, San Francisco, California, [9]Department of Medicine, [10] Department of Surgery, and [11]Department of Immunology, Duke University School of Medicine, Durham, North Carolina

#These authors contributed equally.

Originally published in PLoS Pathogens 8(5):e1002686. May 31, 2012

Abstract

Sexual transmission of human immunodeficiency virus type 1 (HIV-1) most often results from productive infection by a single transmitted/founder (T/F) virus, indicating a stringent mucosal bottleneck. Understanding the viral traits that overcome this bottleneck could have important implications for HIV-1 vaccine design and other prevention strategies. Most T/F viruses use CCR5 to infect target cells and some encode envelope glycoproteins (Envs) that contain fewer potential N-linked glycosylation sites and shorter V1/V2 variable loops than Envs from chronic viruses. Moreover, it has been reported that the gp120 subunits of certain transmitted Envs bind to the gut-homing integrin α4β7, possibly enhancing virus entry and cell-to-cell spread. Here we sought to determine whether subtype C T/F viruses, which are responsible for the majority of new HIV-1 infections worldwide, share biological properties that increase their transmission fitness, including preferential α4β7 engagement. Using single genome amplification, we generated panels of both T/F (n=20) and chronic control (CC, n=20) Env constructs as well as full-length T/F (n=6) and CC (n=4) infectious molecular clones (IMCs). We found that T/F and chronic control Envs were indistinguishable in the efficiency with which they used CD4 and CCR5. Both groups of Envs also exhibited the same CD4+ T cell subset tropism and showed similar sensitivity to neutralization by CD4 binding site (CD4bs) antibodies. Finally, saturating concentrations of anti-α4β7 antibodies failed to inhibit infection and replication of T/F as well as CC viruses, although the growth of the tissue culture-adapted strain SF162 was modestly impaired. These results indicate that the population bottleneck associated with mucosal HIV-1 acquisition is not due to the selection of T/F viruses that use α4β7, CD4 or CCR5 more efficiently.

Introduction

Mucosal transmission of HIV-1 is most often caused by a single variant from amongst the complex viral quasispecies in the infected donor (36, 64, 85, 226, 267, 374, 375, 399). After an eclipse phase of approximately two weeks during which virus is generally not detected in the blood, the progeny of this transmitted/founder (T/F) virus give rise to a productive systemic infection (3, 21, 145, 176, 204, 312, 332). At a minimum, this significant population bottleneck selects for replication competent viruses, most of which use CCR5 as a coreceptor, since viruses that exclusively use CXCR4 are rarely transmitted (51, 176). Whether other phenotypic traits are associated with enhanced mucosal transmission remains uncertain, though addressing this question is of importance because T/F viruses are the targets of vaccines, microbicides, and pre- and post-exposure prophylaxis.

Characterization of T/F virus properties is complicated by the challenges inherent in identifying acutely infected individuals, generating *bona fide* T/F molecular clones, procuring appropriate CC viruses, obtaining sufficient numbers of samples to perform meaningful comparisons, and developing sufficiently sensitive *in vitro* assays to detect phenotypic differences that could impact transmission fitness *in vivo*. Almost all studies examining viral properties associated with mucosal transmission have focused on the viral envelope (Env) glycoprotein, most often in the context of viral pseudotypes (5, 10, 167, 176, 372). In addition, most initial studies examined viruses obtained weeks to months after infection from relatively few transmission events (88, 104, 207). Given the rapidity with which HIV evolves in the face of immune pressures (129), “early” isolates could differ in important ways from true T/F viruses. Nonetheless, analyses of single genome amplification (SGA) derived T/F Env proteins and viruses have shown that mucosal transmission is associated with CD4+ T cell tropism and CCR5 use (176, 257, 313, 372) as well as a variety of signatures in the viral *env* gene (59, 79, 88, 117, 126, 309, 310). These include shorter variable loops, fewer potential N-linked glycosylation sites (PNGs) and, in some cases, enhanced sensitivity to neutralization by CD4 binding site (CD4bs) monoclonal antibodies (mAbs) (372). More recently, it has been shown that the gp120 subunit of

some Env glycoproteins can bind to, and signal through, the integrin α4β7 that is expressed on activated CD4+ T cells in the gut mucosa (9, 63, 250). These findings have been taken to suggest that these interactions play an important role early in sexual transmission of HIV-1 (62, 250). Specifically, it has been hypothesized that genetic signatures associated with transmission of certain subtype A and C viruses, including the absence of some PNGs in V1/V2 and C3/V4 regions, reflect selection for Envs that exhibit strong α4β7 binding and thus increased transmission fitness (250).

To explore the role of α4β7 interactions and other Env properties that might impact mucosal transmission, we employed SGA to generate a panel of T/F (n=20) and CC (n=20) Env constructs from geographically-matched individuals infected with subtype C viruses, the most prevalent HIV-1 lineage worldwide. To examine Env phenotypes in the context of replication competent viruses, we also produced full-length infectious molecular clones (IMCs) for six T/F and four CC subtype C strains. Testing their biological activity in a variety of functional assays, we found no differences in the efficiency with which T/F and CC Envs utilized CD4 or CCR5, mediated infection of primary CD4+ T cell subsets, or were neutralized by mAbs targeting the CD4bs. We confirmed that infection of α4β7-expressing CD4+ T cells by the prototypic subtype B strain HIV-1/SF162 could be partially inhibited by antibodies to α4β7 under some conditions as previously described (9, 63). However, saturating concentrations of α4β7 antibodies had no inhibitory effect on infection of all-*trans* retinoic acid (atRA) stimulated CD4+ T cells from multiple donors by any of the T/F or CC viruses, even though most of their gp120 subunits are predicted to bind this integrin pair based on previously identified genetic signatures (250). These findings indicate that the ability of some gp120 proteins to engage α4β7 may not be recapitulated by their native Env trimers on the surface of infectious particles, and thus suggests that interaction with this integrin pair is not critical for mucosal HIV-1 transmission.

Results

Generation of subtype C T/F and chronic Envs. Previous studies of T/F phenotypes focused almost exclusively on HIV-1 subtype B (171, 176, 258, 372). To examine the extent to which these results are applicable to other subtypes, we focused in this study on the transmission properties of HIV-1 subtype C. To assess viral entry, we assembled a panel of 20 T/F Env clones, six of which have previously been described (191). The remaining 14 clones were derived from 13 acutely infected individuals from South Africa and Zambia (8 males, 5 females) - nine of whom were sampled during the earliest stages of viral infection (Fiebig stages I and II (112); Table 3-1). Plasma viral RNA was extracted, subjected to SGA and direct amplicon sequencing, and used to infer the T/F *env* sequences as previously described (3). Consistent with earlier findings, infection was established by one or a limited number of viral variants. Of the 18 acutely infected individuals included in this panel, 14 acquired a single variant, while three others were infected with two variants and one was infected by four variants (Table 3-1 and Figure 3-1).

To generate an appropriate control group, we obtained 20 Env clones from individuals chronically infected with subtype C viruses (Table 3-1). Seven of these have previously been described (115, 180). The remaining 13 were generated from chronically infected individuals (11 females, 2 males) enrolled in the CHAVI 001 cohort (70). While T/F Envs were derived from individuals of both sexes (10 males; 10 females), chronic Envs were predominantly derived from female subjects (2 males; 18 females). To increase the probability of identifying functional *env* genes, we used SGA to generate up to 42 *env* gene sequences for each chronically infected individual (Figures 3-2 and 3-3). We then constructed phylogenetic trees to identify viruses that had undergone a recent clonal expansion as evidenced by clusters or “rakes” of closely related sequences (Figures 1, 3-2 and 3-3). We reasoned that the common ancestor of such clonally expanded “rakes” would be more likely to encode a fully functional *env* gene than a sequence chosen at random from the quasispecies. To approximate this ancestor, we cloned *env* amplicons whose sequences were either identical to the consensus sequence of the corresponding rake (n=5) or encoded an Env that differed in a single amino acid residue (n=2).

Table 3-1. Origin of T/F and CC HIV-1 *env* clones

Env type	Subject	Env clone designation	Country	Risk factor[a]	Sex	Viral load (RNA copies/ml)	Fiebig stage[b]	Number of SGA sequences	Number of T/F variants	Reference	Cohort[g]
T/F	20258279	20258279-V2_3A5[d] 20258279-V4_3D10[d]	S. Africa	SPD	F	281,838	IV	41	4	this study	SANBS
	2833264	2833264_3G11	S. Africa	SPD	M	234,423	I/II	13	1	this study	SANBS
	21197826	21197826-V1_3A1	S. Africa	SPD	F	343,923	I/II	13	2	this study	SANBS
	21283649	21283649_3E8	S. Africa	SPD	M	3,180	I/II	27	1	this study	SANBS
	20927783	20927783_3E2	S. Africa	SPD	F	1,886	I/II	11	1	this study	SANBS
	1245045	1245045_3C7	S. Africa	SPD	M	234,068	I/II	10	1	this study	SANBS
	19157834	19157834-V1_3C3	S. Africa	SPD	M	275,423	I/II	36	2	this study	SANBS
	2935054	2935054_3A3	S. Africa	SPD	M	>10,000,000	I/II	18	1	this study	SANBS
	ZM246F[c]	ZM246F_C1G[c]	Zambia	HSX	F	10,013,800	II	41	1	312	ZEHRP
	ZM247F	ZM247Fv1.Rev-[d] ZM247Fv2.fs[d]	Zambia	HSX	F	10,823,500	II	44	2	312	ZEHRP
	ZM249M[c]	ZM249M-B10[c]	Zambia	HSX	M	>2,000,000	IV	49	1	312	ZEHRP
	704809221	704809221.1B3	S. Africa	HSX	M	>750,000	I/II	28	1	3	CHAVI
	703010054	703010054.2A2	Malawi	HSX	M	13,936	V	27	1	3	CHAVI
	703010217	703010217.B6	Malawi	HSX	F	102,602	V/VI	25	1	3	CHAVI
	706010018	706010018.2E3	S. Africa	HSX	F	93,700	VI	23	1	3	CHAVI
	704010042[c]	704010042.2E5	S. Africa	HSX	M	181,000	IV	42	1	3	CHAVI
	705010198	705010198.tf	S. Africa	HSX	M	14,950,000	I/II	10	1	in prep[f]	CHAVI
	705010185	705010185.tf	S. Africa	HSX	F	14,800	I/II	10	1	in prep[f]	CHAVI
Chronic	704010330	704010330.G5h	S. Africa	HSX	M	46,100	n/a	26	n/a	this study	CHAVI
	704010207	704010207.D11	S. Africa	HSX	F	15,400	n/a	26	n/a	this study	CHAVI
	702010141	702010141.synR1	Malawi	HSX	F	151,282	n/a	39	n/a	this study	CHAVI
	703010180	703010180.A3[e]	Malawi	HSX	F	105,430	n/a	15	n/a	this study	CHAVI
	702010432[c]	702010432.synR1[c]	Malawi	HSX	M	40,570	n/a	30	n/a	this study	CHAVI
	703010167	703010167.synR1	Malawi	HSX	F	73,505	n/a	30	n/a	this study	CHAVI
	ZM414	ZM414.1[d] ZM414.20[d]	Zambia	HSX	F	213,600	n/a	41	n/a	180	TDRC
	707010457[c]	707010457.synR1[c]	Tanzania	HSX	F	234,671	n/a	20	n/a	this study	CHAVI
	705010534[c]	705010534.synR1[c]	S. Africa	HSX	F	63,300	n/a	36	n/a	this study	CHAVI
	704010499	704010499.H1	S. Africa	HSX	F	15,200	n/a	21	n/a	this study	CHAVI
	704010461	704010461.A7h	S. Africa	HSX	F	22,900	n/a	7	n/a	this study	CHAVI
	704010028	704010028.F6	S. Africa	HSX	F	9,220	n/a	20	n/a	this study	CHAVI
	703010269	703010269.synR1	Malawi	HSX	F	30,434	n/a	30	n/a	this study	CHAVI
	704010273	704010273.E5[e]	S. Africa	HSX	F	25,700	n/a	24	n/a	this study	CHAVI
	709013902	3902.bmG14	Malawi	HSX	F	19,900	n/a	20	n/a	115	CHAVI
	709014707	4707.E1	Malawi	HSX	F	83,400	n/a	22	n/a	115	CHAVI
	709014403	4403.A18[d] 4403.D1[d] 4403.bmB6[d]	Malawi	HSX	F	100,892	n/a	38	n/a	115	CHAVI

[a]SPD = source plasma donors who denied having sex for money or with multiple partners, homosexual activity, injection drug use, or receiving a blood transfusion or a tattoo in the preceding six months; HSX = heterosexual exposure.
[b]defined in (112); n/a = not applicable for subjects enrolled in chronic cohorts.
[c]IMC from subject also tested, see Table 2.
[d]multiple Env clones from single subject.
[e]Env differs from "rake" consensus by a single amino acid.
[f]Kappes et al., manuscript in preparation.
[g]SANBS = South African National Blood Service; ZEHRP = Zambia-Emory HIV Research Project; CHAVI = Center for HIV/AIDS Vaccine Immunology; TDRC = Tropical Diseases Research Centre

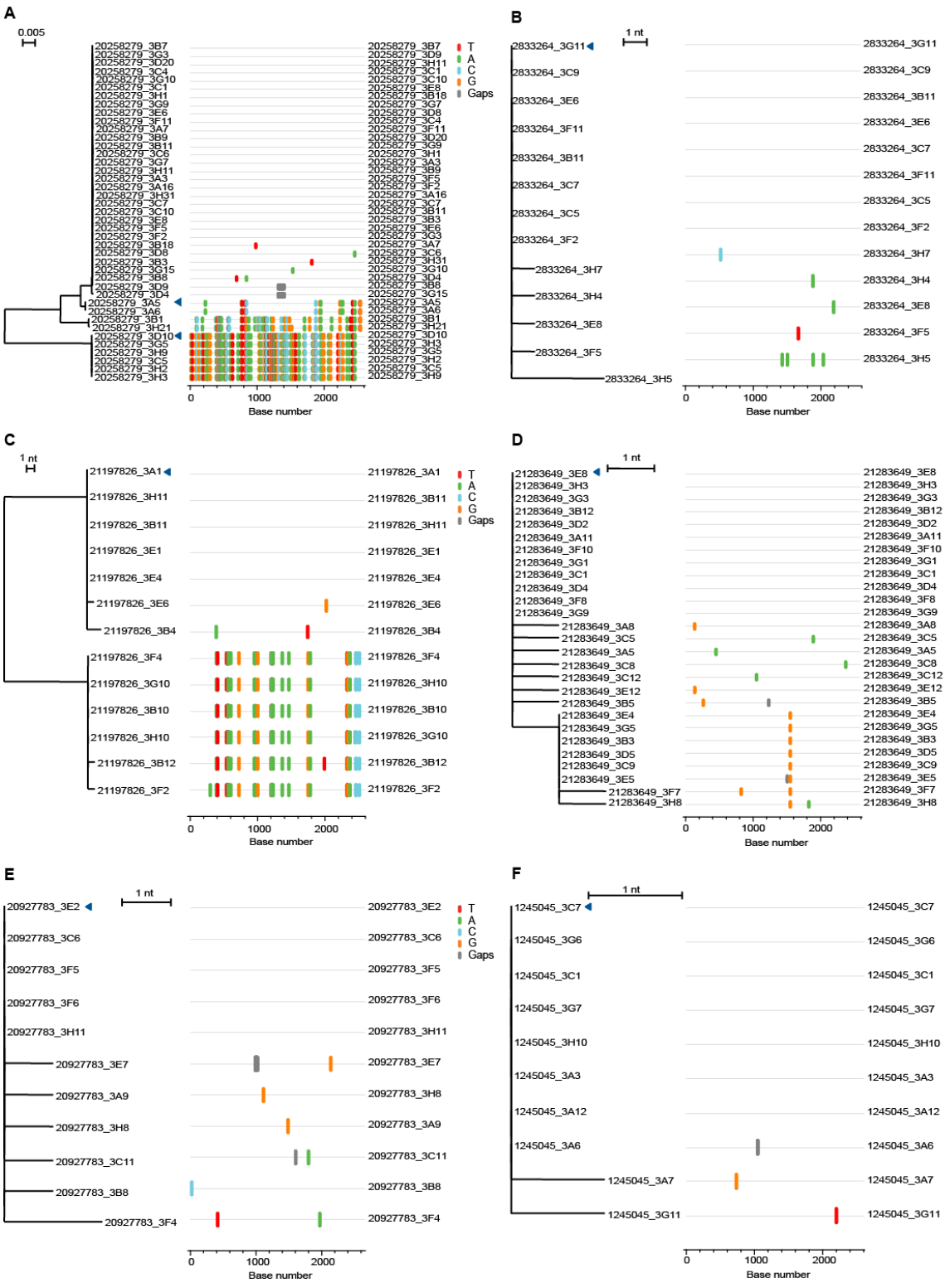
A
0.005
20258279_3B7
20258279_3G3
20258279_3D20
20258279_3C4
20258279_3G10
20258279_3C1
20258279_3H1
20258279_3G9
20258279_3E6
20258279_3F11
20258279_3A7
20258279_3B9
20258279_3B11
20258279_3C6
20258279_3G7
20258279_3H11
20258279_3A3
20258279_3A16
20258279_3H31
20258279_3C7
20258279_3C10
20258279_3E8
20258279_3F5
20258279_3F2
20258279_3B18
20258279_3D8
20258279_3B3
20258279_3G15
20258279_3B8
20258279_3D9
20258279_3D4
20258279_3A5
20258279_3A6
20258279_3B1
20258279_3H21
20258279_3D10
20258279_3G5
20258279_3H9
20258279_3C5
20258279_3H2
20258279_3H3
20258279_3B7
20258279_3D9
20258279_3H11
20258279_3C1
20258279_3C10
20258279_3E8
20258279_3B18
20258279_3G7
20258279_3D8
20258279_3C4
20258279_3F11
20258279_3D20
20258279_3G9
20258279_3H1
20258279_3A3
20258279_3B9
20258279_3F5
20258279_3F2
20258279_3A16
20258279_3C7
20258279_3B11
20258279_3B3
20258279_3E6
20258279_3G3
20258279_3A7
20258279_3C6
20258279_3H31
20258279_3G10
20258279_3D4
20258279_3B8
20258279_3G15
20258279_3A5
20258279_3A6
20258279_3B1
20258279_3H21
20258279_3D10
20258279_3H3
20258279_3G5
20258279_3H2
20258279_3C5
20258279_3H9
T
A
C
G
Gaps
0
1000
2000
Base number
B
1 nt
2833264_3G11
2833264_3C9
2833264_3E6
2833264_3F11
2833264_3B11
2833264_3C7
2833264_3C5
2833264_3F2
2833264_3H7
2833264_3H4
2833264_3E8
2833264_3F5
2833264_3H5
2833264_3G11
2833264_3C9
2833264_3B11
2833264_3E6
2833264_3C7
2833264_3F11
2833264_3C5
2833264_3F2
2833264_3H7
2833264_3H4
2833264_3E8
2833264_3F5
2833264_3H5
0
1000
2000
Base number
C
1 nt
21197826_3A1
21197826_3H11
21197826_3B11
21197826_3E1
21197826_3E4
21197826_3E6
21197826_3B4
21197826_3F4
21197826_3G10
21197826_3B10
21197826_3H10
21197826_3B12
21197826_3F2
21197826_3A1
21197826_3B11
21197826_3H11
21197826_3E1
21197826_3E4
21197826_3E6
21197826_3B4
21197826_3F4
21197826_3H10
21197826_3B10
21197826_3G10
21197826_3B12
21197826_3F2
T
A
C
G
Gaps
0
1000
2000
Base number
D
1 nt
21283649_3E8
21283649_3H3
21283649_3G3
21283649_3B12
21283649_3D2
21283649_3A11
21283649_3F10
21283649_3G1
21283649_3C1
21283649_3D4
21283649_3F8
21283649_3G9
21283649_3A8
21283649_3C5
21283649_3A5
21283649_3C8
21283649_3C12
21283649_3E12
21283649_3B5
21283649_3E4
21283649_3G5
21283649_3B3
21283649_3D5
21283649_3C9
21283649_3E5
21283649_3F7
21283649_3H8
21283649_3E8
21283649_3H3
21283649_3G3
21283649_3B12
21283649_3D2
21283649_3A11
21283649_3F10
21283649_3G1
21283649_3C1
21283649_3D4
21283649_3F8
21283649_3G9
21283649_3A8
21283649_3C5
21283649_3A5
21283649_3C8
21283649_3C12
21283649_3E12
21283649_3B5
21283649_3E4
21283649_3G5
21283649_3B3
21283649_3D5
21283649_3C9
21283649_3E5
21283649_3F7
21283649_3H8
0
1000
2000
Base number
E
1 nt
20927783_3E2
20927783_3C6
20927783_3F5
20927783_3F6
20927783_3H11
20927783_3E7
20927783_3A9
20927783_3H8
20927783_3C11
20927783_3B8
20927783_3F4
20927783_3E2
20927783_3C6
20927783_3F5
20927783_3F6
20927783_3H11
20927783_3E7
20927783_3H8
20927783_3A9
20927783_3C11
20927783_3B8
20927783_3F4
T
A
C
G
Gaps
0
1000
2000
Base number
F
1 nt
1245045_3C7
1245045_3G6
1245045_3C1
1245045_3G7
1245045_3H10
1245045_3A3
1245045_3A12
1245045_3A6
1245045_3A7
1245045_3G11
1245045_3C7
1245045_3G6
1245045_3C1
1245045_3G7
1245045_3H10
1245045_3A3
1245045_3A12
1245045_3A6
1245045_3A7
1245045_3G11
0
1000
2000
Base number

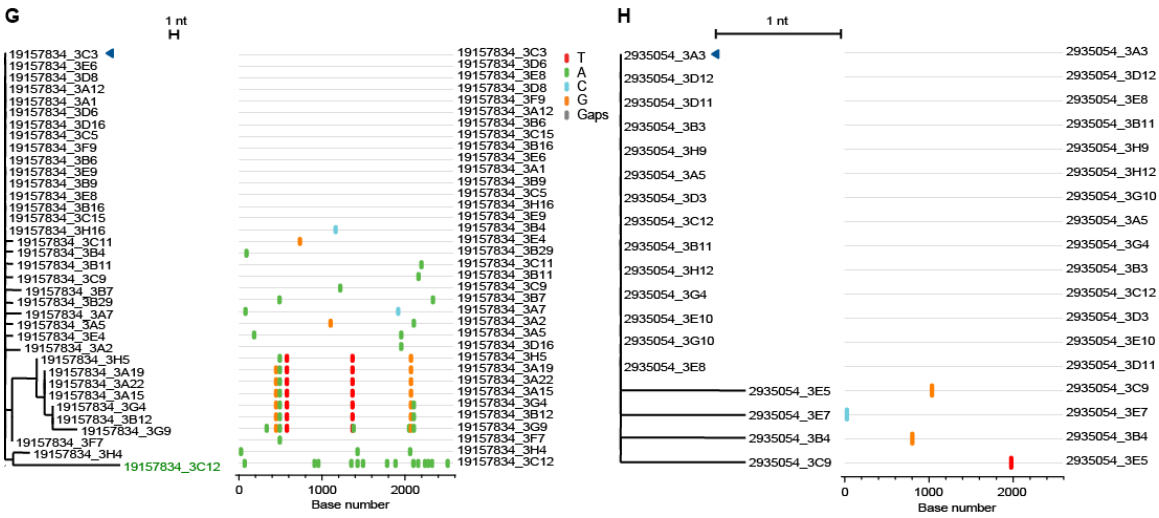

Figure 3-1. Inference of T/F *env* sequences. Maximum likelihood trees of SGA-derived *env* sequences (left) and corresponding Highlighter plots (right) are shown for eight subjects acutely infected with HIV-1 subtype C viruses. Highlighter plots depict sequence alignments (Highlighter v2.1.1; hiv.lanl.gov); tick marks indicate differences compared to the top sequence (red, T; green, A; blue, C; orange, G; grey, gap). The trees were constructed using PhyML (245). Except for in panel A (bar = 0.005 substitutions per site), the scale bar represents a single nucleotide substitution. Sequences chosen for cloning are marked with an arrow. In most subjects, a single low diversity lineage was observed (**B, D, E, F, H**), indicating infection with a single T/F virus. Subjects 20258279 (**A**) and 21197826 (**C**) were infected with four and two T/F viruses, respectively. The tree from subject 19157834 (**G**) shows a lineage with at least four shared mutations, which likely represents a second closely related T/F virus (a single sequence highlighted in green exhibits G->A hypermutation). In all cases, the cloned *envs* represent unambiguously determined T/F viruses. GenBank accession numbers for the *env* sequences are listed in Table 3-3.

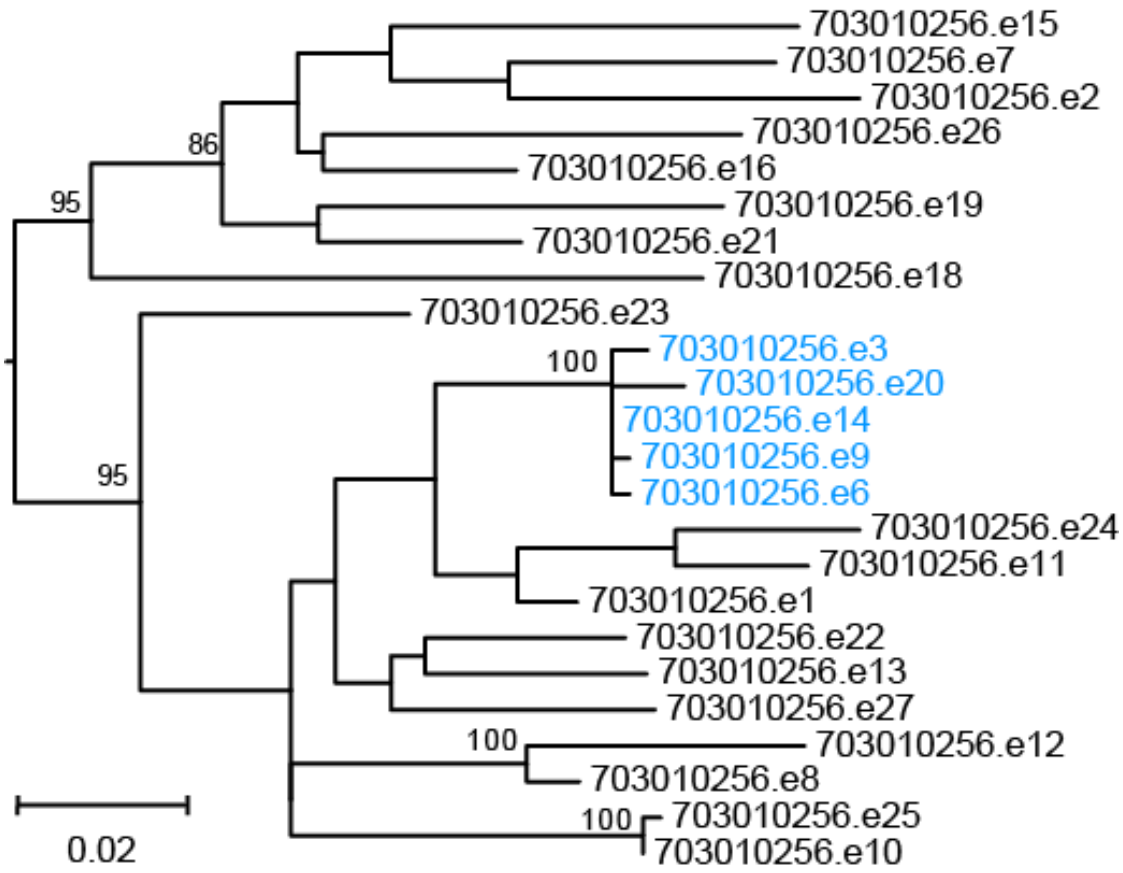

Figure 3-2. Clonal virus expansion in a chronically infected subject. The phylogenetic relationships of SGA-derived 3' half genome sequences depicting the quasispecies complexity in a chronically infected subject are shown. Sequences highlighted in light blue are members of a recently expanded lineage, the consensus sequence of which approximates their most recent common ancestor. The tree was constructed using maximum likelihood methods (140). Nodes with bootstrap support of greater than 80% are labeled (the scale bar represents 0.02 nucleotide substitutions per site).

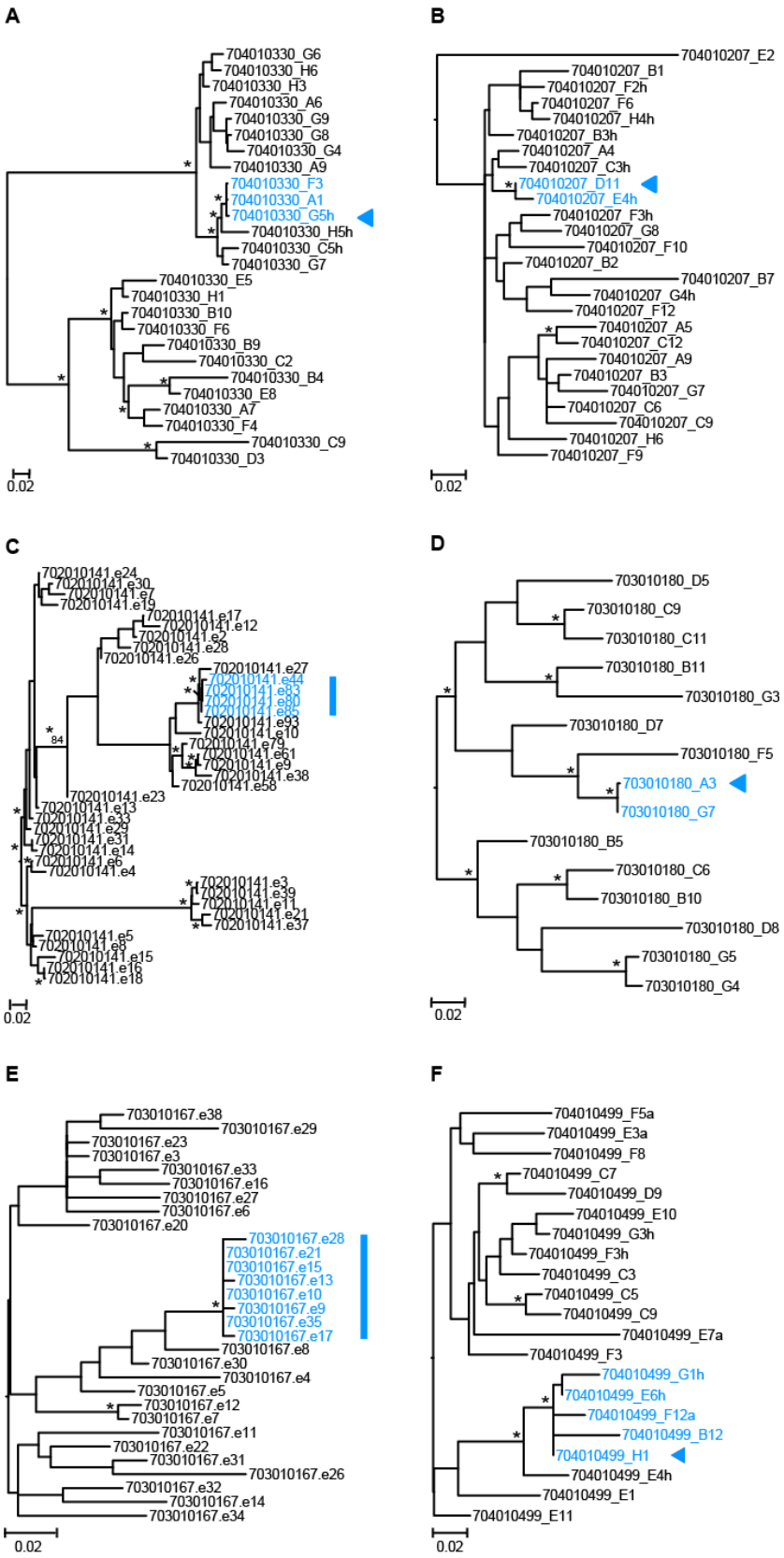
A
704010330_G6
704010330_H6
704010330_H3
704010330_A6
704010330_G9
704010330_G8
704010330_G4
704010330_A9
704010330_F3
704010330_A1
704010330_G5h
704010330_H5h
704010330_C5h
704010330_G7
704010330_E5
704010330_H1
704010330_B10
704010330_F6
704010330_B9
704010330_C2
704010330_B4
704010330_E8
704010330_A7
704010330_F4
704010330_C9
704010330_D3
0.02
B
704010207_E2
704010207_B1
704010207_F2h
704010207_F6
704010207_H4h
704010207_B3h
704010207_A4
704010207_C3h
704010207_D11
704010207_E4h
704010207_F3h
704010207_G8
704010207_F10
704010207_B2
704010207_B7
704010207_G4h
704010207_F12
704010207_A5
704010207_C12
704010207_A9
704010207_B3
704010207_G7
704010207_C6
704010207_C9
704010207_H6
704010207_F9
0.02
C
702010141.e24
702010141.e30
702010141.e7
702010141.e19
702010141.e17
702010141.e12
702010141.e2
702010141.e28
702010141.e26
702010141.e27
702010141.e44
702010141.e83
702010141.e80
702010141.e85
702010141.e93
702010141.e10
702010141.e79
702010141.e61
702010141.e9
702010141.e38
702010141.e58
84
702010141.e23
702010141.e13
702010141.e33
702010141.e29
702010141.e31
702010141.e14
702010141.e6
702010141.e4
702010141.e3
702010141.e39
702010141.e11
702010141.e21
702010141.e37
702010141.e5
702010141.e8
702010141.e15
702010141.e16
702010141.e18
0.02
D
703010180_D5
703010180_C9
703010180_C11
703010180_B11
703010180_G3
703010180_D7
703010180_F5
703010180_A3
703010180_G7
703010180_B5
703010180_C6
703010180_B10
703010180_D8
703010180_G5
703010180_G4
0.02
E
703010167.e38
703010167.e29
703010167.e23
703010167.e3
703010167.e33
703010167.e16
703010167.e27
703010167.e6
703010167.e20
703010167.e28
703010167.e21
703010167.e15
703010167.e13
703010167.e10
703010167.e9
703010167.e35
703010167.e17
703010167.e8
703010167.e30
703010167.e4
703010167.e5
703010167.e12
703010167.e7
703010167.e11
703010167.e22
703010167.e31
703010167.e26
703010167.e32
703010167.e14
703010167.e34
0.02
F
704010499_F5a
704010499_E3a
704010499_F8
704010499_C7
704010499_D9
704010499_E10
704010499_G3h
704010499_F3h
704010499_C3
704010499_C5
704010499_C9
704010499_E7a
704010499_F3
704010499_G1h
704010499_E6h
704010499_F12a
704010499_B12
704010499_H1
704010499_E4h
704010499_E1
704010499_E11
0.02

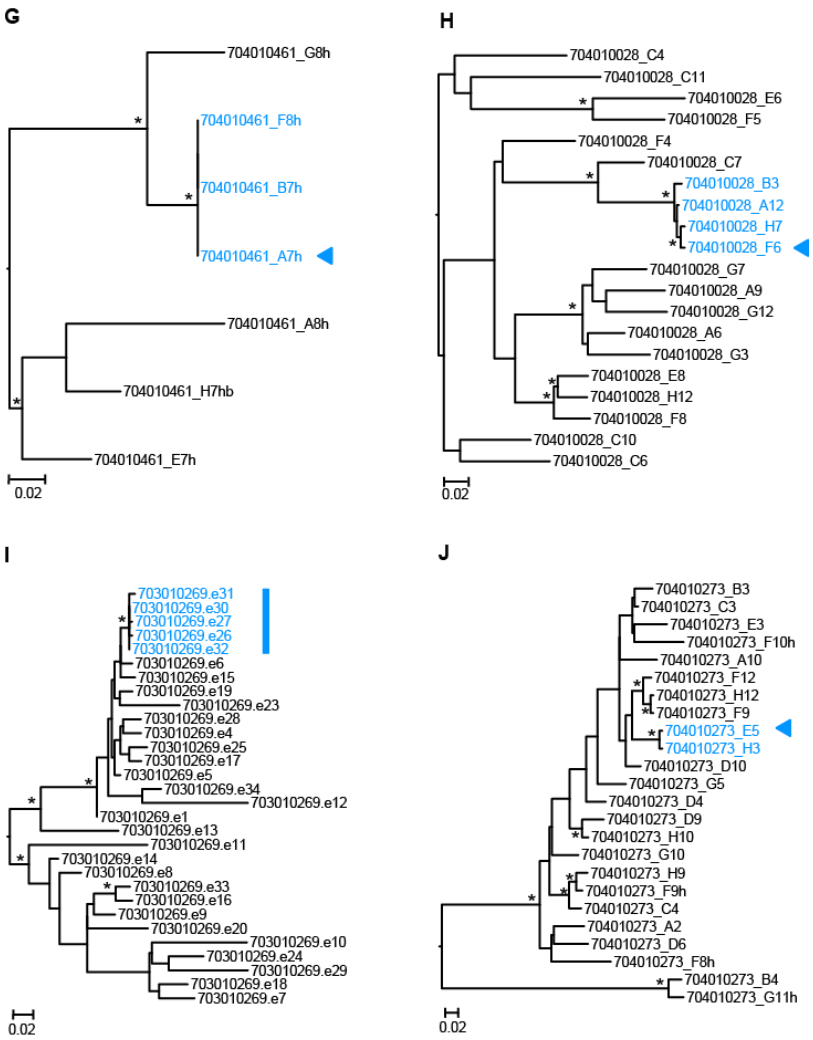

Figure 3-3. Identification of clonally expanded viral lineages in chronically infected individuals. The phylogenetic relationships of SGA-derived *env* sequences depicting the quasispecies complexity in chronically infected subjects are shown (**A-J**). Trees were constructed using maximum likelihood methods (245). Asterisks indicate bootstrap support of greater than 80% (the scale bar represents 0.02 substitutions per site). Sequences highlighted in blue indicate a recently expanded viral lineage, the consensus sequence of which approximates their most recent common ancestor. Red arrows denote *env* amplicons chosen for cloning (**A, B, D, F, G, H, J**) while red lines indicate "rakes" used to infer consensus sequences for chemicalsynthesis (**C, E, I**). GenBank accession numbers for the *env* sequences are listed in Table 3-3.

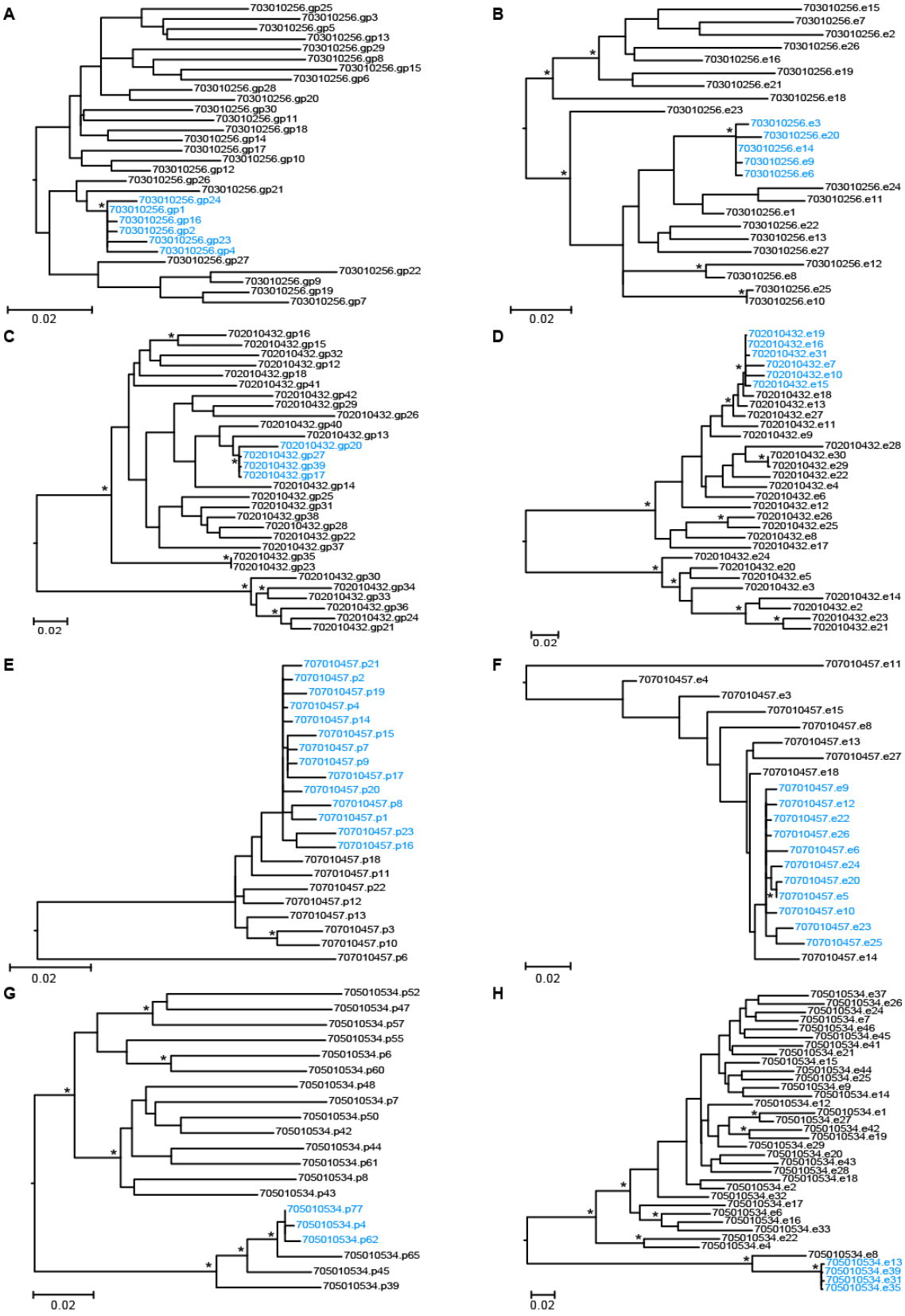
A
703010256.gp25
703010256.gp3
703010256.gp5
703010256.gp13
703010256.gp29
703010256.gp8
703010256.gp15
703010256.gp6
703010256.gp28
703010256.gp20
703010256.gp30
703010256.gp11
703010256.gp18
703010256.gp14
703010256.gp17
703010256.gp10
703010256.gp12
703010256.gp26
703010256.gp21
703010256.gp24
703010256.gp1
703010256.gp16
703010256.gp2
703010256.gp23
703010256.gp4
703010256.gp27
703010256.gp22
703010256.gp9
703010256.gp19
703010256.gp7
0.02
B
703010256.e15
703010256.e7
703010256.e2
703010256.e26
703010256.e16
703010256.e19
703010256.e21
703010256.e18
703010256.e23
703010256.e3
703010256.e20
703010256.e14
703010256.e9
703010256.e6
703010256.e24
703010256.e11
703010256.e1
703010256.e22
703010256.e13
703010256.e27
703010256.e12
703010256.e8
703010256.e25
703010256.e10
0.02
C
702010432.gp16
702010432.gp15
702010432.gp32
702010432.gp12
702010432.gp18
702010432.gp41
702010432.gp42
702010432.gp29
702010432.gp26
702010432.gp40
702010432.gp13
702010432.gp20
702010432.gp27
702010432.gp39
702010432.gp17
702010432.gp14
702010432.gp25
702010432.gp31
702010432.gp38
702010432.gp28
702010432.gp22
702010432.gp37
702010432.gp35
702010432.gp23
702010432.gp30
702010432.gp34
702010432.gp33
702010432.gp36
702010432.gp24
702010432.gp21
0.02
D
702010432.e19
702010432.e16
702010432.e31
702010432.e7
702010432.e10
702010432.e15
702010432.e18
702010432.e13
702010432.e27
702010432.e11
702010432.e9
702010432.e28
702010432.e30
702010432.e29
702010432.e22
702010432.e4
702010432.e6
702010432.e12
702010432.e26
702010432.e25
702010432.e8
702010432.e17
702010432.e24
702010432.e20
702010432.e5
702010432.e3
702010432.e14
702010432.e2
702010432.e23
702010432.e21
0.02
E
707010457.p21
707010457.p2
707010457.p19
707010457.p4
707010457.p14
707010457.p15
707010457.p7
707010457.p9
707010457.p17
707010457.p20
707010457.p8
707010457.p1
707010457.p23
707010457.p16
707010457.p18
707010457.p11
707010457.p22
707010457.p12
707010457.p13
707010457.p3
707010457.p10
707010457.p6
0.02
F
707010457.e11
707010457.e4
707010457.e3
707010457.e15
707010457.e8
707010457.e13
707010457.e27
707010457.e18
707010457.e9
707010457.e12
707010457.e22
707010457.e26
707010457.e6
707010457.e24
707010457.e20
707010457.e5
707010457.e10
707010457.e23
707010457.e25
707010457.e14
0.02
G
705010534.p52
705010534.p47
705010534.p57
705010534.p55
705010534.p6
705010534.p60
705010534.p48
705010534.p7
705010534.p50
705010534.p42
705010534.p44
705010534.p61
705010534.p8
705010534.p43
705010534.p77
705010534.p4
705010534.p62
705010534.p65
705010534.p45
705010534.p39
0.02
H
705010534.e37
705010534.e26
705010534.e24
705010534.e7
705010534.e46
705010534.e45
705010534.e41
705010534.e21
705010534.e15
705010534.e44
705010534.e25
705010534.e9
705010534.e14
705010534.e12
705010534.e1
705010534.e27
705010534.e42
705010534.e19
705010534.e29
705010534.e20
705010534.e43
705010534.e28
705010534.e18
705010534.e2
705010534.e32
705010534.e17
705010534.e6
705010534.e16
705010534.e33
705010534.e22
705010534.e4
705010534.e8
705010534.e13
705010534.e39
705010534.e31
705010534.e35
0.02

Figure S3

Figure 3-4. Construction of CC IMCs from overlapping 5' and 3' half genome sequences. The phylogenetic relationships of SGA-derived 5' and 3' half genome sequences depicting the quasispecies complexity in chronically infected subjects are shown. Trees composed of 5' (**A, C, E, G**) and 3' (**B, D, F, H**) half genome sequences were constructed using maximum likelihood methods (245). Sequences highlighted in blue were used to generate half genome consensus sequences for each subject (**A** and **B** 703010256, **C** and **D** 702010432, **E** and **F** 707010457, **H** and **G** 705010534) that were confirmed to be identical in sequence in the region of overlap then chemically synthesized to generate full-length IMCs. Asterisks indicate bootstrap support of greater than 80% (the scale bar represents 0.02 substitutions per site). GenBank accession numbers for the 5' and 3' half genome sequences are listed in Table 3-3.

For subjects from whom none of the *env* amplicons met these criteria, the rake consensus sequence was inferred and chemically synthesized (n=6). This same approach had also been employed to generate the previously reported CC Env constructs (180, 314). Thus, all 20 CC Envs used in this study were derived from clonally expanded viruses.

Functional analysis of subtype C T/F and CC Envs. Virus pseudotypes containing a luciferase reporter gene and bearing one of the T/F or CC Envs were produced in human 293T cells and then diluted serially on NP2/CD4/CCR5 and NP2/CD4/CXCR4 cells to assess coreceptor usage and to determine the linear range of the assay. All viral pseudotypes were functional, leading to infection of NP2/CD4/CCR5 cells at least 100-fold above Env-negative particles. In contrast, none of the T/F Envs and only one CC Env (4707.E1) mediated entry into NP2/CD4/CXCR4 cells at levels 10-fold above background. However, this Env did not mediate entry of GFP-encoding pseudoviruses into primary CD4+ T cells in the presence of the CCR5 antagonist maraviroc (data not shown). Thus, the small amount of CXCR4-dependent infection seen in NP2/CD4/CXCR4 cells is likely due to the over-expression of this coreceptor and does not reflect CXCR4 use on primary cells. Importantly, all T/F and CC Env constructs were functional, thus validating our methods to correctly infer T/F as well as clonally expanded CC viruses.

Enhanced utilization of CD4 and CCR5 could influence virus transmission since changes in CD4 and CCR5 expression have been shown to impact infection by different HIV-1 strains (74, 95, 96, 274, 336). A previous study of subtype B T/F and CC viral Envs did not reveal differences in their utilization of CCR5 (372). To determine the efficiency with which the newly derived subtype C T/F Envs utilized CD4 relative to the CC Envs, we compared their ability to infect affinofile cells, a 293T cell line that expresses CD4 and CCR5 under independently inducible promoters (172) (Figure 3-5). We induced CCR5 to maximal levels and induced CD4 to high or low expression levels (relative to primary human CD4+ T cells; Figure 2-5B) prior to infection. Infection levels of each pseudovirus in the CD4-low cells were then expressed relative to the values obtained in the CD4-high cells (Figure 3-5A). The macrophage-tropic JR-FL Env, which is known to mediate efficient entry into cells expressing low levels of CD4 (44, 188), was used as a

control. Using this system, we found that virus pseudotypes expressing T/F and clonally expanded CC Envs utilized CD4 with similar efficiency, while CD4 use by JR-FL was 10-fold more efficient than most of the other pseudoviruses (Figure 3-5A). These results demonstrated that the affinofile system is sufficiently sensitive to detect differences in CD4 utilization amongst different virus strains. Additionally, the results confirmed earlier studies of subtype B and C viruses, which indicated that the ability to use limiting levels of CD4 is not a major determinant of transmission fitness (5, 258).

To assess the efficiency of CCR5 use, we infected NP2/CD4/CCR5 cells in the presence of increasing concentrations of the CCR5 antagonist maraviroc and measured the IC_{50} value for each virus. We chose this approach over the use of affinofile cells since we have found that CCR5 expression levels cannot be controlled with sufficient precision at intermediate concentrations of the inducing reagent. Moreover, maraviroc titration should impact CCR5 availability to the same degree on all cells in the population. Therefore, maraviroc sensitivity is a surrogate for the efficiency of CCR5 use, provided that none of the Envs tested can use CCR5 when it is bound to maraviroc (350, 371). This was true of our Env panel; all T/F and chronic Envs examined were sensitive to saturating concentrations of maraviroc with maximal percent inhibitions of >95%. Additionally, T/F and chronic Envs exhibited similar maraviroc IC_{50} values (median T/F=2.22 nM; chronic=1.67 nM; p=0.45). Thus, enhanced CCR5 utilization efficiency does not account for the profound transmission bottleneck of both subtype B (372) and C (Figure 3-5C) (5) infections.

CD4+ T cell subset tropism of subtype C T/F and CC Envs. CD4+ T cell subsets have different activation and coreceptor expression levels, and thus may be differentially susceptible to infection by T/F versus CC viruses (200, 323, 377). Effector memory (T_{EM}) and effector memory RA^+ (T_{EMRA}) cells predominate in mucosal effector sites where the transmission bottleneck likely occurs, while central memory (T_{CM}) and naïve cells are more common in lymph nodes (315, 316). Therefore, an enhanced ability to infect T_{EM} and T_{EMRA} cells

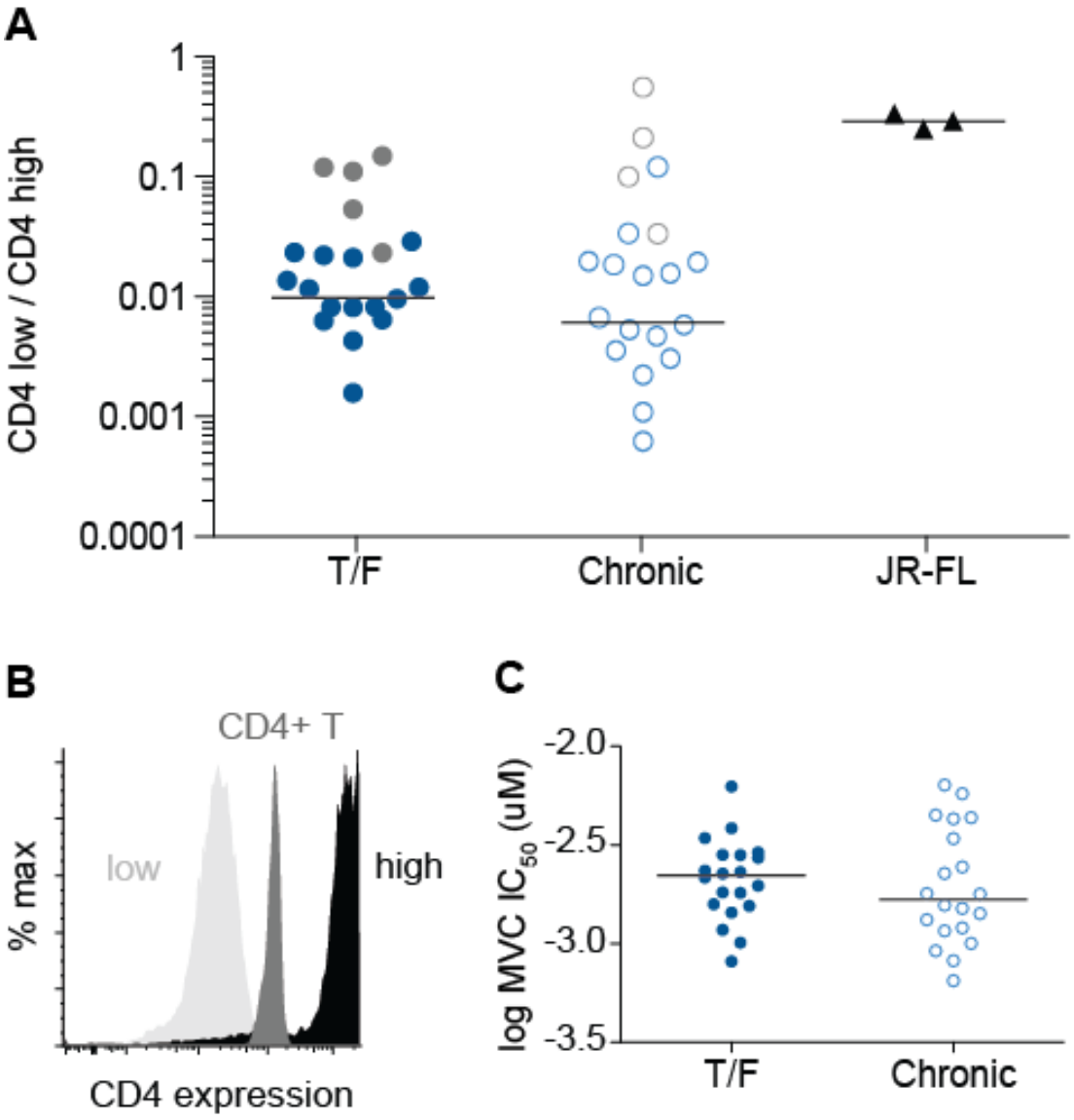

Figure 3-5. T/F and CC Envs utilize CD4 and CCR5 with similar efficiency. (**A**) Efficiency of CD4 usage by T/F and CC Env pseudoviruses. Luciferase-encoding pseudoviruses were used to infect affinofile cells with maximally-induced CCR5 expression and either low or high CD4 expression. Infection of CD4-low cells was measured based on luciferase activity and normalized to infection of CD4-high cells (*y*-axis). Data shown are the mean value from three independent experiments for all T/F and CC Envs, each tested in triplicate; for JR-FL the mean of each of three experiments is plotted. Grey circles indicate poorly infectious Envs for which the CD4 use efficiency is falsely elevated because infection of CD4-low cells was near background, as

described in the methods. The bar represents the median value of each group with these Envs excluded. There was no significant difference in the CD4-use efficiency between T/F and CC envelopes (Mann-Whitney; p=0.35). (**B**) CD4 expression levels from a representative flow cytometry experiment depicting CD4 expression on minimally-induced Affinofile cells (low), fully-induced Affinofile cells (high), and primary human CD4+ T cells (CD4+ T). (**C**) Sensitivity of T/F and CC Envs to inhibition by maraviroc (MVC). Viral pseudotypes were used to infect NP2/CD4/CCR5 cells in the presence of serial three-fold dilutions of the CCR5 antagonist maraviroc. The concentration required to reduce infection by 50% relative to no drug control (IC_{50}) was calculated for each pseudotype. Log MVC IC_{50} values are shown in the y-axis. The bar represents the median value of each group. Higher IC_{50} values indicate that more drug is required to prevent infection corresponding to more efficient CCR5 usage, whereas lower IC_{50} values correspond to less efficient CCR5 usage. No significant difference in IC_{50} values was found between T/F and CC envelope pseudotypes (Mann-Whitney; p=0.46).

could be linked to enhanced mucosal transmission. To explore this, we infected primary CD4+ T cells with GFP-expressing pseudoviruses and then stained for CCR7 and CD45RO to define naïve (CCR7+CD45RO-), T_{CM} (CCR7+CD45RO+), T_{EM} (CCR7-CD45RO+), and T_{EMRA} (CCR7-CD45RO-) cells. As shown in Figure 3-6, we saw no differences in the abilities of subtype C T/F and CC Envs to mediate entry into these CD4+ T cell subsets. Similar to our observations for subtype B T/F and control Envs (372), most infected cells were T_{EM}, but T/F Envs showed no preference for this cell type relative to CC Envs.

Neutralization sensitivity of subtype C T/F and CC Envs. We recently reported that subtype B T/F Envs were more sensitive than CC Envs to the CD4bs mAbs b12 and VRC01, and that this was attributable to increased binding of these antibodies to the native Env trimer (372). To determine whether this was also true for subtype C, we performed neutralization assays with the same antibodies. No significant differences in neutralization sensitivity to b12, VRC01, PG9 or PG16 were observed for T/F and CC Envs (Figure 3-7). As expected, VRC01 generally neutralized subtype C Envs more potently than b12 (379). Using 10 μg/ml of b12, only five Envs were inhibited by 50%, and the most sensitive Env was inhibited by 83%. Using the same concentration of VRC01, 25 Envs were inhibited by 83%, and 16 Envs were inhibited by 95%. Nonetheless, we noted a relationship between the sensitivity to both VRC01 and b12 and the efficiency of CD4 use. When Envs were divided into those that used CD4 most efficiently (top 50% regardless of whether they represented T/F or chronic controls) and those that used CD4 least efficiently, the Envs that used CD4 efficiently were more sensitive to CD4bs (Figure 3-8). In contrast, no relationship between CD4-use efficiency and neutralization sensitivity was observed for PG9, PG16, or purified immunoglobulin pooled from five individuals infected with subtype C HIV-1 (data not shown). Thus, subtype C T/F and chronic Envs used CD4 with similar efficiency, and there was a correlation between CD4 utilization and sensitivity to neutralization by CD4bs mAbs.

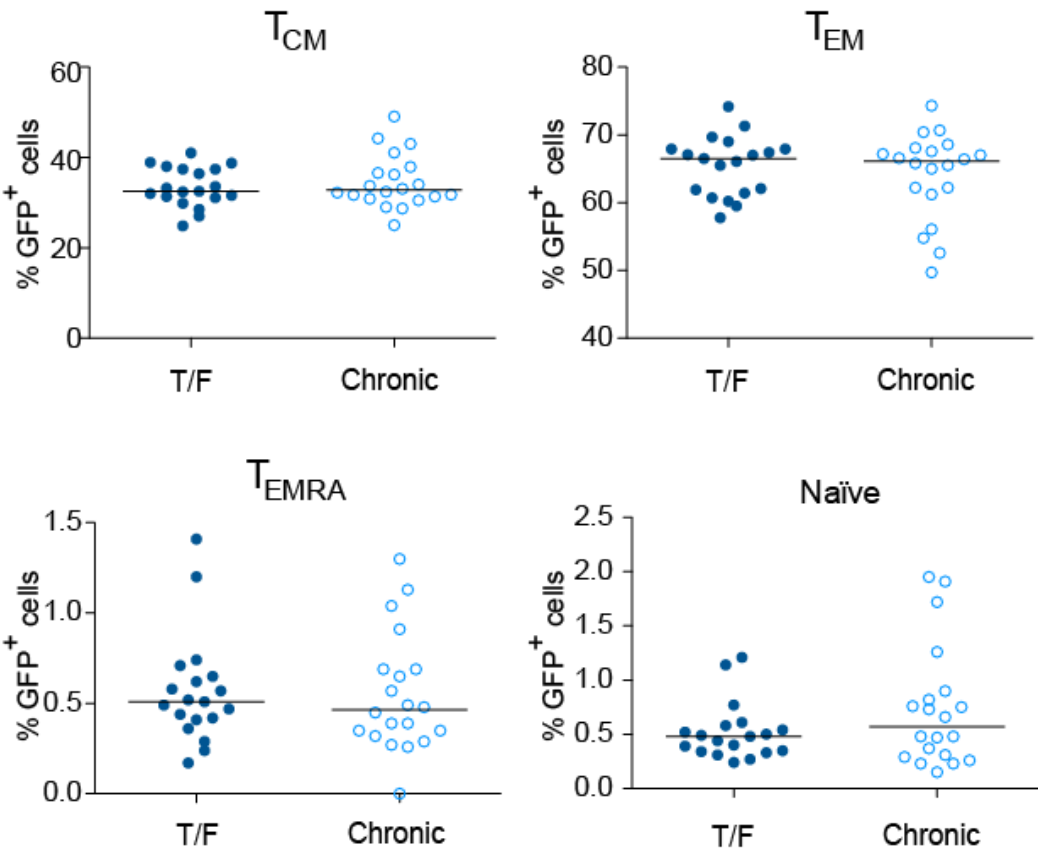

Figure 3-6. T/F and CC Env pseudotypes enter primary CD4+ T cell subsets with similar efficiency. Primary CD4+ T cells were infected with GFP encoding Env pseudotypes to assess the ability of T/F and CC Envs to mediate entry into different CD4+ T cell subsets. Three days post-infection, cells were stained for viability as well as CD3, CD4, CD45RO and CCR7 expression (372). In three independent experiments, cells from different donors cells were analyzed by flow cytometry and GFP+ cells were back-gated onto memory markers to evaluate differential infection of subsets; the average percent of infected cells falling into each subset for each Env is plotted on the *y*-axis. Cells were classified as central memory (T_{CM}: CCR7+CD45RO+), effector memory (T_{EM}: CCR7-CD45RO+), effector memory RA (T_{EMRA}: CCR7-CD45RO-), and naïve (CCR7+CD45RO-). While T_{EM} cells permitted the most efficient infection by Env pseudoviruses, there was no significant difference in infection efficiency between T/F and CC Envs in any of the subsets. The bar represents the median percentage of cells of each subset infected by T/F or CC pseudoviruses.

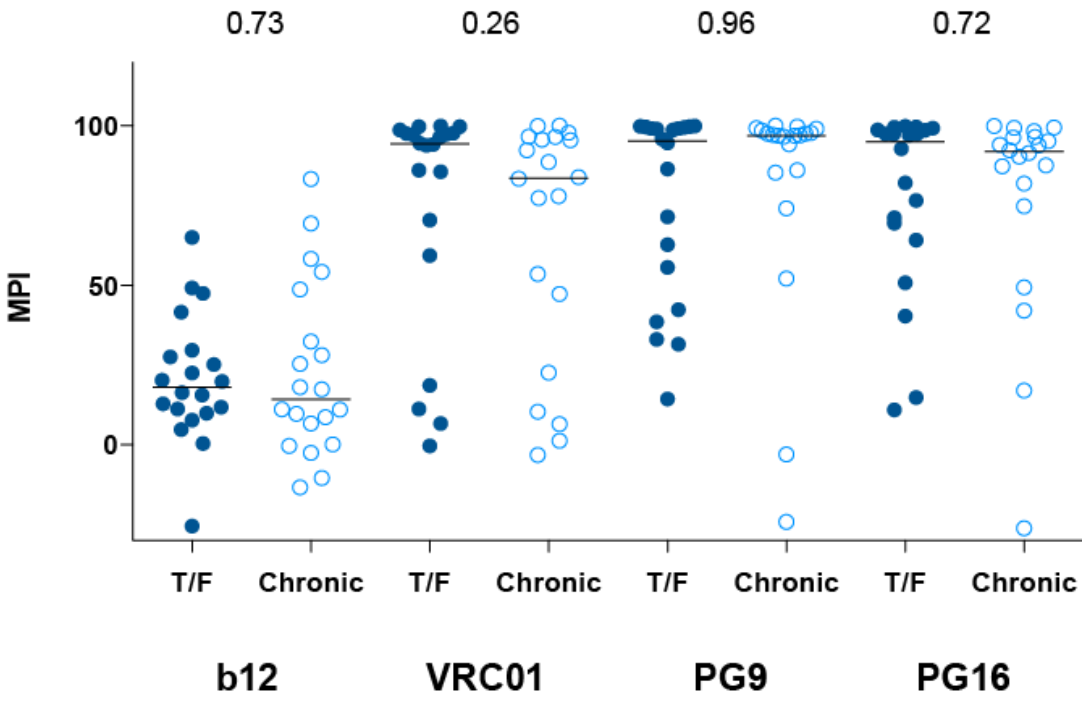

Figure 3-7. Neutralization of T/F and CC Envs. The maximal percent inhibition (MPI) of 10 μg/ml of b12, VRC01, PG9 and PG16 on infection by T/F and CC Env pseudoviruses is shown on the *y*-axis. The bar represents the median MPI. Numbers at the top indicate two-sided Mann-Whitney p-values comparing T/F to CC Envs for each mAb.

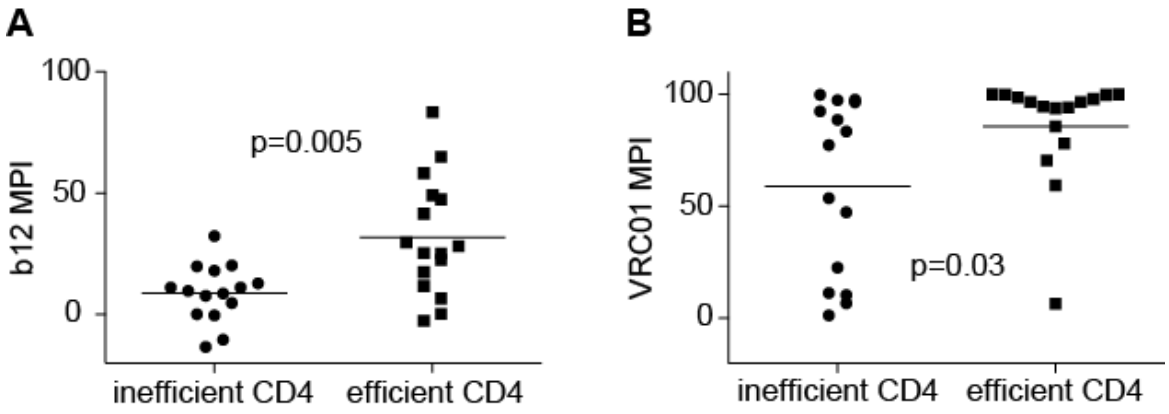

Figure 3-8. CD4-use efficiency correlates with CD4 binding site neutralization sensitivity. The *y*-axis shows sensitivity to CD4bs mAbs b12 **(A)** and VRC01 **(B)** as measured by the maximal percent inhibition (MPI) using 10 μg/ml of each mAb. Envs were divided according to their CD4-use efficiency; those that used CD4 efficiently were more sensitive to CD4bs antibodies than Envs that used CD4 inefficiently. The bar represents the median MPI value and p-values are from two-tailed Mann-Whitney tests.

Effect of α4β7 blockade on infection by Env pseudotypes. The gut-homing integrin α4β7 is expressed on activated CD4+ T cells in the gut (107, 108) and vaginal mucosa (223) and has been shown to bind the gp120 proteins from several recently transmitted subtype A and subtype C viruses (250). In contrast, gp120 proteins from chronic viruses appear to bind α4β7 only rarely, although the subtype B HIV-1/SF162 strain is a notable exception (250). Only a few studies have examined the effect of Env-α4β7 interactions on virus replication (9, 63, 272). It has been shown that mAbs specific for α4β7 partially and transiently inhibit infection of α4β7-positive CD4+ T cells by HIV-1/SF162 at low inocula. Based on these studies, it has been suggested that engagement of α4β7 may enhance HIV-1 infection, especially in the context of mucosal transmission (62, 250).

If the ability of gp120 proteins to bind α4β7 is recapitulated by Env molecules present on virus particles, we reasoned that α4β7 engagement should enhance virus entry, especially at low multiplicities of infection, since binding to the cell surface is a rate-limiting step of virus infection *in vitro* (256, 278). If so, then saturating levels of mAbs to α4β7 should suppress virus infection, as has been shown for the subtype B virus strain HIV-1/SF162 (9, 63). To investigate this, we used a protocol previously developed by Arthos and colleagues in which human CD4+ T cells were stimulated with IL-2 (20 IU/ml), anti-CD3 (1.5 μg/ml) and atRA (10 nM). Under these growth conditions, α4β7 expression was enhanced and detected on 15-65% (median 32%) of CD4+ T cells, predominantly on effector memory cells, from six different donors (data not shown). One donor was non-responsive to atRA and expressed α4β7 on only five to six percent of CD4+ T cells at day six, so these cells were not used for subsequent experiments.

We next titrated two commercially available α4β7 mAbs, Act1 (specific for the α4β7 heterodimer) and 2B4 (specific for α4), both of which have been shown to inhibit gp120 binding and to suppress infection of atRA-treated CD4+ T cells by the laboratory adapted HIV-1/SF162 strain, using concentrations previously reported to be saturating for Act1 (9). To determine if our infection and inhibition conditions were sufficiently sensitive, we used GFP reporter-expressing SF162 Env-containing pseudovirus as the positive control. Pseudovirus expressing the JR-FL Env served as the negative control, since the JR-FL gp120 does not bind α4β7 (250). We failed

to detect any inhibition of infection by either pseudovirus at a broad range of inocula using saturating concentrations of Act1 (Figure 3-9). In fact, Act1 treatment enhanced infection of SF162, JR-FL and VSV-G pseudoviruses by approximately 30% in cells from two different donors. However, gp120-α4β7 binding has recently been described to be critically dependent on Env glycosylation, with high mannose carbohydrates enhancing and complex glycans reducing α4β7 interactions (250). We therefore reasoned that viruses derived from primary CD4+ T cells would be physiologically more relevant, since these cells produce Env proteins with predominantly high-mannose carbohydrates that support α4β7 binding (38).

Effect of α4β7 blockade on replication of subtype C T/F and CC IMCs. To examine the impact of α4β7 blockade on the infectivity and growth kinetics of replication competent viruses, we generated full-length subtype C IMCs representing T/F (n=6) and CC (n=4) viruses (Table 3-2 and Figure 3-4). All but three of these had the LDI/V tripeptide motif in the V2 loop, which has been shown to play a key role in gp120-α4β7 binding (Figure 3-10) (9, 63, 250). Moreover, the number of N-linked glycosylation sites in the V1/V2 region of these IMCs (range from 3 to 8) was comparable to that in gp120 proteins known to interact with α4β7 (range 3 to 9 for the strains SF162, 205F, QA203, and CAP88 (250)). Finally, all replication competent virus stocks were produced in primary human CD4+ T cells to ensure physiologically relevant Env glycosylation, processing and virion incorporation. Using these reagents, we infected atRA-treated primary CD4+ T cells with each virus strain, using a wide range (100-fold) of inocula in the presence of saturating concentrations of Act1. In three independent experiments, we found that Act1 consistently inhibited replication of an SF162 Env-containing molecular clone (NL4-3-SF162, gift from J. Arthos) at six days post-infection. This inhibition was greatest at the lowest multiplicity of infection (Figure 3-11 A and D). We also observed significant Act1-mediated inhibition of an NL4-3 construct that encoded the subtype B Env R3A (231), but again this was seen only at the two lowest virus inputs (Figure 3-11B). No inhibition of infection and replication was observed for YU-2 (Figure 3-11C), which expresses a gp120 that does not bind α4β7 (250).

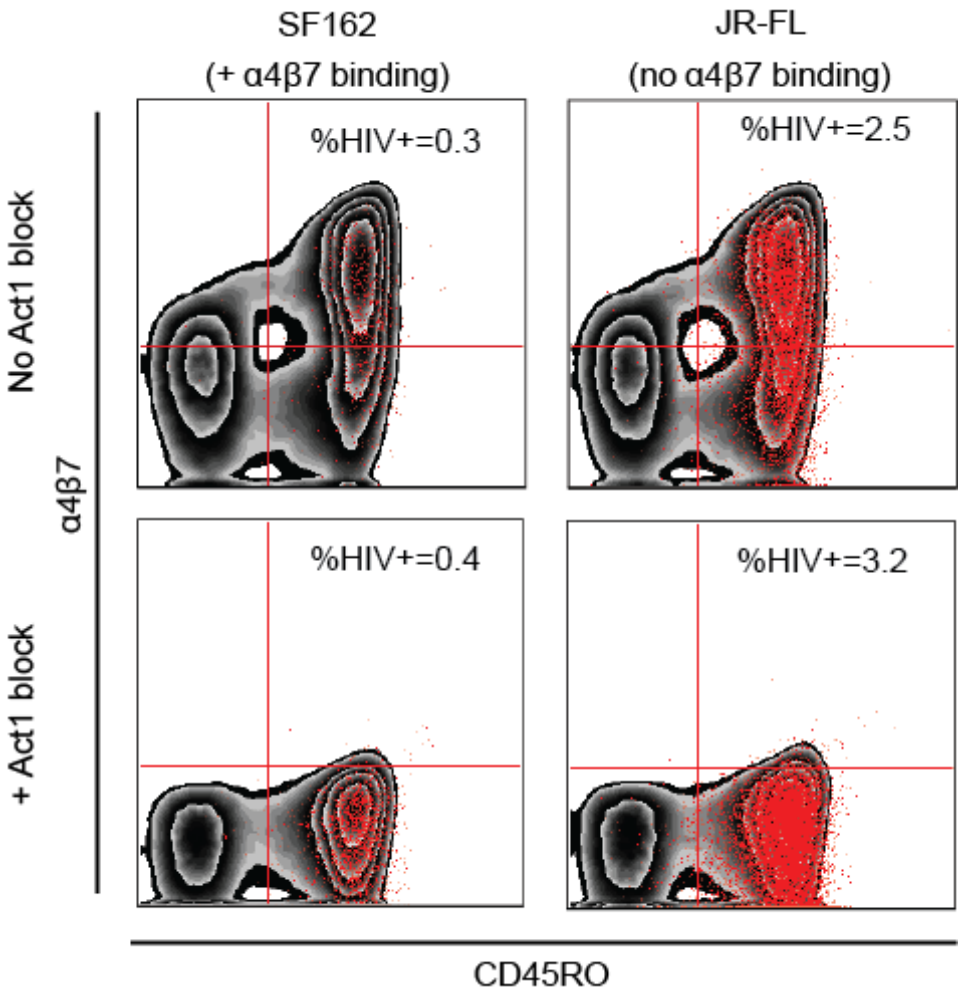

Figure 3-9. Blocking α4β7 enhances pseudovirus infection. Infection of primary CD4+ T cells by Env pseudoviruses is depicted in the presence and absence of Act1 to block α4β7. atRA-treated cells were infected with GFP-expressing pseudotypes containing SF162 and JR-FL Envs whose gp120 proteins do and do not bind α4β7, respectively, in the absence (top two panels) or presence of saturating amounts of the α4β7 specific mAb Act1 (bottom two panels). Infected cells were detected by GFP expression (red overlay). The presence of Act1 resulted in slightly increased infection levels of both pseudotypes. To confirm that saturating levels of Act1 were used, cells were stained with fluorescently labeled Act1 before analysis. The near absence of cells in the upper quadrants of the lower panels shows that binding of labeled Act1 antibody was blocked by unlabeled antibody added before virus infection.

Table 3-2. Description of T/F and CC infectious molecular clones (IMCs)

IMC type	Subject	IMC name	Country	Risk factor[a]	Sex	Viral load (RNA copies/ml)	Fiebig stage[b]	Env AA 179-181[c]	V1V2 PNGs[d]	Reference
T/F	704010042[e]	CH042	South Africa	HSX	M	181,000	IV	LDI	5	in prep[f]
	705010067	CH067	South Africa	HSX	F	639,000	I/II	PDI	5	in prep[f]
	705010162	CH162	South Africa	HSX	M	13,100,000	III	LDI	6	in prep[f]
	703010131	CH131s	Malawi	HSX/MSM	M	411,873	I/II	LDL	5	in prep[f]
	ZM246F[e]	ZM246F-10[e]	Zambia	HSX	F	10,013,800	II	LDI	3	312
	ZM249M[e]	ZM249M-1[e]	Zambia	HSX	M	>2,000,000	IV	LDI	6	312
Chronic	703010256	CH256	Malawi	HSX	F	28,066	n/a	LDV	7	this study
	702010432[e]	CH432[e]	Malawi	HSX	M	40,570	n/a	LDI	8	this study
	707010457[e]	CH457[e]	Tanzania	HSX	F	234,671	n/a	VDI	6	this study
	705010534[e]	CH534[e]	South Africa	HSX	F	63,300	n/a	LDI	5	this study

[a]HSX = heterosexual exposure; MSM = Men who have sex with men.

[b]defined in (112); n/a = not applicable for subjects enrolled in chronic cohorts.

[c]amino acid sequence of α4β7-binding tripeptide in V2 (positions 179-181 in HXB2).

[d]potential N-linked glycosylation sites in the V1V2 region (also see Figure 3-10).

[e]Env from subject also tested, see Table 3-1.

[f]Kappes et al., manuscript in preparation

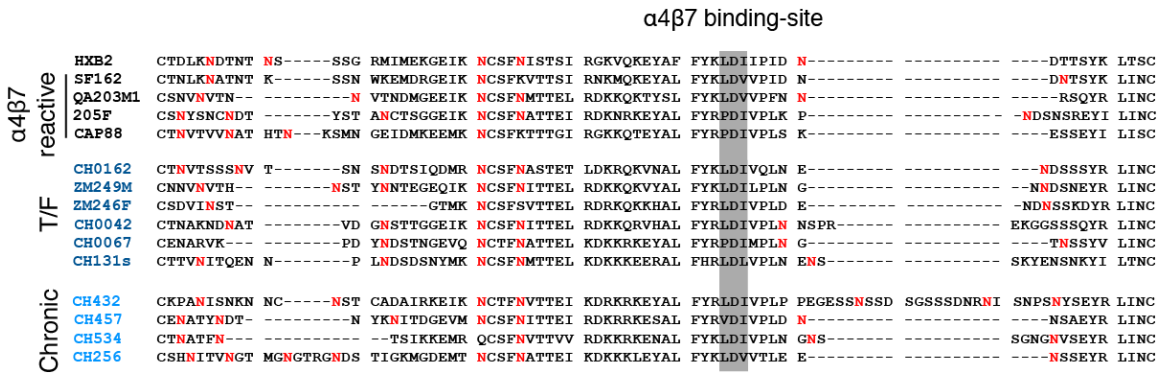

Figure 3-10. Alignment of V1V2 Env protein sequences. An alignment of the first and second variable regions of the HIV-1 Env glycoprotein (HXB2 gp120 residues 131-196) is shown for previously described α4β7-reactive gp120s as well as T/F (dark blue) and CC (light blue) IMCs. Asparagine residues predicted to be glycosylated are shown in red. The α4β7 binding-site (consensus LDV/I; HxB2 residues 179-181) is highlighted in grey. Gaps, shown as dashes, were introduced to optimize the alignment.

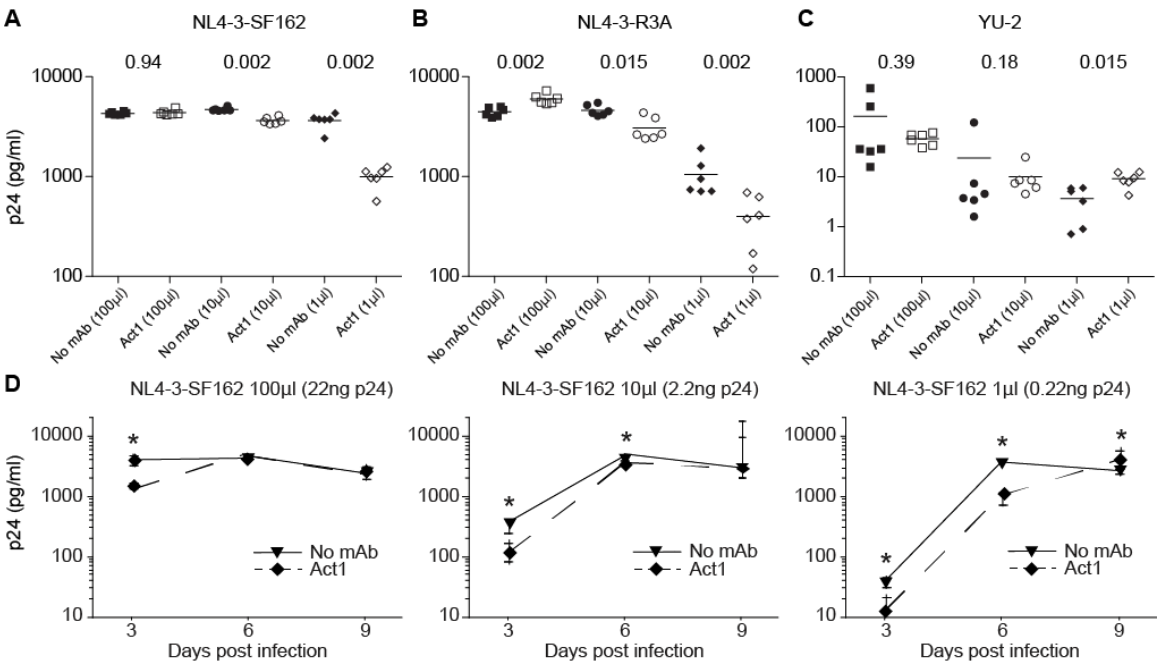

Figure 3-11. Blocking α4β7 inhibits replication of NL4-3-SF162 and NL4-3-R3A but not YU-2. CD4+ T cells with or without Act1 pre-treatment were infected at three different multiplicities using CD4+ T cell derived virus stock (1 µl, 10 µl and 100 µl) to initiate a spreading infection. Infections were performed in six replicate wells, each of which was sampled at days three, six and nine. (**A-C**) Virus production at day six as measured by p24 content in culture supernatants is shown on the y-axis for each of six replicate wells from one of three independent experiments; uncorrected Mann-Whitney *p* values are shown for comparisons of no antibody (solid symbols) versus Act1-treated (open symbols) replicate wells (bar = mean). (**D**) Replication kinetics are shown for NL4-3-SF162 (mean of replicates ± SEM is presented) at three different multiplicities of infection. Inhibition of infection was transient and greatest at six days post infection at the lowest viral input; uncorrected Mann-Whitney p-values less than 0.05 comparing no mAb to Act1 are marked by asterisks.

If mucosal transmission selects for viruses that interact with α4β7, we reasoned that the replication of T/F IMCs would be inhibited when the Env-α4β7 interaction was blocked. Our subtype C IMC infection assays were powered to detect a 30% or higher decrease in virus (p24 antigen) production on day six, a time point when the largest effect on virus growth following α4β7 blockade was observed in previous experiments (63). Two to four ELISA measurements were performed to monitor virus production in each of six replicate wells infected at different multiplicities using CD4+ T cells from three different donors. At the lowest virus inoculum, replication was undetectable in one to four of the six replicate wells from each of the ten subtype C viruses, indicating that virus was added at limiting dilution. Using Act1 at saturating concentrations, we observed no significant inhibition of replication of any subtype C virus (T/F or CC) at any viral inoculum or time point post-infection (Figure 3-12), while replication of the positive control SF162 was reduced. In addition to Act1, we tested the α4 integrin-specific mAb 2B4 using SF162 and three of the subtype C viruses in CD4+ T cells from two donors and obtained similar results: a modest and transient inhibition of SF162, but no inhibition of the other viruses (data not shown). Finally, we tested seven subtype B T/F IMCs (258) using cells from a single donor and again observed no inhibition using the anti-α4β7 mAb Act1 (data not shown). Taken together, these results indicate that blocking the integrin α4β7 does not reduce the replication of T/F and CC subtype C viruses in atRA-stimulated primary CD4+ T cells.

While Act1 failed to inhibit infection and/or replication by any of 13 T/F and four CC viruses, it significantly increased p24 production of five of the ten subtype C viruses (two of six T/F and three of four CC viruses; Figure 3-12). This was observed at multiple time points and with multiple viral inputs. To determine whether antibody binding to α4β7 could lead to enhanced cellular activation (26) and a resulting increase in virus production, we examined the expression of cellular activation markers. We found that neither Act1 nor 2B4 increased the expression of CD25, HLA-DR, Ki67, and CD69 at 1 hour, 2 days, and 5 days post-treatment, nor did these antibodies lead to an increase in CCR5 or α4β7 expression levels (Figure 3-13). However, we noted increased clumping of cells in both Act1 and 2B4 treated cultures (25),

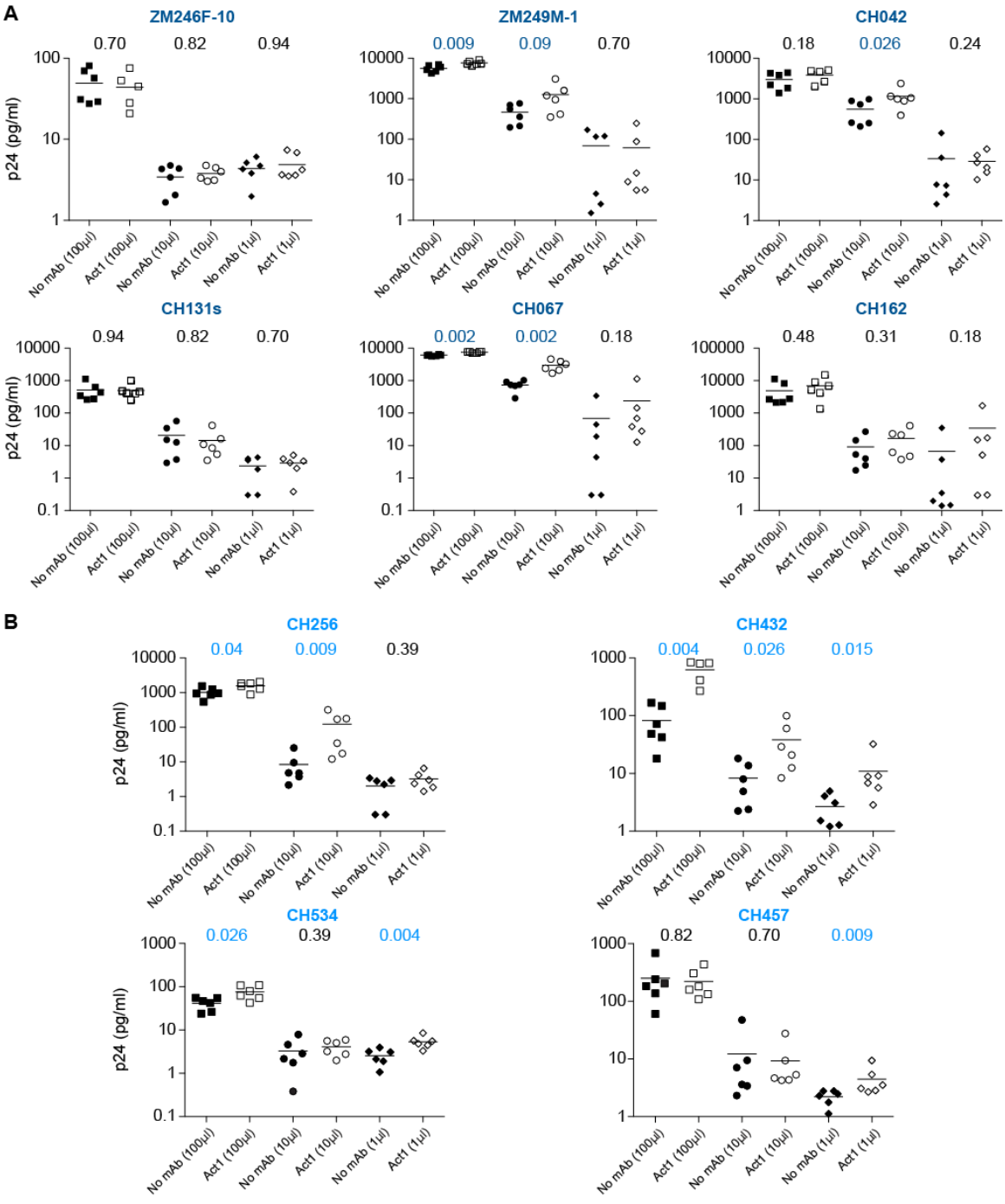

Figure 3-12. Blocking α4β7 does not inhibit replication of subtype C T/F and CC IMCs.

CD4+ T cells were infected at three different multiplicities using CD4+ T cell derived virus stock (1 µl, 10 µl and 100 µl). Virus replication was monitored by measuring p24 content in culture supernatants; each p24 measurement was repeated two to four times. The average p24 value in each of six independent wells at six days post-infection is plotted on the *y*-axis, with the bar

representing the mean p24 value. Uncorrected Mann-Whitney p-values comparing no mAb to Act1 pre-treatment are shown for each viral input. Blocking α4β7 with Act1 increased p24 production for some viruses (colored p-values), but had no reproducible inhibitory effect on any T/F (**A**) or CC (**B**) molecular clones tested, under conditions where reproducible inhibition of NL4-3-SF162 was achieved, as previously described (250).

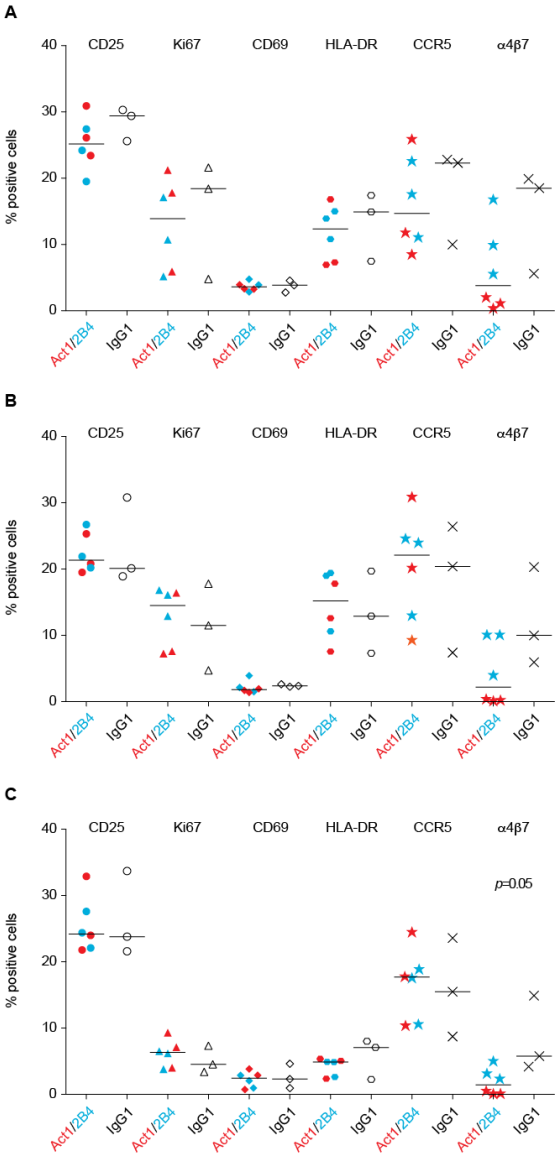

Figure 3-13. Act1 and 2B4 do not affect the activation profile of cells compared to a murine isotype control. Cells from three different donors were treated with Act1 (red) or 2B4 (blue) as well as a murine IgG1 control (open) for one hour (**A**), two days (**B**), or five days (**C**), and analyzed for markers of cellular activation, including CD25, HLA-DR, Ki67, and CD69. The expression of CCR5 and α4β7 was also measured. The percent of live CD4+ T cells expressing each marker is shown on the *y*-axis. No significant differences were observed comparing Act1 or 2B4 treated cells to IgG1, except for decreased α4β7 expression at day five, which reflects decreased detection due to blocking with unlabeled Act1.

which raised the possibility that the enhanced virus production seen in some Act1-treated cultures could be due to increased cell-to-cell viral spread. We thus used high-speed cell imaging to examine cell-cell conjugates in CD4+ T cell cultures from a single donor that were infected with SF162 as well as three subtype C viruses (2 T/F and 1 CC control) after treatment with Act1, 2B4 or a murine IgG1 isotype-control. Neither Act1 nor 2B4 increased expression of the high-affinity form of LFA-1, which is known to be upregulated by α4β7 engagement of gp120 (9). However, we noted a significant increase in the expression of the cell-cell adhesion molecule ICAM-1 in cells exposed to 2B4 or Act1 compared to murine IgG1 (Figure 3-14A). Consistent with increased cell-cell spread, more cell-cell conjugates were virus-positive than predicted, with doublets being more than twice as frequently infected as singlets ($p=0.04$) and triplets being more than three times as frequently infected as singlets ($p=0.06$) (Figure 3-14B). Overall, these results suggest that Act1- and 2B4-mediated increases in cell-cell conjugates could facilitate more efficient spread and replication of some viruses in the absence of increased cellular activation.

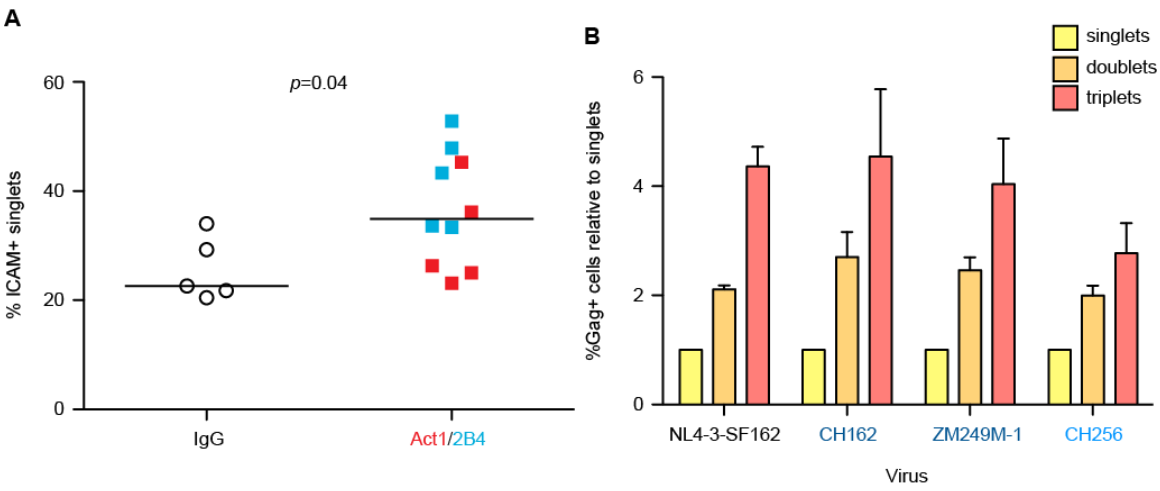

Figure 3-14. Cell-to-cell adhesion and infection analysis. High-speed imaging of single cells and cell aggregates was performed using an ImageStream IS100 cytometer. (**A**) Treatment with Act1 (red) or 2B4 (blue) increased the percent of singlet cells expressing the cell adhesion molecule ICAM-1 (y-axis) relative to a murine isotype (IgG, open) control (p=0.04; Mann-Whitney). Each point represents cells from the same donor infected with a different virus, or mock infected; the bar indicates the group median. (**B**) Cells were gated based on DNA content and size into individual cells (singlets), two cells in contact (doublets) and three cells in contact (triplets). The percent of singlets, doublets, and triplets infected after exposure to different viruses is shown on the y-axis. Cell infection was determined based on Gag (p24) antigen expression compared to mock-infected control. Cell conjugates contained more infected cells than expected by chance, suggesting enhanced cell-to-cell spread (doublets, p=0.04; triplets, p=0.06; two-sided paired T-test).

Discussion

The identification of viral traits that might enhance mucosal transmission is an important goal for vaccine development and other prevention strategies. A first step in characterizing such traits is the identification of T/F viruses, while a second step is the selection of appropriate controls. Virological traits that are strongly associated with transmission, such as CCR5 use, should be readily identifiable when comparing T/F viruses to virtually any CC group, while identifying more subtle phenotypes will greatly depend on the choice of CC viruses, perhaps explaining discrepancies in genetic and phenotypic transmission signatures identified by different groups (5, 59, 88, 104, 117, 126, 167, 309, 310). Finally, the use of *in vitro* assays that recapitulate key steps in mucosal transmission are needed to identify properties unique to T/F viruses. Here, we have compiled a relatively large panel of both Envs and IMCs representing subtype C T/F and CC viruses, and developed a series of infection assays using virus pseudotypes, replication competent viruses, cell lines and primary human CD4+ T cells to improve our ability to identify viral phenotypes associated with transmission.

Env glycoproteins of HIV-1 can differ significantly in the efficiencies with which they utilize CD4 and the viral coreceptors, which in turn can impact viral tropism (74, 95, 96, 274, 336). Given the variability in expression levels of entry cofactors on different cell subsets as well as between individuals (35, 133, 212), it is easy to envision several ways in which Env function could impact transmission efficiency at the level of virus entry. To date, several genetic Env signatures have been reported, with more compact variable loop structures and fewer PNGs being the most frequent findings (59, 117, 126, 309, 310). It is possible that these genetic traits impact Env function in ways that increase transmission fitness. However, to date no consistent T/F phenotype has been described. Thus, it is possible that mucosal transmission is a stochastic event where any reasonably functional R5 or dual tropic Env can initiate a productive infection (152). However, it is also possible that the *in vitro* assays employed thus far have failed to reveal subtler or more transmission-specific phenotypic differences. The recent finding that some gp120 proteins from early HIV-1 infections can bind to the α4β7 integrin is consistent with this, although the ability of T/F viruses to productively interact with α4β7 was not explored.

To determine whether subtype C T/F viruses, which account for the great majority of new infections worldwide, utilize CD4 or CCR5 with enhanced efficiency, we tested both T/F and CC Env constructs in pseudotyping assays. Consistent with previous results for subtype B (372) and subtype C (5), we failed to observe differences in both CCR5 and CD4 utilization. This is in contrast to findings by Etemad and colleagues who reported enhanced CCR5 utilization by Envs from individuals with chronic subtype A infection, although only V1-V5 fragments were tested in the context of chimeric viruses (104). Similarly, Nawaz and colleagues found that gp120s from three subjects acutely infected with subtype A and C viruses bound to dodecameric but not monomeric CD4, while gp120s from subsequent time points of two of the same subjects bound to CD4 in both forms, suggesting an increase in CD4 affinity in later stages of infection (250). These results may be specific to the particular Envs (250) or Env fragments (104) used, or due to the fact that gp120 and particle-associated Env trimers bind CD4 differently. In either case, current data utilizing a large number of Env constructs strongly suggests that the mucosal bottleneck is not the result of selective transmission of viruses with highly efficient CD4 or CCR5 use (5, 167, 372), or with increased efficiency of entry into particular CD4+ T cells subsets (372).

We also examined whether subtype C T/F and CC Envs differed in their interaction with the gut homing integrin α4β7 as recently proposed (250), although previous data are almost entirely based on gp120 binding studies. In many ways, the α4β7 hypothesis is an attractive one. This integrin is expressed at high levels on activated CD4+ T cells in the gut (107) and cervicovaginal mucosa (223), both representing major sites of HIV replication early in infection (41, 158). Moreover, intravenous administration of an anti-α4β7 mAb in rhesus macaques prior to and during acute infection with SIVmac239 resulted in decreased virus loads, perhaps by inhibiting trafficking of α4β7-positive T cells to the GI tract (7). Finally, gp120-induced α4β7 signaling could promote virus replication through increased cell-to-cell adhesion. However, the ability of HIV-1 gp120 to bind α4β7 is far from universal - the commonly studied subtype B gp120s examined to date either do not bind to α4β7 or do so weakly, with the exception of SF162 (250). Nonetheless, several gp120 proteins derived from early subtype A or subtype C infections have been shown to exhibit α4β7 binding capacity, and there is an obvious link between some

α4β7 binding properties (fewer PNGs in the V1-V4 region) and genotypes associated with virus transmission in subtype C viruses (59, 88, 250). While monomeric gp120 binds CD4, viral coreceptors and most broadly neutralizing antibodies, it differs from virion-associated Env trimers in important ways. Perhaps the best example is that numerous antibodies that bind to gp120 fail to neutralize the cognate Env trimer, consistent with both conformational differences and the fact that certain gp120 domains are sequestered in the oligomeric molecule. Thus, a key question that remains relatively unexplored is whether α4β7 binding by gp120 translates into an interaction by trimeric Env that influences virus infection and spread. To address this question, we concentrated on virus infection assays rather than gp120 binding experiments.

In our attempts to define the role of α4β7 in HIV-1 transmission, we were able to replicate a previous key finding, namely that saturating levels of antibodies to α4β7 modestly suppressed infection and replication by the prototypic subtype B strain HIV-1/SF162 (9, 63). The inhibitory effects of α4β7 antibodies on SF162 infection were both transitory and most evident when low levels of virus input were used, which is precisely what would be expected if α4β7 functioned as an attachment factor (63, 250). Attachment of virus particles to the host cell surface is a significant rate-limiting step to virus infection *in vitro*, but can be overcome in part by spinoculation (256), the inclusion of polycations that enhance viral binding (57), or the expression of virus attachment factors such as CD209 or CD209R (279, 281). In the case of attachment factors, their ability to enhance infection is most pronounced when low levels of virus are used. Thus, our finding of a partial inhibition of SF162 replication in α4β7-positive T cells six days post infection at the lowest virus input is entirely consistent with previous reports and shows that our assays are sufficiently sensitive to measure the impact of α4β7 blockade on virus infection. Despite this, we found no inhibition of any T/F or CC subtype B or C virus using cells from multiple donors and levels of virus empirically determined to be barely sufficient to establish a spreading infection. These findings are consistent with those of Pauls and colleagues, who found that a mAb to $\alpha 4$ used for the treatment of multiple sclerosis and Crohn's disease did not impact infection of atRA-treated CD4+ T cells by several HIV-1 strains, including two with the LDI/V tripeptide binding motif in the V2 region (272). Since most of our T/F and CC viruses possessed the α4β7-binding

tripeptide motif as well as below average numbers of PNGs in the V1/V2 region, selection bias - i.e. the preferential inclusion of viruses that would be unlikely to interact with α4β7 - can also be excluded. Thus, we favor the hypothesis that not all Envs that can bind α4β7 in the form of gp120 necessarily do so as unliganded trimers.

Our failure to detect enhancement of viral infection of human CD4+ T cells by primary subtype B or C viruses, including T/F viruses, due to α4β7 interaction is by no means definitive, but does suggest that extrapolating results from gp120 binding assays to more complex virion infectivity studies may be misleading. It is possible that α4β7 interactions will be more important in other types of infection assays. In addition, we have not tested the ability of gp120 proteins derived from our viruses to bind to α4β7, although the relevance of such findings remains uncertain unless the corresponding trimeric Env exhibits similar properties. Our results demonstrate the importance of using replication-competent viruses to study properties associated with mucosal transmission. In contrast to single-round pseudovirus assays, experiments with IMCs are unbiased with respect to the genes that could influence fitness and enable detection of subtle differences following multiple rounds of replication. Thus, T/F and CC IMCs are ideal reagents for future studies of phenotypes that may influence HIV-1 transmission.

Materials and Methods

Study subjects. This study was conducted according to the principles expressed in the Declaration of Helsinki. It was approved by the Institutional Review Boards of the University of Pennsylvania and Duke University. All subjects provided written informed consent for the collection of samples and subsequent analysis. Blood samples were obtained from 26 subjects infected with HIV-1 subtype C. A summary of their geographic origin and infection status is shown in Table 1. Blood specimens were collected in acid citrate dextrose, and plasma was separated and stored at −70°C.

Generation of T/F and CC Envs and IMCs. The inference and cloning of T/F Envs and IMCs from SGA-derived viral sequences has been described (Figure S1) (3, 176, 204, 258, 313). To ensure efficient expression of cloned subtype C Envs for pseudotyping, the sense primer used for amplification of the corresponding *rev1-vpu-env* cassette lacked the *rev* initiation codon (underlined) (5'-*CACC*GGCTTAGGCATCTCCTATAGCAGGAAGAA-3') (191).

Since chronic HIV-1 infections represent complex quasispecies of genetic variants, it is impossible to predict, based on sequence analysis alone, which members of this quasispecies are functional and which are defective or partially defective. To generate biologically relevant CCs, we thus targeted viral variants for both Env and IMC construction that exhibited evidence of a recent clonal expansion. Viral RNA was extracted from the plasma of chronically infected individuals and subjected to SGA and direct amplicon sequencing as described (3, 204), with the following modifications: 5′ half genome amplification: 1st round sense primer 2010ForRC 5′-GTCTCTCTAGGTRGACCAGAT -3′, 1st round antisense primer 2010Rev1C 5′-AAGCAGTTTTAGGYTGRCTTCCTGGATG -3′, 2nd round sense primer 2010R1C 5′-TAGGTRGACCAGATYWGAGCC -3′ and 2nd round antisense primer 2010Rev2C 5′-CTTCTTCCTGCCATAGGAAAT -3′; 3′ half genome: 1st round sense primer 07For7 5′-CAAATTAYAAAAATTCAAAATTTTCGGGTTTATTACAG -3′, 1st round antisense primer 2.R3.B6R 5′- TGAAGCACTCAAGGCAAGCTTTATTGAGGC-3′, 2nd round sense primer VIF1 5′-GGGTTTATTACAGGGACAGCAGAG -3′ and 2nd round antisense primer Low2C 5′-

TGAGGCTTAAGCAGTGGGTTCC -3′. Thermal cycling conditions were identical to (204) except that 60°C was used for primer annealing. Sequences were then aligned using ClustalW (349) and subjected to phylogenetic analysis using PhyML (140). Phylogenetic trees were inspected for clusters of closely related viruses, or "rakes", which are indicative of a recent clonal expansion. (Figures 1, S2 and S3). In five subjects (Table 1), at least one *env* amplicon was identical in sequence to the inferred "rake" consensus and thus selected for cloning using the pcDNA3.1 Directional Topo Expression kit (Invitrogen). In two subjects, observable "rakes" were limited to only two closely related *s*equences, which encoded Env proteins that differed by a single amino acid. In these cases, the amplicon that matched the within patient consensus at this ambiguous site was cloned. In the remaining six subjects, the consensus sequences of the clonal expansion "rakes" were chemically synthesized and cloned (designated .synR1 in Table 3-1). IMCs from chronically infected subjects (CH256, CH432, CH457, and CH534) were generated using the same approach. 3' and 5' half-genome SGA was performed using viral RNA from subjects with evidence of clonal expansion as determined by *env* sequencing. 3' and 5' half genome sequences were used to construct neighbor joining trees (Figure 3-4), and clusters of closely related sequences were selected for further analysis. A consensus sequence of the members of such "rakes" was generated using Consensus Maker (hiv.lanl.gov). 3' and 5' half genome sequences were confirmed to be identical in their 1,040 bp overlapping regions, chemically synthesized in fragments bordered by unique restriction enzymes, and ligated together to construct infectious proviral clones.

Pseudovirus production. Virus pseudotypes were produced by co-transfecting 6 μg of pcDNA3.1^{+} containing the desired *env* clone with 10 μg of HIV-1 backbone (pNL43-ΔEnv-vpr^{+}-luc^{+} or pNL43-ΔEnv-vpr^{+}-eGFP (catalog no. 11100 from the NIH Aids Research and Reference Reagent program (ARRRP) contributed by Haili Zhang, Yan Zhou, and Robert Siliciano (391)) into 293T cells using the calcium phosphate precipitation method. 72 h post-transfection, the pseudovirus-containing supernatant was filtered through a 22 μm filter, aliquoted, and stored at −80°C. Pseudovirus used to infect primary CD4+ T cells was concentrated by ultracentrifugation

through a 20% sucrose cushion. Pelleted pseudovirus was then resuspended in phosphate-buffered saline (PBS) in 1/100th the initial volume. All luciferase-encoding pseudoviral stocks were serially two-fold diluted and used to infect NP2 cells to define the linear range of the assay.

Coreceptor tropism testing and cell line infections. NP2 cells stably expressing CD4 and either CCR5 (NP2/CD4/CCR5) or CXCR4 (NP2/CD4/CXCR4) were infected with luciferase-encoding HIV-1 pseudoviruses by spinoculation in 96-well plates at 450 × g for 90 min at 25°C. Cells were lysed with Brite-Glo (Promega) at 2 h post-infection and analyzed on a Luminoskan Ascent luminometer. To assess sensitivity to coreceptor inhibitor maraviroc, NP2/CD4/CCR5 cells were preincubated for 30 min with saturating concentrations of the CCR5 inhibitor maraviroc (1 μM; ARRRP catalog no. 11580; (103)) or the fusion inhibitor enfuvirtide (10 μg/ml) prior to infection. To assess sensitivity to broadly neutralizing mAbs (HIV-1 gp120 mAb IgG1 b12 (ARRRP catalog no. 2640) from Dennis Burton and Carlos Barbas (47); HIV-1 gp120 mAb VRC01 (ARRRP catalog no. 12033) from Dr. John Mascola (379); HIV-1 mAbs PG9 and PG16 (ARRP catalog no. 12149 and 12150) from IAVI (363)), viral pseudotypes were preincubated with 10 μg/ml of antibody for 1 hour at 37°C. Virus and antibody mixes were then used to infect NP2/CD4/CCR5 cells. All NP2 cell line infections were done in at least triplicate in at least three independent experiments using R5-tropic JR-FL as a positive control and Env-deficient pseudotypes as a negative control.

CD4 utilization efficiency. The ability of Env pseudoviruses to infect cells expressing low levels of CD4 was determined using affinofile cells, which are a modified 293T cell line that stably express CD4 and CCR5 under the control of independently inducible promoters (172). $5x10^2$ cells were plated in each well of a 96-well plate and allowed to grow for two days prior to infection. Cells were induced with 2 μM ponasterone, which induces supraphysiologic levels of CCR5 thus ensuring CD4 is the limiting factor in entry, and either 0.156 ng/ml (CD4-low) or 5 ng/ml (CD4-high) minocycline 18 hours prior to infection. Expression levels were monitored by quantitative FACS analysis (200). At the time of infection, media was exchanged and 25 μl of

luciferase-encoding pseudovirus was added. Cells were then spinoculated at 450g for 90 minutes. Luciferase activity was measured three days post-infection. Each infection condition was done in at least triplicate in each of three independent experiments. Pseudovirus-containing vesicular stomatitis virus glycoprotein (VSV-G) which is CD4-independent and thus infects CD4-high and CD4-low cells equally, HIV-1 JR-CSF Env which requires high levels of CD4, and HIV-1 JR-FL Env which can utilize low levels of CD4 were included in all experiments as controls (322). To calculate CD4-use efficiency, mean relative light units in CD4-low cells were divided by the value obtained in CD4-high cells. The signal-to-noise ratio was higher in affinofile cells than NP2/CD4/CCR5 cells. Nine Envs (5 T/F, 4 CC) infected maximally-CD4-induced afffinofile cells less than 100-fold above background. For these Envs, we noted increased variability across independent assays. Additionally, the ratio of CD4-high to CD4-low infection was likely falsely elevated due to infection of CD4-low cells at background levels. These Envs are highlighted in Figure 2 and were excluded from subsequent analyses.

Maraviroc IC_{50}. Maraviroc IC_{50} values were determined by pretreating NP2/CD4/CCR5 cells with 11 serial 3-fold dilutions of maraviroc, ranging from 5.9 μM to 0.1 nM, or no drug then spinoculating as above with luciferase-encoding pseudovirus and measuring luminescence 72h post-infection. NP2 cells were chosen for this experiment because in the absence of CCR5 (NP2/CD4 only) these cells are highly restrictive to infection (339); thus entry through potential alternative coreceptors when CCR5 is blocked by maraviroc is negligible. IC_{50} was determined using Prism 4.0 to determine the best fitting non-linear curve. Reported IC_{50} values are the mean of four independent experiments, with each drug concentration/pseudovirus condition performed in duplicate.

Primary human CD4+ T cell tropism assay. Primary human CD4+ T cells were purified by negative selection by the University of Pennsylvania's Human Immunology Core. Cells were stimulated with plate-bound anti-CD3 (clone OKT3) (eBiosciences) and anti-CD28 (clone 28.2) (BD Biosciences) and 20 U/ml recombinant interleukin-2 (IL-2) (aldesleukin, Prometheus Laboratories) in RPMI supplemented with 10% fetal bovine serum (FBS, Sigma-Aldrich). Three

days after stimulation, cells were transferred to 96-well V-bottom plates. Five microliters of concentrated GFP-expressing pseudovirus was used to infect 6.7 × 10^5 cells in triplicate by spinoculating at 1,200 × *g* for 2 hours. Cells were then transferred to new 24-well plates, and new medium containing 20 U/ml IL-2 was added. Three days post-infection, cells were stained for flow cytometry (350, 372).

Flow cytometry. A total of 1-2 × 10^6 cells from each condition were stained for flow cytometry. Incubations were done at room temperature in fluorescence-activated cell sorter (FACS) wash buffer (PBS, 2.5% FBS, 2 mM EDTA). Cells were first washed in PBS, then live/dead Aqua (Invitrogen) was added and incubated for 10 min. Next, anti-CCR7 IgM (BD) in FACS wash buffer was added and incubated for 30 min. Cells were then washed in FACS wash buffer before staining with anti-CD3–Qdot 655 (Invitrogen), anti-CD4–Alexa Fluor 700 (BD), anti-CD45RO–phycoerythrin (PE)-Texas Red (Beckman Coulter), and anti-IgM–PE (Invitrogen) for 30 min. Cells were then washed in FACS wash buffer and resuspended in 1% paraformaldehyde (PFA). Samples were run on an LSRII (BD) instrument and analyzed with FlowJo 8.8.6 (Treestar). Cells were gated as follows: singlets (FSC-A by FSC-H), then live cells (SSC-A by live/dead), then lymphocytes (SSC-A by FSC-A), then $CD3^+$ cells (SSC-A by CD3), then memory markers (CCR7 by CD45RO).

To examine activation of cells treated with Act1, 2B4, isotype control murine IgG1, or no antibody, cells were pretreated with 33nm of the specified antibody for 1 hour, 2 days, or 5 days. At each time point, 1 × 10^6 cells were washed in PBS, then live/dead Aqua was added for 10 minutes. Anti-CCR5-PE (BD), anti-CD4-PerCP-Cy5.5, anti-CD25-APC-Cy7, anti-HLA-DR-PE-Cy7, anti-α4β7-Alexa Fluor 680 (clone Act1) and anti-CD45RO-TexasRed-PE were added in FACS wash buffer for 30 minutes. Cells were then washed in FACS wash buffer and treated with cytofix/cytoperm buffer (BD) for 17 minutes. Anti-CD3-V450, anti-CD69-APC, and anti-Ki67-FITC in perm/wash buffer were added and incubated for 1 hour at room temperature. Cells were washed in perm/wash buffer, fixed in 0.1% paraformaldehyde, run on an LSRII instrument and

data was analyzed with FlowJo. Live cells expressing CD3 and CD4 were analyzed for expression of activation markers.

Production of HIV in primary CD4+ T cells. Replication competent viral stocks were generated by transfecting a 10cm dish 30% confluent with 293T cells with 6 μg of IMC DNA. Virus was harvested 72 hours post-transfection and filtered through a 45 micron low protein binding filter. 293T-derived HIV was then used to infect stimulated human CD4+ T cells. 18 hours after infection cells were washed twice to remove unbound 293T-derived virus. CD4+ T cell derived HIV was then harvested 11 days post infection, filtered through a 45 micron filter, aliquoted and frozen at -80°C. p24 antigen concentration of viral stocks was assessed by Alliance ELISA and high sensitivity alphaLISA (Perkin Elmer); these methods were in good agreement for all IMCs tested.

Infection assay to assess effect of α4β7 blockade. Freshly isolated human CD4+ T cells purified by negative selection were stimulated with 1.5μg/ml anti-CD3 clone OKT3, 20 units/ml IL-2, and 10 nM atRA. atRA was resuspended in DMSO, filter sterilized, aliquoted in the dark, and immediately frozen at -80°C for no longer than one month. 24 hours after stimulation, media was removed, and new media with IL-2 and atRA was added. Media was changed and new IL-2 and atRA were added every two to three days. Efforts were made to precisely follow previously reported methods (9, 63). Cells were infected six days post-stimulation for both pseudotype and replication competent HIV infection. Cells were pre-treated for 1 hour with 33 nM Act1 (an α4β7 heterodimer specific mAb; ARRRP catalog no. 11718 from Dr. A. A. Ansari (198)) at 37°C prior to infection. α4β7 expression and saturating mAb blockade was confirmed on the day of infection by flow cytometry. α4β7 expression was determined with Alexa Fluor 680-conjugated Act1 (Invitrogen). GFP-expressing pseudotype infections were performed as described above. SF162 and JR-FL pseudovirions were used as positive and negative controls, respectively (250). For infections with replication competent HIV, virus made in CD4+ T cells was used to limit potentially non-physiologic properties of 293T-derived HIV. $2x10^5$ stimulated atRA-treated CD4+ T cells were plated in 100 μl per well of a 96-well plate. After incubation with Act1

or media only, 100 μl of CD4+ T cell-derived virus was added at a neat, 1:10, or 1:100 dilution. Cells were infected for five hours at 37°C without spinoculation and then cells were washed four times to remove unbound HIV. Three, six, and nine days post-infection, media was changed and p24 antigen concentration was assessed in the supernatant using an alphaLISA high sensitivity kit (Perkin Elmer) read on a Synergy H4 plate reader (BioTek instruments). Either four or six replicate wells were used per condition, and each alphaLISA measurement was performed 2-4 times. AlphaLISA assays were performed in 25 μl volume in 384 well plates. Each plate contained an internal standard curve ranging four orders of magnitude with each standard concentration repeated in eight wells. The lower limit of detection for most assays ranged between 3 and 10 pg p24 per mL.

High-speed cell imaging. Purified CD4+ T cells were treated with atRA, anti-CD3, and IL-2, and infected as described for α4β7 blocking experiments. Nine days post infection, cells exposed to 10 μl of NL4-3-SF162, ZM249, CH162, CH256, and mock infected were pooled from six replicate wells, washed in PBS and then FACS wash buffer. Anti-CCR5-PE-Cy7, anti-CD54 (ICAM-1)-PE-Cy5, anti-LFA-1-PE (clone MEM-148), and anti-α4β7-Alexa Fluor 680 (clone Act1) were added in FACS wash buffer and allowed to incubate for 30 minutes. Cells were then washed in FACS wash buffer and treated with cytofix/cytoperm buffer for 17 minutes. Anti-Gag-FITC (clone KC-57) was added for 1 hour. Cells were fixed in 1% paraformaldehyde and DAPI was added 30 minutes prior to analysis. Samples were run on an ImageStream IS100 equipped with two cameras and 405, 488, and 658 nm excitation lasers. At least 20,000 images were collected per condition, and the upper limit of images classified as cells was set to 600 pixels to allow collection of cell-cell conjugates. Cells were gated as follows: singlets, doublets, and triplets (DAPI by brightfield area), then Gag+ (Gag intensity by Gag median pixel). Gag positivity was gated such that the percent of mock-infected Gag+ cells was equal in singlet, doublet, and triplet populations. A single Gag-expressing cell was sufficient for a doublet or triplet image to be considered Gag+, as confirmed by visual inspection of Gag+ images. LFA-1 and ICAM-1

expression were analyzed on nucleated (DAPI+), focused (brightfield gradient root mean square-high), singlets (brightfield aspect ratio ~1) to ensure that all analyzed images were of high quality.

Statistical analysis. To test the hypothesis that T/F Envs as a group were different from CC Envs in various functional measures, we used two-tailed Mann-Whitney tests. To test the hypothesis that Act1 treatment inhibited viral replication in CD4+ T cells, we again used two-tailed Mann-Whitney tests comparing the six biological replicates with and without Act1 treatment for each virus. No attempts were made to correct for multiple testing, largely because Act1 treatment did not have the expected effect on T/F viruses. Because six values from each group were compared, the minimum uncorrected *p*-value was 0.002. Applying the conservative Bonferroni correction would render all comparisons insignificant (α level of 0.05 divided by 39 tests = 0.001). Thus, we conclude that Act1 inhibits or enhances only when multiple input levels of the same virus show a consistent effect. To determine if cell-cell conjugates were infected more than expected by chance, the percent of Gag+ doublets was compared in a paired *t*-test to double the percent Gag+ singlets, and the percent of Gag+ triplets was compared to triple the percent Gag+ singlets.

Nucleotide accession numbers. All newly obtained HIV-1 sequences have been submitted to GenBank and are available under accession numbers listed in Table 3-3.

Table 3-3. GenBank accession numbers of sequences generated for this study

Infection stage	Subject	*env* clone accession numbers	*env* SGA accession numbers	5' half accession numbers	3' half accession numbers
Acute	20258279	HQ595763 and HQ595764 (env)	JQ753730-JQ753770	n/a	n/a
	2833264	HQ595757 (env)	JQ754177-JQ754189	n/a	n/a
	21197826	HQ595753 (env)	JQ754190-JQ754202	n/a	n/a
	21283649	HQ595756 (env)	JQ754203-JQ754229	n/a	n/a
	20927783	HQ595750 (env)	JQ754230-JQ754240	n/a	n/a
	1245045	HQ595742 (env)	JQ754241-JQ754250	n/a	n/a
	19157834	HQ595743 (env)	JQ754251-JQ754286	n/a	n/a
	2935054	HQ595758 (env)	JQ754287-JQ754304	n/a	n/a
Chronic	704010330	JQ777128 (env)	JQ777111-JQ777136	n/a	n/a
	704010207	JQ777073 (env)	JQ777061-JQ777086	n/a	n/a
	702010141	702010141.synR1[a] (env)	JQ779286-JQ779324	n/a	n/a
	703010180	JQ777046 (env)	JQ777046-JQ777060	n/a	n/a
	703010167	703010167.synR1[a] (env)	JQ779884-JQ779913	n/a	n/a
	704010499	JQ777164 (env)	JQ777144-JQ777164	n/a	n/a
	704010461	JQ777137 (env)	JQ777137-JQ777143	n/a	n/a
	704010028	JQ777039 (env)	JQ777026-JQ777045	n/a	n/a
	703010269	703010269.synR1[a] (env)	JQ777165-JQ777194	n/a	n/a
	704010273	JQ777098 (env)	JQ777087-JQ777110	n/a	n/a
	707010457	707010457.synR1[a] (*env*); CH457[a] (IMC)	n/a	JQ779148-JQ779169	JQ779128-JQ779147
	705010534	705010534.synR1[a] (*env*); CH534[a] (IMC)	n/a	JQ779206-JQ779225	JQ779170-JQ779205
	702010432	702010432.synR1[a] (*env*); CH432[a] (IMC)	n/a	JQ779256-JQ779285	JQ779226-JQ779255
	703010256	CH256[a] (IMC)	n/a	JQ779098-JQ779127	JQ779074-JQ779097

[a]chemically synthesized sequences available in Table S1 of online version of this manuscript (doi:10.1371/journal.ppat.1002686).

Acknowledgements

We thank James Arthos for the replication competent NL4-3-SF162 clone as well as technical advice and unpublished data regarding HIV-1 gp120 and α4β7 interactions. We also thank the University of Pennsylvania's Center for AIDS Research (CFAR) human immunology, flow cytometry, and viral and molecular core facilities for reagents and protocols, Susan Ellenberg and Liyi Cen for statistical consultation, Jay Gardner for antibody conjugation, Elizabeth Henning for pseudovirus production, Jamie White and Patricia Crystal for manuscript preparation, and Tony Fauci for helpful discussions.

CHAPTER 4

Primary Infection by a Human Immunodeficiency Virus with Atypical Coreceptor Tropism

Nicholas F. Parrish[1,2#], Chunlai Jiang[3,4#@] Craig B. Wilen[2#], Hui Li[1,2#], Yue Chen[3,4#], Jeffrey W. Pavlicek[3,4], Anna Berg[3,4], Xiaozhi Lu[3,4], Hongshuo Song[3,4], John C. Tilton[5], Jennifer M. Pfaff[2], Elizabeth A. Henning[2], Julie M. Decker[6], M. Anthony Moody[3,7], Mark S. Drinker[4], Robert Schutte[3,4], Stephanie Freel[3,4], Georgia D. Tomaras[3,4,8,9], Rebecca Nedellec[10], Donald E Mosier[10], Barton F. Haynes[3,4,9], George M. Shaw[1,2], Beatrice H. Hahn[1,2], Robert W. Doms[2*] and Feng Gao[3,4]

Departments of [1]Medicine and [2]Microbiology, Perlman School of Medicine at the University of Pennsylvania, Philadelphia, PA 19104, [3]Duke Human Vaccine Institute and [4]Department of Medicine, Duke University Medical Center, Durham, NC 27710, [5]Department of General Medical Sciences, Center for Proteomics, Case Western Reserve University School of Medicine, Cleveland, OH 44106, [6]University of Alabama at Birmingham, Birmingham, AL 35294, Departments of [7]Pediatrics, [8]Surgery, [9]Immunology and Duke University Medical Center, Durham, NC 27710, and [10]Department of Immunology & Microbial Science, The Scripps Research Institute, La Jolla, CA 92037, USA.

[@]Current address: National Engineering Laboratory of AIDS Vaccine, School of Life Science, Jilin University, Changchun, Jilin, 130012, P. R. China

#These authors contributed equally.

Originally published in Journal of Virology 85(20):10669-81. Published online ahead of print August 10, 2011.

Abstract

The great majority of human immunodeficiency virus type 1 (HIV-1) strains enter CD4+ target cells by interacting with one of two coreceptors, CCR5 and CXCR4. Here we describe a transmitted/founder (T/F) virus (ZP6248) that was profoundly impaired in its ability to utilize CCR5 and CXCR4 coreceptors on multiple CD4+ cell lines as well as primary human CD4+ T cells and macrophages *in vitro,* yet replicated to very high titers (>80 million RNA copies/ml) in an acutely infected individual. Interestingly, the envelope (Env) glycoprotein of this subtype B virus had a rare GPEK sequence in the crown of its third variable loop (V3) rather than the consensus GPGR sequence. Extensive sequencing of sequential plasma samples showed that the GPEK sequence was present in virtually all Envs, including those from the earliest time points after infection. The molecularly cloned T/F virus was able to replicate, albeit poorly, in cells obtained from *ccr5Δ32* homozygous donors. The ZP6248 T/F virus could also infect cell lines overexpressing the alternative coreceptors GPR15, APJ and FPRL-1. A single mutation in the V3 crown sequence (GPEK->GPGK) of ZP6248 restored its infectivity in CCR5+ cells but reduced its ability to replicate in GPR15+ cells, indicating that the V3 crown motif played an important role in usage of this alternative coreceptor. These results suggest that the ZP6248 T/F virus established acute infection *in vivo* by using coreceptor(s) other than CCR5 or CXCR4, or that the CCR5 coreceptor existed in an unusual conformation in this individual.

Introduction

Human immunodeficiency virus type I (HIV-1) enters target cells by first binding to the primary receptor CD4 and then to a coreceptor, generally either the chemokine receptors CCR5 or CXCR4 (28). CD4 binding induces structural changes in the envelope (Env) glycoprotein that form and expose the coreceptor binding site. There are two main interactions between Env and coreceptor (77, 78, 164, 300, 301): the base of the third variable loop (V3) loop engages the N-terminus of the coreceptor, while the crown of the V3 loop that includes the highly conserved GPGR/Q arch motif binds to the extracellular loops of the coreceptor, with the second extracellular loop of the coreceptor being particularly important (94, 164, 194, 291, 354). Although some HIV-1 strains are able to use a variety of different G protein-coupled receptors to gain entry into CD4+ cell lines, the great majority of these viruses use CCR5 and/or CXCR4 as coreceptors to infect primary cells (27, 28, 65, 128, 280, 381). CCR3, GPR15, APJ, and FPRL-1 are among the most frequently used alternative coreceptors when over-expressed on cell lines (66, 167, 251, 280, 335). Rare cases of HIV-1 strains that are able to use FPRL-1 and GPR1, but not CCR5 or CXCR4, have been reported (335).

To characterize the biological processes underlying HIV/SIV transmission, we recently developed an experimental strategy that permits the identification, enumeration and molecular cloning of transmitted/founder (T/F) viruses (176, 312). This strategy, which employs single genome amplification (SGA) and direct amplicon sequencing of HIV/SIV RNA or DNA from the plasma or infected cells, makes it possible to infer the nucleotide sequence of the viral strain(s) that initiated productive infection weeks earlier (3, 176, 177, 201, 312, 346, 384). An important prediction of this approach has been that inferred T/F viruses are fully functional and encode all proteins necessary to establish a new infection. Indeed, this prediction has been borne out in numerous studies, which have shown that T/F viral genes as well as full-length genomes are biologically active. Sets of T/F Envs have been shown to mediate efficient virus entry in single round infection assays, and they invariably use CCR5 as a coreceptor (176, 191). Similarly, T/F infectious molecular clones (IMCs) of HIV-1, SIVmac and SIVagm all produce replication

competent virus that grow to high titers in primary CD4+ T cells (125, 204, 313).

To generate a comprehensive panel of T/F Env constructs for biological studies, we recently characterized more than 100 plasma samples from acute infection cases, including commercially available seroconversion panels of serial plasma donors (176). Sequences spanning the *rev-vpu-env* region of the HIV-1 genome were amplified using the SGA method and used to infer the T/F *env* sequences (176, 313). A subset of these were then cloned and subjected to functional studies. When a panel of subtype B *env* genes derived by this method was tested, all but one were highly functional in single round infection assays. The exception was an Env construct from an acutely infected plasma source donor with a highly unusual GPEK V3 loop crown sequence that failed to utilize CCR5 or CXCR4 efficiently to infect cell lines or primary CD4+ cells, although function was restored when the V3 crown sequence was changed to GPER. The poor functionality of this unambiguously identified T/F Env was in stark contrast to the ability of the corresponding virus to replicate *in vivo*, as evidenced by high plasma viral load (>80 million RNA copies/ml) in the infected host. Here, we investigated the mechanisms underlying this highly unusual T/F virus phenotype.

Materials and Methods

Amplification of the HIV-1 *env* gene. Serial plasma samples collected from an acutely infected plasma donor, ZP6248, were purchased from ZeptoMetrix. A total of seven plasma samples were collected between February 12 and March 9, 1997, and viral loads (VLs) were determined by the COBAS AMPLICOR HIV-1 MONITOR Test. Viral RNA was extracted from plasma collected on February 26, March 2 and March 9 using the PureLink viral RNA/DNA mini kit (Invitrogen, Carlsbad, CA) and used for cDNA synthesis using Superscript III (Invitrogen, Carlsbad, CA) and primer Env3'ex 5'-TTGCTACTTGTGATTGCTCCATGT-3' (nt 8913-8936 in HXB2) in a 50 µl volume. Single genome amplification (SGA) was used to obtain *rev-vpu-env* cassettes as previously described (176, 181). The first round PCR was carried out with primers Env5'ex 5′-TAGAGCCCTGGAAGCATCCAGGAAG-3′ (nt 5853-5877) and Env3'ex, and the second round PCR with primers Env1Atopo 5'-caccGGCTTAGGCATCTCCTATGG CAGGAAGAA-3' (nt 5957-5983) and Env3'in 5'-GTCTCGAGATACTGCTCCCACCC-3' (nt 8904-8882).

Sequence analysis. All SGA amplicons were sequenced directly by cycle sequencing and dye terminator methods using an ABI 3730xl genetic analyzer (Applied Biosystems, Foster City, CA). Individual sequences were assembled and edited using the Sequencher program 4.7 (Gene Codes, Ann Arbor, MI). The *env* sequences were aligned using CLUSTAL W (349), and manual adjustment for optimal alignment was done using MASE (110). The *env* sequence of the T/F virus was inferred as previously described (176). A phylogenetic tree was constructed with complete *env* gene sequences using the Neighbor-joining method (311) and the Kimura two-parameter model (179). Highlighter analysis was performed through the LANL database website (http://www.hiv.lanl.gov/content/sequence/HIGHLIGHT/highlighter.html). The accession numbers are EU575573-EU575592.

Generation of V3 mutants. Site-directed mutagenesis was carried out to introduce mutations into the V3 region of the *env* gene using the Quikchange Site-Directed Mutagenesis kit

(Stratagene, La Jolla, CA) as previously described (214). A single mutation (E312G) was introduced into the ZP6248.wt *env* gene to make the ZP6248.E312G mutant. The mutagenesis reaction was transformed into XL1-Blue supercompetent cells and positive clones were confirmed by sequencing.

Construction of YU2-ZP4248 chimeras. To conveniently insert a foreign *env* gene into the replication competent YU2 proviral clone, we first generated a modified YU2 clone (pYU2-ΔenvMN), in which the partial *vpu* gene*,* complete *env,* and partial *nef* gene (nt 6186-8800) were replaced by a multiple cloning site fragment **ACGCGT**ATCACAAGATTAGT**GcGGCcgc** (MluI-14bp spacer-NotI). The unique MluI and NotI sites (bold letters) that are rare among HIV-1 *env* genes were introduced. The first 2 bp and the last 8 bp (underlined) are from the *vpu* and *nef* coding regions, respectively. The small letters indicate those bases that are different from the original YU2 sequence.

To clone the ZP6248.wt *env* gene into pYU2-ΔenvMN, both ZP6248.wt and ZP6248.E312G were amplified with Platinum *Taq* High Fidelity polymerase. MluI and NotI restriction sites were introduced at the 5' and 3' ends of the amplified *env* genes, respectively, at the corresponding positions in the HIV-1 genome. The PCR products were purified, digested with MluI and NotI, and ligated into the pre-treated pYU2-ΔenvMN vector. The positive clones from transformed JM109 cells were identified and confirmed by sequencing.

Single round infection assay. TZM-bl cells were infected with pseudovirions as previously described (180). Infectivity was determined by measuring luciferase activity in the cell lysates using the Bright-Glo Luciferase Assay System (Promega Corp., Madison, WI) on a Victor 2 luminometer (Perkin-Elmer Life Sciences, Shelton, CT).

Determination of coreceptor usage. GHOST(3) indicator cell lines expressing CCR1, CCR2b, CCR3, CCR4, CCR8, CXCR4, Hi5, X4R5, GPR15/BOB, STRL33/Bonzo, CX3CR1 were obtained from the NIH AIDS Research and Reference Reagent Program. Cells (3×10^5) were seeded in 12-well plates the day before infection. 100 ng p24 of each pseudovirion or infectious

virus prepared from transfected 293T cells was added to each well. After absorption for six hours at 37^{o}C, complete medium was added, and cell culture was maintained at 37^{o}C with 5% CO_2. Supernatant was collected daily, and virus replication was monitored by measuring the p24 antigen content using the Alliance HIV-1 p24 ANTIGEN ELISA Kit (PerkinElmer, Boston, MA). Coreceptor usage was also determined on NP-2 cells expressing CD4 along with either CCR5, CXCR4, or other G protein-coupled receptors with Env pseudovirions as previously described (251, 335).

Molecular cloning of the full-length ZP6248 T/F virus. To obtain an infectious molecular clone (IMC) of the ZP6248 T/F virus, SGA methods were used to amplify overlapping 5' and 3' half genomes as well as the viral LTR from plasma viral RNA. The full-length T/F sequence was inferred as described (125, 204, 313) and chemically synthesized as three subgenomic fragments. These fragments were then cloned using unique restriction enzyme sites into a low copy number plasmid (modified pBR322 vector), which has been shown to prevent construct instability (313). The integrity of the IMC was confirmed by nucleotide sequence analysis following large scale plasmid grow-up.

Western blot. HIV-1 infectious clones were transfected into 293T cells in a T75 flask using FuGENE6 transfection reagent (Roche Diagnostics; Indianapolis, IN). Briefly, 40 µg DNA was mixed with 120 µl of FuGENE6 in a total volume of 1.5 ml of serum-free DMEM, incubated for 30 minutes, and added to 293T cells (70% confluence) seeded one day earlier at 1.5 x10^7 cells per flask. Forty-eight hours after transfection, the supernatants were harvested, and the viruses were pelleted through a 20% sucrose cushion at 27,000 rpm for 2 hours using an AH-629 Swinging Bucket Aluminum Rotor. The pelleted virus particles and transfected 293T cells were lysed with 250 µl of lysis buffer (50mM Tris-HCl, 150mM NaCl, 20mM EDTA, 1% Triton-X100, 0.1% SDS, pH 7.4). Western blot analysis was performed as previously described (180). The same amount of each virus (based on the p24 contents: 300 ng of the cell lysate and 10 ng of pelleted virus particles) was loaded on a NuPAGE Novex 4-12% Bis-Tris gel (Invitrogen; Carlesbad, CA). After the samples were transferred to a nitrocellulose membrane, the membrane

was blocked in PBS containing 1% casein and 0.01% NaN_3 for 1 hour. The blot was reacted with purified HIVIG (Quality Biological, Gaithersburg, MD) and a mouse mAb 13D5 (1 µg/ml) to the HIV-1 Env protein. Finally, the membrane was reacted with IRDye® 700DX conjugated affinity purified anti-human IgG (Rockland Immunochemicals; Gilbertsville, PA) and Alexa-Fluor 680-conjugated goat anti-mouse IgG (Invitrogen; Carlesbad, CA). Fluorescence was detected on an Odyssey Infrared Imaging system (LiCor Biosciences; Lincoln, NE).

Infection of CD4+ T cells and macrophages. Human CD4+ T cells were obtained from the Center for AIDS Research's Immunology Core at the University of Pennsylvania. All donors gave written informed consent. *Ccr5 wt* and *ccr5Δ32* homozygous cells were stimulated with plate-bound anti-CD3 (eBiosciences, San Diego, CA) and anti-CD28 (BD Biosciences, San Jose, CA) for three days prior to infection. Cells were maintained in RPMI with 10% FBS and IL-2 (20 units/ml) throughout the experiment. Cells were then infected with HIV-1 pseudovirions expressing GFP in the presence or absence of 50 µM AMD3100 as previously described (274). Prototype R5 (JRFL) and X4 (LAI) pseudovirions were used as controls.

GFP pseudovirions were made by co-transfecting Env-pcDNA3.1 with pNL4-3deltaE-EGFP in 293T cells. Viruses were harvested 72 hours post-transfection and pelleted through a 20% sucrose cushion. Cells were then spinoculated with HIV-GFP pseudovirions for two hours at 1200g. Three days post-infection cells were analyzed by flow cytometry. Experiments were repeated in two different *ccr5Δ32* homozygous donors, each time with a *ccr5* wt control donor.

Infections of matched donor CD4+ T cells and macrophages with the ZP6248 T/F and control IMCs were performed as previously described (313). Briefly, virus stocks were prepared by transfecting a 10 cm dish 30% confluent with 293T cells with 6 µg of IMC DNA using FuGene (Roche, Indianapolis, IN). CD4+ cells were positively selected and plated in polystyrene tissue culture dishes for two hours in HBSS with 10 mM Ca2+ and Mg2+ to remove adherent monocytes, then stimulated for 48 hours with 3 µg/ml Staphylococcal enterotoxin B. CD4+ T cells ($5x10^5$) were inoculated overnight with 50,000 IU of the control viruses (or 100ng p24 for

ZP6248.wt). Monocyte-derived macrophages were derived by similarly plating peripheral blood mononuclear cells (PBMCs) in 24-well polystyrene plates to isolate monocytes, which were cultured with DMEM supplemented with 10% giant-cell conditioned media, 10% human AB serum, and 5 U/ml rhM-CSF (R&D systems, Minneapolis, MN). After 6 days, macrophages were inoculated overnight with 100,000 IU of the control viruses (or 200 ng p24 for ZP6248.wt), then washed three times. Virus replication was monitored by measuring p24 antigen concentration in the supernatant.

Flow cytometry analysis of HIV-1-infected CD4+ T cells. CD4+ T cells (1-2 x 10^6) per condition were stained with live/dead Aqua (Invitrogen, Carlsbad, CA), anti-CD3 Qdot655 (Invitrogen, Carlsbad, CA), anti-CD4 Alexa 700 (BD Biosciences, San Jose, CA), anti-CD45RO PE Texas Red (Beckman Coulter, Miami, FL), anti-CCR7 IgM (BD Biosciences, San Jose, CA), and anti-IgM PE (Invitrogen, Carlsbad, CA). Approximately 10^6 events were collected per condition. The gating strategy was as follows: singlets (FSC-A by FSC-H), live cells (SSC-A by live/dead), lymphocytes (SSC-A by FSC-A), and T cells (SSC-A by CD3). To assess viral tropism, infected cells, defined as GFP+, were back-gated on memory markers CCR7 and CD45RO. Flow cytometry was performed on a BD LSR II and data was analyzed with FlowJo 8.8.6 (TreeStar, Inc., Ashland, OR).

CD4 and CCR5 dependent infection determined by Affinofile analysis. 293T cells expressing CD4 and CCR5 under independent inducible promoters, called affinofiles, were used to assess the CD4 and CCR5 utilization efficiency of ZP6248.wt and ZP6248.E312G as previously described (172). Briefly, cells were plated in 96-well plates 48 hours prior to induction. An entire 96-well plate was used per virus representing 48 different CD4 and CCR5 conditions each in duplicate. To induce cells two-fold serial dilutions of ponasterone A and minocycline (Invitrogen, Carlsbad, CA), starting at 2 uM and 5 ng/ml respectively, were added and cells were incubated for 18 hours prior to infection. To infect cells, approximately 25 ng p24 of HIV-NL43-luc+vpr+ pseudovirions were added to each well in the 96-well plate. At 72 hours post-infection, luciferase activity was assessed using the Bright-Glo Luciferase Assay system and vector angles

and magnitude were quantified by VERSA (http://versa.biomath.ucla.edu/). Control viruses TA1 (194) and maraviroc-resistant R3 (351) were included in all experiments which were repeated in duplicate in each of at least three independent experiments.

Detection of the minority variant by parallel allele-specific sequencing (PASS). The PASS assay was performed as previously described (49). Briefly, 20 µl of 6% acrylamide gel mix, containing 1 µM acrydite-modified primer 1H1 5'Acr-CAATAATTGTCTGGCCTGTACCGTCA-3' (nt 7834-6859), cDNA template, 0.3% diallyltartramide, 5% rhinohide, 0.1% APS, 0.1% TEMED, 0.2% BSA and 17 µl cDNA were used to cast a gel on a bind-saline- (Amersham Biosciences, Piscataway, NJ) treated glass slide. The in-gel PCR amplification was then performed in a PTC-200 Thermal Cycler with a mix of 1 µM primer 1C1 5'-GGATCAAAGCCTAAAGCCATGTGT-3' (nt 6560-6583), 0.1% Tween-20, 0.2% BSA, 1x PCR buffer, 100uM dNTP mix, 3.3 units of Jumpstart Taq DNA polymerase (Sigma, St. Louis, MO), and H_2O (up to 300 µl) under a sealed SecureSeal chamber (Grace Bio-Labs, Inc., Bend, OR). PCR was carried out as follows: 94^oC for 3 minutes; 65 cycles of 94^oC for 30 seconds, 56^oC for 45 seconds, and 72^oC for 1 minute; 72^oC for 3 minutes. After PCR amplification, single-base extension (SBE) was performed with mutant and WT bases distinctively labeled with Cy3 and Cy5, respectively, using the sequencing primer 5'-AACAACACAAGAAAAGGTGTACATATAGGACCAG-3' (nt 7125-7164) that annealed just upstream of the mutation site (G<u>A</u>A->G<u>G</u>A). The gel was scanned to obtain images with a GenePix 4000B Microarray Scanner (Molecular Devices, Sunnyvale, CA) and then analyzed with the Progenesis PG200 (Nonlinear Dynamics, Durham, NC) software. Wild type and mutant viruses were determined by comparing their relative fluorescence intensities to normalized values.

Coreceptor expression on PBMCs. A panel of antibodies was used to examine coreceptor surface expression on peripheral blood lymphocytes (PBLs), either PHA-stimulated or -unstimulated, using flow cytometry. Four labeling steps were carried out: 1) 2.5 x 10^5 cells were incubated with 20 µg/ml of each of the following antibodies: anti-GPR15 (R&D Systems,

Minneapolis, MN), anti-FPRL-1 (R&D Systems, Minneapolis, MN), anti-APJ (R&D Systems, Minneapolis, MN), anti-CXCR4 (BD Pharmingen, San Diego, CA), or anti-CCR5 (BD Pharmingen, San Diego, CA); 2) cells were incubated with 10 μg/ml of FITC-labeled anti-mouse IgG (H+L) antibody (KPL, Gaithersburg, Maryland); 3) PE-Cy7-labled anti-CD4 antibody (BD Pharmingen, San Diego, CA) was incubated with the cells; and 4) the cells were finally incubated with Aqua Vital Dye (Invitrogen, Carlsbad, CA). Each labeling step was carried out for 30 minutes at 4°C. Lymphocytes were washed with 3 ml of PBS containing 1% BSA between steps. Lymphocytes fixed in PBS containing 1% paraformaldehyde were analyzed on a BD LSRII.

Results

Viral kinetics during acute HIV-1 infection in subject ZP6248. Serial samples from an acutely infected male plasma source donor, ZP6248, infected with a subtype B HIV-1 were obtained before and after seroconversion, and virus load (VL), p24 and HIV-1 specific antibody levels were determined (Figure 4-1). VLs were below detection limits (400 copies/ml) for the first four time points (between February 12 and 23, 1997) and then began to rise, reaching 87.7 million copies/ml within the next 11 days (Figure 4-1). Subsequent samples were not available for analysis. P24 antigen was detected at the last two time points, and HIV-1 specific antibodies (Abs) were detected by EIA, but not by Western blot analysis at the final time point. According to the Fiebig staging system that is based on the sequential appearance of viral RNA, p24 antigen, and antibodies in plasma during acute infection (112), subject ZP6248 met the criteria for Fiebig stage I, Fiebig stage II and Fiebig stage III at the indicated time-points (Figure 4-1). The time course from Fiebig stage I to Fiebig stage III was similar to those observed in other acute HIV-1-infections (201).

Infection by a single T/F virus with an unusual V3 crown. Twenty full-length *env* gene sequences were obtained from the March 9 plasma sample using the SGA method. Sequence analysis showed limited genetic diversity in the virus population, except for one *env* sequence which contained 13 G-to-A substitutions, characteristic of APOBEC-mediated hypermutation (Figure 4-2A). A single T/F *env* gene sequence was inferred, which like most previously characterized T/F Envs was genotypically consistent with an R5 phenotype (176). Examination of the deduced amino acid sequences of 20 SGA amplicons revealed a highly unusual V3 sequence that contained a GPEK rather than the subtype B consensus GPGR crown motif (Figure 4-2B). Only 13 of more than 90,000 HIV-1 V3 sequences in GenBank had this same GPEK V3 crown motif. Six additional V3 sequences obtained from two earlier samples (February 26 and March 2) all had the identical GPEK crown sequences (Figure 4-2B). Thus, subject ZP6248 appears to have become productively infected with a single T/F virus that exhibited an unusual V3 crown.

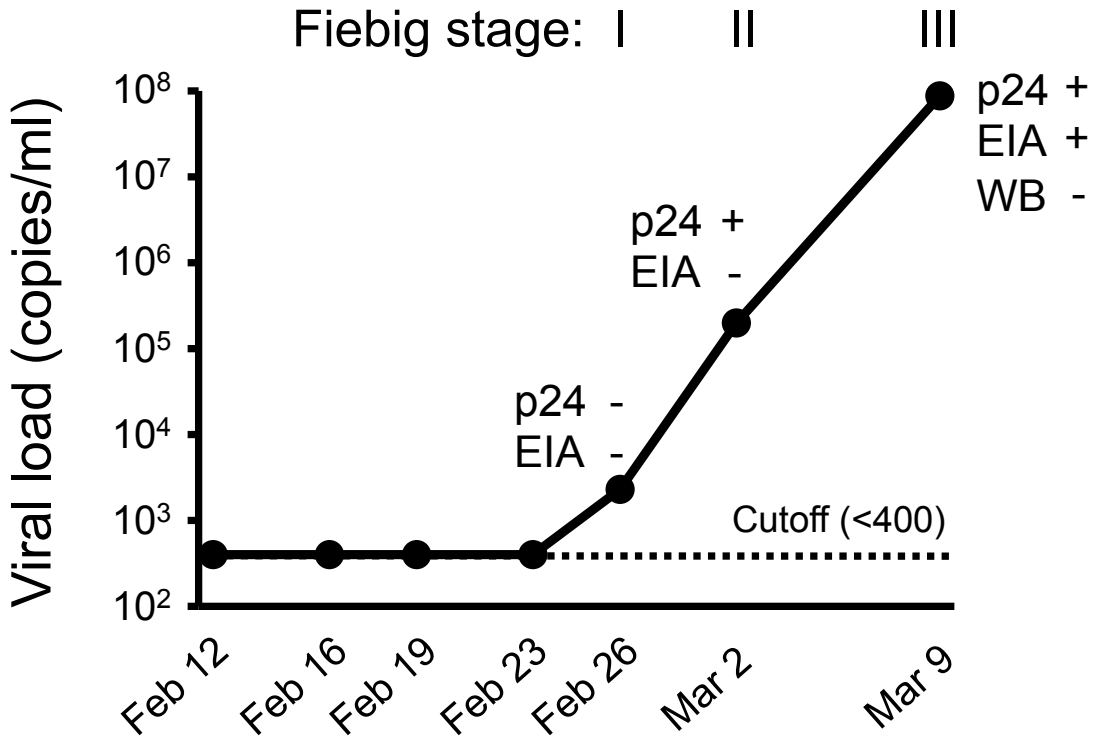

Figure 4-1. Laboratory staging of acute HIV-1 infection in subject ZP6248. Plasma viral load (RNA copies/ml) was determined using the COBAS AMPLICOR HIV-1 MONITOR test (the threshold of the assay is 400 copies/ml). P24 antigen was detected using the Alliance HIV-1 p24 ANTIGEN ELISA Kit (PerkinElmer, Boston, MA). HIV-1 specific antibodies were detected using the GS HIV-1/HIV-2 plus O EIA Kit and GS HIV-1 Western Blot Kit (Bio-Rad, Hercules, CA). The temporal appearance of HIV-1 specific markers according to the classification by Fiebig (112) is shown.

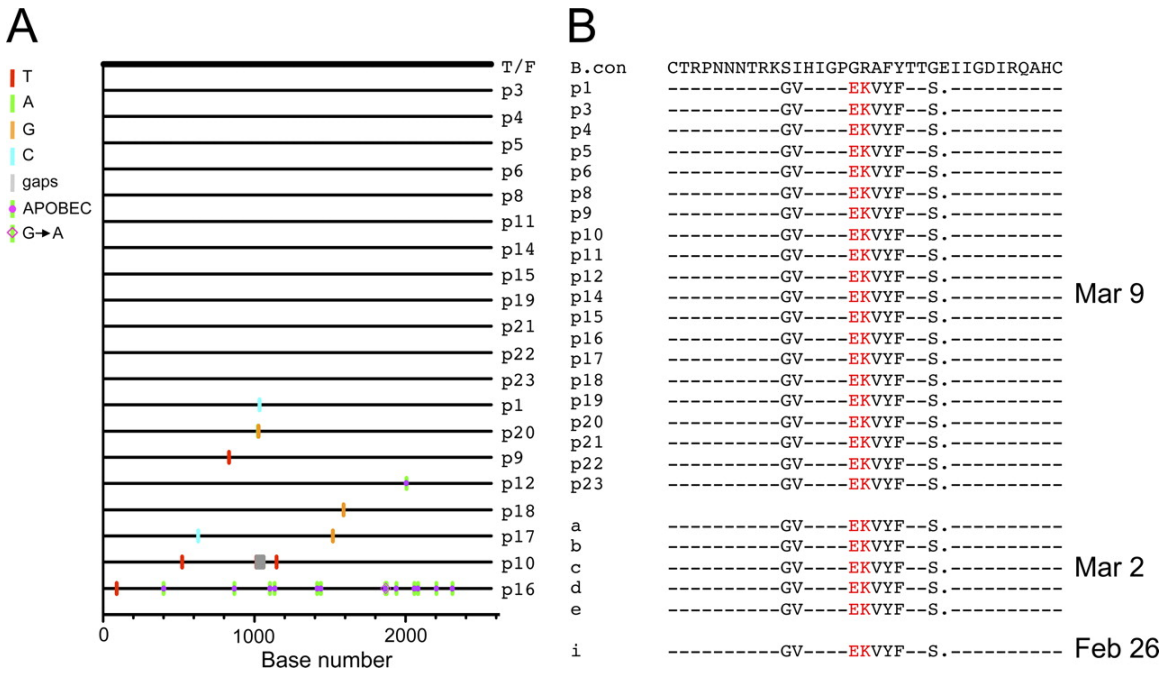

Figure 4-2. Identification of a rare GPEK V3 crown sequence in the ZP6248 envelope glycoprotein. (A) Single genome amplification (SGA) was used to infer the transmitted founder (T/F) env sequence. A Highlighter plot denotes the location of nucleotide substitutions in each SGA derived env sequence compared to the T/F virus. The position of these substitutions is indicated on the bottom (p16 contains G-to-A changes characteristic of APOBEC-mediated hypermutation). Nucleotide substitutions and gaps are color-coded (all *env* sequences were derived from the March 9 time point). (B) Alignment of Env protein sequences in the V3 domain. Sequences from three time points (March 9, March 2 and February 26) are compared to the subtype B consensus sequence. The rare EK V3 crown motif found in all ZP6248 sequences is highlighted in red. Dashes in the alignment indicate sequence identity to the consensus; dots indicate deletions.

ZP6248 T/F Env fails to mediate virus entry into TZM-bl and GHOST cells. To examine its biological activity, the molecularly cloned ZP6248 T/F *env* gene was co-transfected with an *env*-minus HIV-1 backbone (SG3Δenv). Infectivity of the resulting pseudovirions was assessed in TZM-bl cells, which express CD4 as well as CCR5 and CXCR4. Unlike all previously analyzed T/F Envs (176, 191, 204), the ZP6248 T/F Env construct failed to mediate infection in both TZM-bl cells (Figure 4-3) as well as GHOST(3) cells expressing CD4 and either CCR5 or CXCR4 (data not shown). Thus, despite a very high virus load in the infected individual, the inferred T/F Env failed to mediate detectable virus infection in two commonly used reporter cell lines.

Since it is known that V3 plays an important role in coreceptor binding (77, 78, 164, 300, 301), we introduced a single nucleotide substitution (A->G) into the ZP6248.wt Env to generate a mutant, ZP6248.E312G with a consensus glycine (G) rather than the aspartic acid (E) at position 312. Pseudovirions generated with the ZP6248.E312G Env mutant were fully infectious in TZM-bl cells expressing CCR5 and CXCR4 (Figure 4-3). This finding thus identified the rare GPEK crown motif as the reason for the inability of the ZP6248 Env to mediate infection of TZM-bl cells via either of the two major HIV coreceptors, and that a single mutation in the V3 crown sequence restored its infectivity to levels comparable to other primary R5 Envs. Given this, we used a parallel allele-specific sequencing method (49) to determine if viral genomes bearing subtype B consensus V3 loop sequences were present in this individual. We analyzed 1390 viral genomes from the March 9 plasma sample and found only two that contained the E312G sequence (Figure 4-4). Therefore, we conclude that the inferred T/F Env accurately reflects the dominant viral genotype in this individual, and that virions bearing the unusual GPEK motif were responsible for the primary infection.

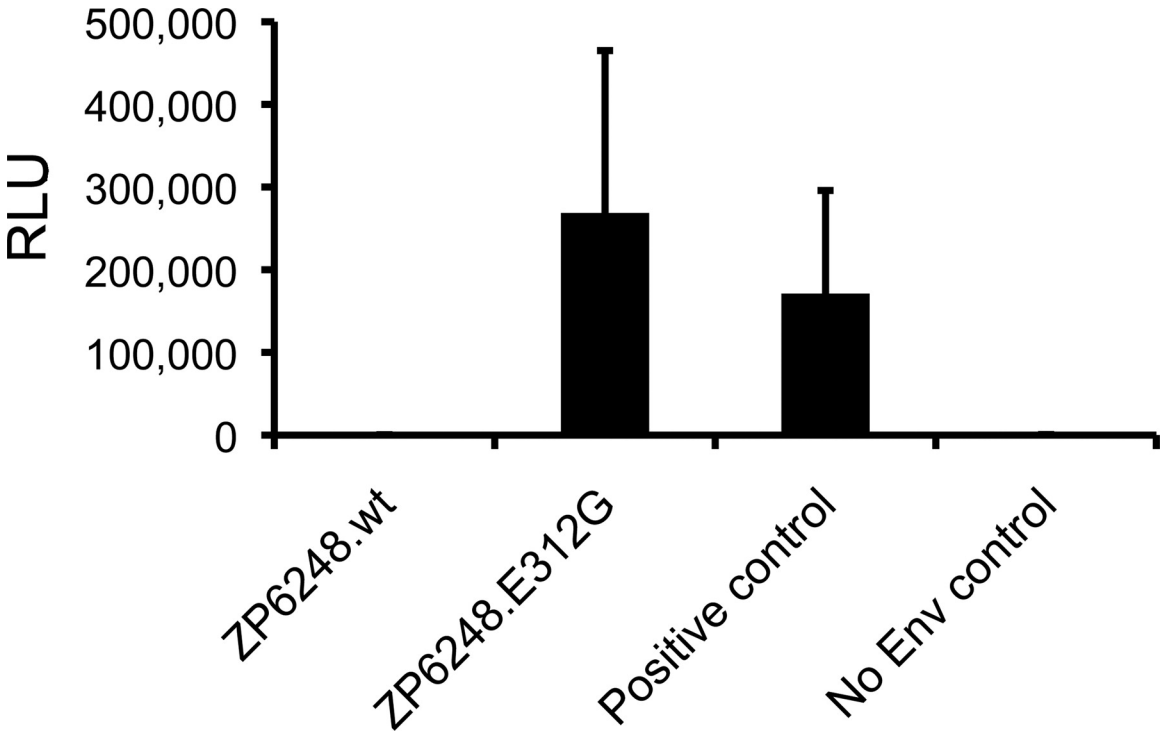

Figure 4-3. Infectivity of pseudoviruses containing ZP6248 Env glycoproteins. Viral pseudotypes bearing the indicated Env glycoproteins were used to infect TZM-bl cells stably expressing CD4 and CCR5. Infectivity was determined by measuring relative light units (RLU) in cell lysates 48 hours after infection (*y* axis). ZP6248.wt represents the T/F Env, while ZP6248.E312G contained a single amino acid substitution in the V3 crown. A subtype C Env (ZM53) was used as a positive control, while Env-negative pseudotypes (SG3Δenv) were used as a negative control.

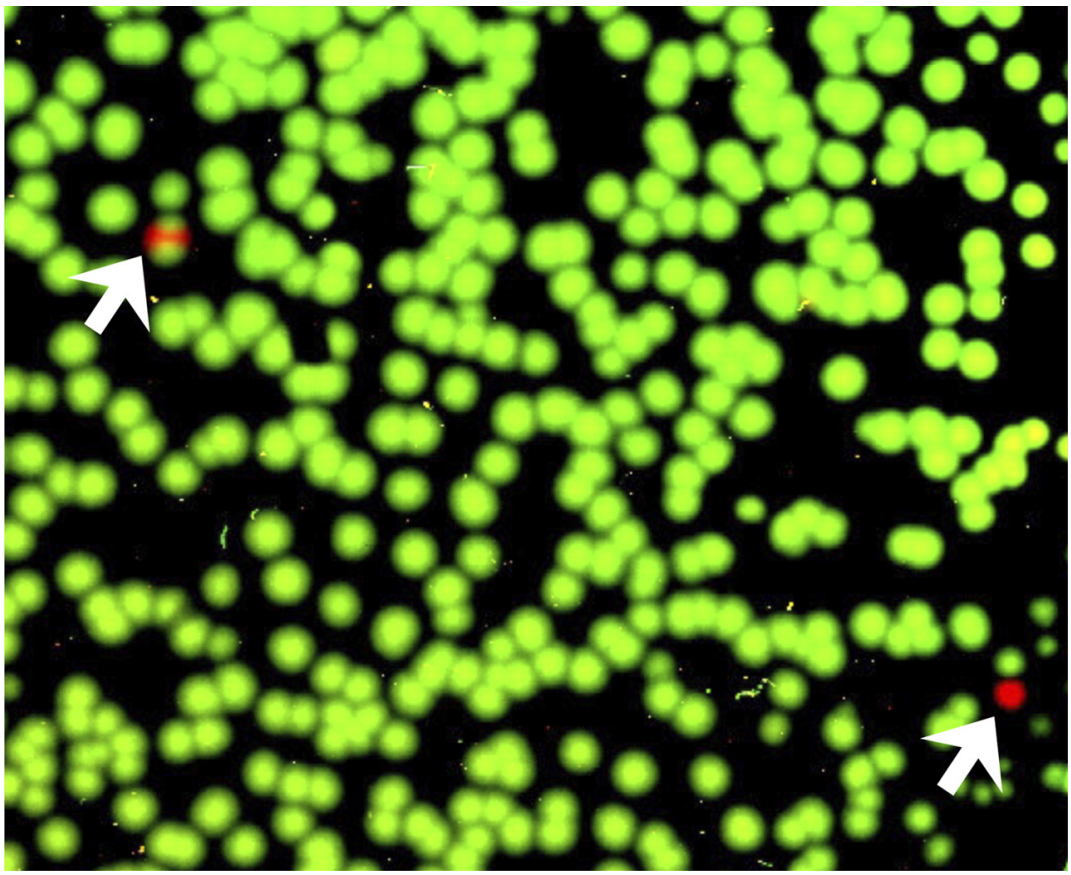

Figure 4-4. Detection of the rare ZP6248.E321G mutation during acute infection. The presence of the ZP6248.E321G mutation (A to G) was examined by parallel allele-specific sequencing (PASS) analysis in plasma collected at the 9 March time point. In this assay, cDNA annealed to an acrydite-modified primer is immobilized in an acrylamide gel, after which in-gel PCR is performed, with the resulting products accumulating around the individual cDNA templates. Sequencing primers that anneal just upstream of the mutation site in V3 (GAA->GGA) can be used to distinguish wt and mutant bases at the same position by single-base extension using Cy3- and Cy5-labeled adenosine (wt) and guanosine (mutant), respectively. The gel was scanned to obtain images with a GenePix 4000B microarray scanner, and the spot number was counted using the Progenesis PG200 software. Green and red spots indicate wt and mutant bases, respectively, detected in individual viral genomes. Two mutants were identified by arrows. A partial image from one of the three experiments is shown.

ZP6248 T/F Env uses multiple alternative coreceptors for cell entry. The fact that the T/F Env clone failed to mediate efficient virus entry, coupled with our finding that a single amino acid substitution in the V3 loop rendered the ZP6248 Env functional in the TZM-bl assay, raised the possibility that the T/F virus from which it was derived had an altered *in vivo* coreceptor preference. It was also possible that the ZP6248 T/F Env recognized CCR5 only when expressed in specific cell types, or that it did not pseudotype efficiently. To differentiate between these possibilities, we generated replication-competent YU2 chimeras containing either wild type (YU2-6248.wt) or mutant (YU2-6248.E312G) ZP6248 *env* genes and tested these constructs in a panel of GHOST(3) cells expressing CCR1, CCR2b, CCR3, CX3CR1, CCR4, CCR8, CXCR4, CCR5, CCR5/CXCR4, GPR15/BOB, and STRL33/Bonzo. Consistent with the results obtained with pseudovirions, YU2-6248.wt did not infect CCR5+, CXCR4+, or CCR5/CXCR4+ cells, but replicated, albeit at very low titers, in GPR15+ cells (Figure 4-5). Conversely, YU2-ZP6248.E312G replicated well in CCR5+ and CCR5/CXCR4+ cells, but grew somewhat more poorly in GPR15+ cells.

To further test the coreceptor preference of the ZP6248 envelope glycoprotein in a different cellular context, we infected NP-2 cells expressing CD4 along with either CCR5, CXCR4, or other G protein-coupled receptors with Env pseudovirions (335). We found that ZP6248.wt mediated nearly equivalent levels of infection on cells expressing GPR15 or APJ, and weakly infected cells expressing FPRL-1 or CCR5 (Table 4-1). It was not unexpected that NP2/CD4/CCR5 cells were weakly infected but not TZM-bl cells by ZP6248 pseudovirus because the background of NP2 cells is 2-3 logs lower than TZM-bl cells (206). Once again, the virus with the E312G mutant exhibited greatly enhanced infectivity in cells expressing CD4 and CCR5. Finally, we compared the coreceptor usage of the ZP6248 Env to that of 24 subtype B T/F psudovirions using a panel of NP-2 cells expressing various G protein coupled receptors. In stark contrast to the other Envs in this panel which used CCR5 or CXCR4 most efficiently, ZP6248.wt predominantly used GPR15 and APJ, while the use of other coreceptors was negligible (Figure 4-6). Additionally, we noted that ZP6248 used GPR15 much better than any other Envs in this

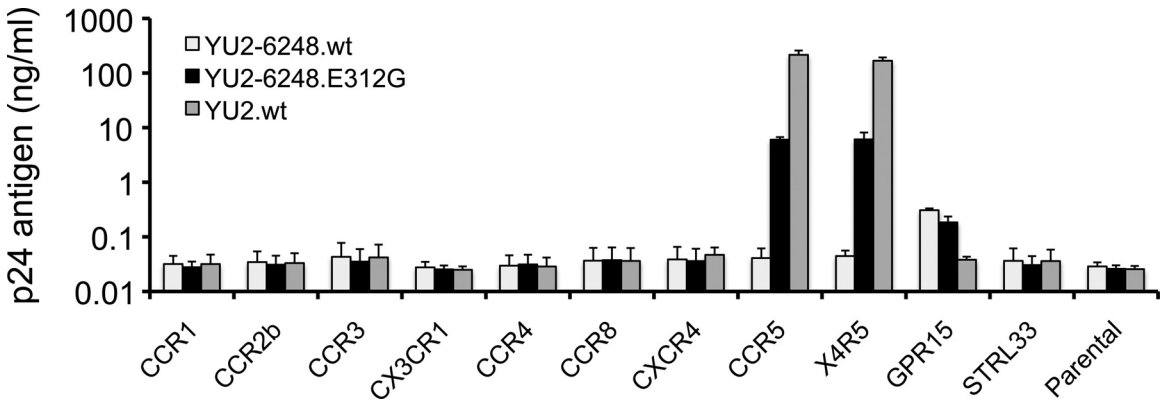

Figure 4-5. Coreceptor usage of ZP6248 Env. GHOST (3) cell lines expressing CD4 and the indicated coreceptors were infected with two replication-competent YU2/ZP6248 chimeras (YU2-6248.wt and YU2-6248.E312G) as well as wild-type HIV-1 YU2.wt. Viruses normalized by p24 content (100 ng) were used to infect cells, and virus replication was monitored by measuring p24 antigen in culture supernatants 7 days after infection. The *y* axis shows the mean of p24 concentrations from three independent experiments. Error bars represent one standard error of the mean.

Table 4-1. Determination of coreceptor usage of ZP6248 in NP-2 cell lines[a]

Env	GPR15	APJ	FPRL-1	CCR5	CD4 only
ZP6248.wt	10991	9972	355	1183	11
ZP6248.E312G	1331	6428	2300	45542	6
NL4-3 (X4)	82	9433	6	220	23
YU2 (R5)	101	940	2256	342801	7
NL4-3 without Env	7	6	8	13	8

[a] NP-2 cells expressing CD4 and the various potential coreceptors as noted were infected with NL4-3 luc$^+$ pseudovirions. The ability to use the coreceptor was assessed by measuring relative light units (RLUs) in cell lysates and comparing the results to those for CXCR4- and CCR5-using control Envs.

panel (data not shown). The ZP6248.E312G mutant, on the other hand, showed a pattern of entry into NP-2 cells indistinguishable from many other T/F Envs (Figure 4-6). Thus, the ZP6248 T/F Env is clearly distinct from other T/F Envs we have analyzed, and failed to mediate efficient infection of cell lines expressing CD4 and CCR5 unless residue 312 in the V3 crown sequence was changed to consensus subtype B glycine.

To determine if ZP6248.wt Env was expressed and incorporated into virions properly, we analyzed Env content in cell lysates and secreted virus particles from transfected 293T cells by Western blot. Compared to YU2, both YU2-6248.wt and YU2-6248.E312G contained lower amounts of Env though cleavage efficiency appeared normal (Figure 4-7). However, since the YU2-6248.E312G virus exhibited high levels of infection on cells expressing CD4 and CCR5, it is evident that the amount of Env on YU2-6248.wt was not limiting for virus infection.

Full-length ZP6248 T/F virus infects GPR15+ but not CCR5+ GHOST cells. To determine whether the atypical function of the ZP6248 Env would be recapitulated in its regular genomic context, we inferred the sequence of the entire ZP6248 T/F provirus and generated a full-length IMC. Overlapping genomic halves were amplified from plasma viral RNA from the March 9 sample using the SGA method as previously described (313). As observed for the *env* gene, both half-genome sequences were homogenous and coalesced to an unambiguous consensus sequence representing the T/F virus (Figure 4-8A), which was then synthesized and cloned using three subgenomic fragments (Figure 4-8B). When virus derived from the molecular clone was used to infect a GHOST cell panel, only GPR15 expressing cells became weakly infected, demonstrating that the full-length ZP6248 T/F virus exhibited the same coreceptor preferences as the viral pseudotypes and the YU2-ZP6248 chimera (data not shown).

ZP6248 T/F virus infects CD4+ T cells from *ccr5*Δ*32* homozygous donors. We next sought to determine if ZP6248 Env could mediate efficient infection of primary human CD4+ T cells, and if so, to identify the receptors used for virus entry. Unfortunately, cells were not available from this donor, though we were able to determine that this individual had a wildtype

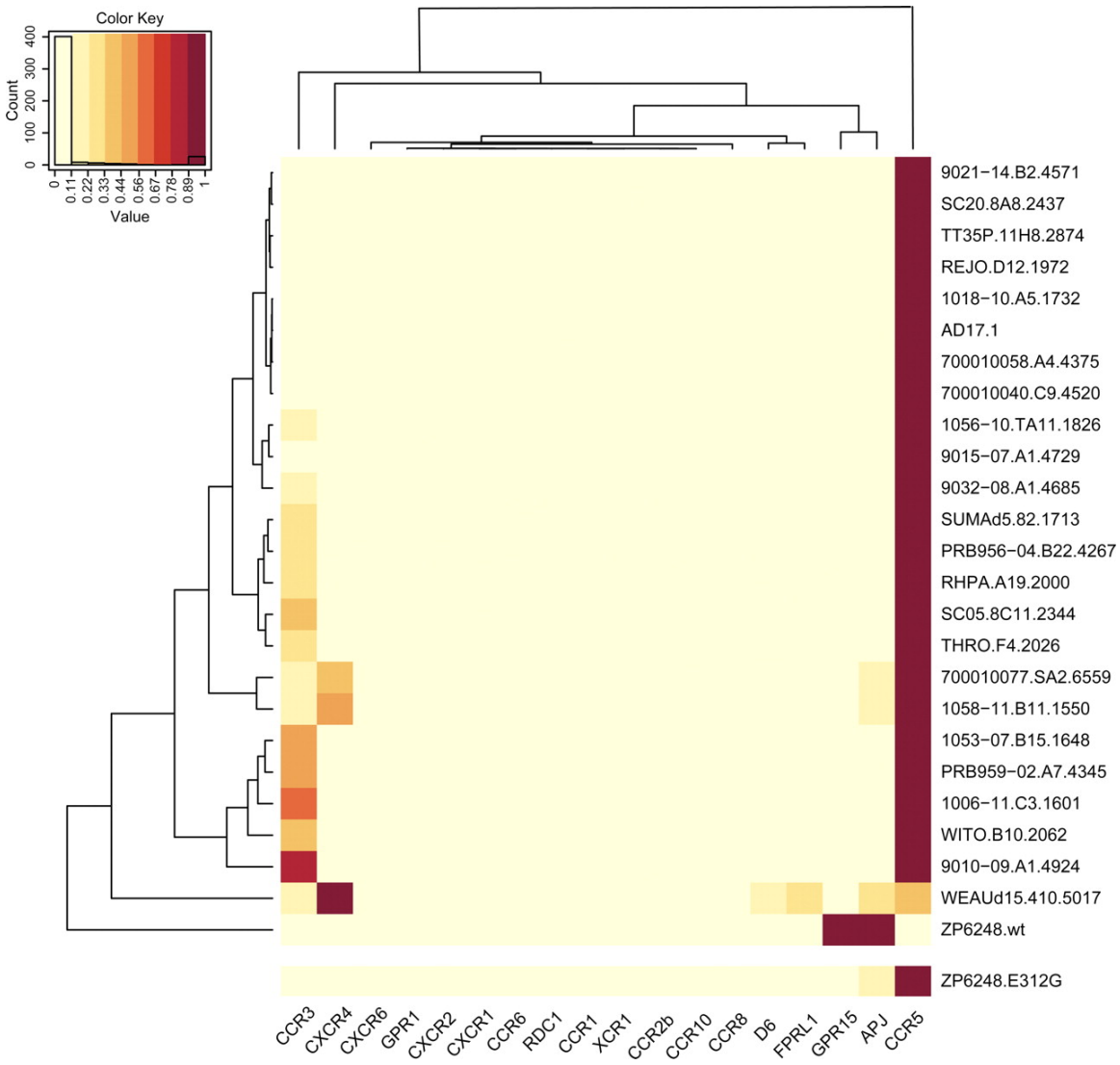

Figure 4-6. Comparison of the ZP6248 Env tropism to that of other subtype B T/F Envs. Entry of ZP6248.wt and ZP6248.E312G pseudotypes into 18 different NP-2 cell lines stably expressing CD4 and the indicated seven-transmembrane domain receptors was compared to that of 24 subtype B T/F Envs. The cell line that was infected most efficiently for each virus was normalized to one (dark red), while the entry into the other cell lines was expressed as a fraction of this value as indicated by the key within the figure. Dendrograms on the top and left of the heat map represent hierarchical clustering of the data that show coreceptors with similar patterns of usage by Envs (top) and Envs with similar coreceptor tropism (left).

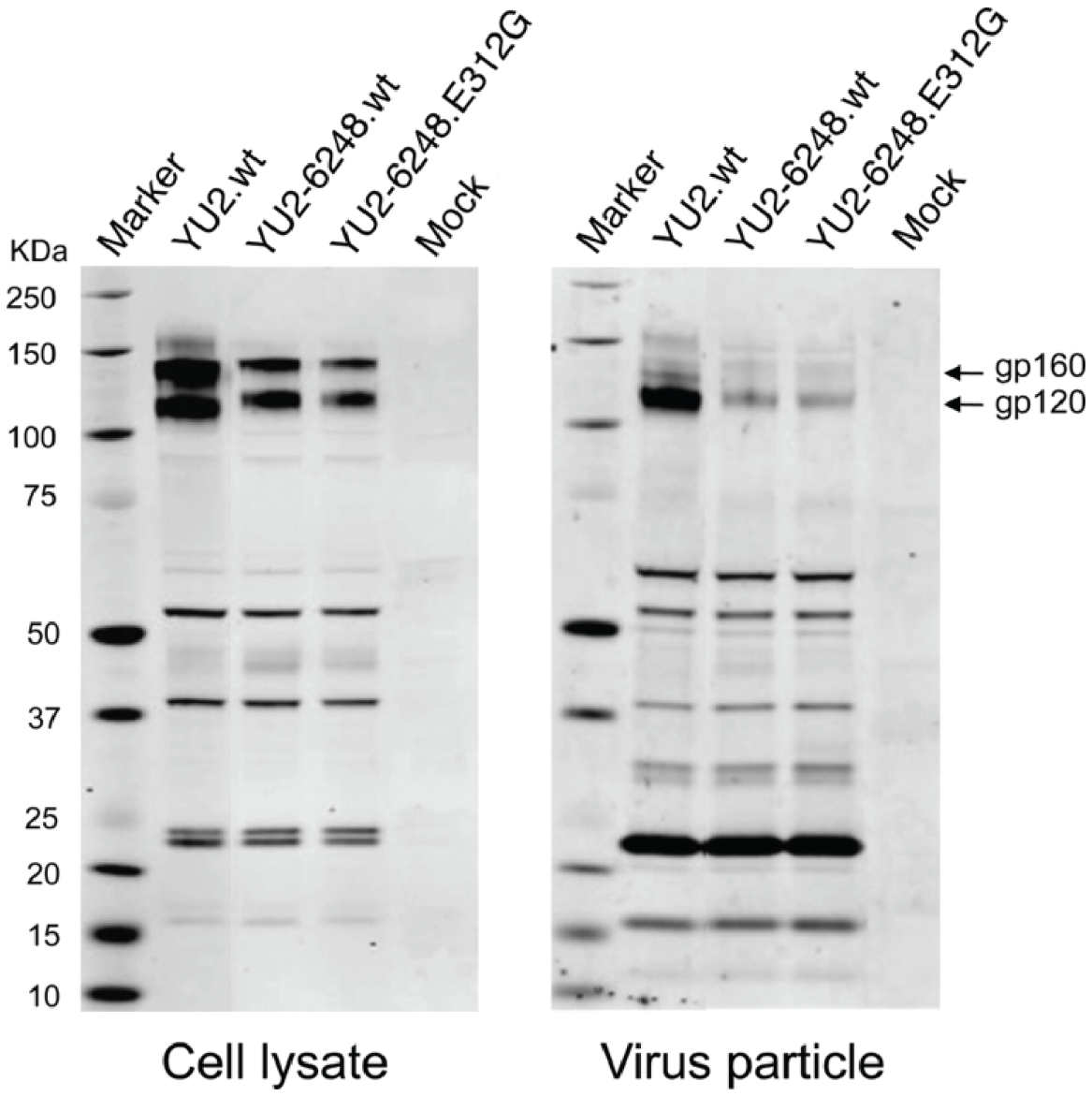

Figure 4-7. Protein expression from transfected cells. 293T cells were transfected with the proviral clones indicated, and cell lysates and viral supernatants were harvested 48 h post-transfection. Protein expression and processing was examined by Western blot analysis using an HIV-1-positive human serum sample and a mouse MAb (13D5) specific for the HIV-1 Env protein (31). The position of the Env precursor (gp160) and the extracellular domain (gp120) are indicated. Protein standards are indicated on the left.

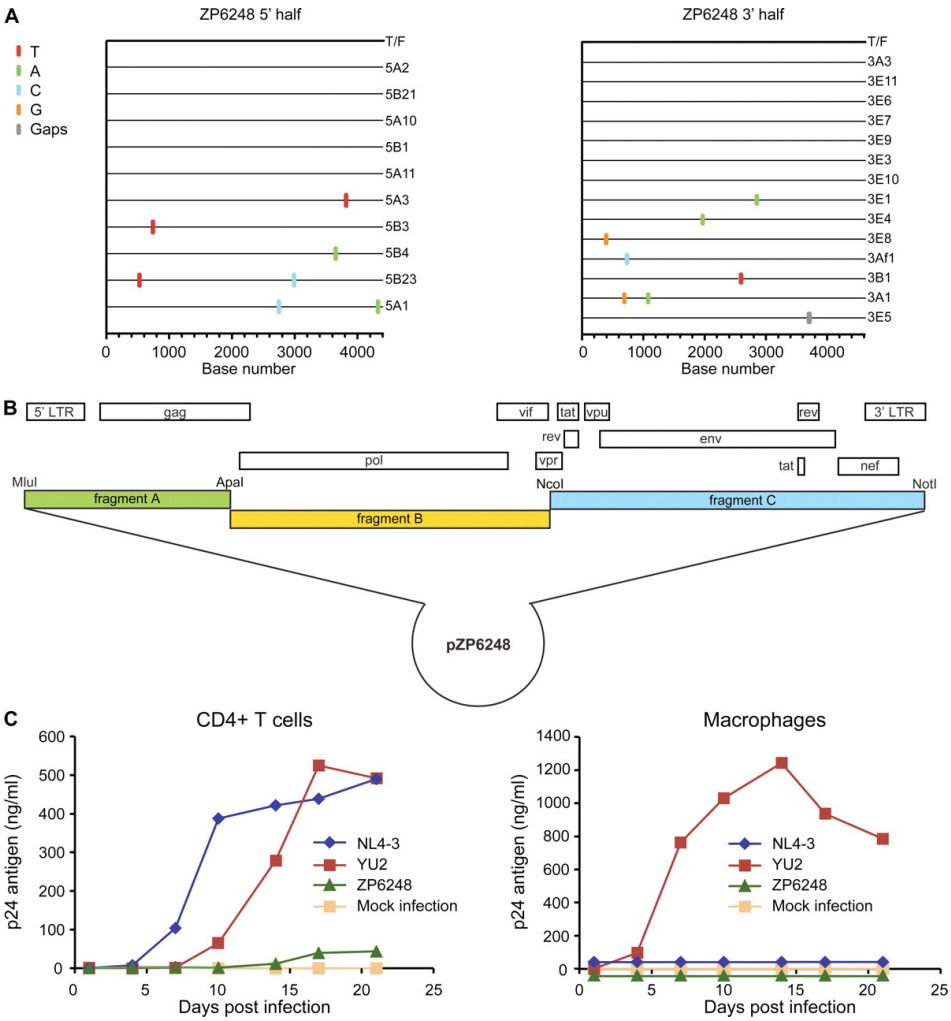

Figure 4-8. Molecular cloning and biological characterization of the T/F virus of subject ZP6248. (A) 5' (4377bp) and 3' (4528bp) half-genomes overlapping by 66bp were amplified by SGA from plasma viral RNA (March 9 time point) and used to infer the sequence of the single T/F virus infecting subject ZP6248 as previously described (125, 204, 313). The Highlighter plots denote the location of nucleotide substitutions compared to the inferred T/F sequence, with their position indicated on the bottom. Nucleotide substitutions and gaps are color coded. (B) The full-length ZP6248 genome was synthesized in three overlapping fragments and cloned into a modified pBR322 vector as described (347). (C) Viruses harvested from transfected 293T cells were examined for their ability to replicate in activated primary human CD4+ lymphocytes (left) and monocyte-derived macrophages (right) from the same donor. The *x*-axis indicates days post infection; the *y*-axis denotes p24 antigen concentration (ng/ml) in the culture supernatant.

ccr5 genotype (not shown). We obtained both *ccr5* wt and *ccr5*Δ*32* homozygous human CD4+ T cells from several donors and performed infection assays using ZP6248.wt and ZP6248.E312G Env pseudovirions expressing a GFP reporter. One of two representative experiments using cells from different *ccr5* wt and *ccr5*Δ*32* homozygous donors is shown in Figure 4-9A. In the presence of the CXCR4 inhibitor AMD3100, ZP6248.wt pseudoviruses infected 0.17% of *ccr5* wt cells and 0.047% of *ccr5*Δ*32* homozygous cells compared to 1.53% and 0.009% for ZP6248.E312G pseudovirions, respectively. Similar results were obtained in the absence of AMD3100, and using cells from a second donor. In addition, the replication competent ZP6248 T/F virus replicated with severely delayed kinetics and to a much lower titer in CD4+ T cells, and failed to replicate in macrophages (Figure 4-8C). Interestingly, prolonged culture of the ZP6248 T/F virus in CD4+ T cells resulted in the selection of a variant with a GPGK V3 crown motif that conferred efficient CCR5 use (data not shown). Finally, the ZP6248 T/F virus replicated even more poorly in *ccr5*Δ*32* homozygous CD4+ T cells, and only at high inocula (data not shown). Thus, Env pseudovirions and IMC-derived virus bearing an unusual V3 loop sequence could utilize one or more alternative coreceptors to mediate inefficient entry into *ccr5*Δ*32* homozygous cells although it also used CCR5 poorly.

Tropism analysis of the ZP6248 T/F virus. The failure of the ZP6248 T/F Env to mediate efficient infection of primary CD4+ T cells raised the possibility that it was uniquely adapted to its host which in turn could have exhibited unusual features, such as unusual CCR5 expression, post-translational processing, or conformation. While cells were not available from this donor, we reasoned that a more detailed analysis of viral tropism might shed light on this issue. Therefore, we employed a highly sensitive CD4+ T cell subset tropism assay to determine if virions bearing the ZP6248.wt or ZP6248.E312G Envs exhibited any unusual properties. CD4+ T cells were obtained from several donors and infected with GFP-expressing pseudovirions. Cells from individual donors were stained with CCR7 and CD45RO to define naïve, central memory, effector memory, and effector memory RA cell subsets (T_{EMRA}). HIV-1-infected cells were then back-gated to evaluate tropism among different CD4+ T cell subsets. 5.2% of ZP6248.wt

pseudovirus-infected cells were naïve, 35.6% were central memory, 58.6% were effector memory, and 0.6% were T_{EMRA} compared to 0.3%, 19.3%, 79.4%, and 1.0% for ZP6248.E312G, respectively (Figure 4-9B). This distribution of infected cells amongst the various CD4+ T cell subsets is similar to what we have observed for other subtype B viruses, indicating that the ZP6248.wt Env and ZP6248.E312G Envs did not exhibit unusual CD4+ T cell subset preference. However, once again, ZP6248.wt was poorly infectious compared to ZP6248.E312G.

We also took a second approach to examine the tropism of ZP6248 Env pseudovirions, performing infection assays on affinofile cells, which are a human 293T cell line that expresses CD4 and CCR5 under independent inducible promoters making it possible to modulate receptor levels across a broad physiologic range (172). The affinofile cells were infected under various CD4 and CCR5 expression conditions with pseudoviruses bearing the ZP6248.wt or ZP6248.E312G Envs. We also performed infection assays with two control viruses: TA1 requires high levels of CCR5 for efficient virus infection, while MVC R3 can infect cells expressing very low levels of CCR5 (44). We found that ZP6248.wt Env required relatively high levels of both CCR5 and CD4 for infectivity, while ZP6248.E312G Env could utilize very low levels of CCR5 at moderate CD4 expression levels (Figure 4-10A). In the affinofile cell system, the sensitivity to changes in CD4 and CCR5 use can be quantified by determining a vector angle (172). A low vector angle is consistent with very efficient CCR5 use, while a high vector angle is associated with inefficient CCR5 use (194, 351). The ZP6248.wt Env had a vector angle of 45°, consistent with its being equally dependent upon CCR5 and CD4 expression levels, while the ZP6248.E312G Env had a very low vector angle, consistent with very efficient CCR5 use at intermediate to high expression levels of CD4 (Figure 4-10B). Of note, the infection level of ZP6248.wt pseudovirions was nearly one order of magnitude lower than that of ZP6248.E312G pseudovirions and TA1, and nearly two orders of magnitude lower than that of MVC R3 (Figure 4-10B). Taken together, these findings are consistent with previous cell line and primary cell data, which show that ZP6248.wt Env can utilize CCR5 for entry, but does so very inefficiently and only when CCR5 and CD4 expression levels are high.

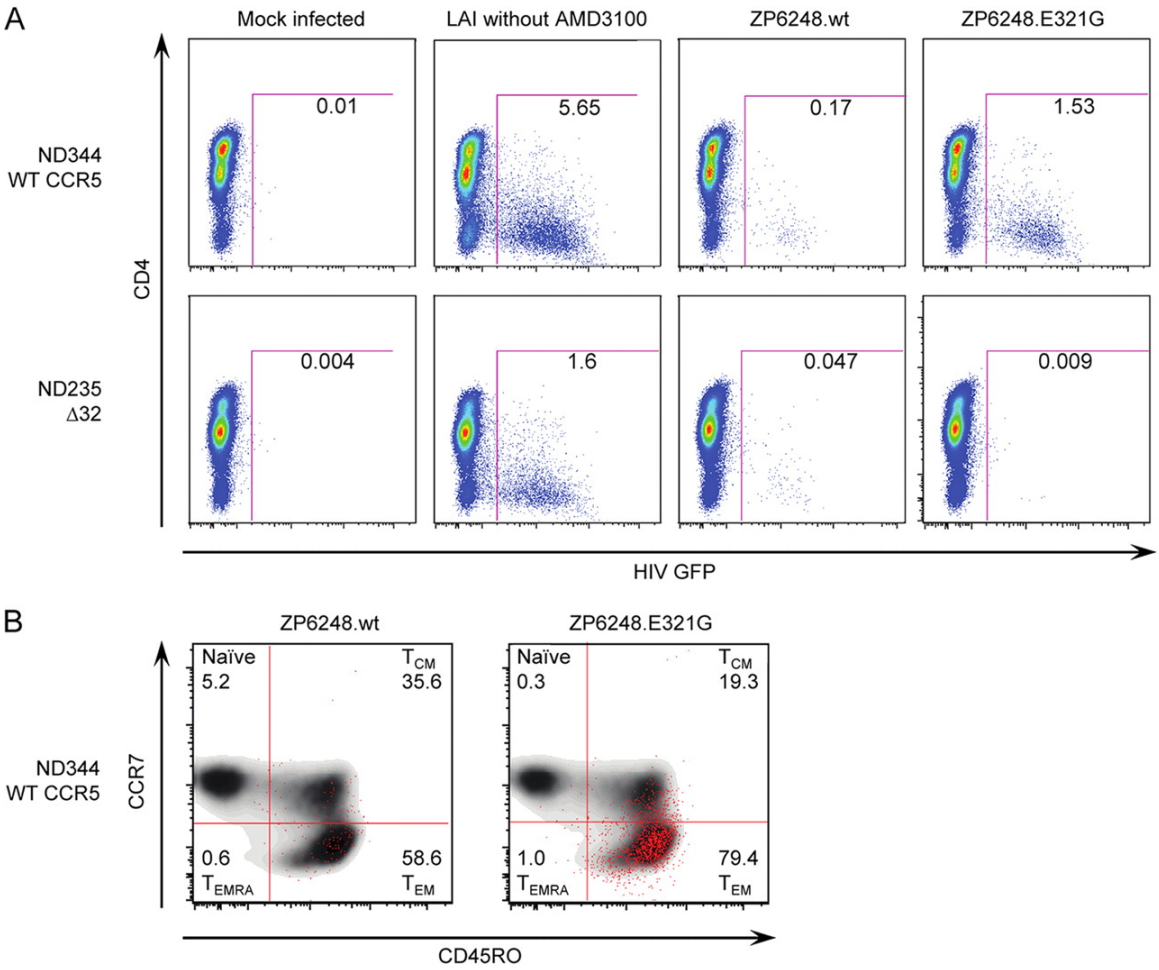

Figure 4-9. Infection of human CD4+ T cells. Env pseudovirions expressing a GFP reporter were used to infect primary *ccr5* Δ32/Δ32 or *ccr5* wt CD4+ T cells in the presence of the CXCR4 antagonist AMD3100. Viral infection was assessed by flow cytometry after gating on live, CD3+ cell singlets. (A) *ccr5* Δ32/Δ32 or *ccr5* wt CD4+ T cells were infected with ZP6248.wt and ZP6248.E312G in the presence of AMD3100. Mock-infected cells were used as a negative control while the X4 HIV-1 strain LAI was used as a positive control in the absence of AMD3100. (B) Infected cells were back-gated onto memory markers CCR7 and CD45R0 (CCR7+CD45RO-, naïve; CCR7+CD45RO+, central memory; CCR7-CD45RO+ effector memory; CCR7-CD45RO-, effector memory RA) to evaluate memory subset tropism of ZP6248.wt and ZP6248.E312G. The data is shown from one of two independent experiments from different donors.

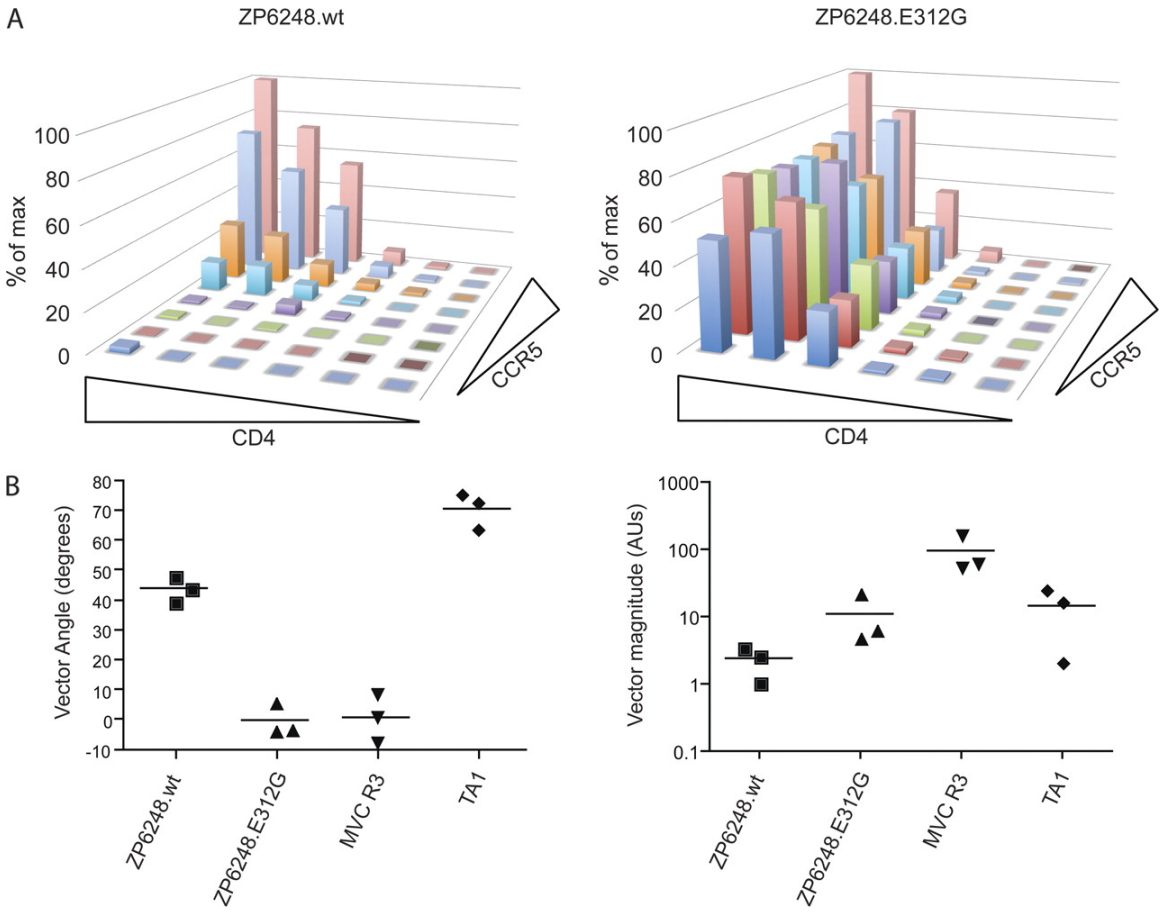

Figure 4-10. ZP6248.wt uses CCR5 inefficiently. (A) ZP6248.wt and ZP6248.E312G pseudovirions were used to infect Affinofile cells which express CD4 and CCR5 with independent induction systems. ZP6248.wt requires high CCR5 expression for infection compared to ZP6248.E312G which can utilize very low levels of CCR5. Both Envs require moderate CD4 expression for infection. (B) The sensitivity to changes in CD4 and CCR5 levels was quantified by Viral Entry Receptor Sensitivity Analysis (VERSA) which yields a single vector angle. Lower vector angles correspond to Envs that utilize CCR5 very efficiently as seen with the maraviroc-resistant Env MVC R3 (1°), while higher vector angles are associated with inefficient CCR5 use as seen with the V3-loop truncated virus TA1 (71°). ZP6248.wt has a vector angle of 44° compared to 0° for ZP6248.E312G. In addition, the vector magnitude can be quantified to assess overall infectivity. ZP6248.wt is 5-fold less infectious than ZP6248.E312G and 40-fold less infectious than MVC R3, consistent with other cell lines and primary cell data.

Expression of coreceptors on the surface of CD4+ T cells. Since ZP6248 was able to infect CD4+ T cells without using CCR5 or CXCR4 coreceptors, albeit inefficiently, we asked whether alternative coreceptors, such as GPR15, APJ, and FPRL-1, were expressed on the surface of these target cells. We thus performed flow cytometry analysis of PBMCs from five normal healthy donors using antibodies specific for GPR15, APJ, and FPRL-1. GPR15 was detected on 7.4% of CD4+ T cells, while APJ was present on 53.4% of CD4+ T cells (Figure 4-11). FPRL-1 was also detected, but at a much lower frequency (1.1% of CD4+ T cells). As expected, CXCR4 was found on nearly all CD4+ T cells, while CCR5 was expressed on 12.5% CD4+ T cells. Similar results were obtained for GPR15, APJ, and FPRL-1 on both unstimulated and PHA-treated PBMCs. These results demonstrate that GPR15, APJ and FPRL-1 are all expressed on the surface of CD4+ T cells and could thus serve as alternative coreceptor for ZP6248 *in vivo*.

Discussion

HIV-1 infection is primarily established by viruses that use CCR5 for entry (131, 176, 234, 255, 313). In this study, we identified and characterized a T/F virus, ZP6248, that replicated to a VL of 87.7 million copies/ml during acute infection *in vivo*, yet its Env glycoprotein failed to efficiently facilitate virus entry into CCR5 or CXCR4-bearing target cells *in vitro*. This finding was clearly at odds with previous results showing that T/F viruses are fully functional and invariably use CCR5 alone or, less commonly, in combination with CXCR4 to infect cells (176, 191). We sought to determine if the poor functionality of this T/F Env was due to methodological issues or whether this virus established infection in a naïve host by utilizing unusual viral and/or host factors that could provide insight into the mechanisms of HIV-1 transmission.

A trivial explanation that could account for the poor functionality of the ZP6248 T/F Env is that its sequence does not reflect that of the virus that established infection in this host. Because the SGA and bioinformatics approaches we have taken to identify multiple T/F Envs have invariably yielded fully functional Env proteins that utilize CCR5 (and sometimes CXCR4 as well) to infect cells, this explanation is highly unlikely. As is common in recently infected individuals, extensive sequencing of *env* shortly after this individual became infected showed very limited genetic diversity and so our inference of the T/F *env* sequence is unambiguous. In addition, the ZP6248 T/F Env exhibited a highly unusual GPEK V3 crown sequence. All *envs* sequenced at three early time-points after infection contained this motif, as did all but two of 1390 genomes analyzed by PASS. It is important to note that this frequency (0.15%) is well above the level of background in this assay (211); therefore a variant which was capable of using CCR5 efficiently *in vitro* was present, but was overshadowed *in vivo* by the variant with poorer *in vitro* CCR5 use. Overall, our data demonstrates that this individual was infected by a virus with a very unusual phenotype.

Another technical issue that could account for poor viral infectivity would be if the ZP6248 T/F Env is packaged into virions poorly. We think this possibility is unlikely, as we analyzed the ZP6248 T/F Env in four viral backgrounds: viral pseudotypes based on HIV-1 HxB2 and SG3

backbones, a replication competent HIV-1 YU2 chimera, and a replication competent, full-length molecular clone derived from subject ZP6248. In addition, immunoblots revealed levels of correctly processed ZP6248 Env in virus particles that were comparable to levels of the fully functional ZP6248.E312G mutant. Therefore, we feel that the low infection levels cannot be explained by poor Env expression, processing, or virion incorporation. In addition, it is important to stress that the single E312G mutation in the V3 loop rendered the Env as functional in virus infection assays as most other primary R5 Envs, and it is difficult to envision how such a change could influence Env incorporation into virus particles.

Despite adequate levels of expression and processing, the ZP6248 Env exhibited poor functionality on two different, commonly used cell lines as well as on primary human CD4+ T cells from 14 different donors. Detailed tropism studies revealed no unusual properties with regards to T cell subset infection, though relatively high levels of CCR5 and CD4 were needed to support infection. In addition, the sequence of the ZP6248 Env has no unusual genetic features save for the highly atypical V3 loop crown. Based on its sequence, this Env is predicted to use CCR5. Might this virus have used CCR5 to mediate efficient virus infection *in vivo*, even though it failed to do so *in vitro*? If so, we would predict that there was something unusual about the manner in which CCR5 was presented on the surface of cells in this individual - otherwise we should have observed robust infection in our *in vitro* assays. Unfortunately, we cannot rule-out this possibility as cells from this individual are not available for study, although we were able to obtain enough cellular debris from plasma to determine that both CCR5 alleles had wild-type sequences in the ORF. In addition, the unusual V3 loop sequence in this individual provides some clues: it is thought that the tip of the V3 loop interacts with the second extracellular loop of the viral coreceptors (164, 380), and this region of CCR5 (and CXCR4) can exhibit conformational heterogeneity (30, 199). In fact, CCR5 inhibitors such as maraviroc alter the conformation of the extracellular loops of CCR5 thus blocking interactions with Env (97, 185, 328). One mechanism by which HIV-1 can become resistant to these allosteric inhibitors is through mutations in the V3 loop that enable it to interact with the altered receptor conformation (14, 32, 259, 274, 351, 355).

In addition, several studies have shown via the use of panels of conformation-specific monoclonal antibodies that CCR5 exhibits conformational heterogeniety on the surface of human CD4+ T cells, though the mechanisms that account for this as well as the implications of altered conformation on viral infectivity are not known (30, 199). Thus, it is possible that CCR5 in this individual exhibited an unusual conformation that was not recapitulated by the cells used in our *in vitro* assays, and that the ZP6248 T/F Env with its unusual V3 sequence was well-adapted to use this conformation.

Another possibility is that virus in this patient used a coreceptor other than CCR5 to initiate infection. If so, this would be unprecedented for HIV-1, but not for SIV; SIVrcm from red-capped mangabeys often uses CCR2 as a coreceptor as genetic absence of CCR5 is common in this species (54). In addition, SIVsmm from sooty mangabeys can also use a coreceptor other than CCR5 to mediate infection *in vivo*: genetic absence of CCR5 is relatively common in sooty mangabeys, but CCR5-negative animals are still infected with SIVsmm, though their virus loads are on average one-half log less than what is typically seen in CCR5+ animals (298). The coreceptor used by SIVsmm to replicate in sooty mangabeys has not yet been identified, though *in vitro* and genetic studies appear to rule-out the use of CXCR4. Therefore, in at least two non-human primate species, robust *in vivo* replication by SIV can be achieved by utilization of coreceptors other than CCR5 or CXCR4.

Several HIV-1 strains have been shown to employ coreceptors other than CCR5 or CXCR4 to infect cells (27, 28, 65, 128, 280, 381), with CCR3, GPR15, APJ, and FPRL-1 being among those most frequently used (66, 167, 251, 280, 335). However, these studies have typically employed cell lines that likely over-express these coreceptors, so it is difficult to assess whether utilization of these coreceptors can lead to infection of primary human cell types. In fact, with few exceptions, HIV-1 strains fail to infect human T cells from individuals who lack CCR5 in the presence of the CXCR4 inhibitor AMD3100, arguing that in this context alternative coreceptors typically cannot mediate infection (66, 330). However, ZP6248 was able to use three alternative coreceptors (GPR15, APJ and FPRL-1) to infect cell lines, using the former two much

more efficiently than CCR5. This pattern is strikingly different from that of all other subtype B T/F Envs recently analyzed in NP2 cells expressing various putative alternative coreceptors. Therefore it is reasonable to ask if these receptors are expressed *in vivo* on cell types relevant to transmission. Previous studies showed GPR15 mRNA in human colon tissue and CD4+ T lymphocytes as well as rhesus macaque peripheral blood mononuclear cells (67, 86, 109), FPRL-1 in a large variety of cells and organs, including T and B lymphocytes (235), and APJ in the human brain (100) and also in activated PBMCs (58). Using currently available antibodies, we have found that GPR15 and APJ are expressed on the surface of 7.7% and 56% of CD4+ T cells, respectively, while FPRL-1 can be found on only about 1% of CD4+ T cells. The presence of these coreceptors on the surface of CD4+ T cells suggests that they may be used by ZP6248 *in vivo*. Since GPR15 is widely present in gut tissue, was the coreceptor used most efficiently by ZP6248, and is known to be used by some SIV and HIV-2 strains (86, 100, 357), it is the most likely candidate.

Almost all T/F HIV-1 Envs use CCR5 efficiently *in vitro* and presumably *in vivo* as well, given the relative resistance of individuals who lack CCR5 to virus infection. However, this study reinforces the idea that the Env glycoprotein is incredibly plastic, and shows that our *in vitro* assays at times fail to recapitulate important virological properties that operate *in vivo*. Whether by exploiting an atypical CCR5 conformation or by using coreceptors not previously known to mediate transmission, the virus that infected subject ZP6248 did so without efficient use of CCR5 in its standard form in multiple assays. In light of this, while attempting to block CCR5 use as an option for target cell entry (e.g., by maraviroc-containing microbicides) will likely be an effective prevention strategy, our report cautions that atypical presentations of CCR5 or alternative coreceptors may sometimes be used by HIV to result in establishment of primary infection.

Acknowledgements

We thank Dr. Hiroo Hoshino for NP-2 cell lines; Drs. Haili Zhang, Yan Zhou, and Robert Siliciano for bicyclam JM-2987 and pNL4-3-deltaE-EGFP; Brooke Walker for editorial assistance; and the NIH AIDS Research and Reference Reagent Program, Division of AIDS, NIAID, NIH for GHOST(3) cell lines. This work was supported by NIH grants AI067854 (BFH, BHH, GMS and FG), AI040880 (RWD), Bill and Melinda Gates Foundation grants 37874, 38691 and 38643 (BFH, BHH, GMS), and the Duke and UAB Centers for AIDS Research (AI064518 and AI27767). CBW and NFP were supported by T32 AI007632 and T32 GM008361, respectively.

CHAPTER 5

Phenotypic Characteristics of Transmitted Founder HIV-1

Nicholas F. Parrish[a,b], Feng Gao[c,d], Hui Li[a], Elena E. Giorgi[e], Hannah J. Barbian[a,b], Erica H. Parrish[a], Lara Zajic[a], Shilpa S. Iyer[a,b], Julie M. Decker[f], Amit Kumar[c], Bhavna Hora[c], Anna Berg[c], Fangping Cai[c], Jennifer Hopper[c], Thomas N. Denny[c,d], Haitao Ding[f], Christina Ochsenbauer[f], John C. Kappes[f], Rachel P. Galimidi[g], Anthony P. West[g], Pamela J. Bjorkman[g,h], Craig B. Wilen[a,b], Robert W. Doms[b,i], Meagan O'Brien[j], Nina Bhardwaj[j,k,l], Persephone J. Borrow[m], Barton F. Haynes[c,d,n], Mark Muldoon[o], James P. Theiler[e], Bette Korber[e], George M. Shaw[a,b], Beatrice H. Hahn[a,b]*

Departments of Medicine[a] and Microbiology[b], Perelman School of Medicine, University of Pennsylvania, Philadelphia, PA 19104; [c]Duke Human Vaccine Institute and [d]Department of Medicine, Duke University School of Medicine, Durham, NC 27710; [e]Theoretical Biology and Biophysics, Theoretical Division, Los Alamos National Laboratory, Los Alamos, NM 87545; [f]Department of Medicine, University of Alabama at Birmingham, Birmingham, AL 35294; [g]Division of Biology, California Institute of Technology, Pasadena, CA, 91125; [h]Howard Hughes Medical Institute; [i]Department of Pathology and Laboratory Medicine, Children's Hospital of Philadelphia, Philadelphia, PA 19104; Departments of Medicine[j], Pathology[k], and Dermatology[l], New York University School of Medicine, New York, NY 10016; [m]Nuffield Department of Clinical Medicine, University of Oxford, Weatherall Institute of Molecular Medicine, John Radcliffe Hospital, Headington, Oxford OX3 9DS, UK; [n]Department of Immunology, Duke University School of Medicine, Durham, NC 27710; [o]School of Mathematics, University of Manchester, Manchester, UK M13 9PL.

Abstract

Defining the virus-host interactions responsible for HIV-1 transmission, including the phenotypic requirements of viruses capable of establishing *de novo* infections, could be important for AIDS vaccine development. Previous analyses have failed to identify viral properties other than CCR5 and T cell tropism that are preferentially associated with transmission. However, most of these studies were limited to using viral pseudotypes to examine envelope (Env) function. Here, we generated full-length infectious molecular clones (IMCs) of mucosally transmitted founder (TF; n=27) and chronic control (CC; n=14) viruses of subtypes B (n=18) and C (n=23), and compared their phenotypic properties in assays specifically designed to probe the earliest stages of HIV-1 infection. We found that TF virions were 1.7-fold more infectious (p=0.049) and contained 1.9-fold more Env per particle (p=0.048) compared with CC viruses. TF viruses were also captured by monocyte-derived dendritic cells (moDCs) 1.7-fold more efficiently (p=0.035) and were more readily transferred to CD4+ T cells (p=0.025) than CC viruses. In primary CD4+ T cells, TF and CC viruses replicated with comparable kinetics; however, when propagated in the presence of interferon alpha (IFN-α), TF viruses replicated to significantly higher titers than did CC viruses (p=0.012). This difference was more pronounced for subtype B (62-fold) than subtype C (1.7-fold) viruses, possibly reflecting demographic differences of the respective patient cohorts. Together these data indicate that TF viruses are enriched for higher Env content, enhanced cell-free infectivity, improved dendritic cell interaction and relative IFN-α resistance. These viral properties, which could act in concert, should be considered in the development and testing of future prevention strategies.

Introduction

Understanding the host and viral factors that influence the ability of human immunodeficiency virus type 1 (HIV-1) to cross mucosal barriers may be critical for the development of an effective AIDS vaccine (331). HIV-1 virions or infected cells are believed to cross the epithelium shortly after sexual exposure, although the mechanisms by which this occurs remain largely unknown. Within the mucosa, viruses are believed to interact with dendritic cells (DCs), such as Langerhans cells, but do not productively infect these cells (159). In the simian model of HIV-1, the first cells to become productively infected are resting intraepithelial CD4+ T cells, which represent the most abundant target cell type in the lamina propria (395). Simultaneous with initial infection events, local innate immune responses are elicited, with plasmacytoid DCs accumulating rapidly at sites of virus entry. These cells secrete cytokines and chemokines, such as MIP1-β and type I interferons, and orchestrate an early local innate immune response (209). After local infection in mucosal and submucosal tissues is established, HIV-1 spreads to regional and distant lymphoid tissues including gut-associated lymphoid tissue (GALT) where virus expands exponentially, triggering a systemic cytokine storm preceding peak viremia (319, 343).

Many host factors can influence whether virus exposure leads to productive infection, including the physical barrier of the mucosa and its associated mucous secretions (136, 248), target cell availability (212, 266, 398), immune activation (224), genital inflammation (195), and altered mucosal microbiota (12). While HIV-1 is characterized by high genotypic and phenotypic diversity, the extent to which this variation influences the transmission process remains unclear. Transmission across intact mucosal barriers is inherently inefficient and invariably associated with a viral population bottleneck (159, 365). Indeed, in 60-80% of mucosal infections, a single transmitted founder (TF) virus is responsible for productive clinical infection (176). This finding has raised the question whether the transmission process represents a stochastic event, in which every replication competent virus has a roughly equal chance of establishing a new infection, or whether the bottleneck selects for viruses that exhibit particular biological properties that

predispose them to cross the mucosa and replicate efficiently. In support of the latter, transmitted viruses have generally been found to exhibit CCR5 tropism and share certain genetic features, including shorter variable loops, fewer potential N-linked glycosylation sites and amino acid signatures in their envelope glycoproteins (Envs) which may affect Env surface expression and/or other viral properties (59, 79, 88, 126, 203, 213, 309). However, to date no consistent phenotypic correlate of these latter signatures with transmission biology has been identified.

Initial phenotypic studies of viruses obtained in acute or early infection were generally limited to analyses of Env functions, which were almost exclusively conducted in the context of Env pseudoviruses. These analyses led to a number of hypotheses as to how transmitted viruses might differ from their chronic counterparts. Such differences included more efficient engagement of receptor or coreceptor by transmitted Envs (5, 167), greater sensitivity to neutralizing antibodies resulting from a more open or accessible Env conformation (88, 390), or preferential interaction of Env with the integrin pair $\alpha 4\beta 7$ (250). A limitation of these studies, however, was that they employed viruses and/or Envs obtained weeks or months after the transmission event when substantial virus evolution and selection could have occurred. Using single genome amplification (SGA) (312) and a model of random virus evolution (176), we generated Env sequences and molecular clones corresponding to actual TF viral genomes and showed for the first time that, at the moment of virus transmission and infection of the first cell, TF viruses use CCR5 as the coreceptor for entry (171, 176, 270, 372). We failed, however, to find corroborate previous evidence that TF Envs used CD4 and CCR5 more efficiently (270, 372), interacted specifically with $\alpha 4\beta 7$ (270), or exhibited a preferential tropism for particular CD4+ T cell subsets (270, 372). We also failed to identify an enhanced overall sensitivity TF Envs to neutralization, although subtype B TF Envs were slightly more sensitive to CD4 binding site neutralizing antibodies than subtype C TF Envs (372). Most recently, we discovered that TF Envs are more completely inhibited by small molecule CCR5 antagonists than chronic control (CC) Envs consistent with altered CCR5 interactions, although the biological relevance of this finding remains to be determined (268). Thus, except for preferential CCR5 coreceptor usage and T-cell

tropism, no other consistent phenotypic difference between TF and CC viruses has been identified.

Env pseudotypes are generated by co-transfection of an *env* expression cassette with an *env*-minus proviral backbone. Since this backbone represents a standard (non-TF) HIV-1 genome, the contribution of gene products other than Env to the TF phenotype cannot be assessed. Moreover, overexpression of Env, which is inherent in the co-transfection assay, precludes a meaningful assessment of virus-host cell interactions and particle composition. Reasoning that these shortcomings may have obscured phenotypic differences that could enhance mucosal transmission, we developed methods to clone full-length TF genomes and showed that these produced replication competent viruses that grew efficiently in CD4+ T cells but not macrophages (204, 257, 313). However, a systematic evaluation of the TF phenotype also required a sufficient number of chronic control (CC) viruses, also derived as full-length IMCs, for comparison. Here, we describe the generation and biological characterization of a comprehensive set of TF (n=27) and CC (n=14) IMCs, representing two major HIV-1 group M subtypes. Using these novel reagents, we compared biological properties that would be expected to influence viral fitness during the earliest stages of the transmission process. Our results reveal that TF viruses share common traits that likely enhance their fitness in crossing mucosal surfaces and in promoting the establishment of a productive local infection.

Results

Infectious molecular clones of transmitted founder and chronic control viruses. Although a limited number of TF and CC IMCs has previously been reported (204, 257, 270, 313), available clones were too few to conduct meaningful phenotypic comparisons. This has especially been true for viruses from chronically infected individuals, for which only four IMCs (all from subtype C infections) have been constructed (270). To create a more balanced panel, both with respect to the number of TF and CC IMCs as well as their subtype representation, we cloned additional viral genomes from individuals enrolled in acute and chronic HIV-1 infection cohorts. Using previously reported methods (204, 257, 313), we inferred 12 additional TF genomes (Fig. 5-1) representing mucosally transmitted viruses from single (n=8) or multivariant (n=4) transmissions. Together with existing constructs, these comprised a panel of 27 TF IMCs, with equal representation of subtype B (n=13) and subtype C (n=14) viruses (Table 5-1).

Chronically HIV-1 infected individuals harbor complex quasispecies of genetically diverse HIV-1 variants. Since it is impossible to predict based on sequence inspection alone which variants are biologically active and which are functionally impaired, we amplified between 20 and 40 *env* genes or 3' half genomes from chronic infection plasmas and searched for clusters of nearly identical sequences as indicators of recent clonal expansions (Fig. 5-2). We reasoned that the inferred common ancestors of these clusters must encode persistently replicating viruses and thus represented relevant controls for biological comparisons with TF viruses. Consistent with this interpretation, we found that all chronic IMCs generated from expansion rakes produced viruses that grew to high titers in CD4+ T cells. However, not all chronic infection samples were suitable for IMC construction. Analyzing over 60 plasmas, we identified only 14, including four reported previously (270), that exhibited clonal expansion rakes in both 3' and 5' halves of their viral genomes (Fig. 5-2). These were used to construct CC IMCs representing both subtype B (n=5) and subtype C (n=9) infections (Table 5-1).

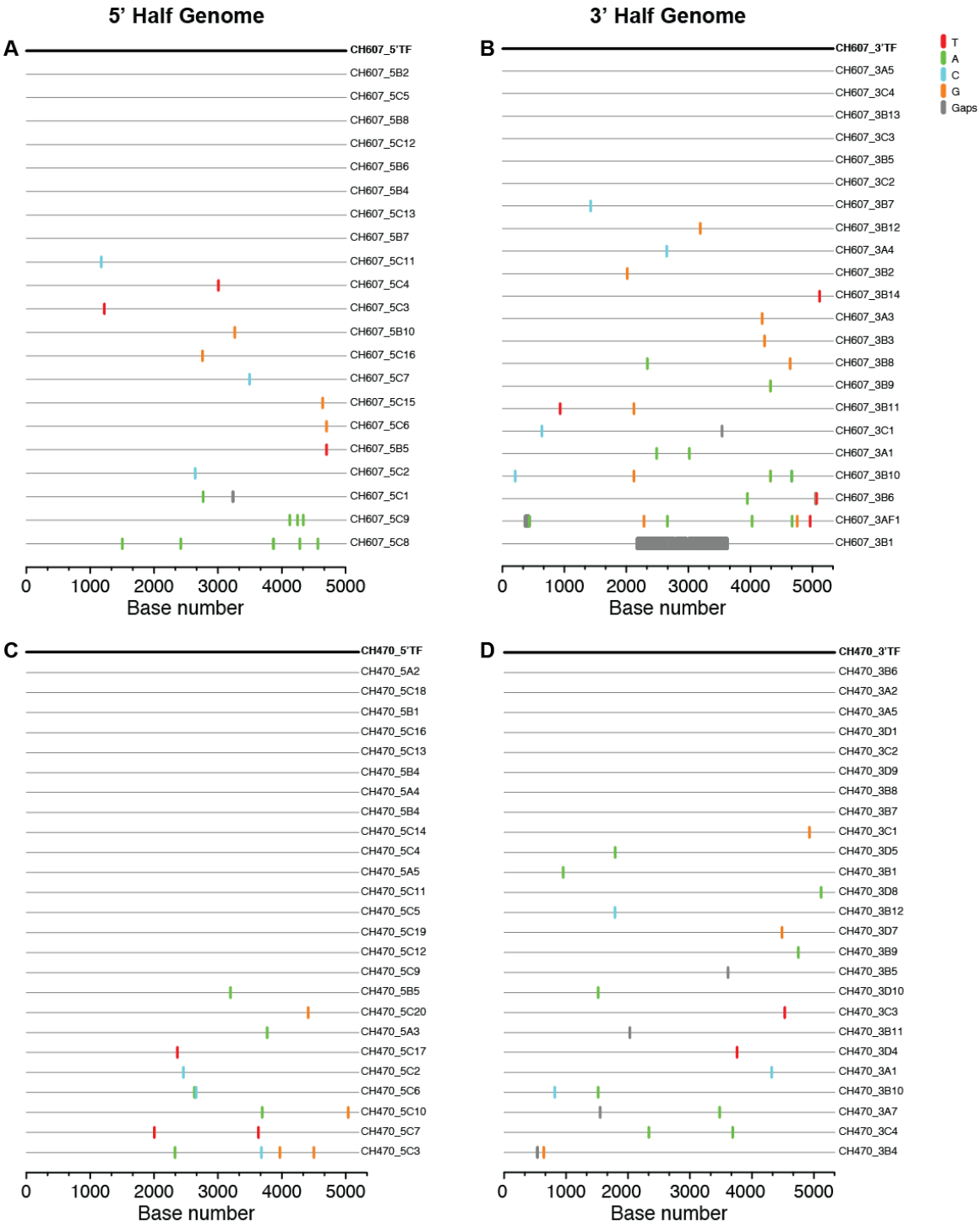
5' Half Genome
3' Half Genome
A
B
C
D
T
A
C
G
Gaps
CH607_5'TF
CH607_5B2
CH607_5C5
CH607_5B8
CH607_5C12
CH607_5B6
CH607_5B4
CH607_5C13
CH607_5B7
CH607_5C11
CH607_5C4
CH607_5C3
CH607_5B10
CH607_5C16
CH607_5C7
CH607_5C15
CH607_5C6
CH607_5B5
CH607_5C2
CH607_5C1
CH607_5C9
CH607_5C8
CH607_3'TF
CH607_3A5
CH607_3C4
CH607_3B13
CH607_3C3
CH607_3B5
CH607_3C2
CH607_3B7
CH607_3B12
CH607_3A4
CH607_3B2
CH607_3B14
CH607_3A3
CH607_3B3
CH607_3B8
CH607_3B9
CH607_3B11
CH607_3C1
CH607_3A1
CH607_3B10
CH607_3B6
CH607_3AF1
CH607_3B1
CH470_5'TF
CH470_5A2
CH470_5C18
CH470_5B1
CH470_5C16
CH470_5C13
CH470_5B4
CH470_5A4
CH470_5B4
CH470_5C14
CH470_5C4
CH470_5A5
CH470_5C11
CH470_5C5
CH470_5C19
CH470_5C12
CH470_5C9
CH470_5B5
CH470_5C20
CH470_5A3
CH470_5C17
CH470_5C2
CH470_5C6
CH470_5C10
CH470_5C7
CH470_5C3
CH470_3'TF
CH470_3B6
CH470_3A2
CH470_3A5
CH470_3D1
CH470_3C2
CH470_3D9
CH470_3B8
CH470_3B7
CH470_3C1
CH470_3D5
CH470_3B1
CH470_3D8
CH470_3B12
CH470_3D7
CH470_3B9
CH470_3B5
CH470_3D10
CH470_3C3
CH470_3B11
CH470_3D4
CH470_3A1
CH470_3B10
CH470_3A7
CH470_3C4
CH470_3B4
0
1000
2000
3000
4000
5000
Base number

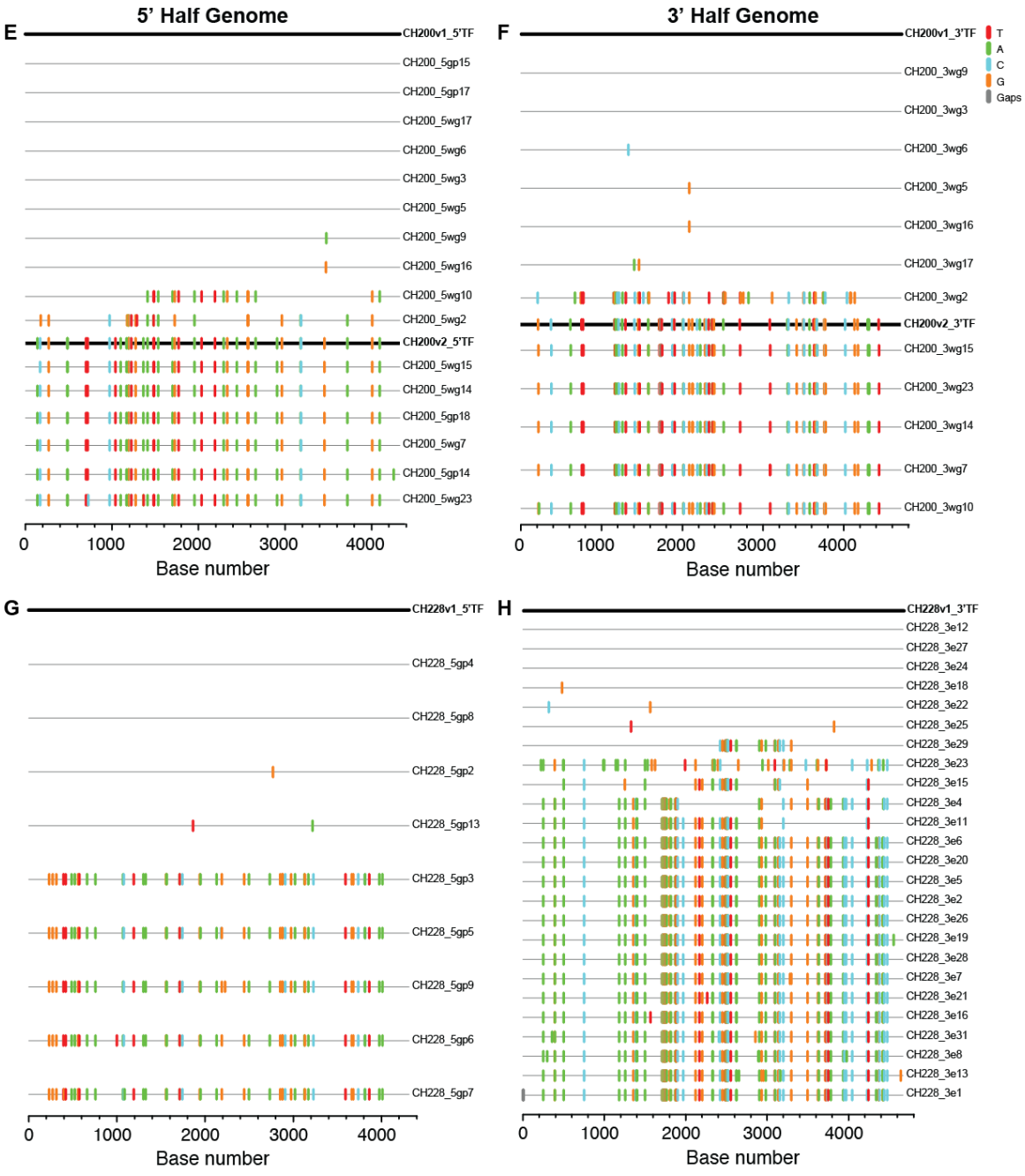
E
5' Half Genome
CH200v1_5'TF
CH200_5gp15
CH200_5gp17
CH200_5wg17
CH200_5wg6
CH200_5wg3
CH200_5wg5
CH200_5wg9
CH200_5wg16
CH200_5wg10
CH200_5wg2
CH200v2_5'TF
CH200_5wg15
CH200_5wg14
CH200_5gp18
CH200_5wg7
CH200_5gp14
CH200_5wg23
0
1000
2000
3000
4000
Base number
F
3' Half Genome
CH200v1_3'TF
CH200_3wg9
CH200_3wg3
CH200_3wg6
CH200_3wg5
CH200_3wg16
CH200_3wg17
CH200_3wg2
CH200v2_3'TF
CH200_3wg15
CH200_3wg23
CH200_3wg14
CH200_3wg7
CH200_3wg10
T
A
C
G
Gaps
0
1000
2000
3000
4000
Base number
G
CH228v1_5'TF
CH228_5gp4
CH228_5gp8
CH228_5gp2
CH228_5gp13
CH228_5gp3
CH228_5gp5
CH228_5gp9
CH228_5gp6
CH228_5gp7
0
1000
2000
3000
4000
Base number
H
CH228v1_3'TF
CH228_3e12
CH228_3e27
CH228_3e24
CH228_3e18
CH228_3e22
CH228_3e25
CH228_3e29
CH228_3e23
CH228_3e15
CH228_3e4
CH228_3e11
CH228_3e6
CH228_3e20
CH228_3e5
CH228_3e2
CH228_3e26
CH228_3e19
CH228_3e28
CH228_3e7
CH228_3e21
CH228_3e16
CH228_3e31
CH228_3e8
CH228_3e13
CH228_3e1
0
1000
2000
3000
4000
Base number

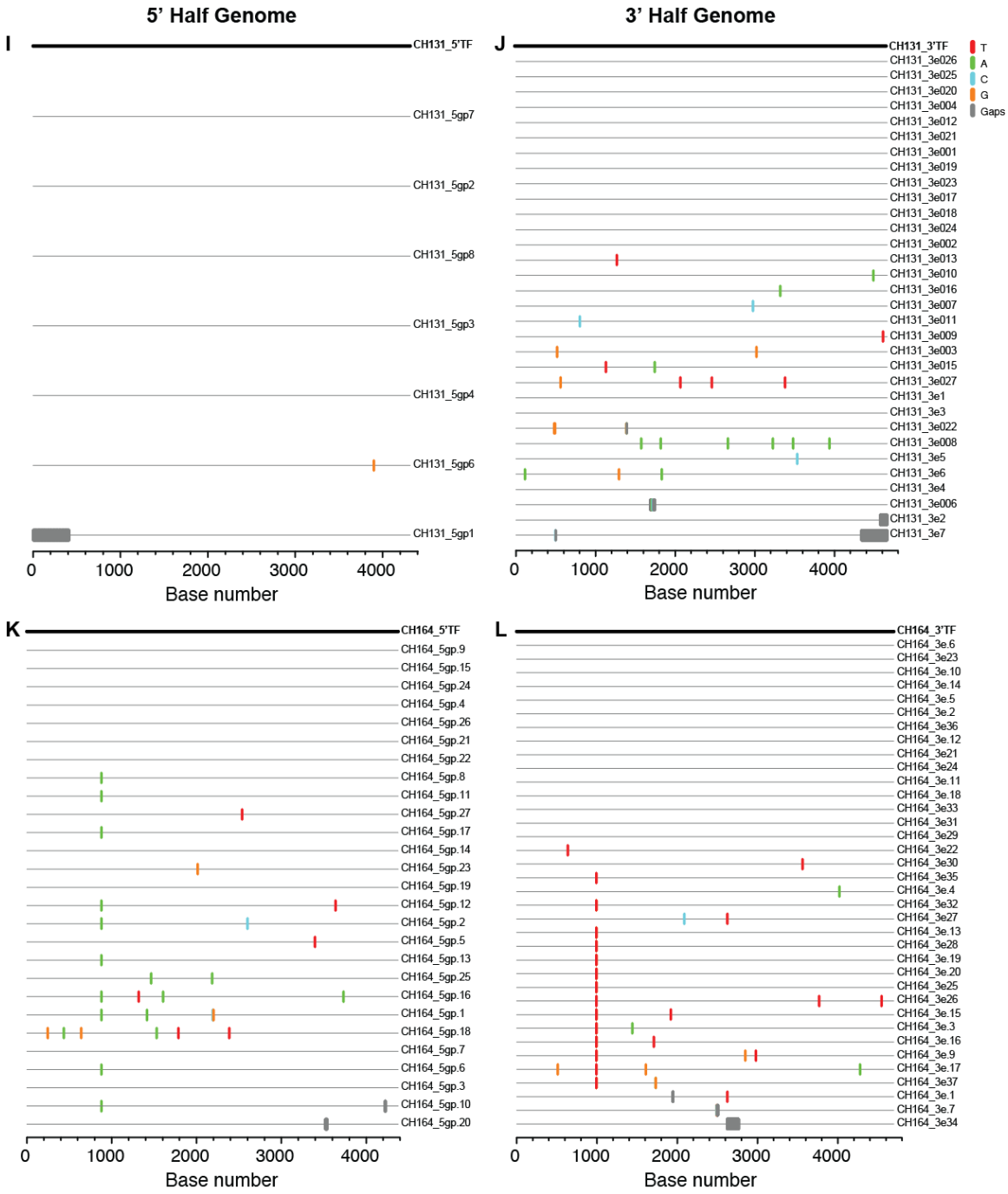
5' Half Genome
3' Half Genome
I
CH131_5'TF
CH131_5gp7
CH131_5gp2
CH131_5gp8
CH131_5gp3
CH131_5gp4
CH131_5gp6
CH131_5gp1
0
1000
2000
3000
4000
Base number
J
CH131_3'TF
CH131_3e026
CH131_3e025
CH131_3e020
CH131_3e004
CH131_3e012
CH131_3e021
CH131_3e001
CH131_3e019
CH131_3e023
CH131_3e017
CH131_3e018
CH131_3e024
CH131_3e002
CH131_3e013
CH131_3e010
CH131_3e016
CH131_3e007
CH131_3e011
CH131_3e009
CH131_3e003
CH131_3e015
CH131_3e027
CH131_3e1
CH131_3e3
CH131_3e022
CH131_3e008
CH131_3e5
CH131_3e6
CH131_3e4
CH131_3e006
CH131_3e2
CH131_3e7
T
A
C
G
Gaps
0
1000
2000
3000
4000
Base number
K
CH164_5'TF
CH164_5gp.9
CH164_5gp.15
CH164_5gp.24
CH164_5gp.4
CH164_5gp.26
CH164_5gp.21
CH164_5gp.22
CH164_5gp.8
CH164_5gp.11
CH164_5gp.27
CH164_5gp.17
CH164_5gp.14
CH164_5gp.23
CH164_5gp.19
CH164_5gp.12
CH164_5gp.2
CH164_5gp.5
CH164_5gp.13
CH164_5gp.25
CH164_5gp.16
CH164_5gp.1
CH164_5gp.18
CH164_5gp.7
CH164_5gp.6
CH164_5gp.3
CH164_5gp.10
CH164_5gp.20
0
1000
2000
3000
4000
Base number
L
CH164_3'TF
CH164_3e.6
CH164_3e23
CH164_3e.10
CH164_3e.14
CH164_3e.5
CH164_3e.2
CH164_3e36
CH164_3e.12
CH164_3e21
CH164_3e24
CH164_3e.11
CH164_3e.18
CH164_3e33
CH164_3e31
CH164_3e29
CH164_3e22
CH164_3e30
CH164_3e35
CH164_3e.4
CH164_3e32
CH164_3e27
CH164_3e.13
CH164_3e28
CH164_3e.19
CH164_3e.20
CH164_3e25
CH164_3e26
CH164_3e.15
CH164_3e.3
CH164_3e.16
CH164_3e.9
CH164_3e.17
CH164_3e37
CH164_3e.1
CH164_3e.7
CH164_3e34
0
1000
2000
3000
4000
Base number

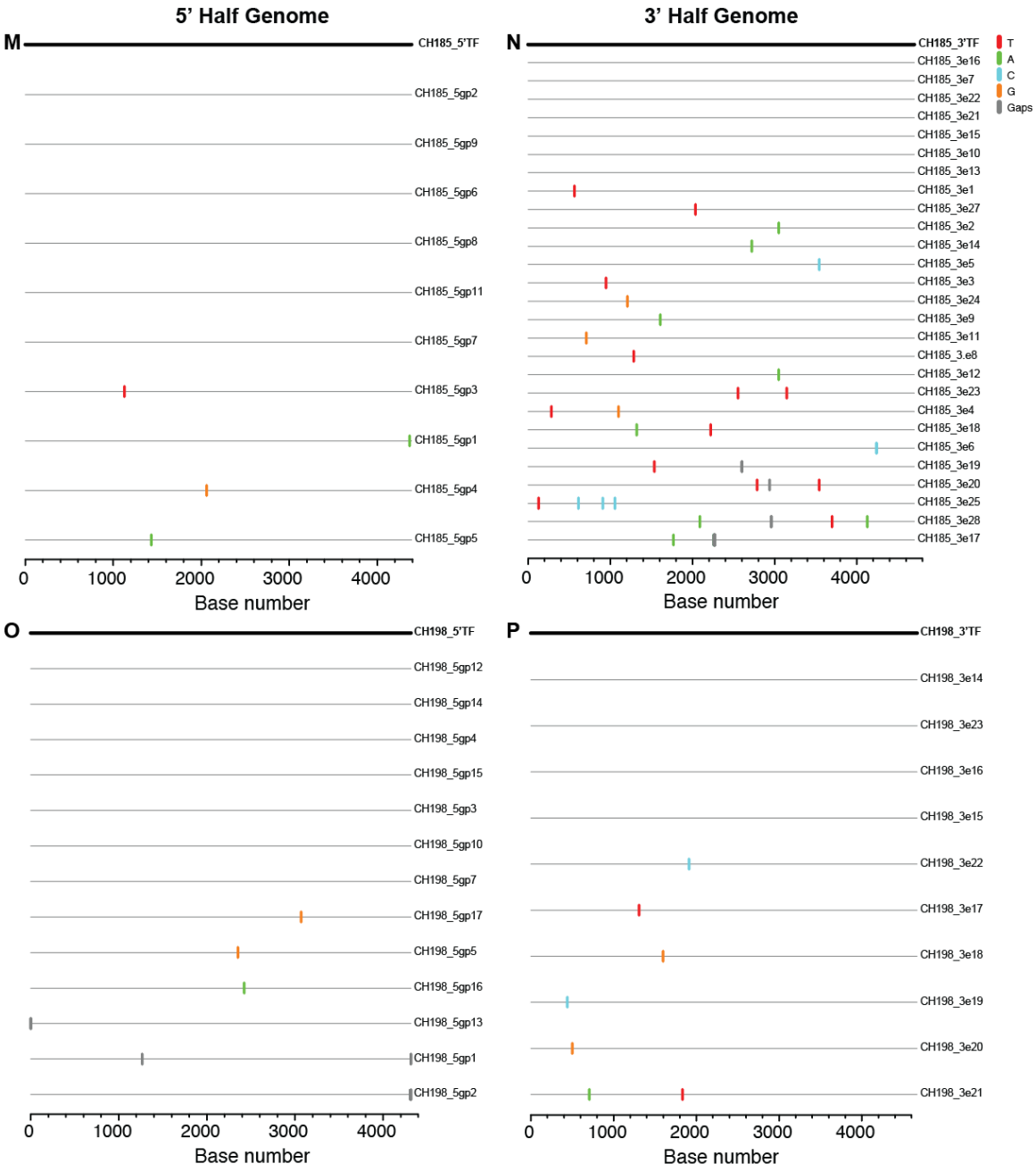
5' Half Genome
3' Half Genome
M
CH185_5'TF
CH185_5gp2
CH185_5gp9
CH185_5gp6
CH185_5gp8
CH185_5gp11
CH185_5gp7
CH185_5gp3
CH185_5gp1
CH185_5gp4
CH185_5gp5
0
1000
2000
3000
4000
Base number
N
CH185_3'TF
CH185_3e16
CH185_3e7
CH185_3e22
CH185_3e21
CH185_3e15
CH185_3e10
CH185_3e13
CH185_3e1
CH185_3e27
CH185_3e2
CH185_3e14
CH185_3e5
CH185_3e3
CH185_3e24
CH185_3e9
CH185_3e11
CH185_3.e8
CH185_3e12
CH185_3e23
CH185_3e4
CH185_3e18
CH185_3e6
CH185_3e19
CH185_3e20
CH185_3e25
CH185_3e28
CH185_3e17
T
A
C
G
Gaps
O
CH198_5'TF
CH198_5gp12
CH198_5gp14
CH198_5gp4
CH198_5gp15
CH198_5gp3
CH198_5gp10
CH198_5gp7
CH198_5gp17
CH198_5gp5
CH198_5gp16
CH198_5gp13
CH198_5gp1
CH198_5gp2
P
CH198_3'TF
CH198_3e14
CH198_3e23
CH198_3e16
CH198_3e15
CH198_3e22
CH198_3e17
CH198_3e18
CH198_3e19
CH198_3e20
CH198_3e21

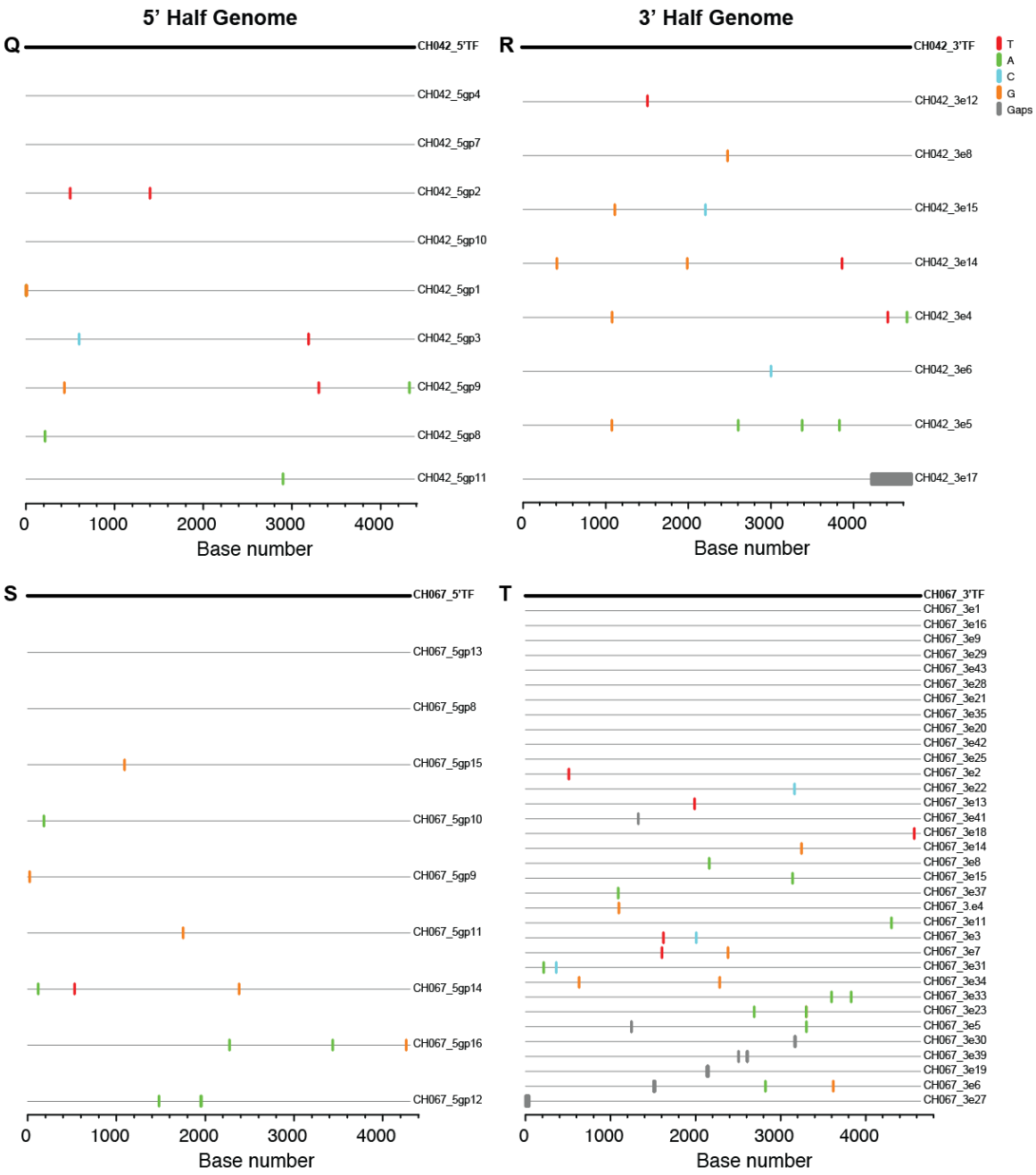
5' Half Genome
3' Half Genome
Q
CH042_5'TF
CH042_5gp4
CH042_5gp7
CH042_5gp2
CH042_5gp10
CH042_5gp1
CH042_5gp3
CH042_5gp9
CH042_5gp8
CH042_5gp11
R
CH042_3'TF
CH042_3e12
CH042_3e8
CH042_3e15
CH042_3e14
CH042_3e4
CH042_3e6
CH042_3e5
CH042_3e17
T
A
C
G
Gaps
S
CH067_5'TF
CH067_5gp13
CH067_5gp8
CH067_5gp15
CH067_5gp10
CH067_5gp9
CH067_5gp11
CH067_5gp14
CH067_5gp16
CH067_5gp12
T
CH067_3'TF
CH067_3e1
CH067_3e16
CH067_3e9
CH067_3e29
CH067_3e43
CH067_3e28
CH067_3e21
CH067_3e35
CH067_3e20
CH067_3e42
CH067_3e25
CH067_3e2
CH067_3e22
CH067_3e13
CH067_3e41
CH067_3e18
CH067_3e14
CH067_3e8
CH067_3e15
CH067_3e37
CH067_3.e4
CH067_3e11
CH067_3e3
CH067_3e7
CH067_3e31
CH067_3e34
CH067_3e33
CH067_3e23
CH067_3e5
CH067_3e30
CH067_3e39
CH067_3e19
CH067_3e6
CH067_3e27
0
1000
2000
3000
4000
Base number

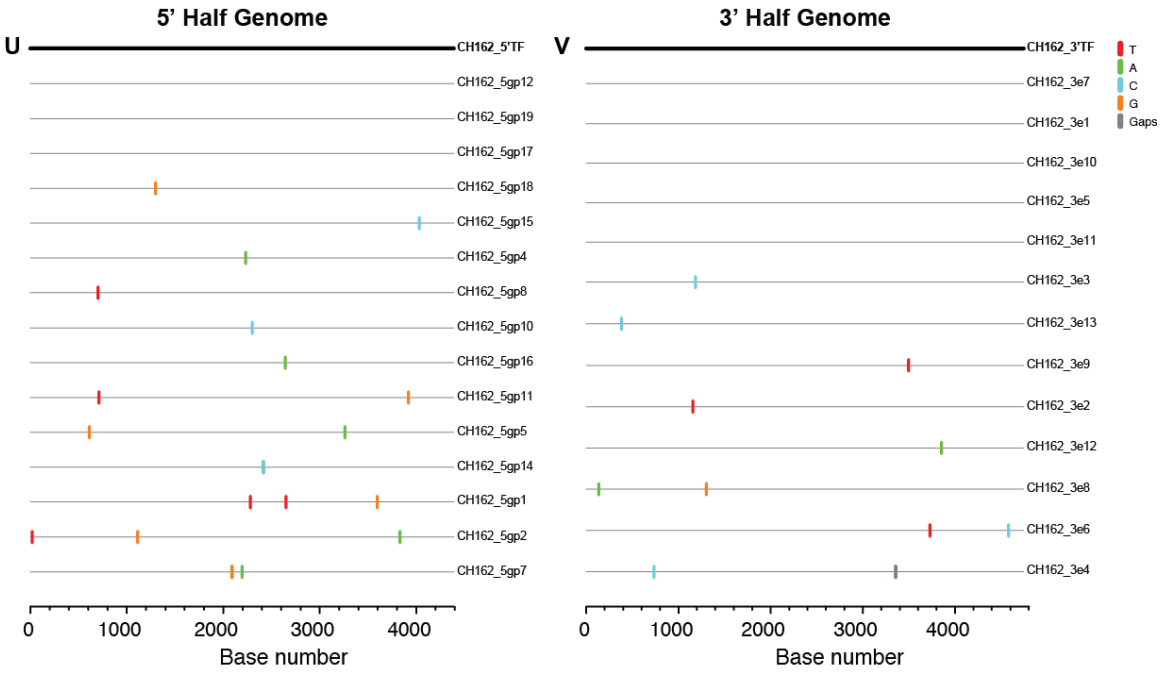

Figure 5-1. Inference of TF genome sequences. (*A*-*V*) Highlighter plots of SGA derived 5' (left panel) and 3' (right panel) half genome sequences are shown for two subjects acutely infected with subtype B (*A*-*D*) and nine subjects acutely infected with subtype C (*E*-*V*) viruses (Highlighter v2.1.1; hiv.lanl.gov); tick marks indicate differences compared to the top sequence (red, T; green, A; blue, C; orange, G; grey, gap), which is identical to the inferred TF sequence (*A, B* - CH607; *C, D* - CH470; *E, F* - CH200v1; *G, H* - CH228v1; *I, J* - CH131; *K, L* - CH164; *M, N* - CH185; *O, P* - CH198; *Q, R* - CH042; *S, T* - CH067; *U, V* - CH162). Two TF viruses were inferred from subject 703010200, with the second variant shown in bold below the sequences used to infer the first TF variant.

Table 5-1. Infectious molecular clones of mucosally transmitted founder and chronic control viruses.

Subject	IMC	Subtype	Type	Sex	Risk factor[b]	CD4 count	VL[c]	Sample date	Stage	Country of origin	# TFs	CoR[f]	Reference
AD17	AD17	B	TF	M	MSM	n/a	47,600,000	6/14/99	II[d]	USA	1	R5	204
700010040	CH040	B	TF	M	MSM	n/a	2,197,248	7/25/06	II[d]	USA	1	R5	258
700010106	CH106	B	TF	M	MSMW	n/a	84,545,454	10/19/06	II[d]	USA	1	R5	258
700010470	CH470	B	TF	M	MSM	n/a	84,193	1/25/08	IV[d]	USA	1	R5	this study
700010607	CH607	B	TF	M	MSM	n/a	8,009	7/8/08	IV[d]	USA	2	R5	this study
REJO4541	REJO	B	TF	M	HSX	n/a	722,349	9/28/01	V[d]	USA	1	R5	258
RHPA4256	RHPA	B	TF	F	HSX	n/a	1,458,354	12/5/00	V[d]	USA	1	R5	258
SUMA0874	SUMA	B	TF	M	MSM	n/a	939,260	5/13/91	II[d]	USA	1	R5	258
THRO4156	THRO	B	TF	M	MSM	n/a	5,413,140	8/1/00	V[d]	USA	1	R5	258
700010058	CH058	B	TF	M	MSM	n/a	3,565,728	9/8/06	II[d]	USA	1	R5	258
700010077	CH077	B	TF	M	MSM	n/a	394,649	8/31/06	II/III[d]	USA	1	R5/X4	258
TRJO4551	TRJO	B	TF	M	MSM	n/a	8,121,951	10/10/01	II[d]	USA	1	R5	258
WITO4160	WITO	B	TF	M	HSX	n/a	325,064	8/4/00	II[d]	USA	1	R5	258
ZM247F	ZM247Fv1	C	TF	F	HSX	n/a	10,823,500	10/28/03	II[d]	Zambia	2	R5	312
ZM247F	ZM247Fv2	C	TF	F	HSX	n/a	10,823,500	10/28/03	II[d]	Zambia	2	R5	312
704010042	CH042	C	TF	M	HSX	n/a	181,000	1/29/07	IV[d]	S. Africa	1	R5	this study
705010067	CH067	C	TF	F	HSX	n/a	639,000	1/10/07	I/II[d]	S. Africa	1	R5	this study
703010131	CH131	C	TF	M	MSMW	n/a	411,873	3/8/07	I/II[d]	Malawi	1	R5	this study
705010162	CH162	C	TF	M	HSX	n/a	13,100,000	6/22/07	III[d]	S. Africa	1	R5	this study
706010164	CH164	C	TF	M	MSMW	n/a	23,600	8/16/07	IV[d]	S. Africa	1	R5	this study
703010228	CH228v1	C	TF	M	HSX	n/a	47,549	6/1/07	III[d]	Malawi	2	R5	this study
705010185	CH185	C	TF	F	HSX	n/a	14,800	7/13/07	I/II[d]	S. Africa	1	R5	this study
705010198	CH198	C	TF	M	HSX	n/a	14,950,000	7/13/07	I/II[d]	S. Africa	1	R5	this study
703010200	CH200v1	C	TF	M	HSX	n/a	165,501	5/11/07	I/II[d]	Malawi	3	R5	this study
703010200	CH200v2	C	TF	M	HSX	n/a	165,501	5/12/07	I/II[d]	Malawi	3	R5	this study
ZM246F	ZM246F	C	TF	F	HSX	n/a	10,013,800	1/14/03	II[d]	Zambia	1	R5	312
ZM249M	ZM249M	C	TF	M	HSX	n/a	>2,000,000	8/5/03	IV[d]	Zambia	1	R5	312
STCO5453	STCOr1	B	CC	M	MSM	796	67,964	2/15/05	2[e]	USA	n/a	R5/X4	this study
STCO5453	STCOr2	B	CC	M	MSM	796	67,964	2/15/05	2[e]	USA	n/a	R5/X4	this study
WARO5662	WARO	B	CC	F	HSX	598	16,758	10/17/07	2.5[e]	USA	n/a	R5	this study
MCST4474	MCST	B	CC	M	MSM	634	29,500	7/2/07	9.5[e]	USA	n/a	R5	this study
RHGA1581	RHGA	B	CC	M	MSM	571	50,000	2/20/03	9.6[e]	USA	n/a	R5	this study
703010269	CH269	C	CC	F	HSX	195	30,434	4/9/08	n/a	Malawi	n/a	R5	this study
702010293	CH293	C	CC	F	HSX	339[g]	27,169	4/1/08	n/a	Malawi	n/a	R5	this study
702010432	CH432	C	CC	M	HSX	261[g]	40,570	5/7/08	n/a	Malawi	n/a	R5	270
702010440	CH440	C	CC	F	HSX	125[g]	25,583	5/12/08	n/a	Malawi	n/a	R5	this study
705010534	CH534	C	CC	F	HSX	303[g]	63,300	8/26/08	n/a	S. Africa	n/a	R5	270
702010141	CH141	C	CC	F	HSX	326[h]	151,282	11/13/07	n/a	Malawi	n/a	R5	this study
703010167	CH167	C	CC	F	HSX	358[g]	73,505	5/24/07	n/a	Malawi	n/a	R5	this study
703010256	CH256y2	C	CC	F	HSX	531	28,066	6/30/09	2[e]	Malawi	n/a	R5	270
707010457	CH457	C	CC	F	HSX	450[g]	234,671	6/10/08	n/a	Tanzania	n/a	R5	270

[a] TF, transmitted founder; CC, chronic control.
[b]MSM, men who have sex with men; HSX, heterosexual exposure; MSMW, men who have sex with men and women.
[c] VL= viral load (RNA copies per ml of plasma).
[d]defined in (112).
[e]duration of infection is given in years; n/a, data not available.
[f]coreceptor tropism as determined by AMD3100 and TAK779 inhibition: R5, CCR5 tropic; R5/X5 = CCR5/CXCR4 dual tropic.
[g]average CD4 count from samples taken before and after IMC generation.
[h]a single CD4 count is available for a sample taken 12 weeks prior to IMC generation.

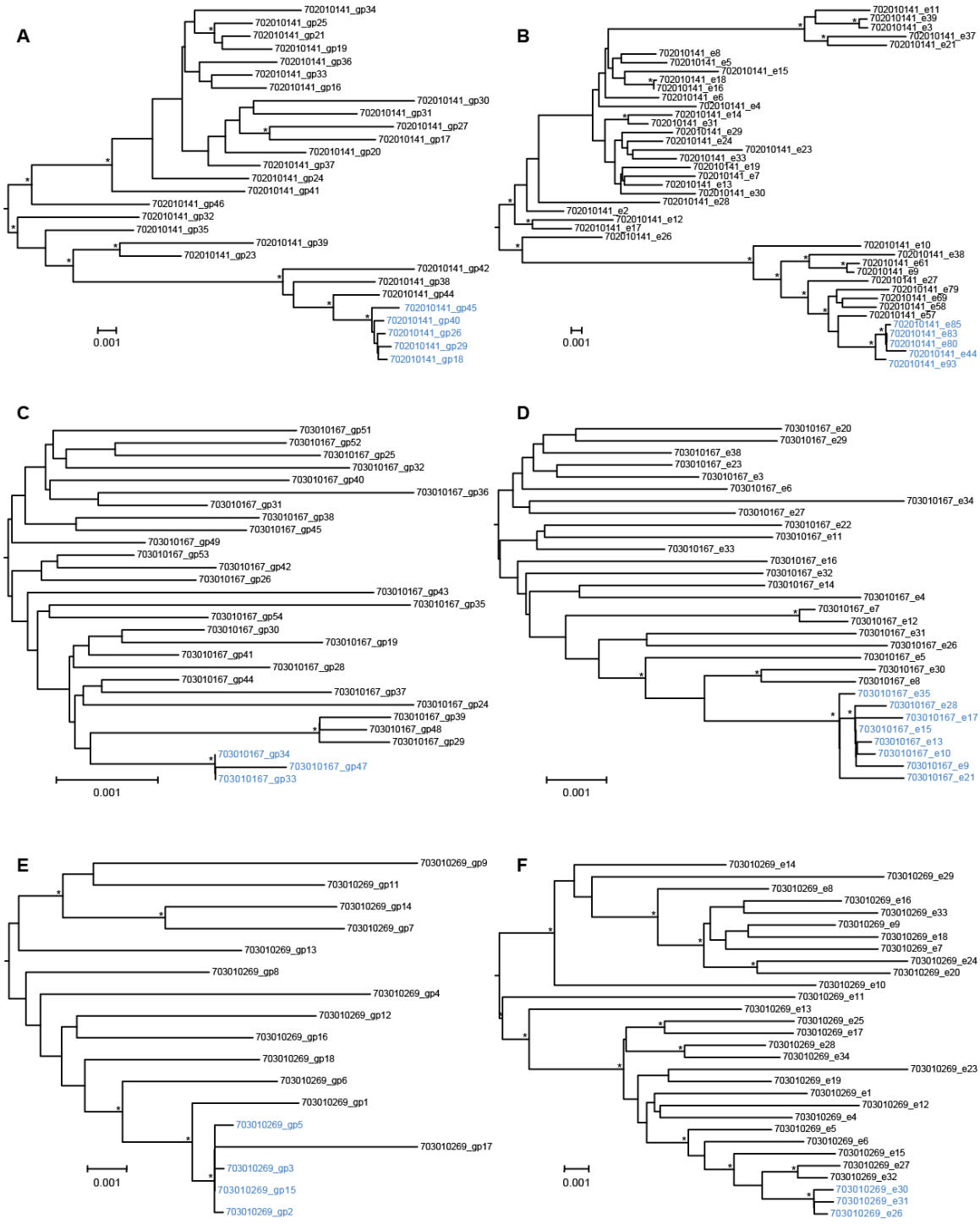
A
702010141_gp34
702010141_gp25
702010141_gp21
702010141_gp19
702010141_gp36
702010141_gp33
702010141_gp16
702010141_gp30
702010141_gp31
702010141_gp27
702010141_gp17
702010141_gp20
702010141_gp37
702010141_gp24
702010141_gp41
702010141_gp46
702010141_gp32
702010141_gp35
702010141_gp39
702010141_gp23
702010141_gp42
702010141_gp38
702010141_gp44
702010141_gp45
702010141_gp40
702010141_gp26
702010141_gp29
702010141_gp18
0.001
B
702010141_e11
702010141_e39
702010141_e3
702010141_e37
702010141_e21
702010141_e8
702010141_e5
702010141_e15
702010141_e18
702010141_e16
702010141_e6
702010141_e4
702010141_e14
702010141_e31
702010141_e29
702010141_e24
702010141_e23
702010141_e33
702010141_e19
702010141_e7
702010141_e13
702010141_e30
702010141_e28
702010141_e2
702010141_e12
702010141_e17
702010141_e26
702010141_e10
702010141_e38
702010141_e61
702010141_e9
702010141_e27
702010141_e79
702010141_e69
702010141_e58
702010141_e57
702010141_e85
702010141_e83
702010141_e80
702010141_e44
702010141_e93
0.001
C
703010167_gp51
703010167_gp52
703010167_gp25
703010167_gp32
703010167_gp40
703010167_gp36
703010167_gp31
703010167_gp38
703010167_gp45
703010167_gp49
703010167_gp53
703010167_gp42
703010167_gp26
703010167_gp43
703010167_gp35
703010167_gp54
703010167_gp30
703010167_gp19
703010167_gp41
703010167_gp28
703010167_gp44
703010167_gp37
703010167_gp24
703010167_gp39
703010167_gp48
703010167_gp29
703010167_gp34
703010167_gp47
703010167_gp33
0.001
D
703010167_e20
703010167_e29
703010167_e38
703010167_e23
703010167_e3
703010167_e6
703010167_e34
703010167_e27
703010167_e22
703010167_e11
703010167_e33
703010167_e16
703010167_e32
703010167_e14
703010167_e4
703010167_e7
703010167_e12
703010167_e31
703010167_e26
703010167_e5
703010167_e30
703010167_e8
703010167_e35
703010167_e28
703010167_e17
703010167_e15
703010167_e13
703010167_e10
703010167_e9
703010167_e21
0.001
E
703010269_gp9
703010269_gp11
703010269_gp14
703010269_gp7
703010269_gp13
703010269_gp8
703010269_gp4
703010269_gp12
703010269_gp16
703010269_gp18
703010269_gp6
703010269_gp1
703010269_gp5
703010269_gp17
703010269_gp3
703010269_gp15
703010269_gp2
0.001
F
703010269_e14
703010269_e29
703010269_e8
703010269_e16
703010269_e33
703010269_e9
703010269_e18
703010269_e7
703010269_e24
703010269_e20
703010269_e10
703010269_e11
703010269_e13
703010269_e25
703010269_e17
703010269_e28
703010269_e34
703010269_e23
703010269_e19
703010269_e1
703010269_e12
703010269_e4
703010269_e5
703010269_e6
703010269_e15
703010269_e27
703010269_e32
703010269_e30
703010269_e31
703010269_e26
0.001

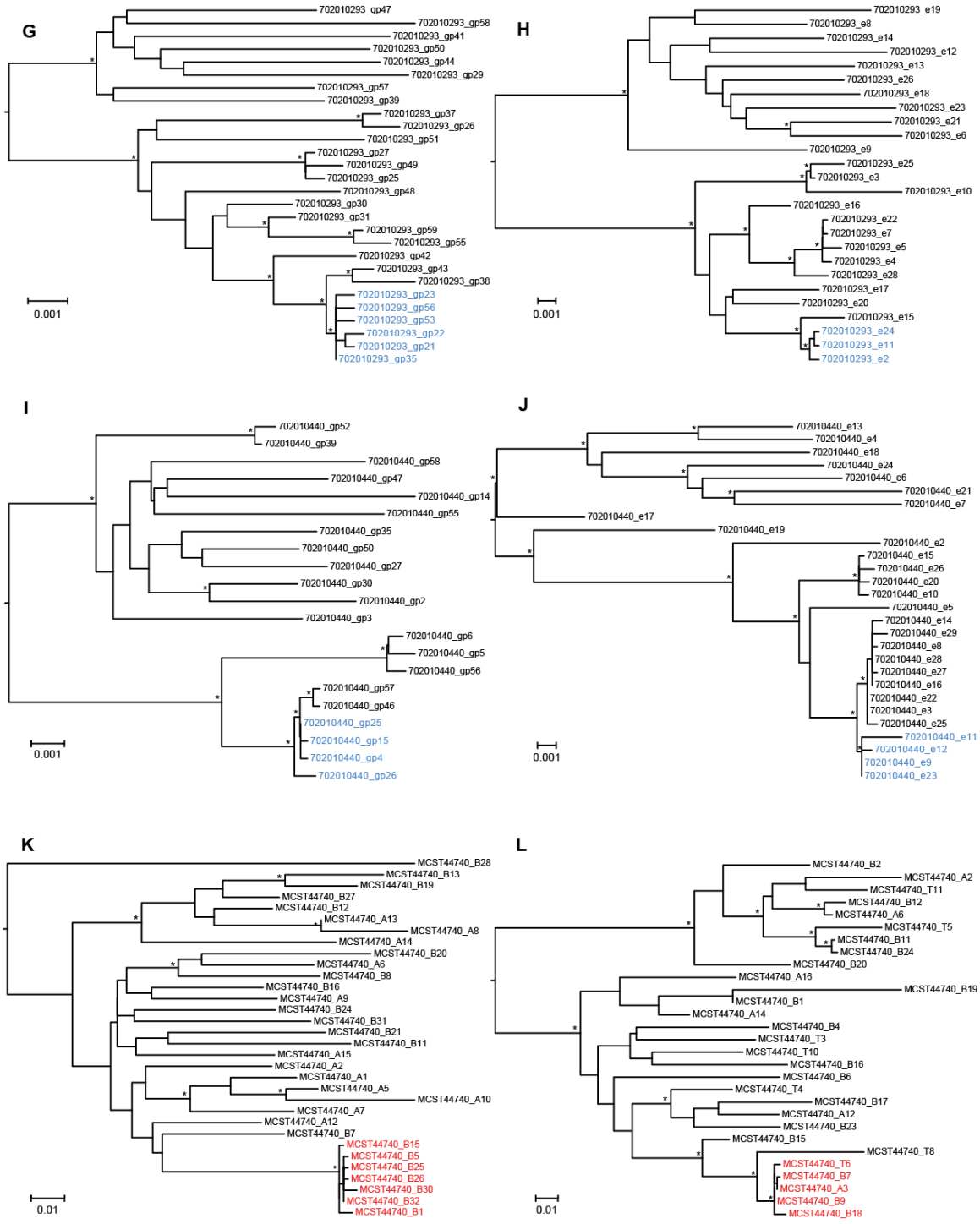
G
702010293_gp47
702010293_gp58
702010293_gp41
702010293_gp50
702010293_gp44
702010293_gp29
702010293_gp57
702010293_gp39
702010293_gp37
702010293_gp26
702010293_gp51
702010293_gp27
702010293_gp49
702010293_gp25
702010293_gp48
702010293_gp30
702010293_gp31
702010293_gp59
702010293_gp55
702010293_gp42
702010293_gp43
702010293_gp38
702010293_gp23
702010293_gp56
702010293_gp53
702010293_gp22
702010293_gp21
702010293_gp35
0.001
H
702010293_e19
702010293_e8
702010293_e14
702010293_e12
702010293_e13
702010293_e26
702010293_e18
702010293_e23
702010293_e21
702010293_e6
702010293_e9
702010293_e25
702010293_e3
702010293_e10
702010293_e16
702010293_e22
702010293_e7
702010293_e5
702010293_e4
702010293_e28
702010293_e17
702010293_e20
702010293_e15
702010293_e24
702010293_e11
702010293_e2
0.001
I
702010440_gp52
702010440_gp39
702010440_gp58
702010440_gp47
702010440_gp14
702010440_gp55
702010440_gp35
702010440_gp50
702010440_gp27
702010440_gp30
702010440_gp2
702010440_gp3
702010440_gp6
702010440_gp5
702010440_gp56
702010440_gp57
702010440_gp46
702010440_gp25
702010440_gp15
702010440_gp4
702010440_gp26
0.001
J
702010440_e13
702010440_e4
702010440_e18
702010440_e24
702010440_e6
702010440_e21
702010440_e7
702010440_e17
702010440_e19
702010440_e2
702010440_e15
702010440_e26
702010440_e20
702010440_e10
702010440_e5
702010440_e14
702010440_e29
702010440_e8
702010440_e28
702010440_e27
702010440_e16
702010440_e22
702010440_e3
702010440_e25
702010440_e11
702010440_e12
702010440_e9
702010440_e23
0.001
K
MCST44740_B28
MCST44740_B13
MCST44740_B19
MCST44740_B27
MCST44740_B12
MCST44740_A13
MCST44740_A8
MCST44740_A14
MCST44740_B20
MCST44740_A6
MCST44740_B8
MCST44740_B16
MCST44740_A9
MCST44740_B24
MCST44740_B31
MCST44740_B21
MCST44740_B11
MCST44740_A15
MCST44740_A2
MCST44740_A1
MCST44740_A5
MCST44740_A10
MCST44740_A7
MCST44740_A12
MCST44740_B7
MCST44740_B15
MCST44740_B5
MCST44740_B25
MCST44740_B26
MCST44740_B30
MCST44740_B32
MCST44740_B1
0.01
L
MCST44740_B2
MCST44740_A2
MCST44740_T11
MCST44740_B12
MCST44740_A6
MCST44740_T5
MCST44740_B11
MCST44740_B24
MCST44740_B20
MCST44740_A16
MCST44740_B19
MCST44740_B1
MCST44740_A14
MCST44740_B4
MCST44740_T3
MCST44740_T10
MCST44740_B16
MCST44740_B6
MCST44740_T4
MCST44740_B17
MCST44740_A12
MCST44740_B23
MCST44740_B15
MCST44740_T8
MCST44740_T6
MCST44740_B7
MCST44740_A3
MCST44740_B9
MCST44740_B18
0.01

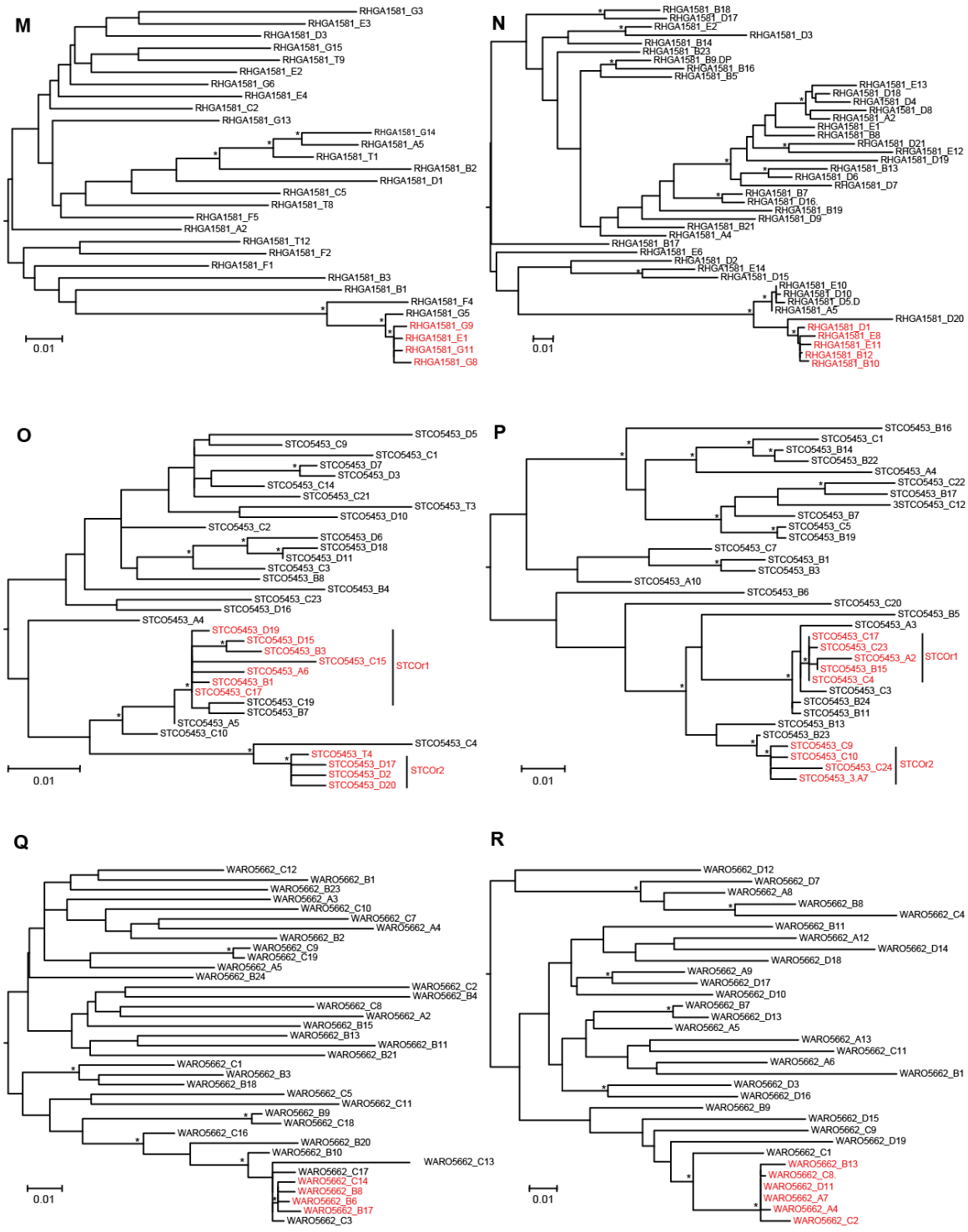
M
RHGA1581_G3
RHGA1581_E3
RHGA1581_D3
RHGA1581_G15
RHGA1581_T9
RHGA1581_E2
RHGA1581_G6
RHGA1581_E4
RHGA1581_C2
RHGA1581_G13
RHGA1581_G14
RHGA1581_A5
RHGA1581_T1
RHGA1581_B2
RHGA1581_D1
RHGA1581_C5
RHGA1581_T8
RHGA1581_F5
RHGA1581_A2
RHGA1581_T12
RHGA1581_F2
RHGA1581_F1
RHGA1581_B3
RHGA1581_B1
RHGA1581_F4
RHGA1581_G5
RHGA1581_G9
RHGA1581_E1
RHGA1581_G11
RHGA1581_G8
0.01
N
RHGA1581_B18
RHGA1581_D17
RHGA1581_E2
RHGA1581_D3
RHGA1581_B14
RHGA1581_B23
RHGA1581_B9.DP
RHGA1581_B16
RHGA1581_B5
RHGA1581_E13
RHGA1581_D18
RHGAT581_D4
RHGA1581_D8
RHGA1581_A2
RHGA1581_E1
RHGA1581_B8
RHGA1581_D21
RHGA1581_E12
RHGA1581_D19
RHGA1581_B13
RHGA1581_D6
RHGA1581_D7
RHGA1581_B7
RHGA1581_D16.
RHGA1581_B19
RHGA1581_D9
RHGA1581_B21
RHGA1581_A4
RHGA1581_B17
RHGA1581_E6
RHGA1581_D2
RHGA1581_E14
RHGA1581_D15
RHGA1581_E10
RHGA1581_D10
RHGA1581_D5.D
RHGA1581_A5
RHGA1581_D20
RHGA1581_D1
RHGA1581_E8
RHGA1581_E11
RHGA1581_B12
RHGA1581_B10
0.01
O
STCO5453_D5
STCO5453_C9
STCO5453_C1
STCO5453_D7
STCO5453_D3
STCO5453_C14
STCO5453_C21
STCO5453_T3
STCO5453_D10
STCO5453_C2
STCO5453_D6
STCO5453_D18
STCO5453_D11
STCO5453_C3
STCO5453_B8
STCO5453_B4
STCO5453_C23
STCO5453_D16
STCO5453_A4
STCO5453_D19
STCO5453_D15
STCO5453_B3
STCO5453_C15
STCO5453_A6
STCO5453_B1
STCO5453_C17
STCOr1
STCO5453_C19
STCO5453_B7
STCO5453_A5
STCO5453_C10
STCO5453_C4
STCO5453_T4
STCO5453_D17
STCO5453_D2
STCO5453_D20
STCOr2
0.01
P
STCO5453_B16
STCO5453_C1
STCO5453_B14
STCO5453_B22
STCO5453_A4
STCO5453_C22
STCO5453_B17
3STCO5453_C12
STCO5453_B7
STCO5453_C5
STCO5453_B19
STCO5453_C7
STCO5453_B1
STCO5453_B3
STCO5453_A10
STCO5453_B6
STCO5453_C20
STCO5453_B5
STCO5453_A3
STCO5453_C17
STCO5453_C23
STCO5453_A2
STCOr1
STCO5453_B15
STCO5453_C4
STCO5453_C3
STCO5453_B24
STCO5453_B11
STCO5453_B13
STCO5453_B23
STCO5453_C9
STCO5453_C10
STCO5453_C24
STCOr2
STCO5453_3.A7
0.01
Q
WARO5662_C12
WARO5662_B1
WARO5662_B23
WARO5662_A3
WARO5662_C10
WARO5662_C7
WARO5662_A4
WARO5662_B2
WARO5662_C9
WARO5662_C19
WARO5662_A5
WARO5662_B24
WARO5662_C2
WARO5662_B4
WARO5662_C8
WARO5662_A2
WARO5662_B15
WARO5662_B13
WARO5662_B11
WARO5662_B21
WARO5662_C1
WARO5662_B3
WARO5662_B18
WARO5662_C5
WARO5662_C11
WARO5662_B9
WARO5662_C18
WARO5662_C16
WARO5662_B20
WARO5662_B10
WARO5662_C13
WARO5662_C17
WARO5662_C14
WARO5662_B8
WARO5662_B6
WARO5662_B17
WARO5662_C3
0.01
R
WARO5662_D12
WARO5662_D7
WARO5662_A8
WARO5662_B8
WARO5662_C4
WARO5662_B11
WARO5662_A12
WARO5662_D14
WARO5662_D18
WARO5662_A9
WARO5662_D17
WARO5662_D10
WARO5662_B7
WARO5662_D13
WARO5662_A5
WARO5662_A13
WARO5662_C11
WARO5662_A6
WARO5662_B1
WARO5662_D3
WARO5662_D16
WARO5662_B9
WARO5662_D15
WARO5662_C9
WARO5662_D19
WARO5662_C1
WARO5662_B13
WARO5662_C8.
WARO5662_D11
WARO5662_A7
WARO5662_A4
WARO5662_C2
0.01

Figure 5-2. Inference of CC genome sequences. The phylogenetic relationships of SGA-derived 5' and 3' half genome sequences from chronically infected subjects are shown. Trees composed of 5' (*A, C, E, G, I, K, M, O, Q*) and 3' (*B, D, F, H, J, L, N, P, R*) half genome sequences were constructed using maximum likelihood methods. Sequences highlighted in blue (subtype C) and red (subtype B) represent clonal viral expansions that were used to generate half genome consensus sequences for each subject (*A, B* - 702010141; *C, D* - 703010167; *E, F* - 703010269; *H, G* 702010293; *I, J* - 702010440; *K, L* - MSCT4474; *M, N* - RHGA1581; *O, P* - STCO5453; *Q, R* - WARO5662). These consensus sequences, which were identical in a 1 kb region of overlap, were chemically synthesized and combined to generate full-length IMCs. Asterisks indicate bootstrap support of greater than 70% (the scale bar represents 0.001 or 0.01 substitutions per site as indicated).

To determine the coreceptor usage of the 22 new IMCs, we infected CCR5 and CXCR4 expressing reporter cells both in the presence and absence of their respective inhibitors (176). Consistent with previous analyses of Env pseudotypes (171, 176, 270, 372), the results indicated that all IMCs were CCR5 tropic, except for one TF and two CC viruses that were dual tropic for CCR and CXCR4 (Table 5-1).

Phenotypic studies. All biological experiments were performed using viral stocks that were CD4+ T cell derived, sucrose cushion purified and depleted of CD45+ microvesicles. Virus was quantified by measuring reverse transcriptase (RT) activity, viral RNA (vRNA) copy number and p24 antigen content. Comparing these values, we noticed that subtype C stocks appeared to contain about 5-fold less p24 antigen per unit of RT activity than subtype B stocks (Fig. 5-3*A*). This discrepancy was also seen when p24 antigen was normalized using RNA copy numbers (Fig. 5-3*B*). However, no such difference was observed when virion RT activity was compared to RNA copy number (Fig. 5-3*C* and *D*). Similar results were obtained when viral stocks were tested in two additional p24 detection assays (Fig. 5-3*E* and *F*). Thus, three commonly used p24 capture assays recognized subtype C core proteins considerably less efficiently than subtype B core proteins, leading to a systematic underestimation of the number of viral particles in subtype C viral stocks. We therefore used RT activity to normalize virus input and measure virus replication in all subsequent experiments.

To determine whether TF and CC viruses differed in their phenotypic properties, we used two complementary statistical approaches. First, we used a conservative non-parametric permutation test (perm test) to address the central question of whether TF and CC viruses exhibited reproducible phenotypic differences. Second, we used a generalized linear model (GLM) to test for interactions between different parameters such as subtype and cell donors in replicate experiments, and to test for the independence of viruses from the same subjects. Since both virus status (TF or CC) and subtype (B or C) influenced the biological outcome, the GLM test allowed us to interpret the data with these variables taken into account.

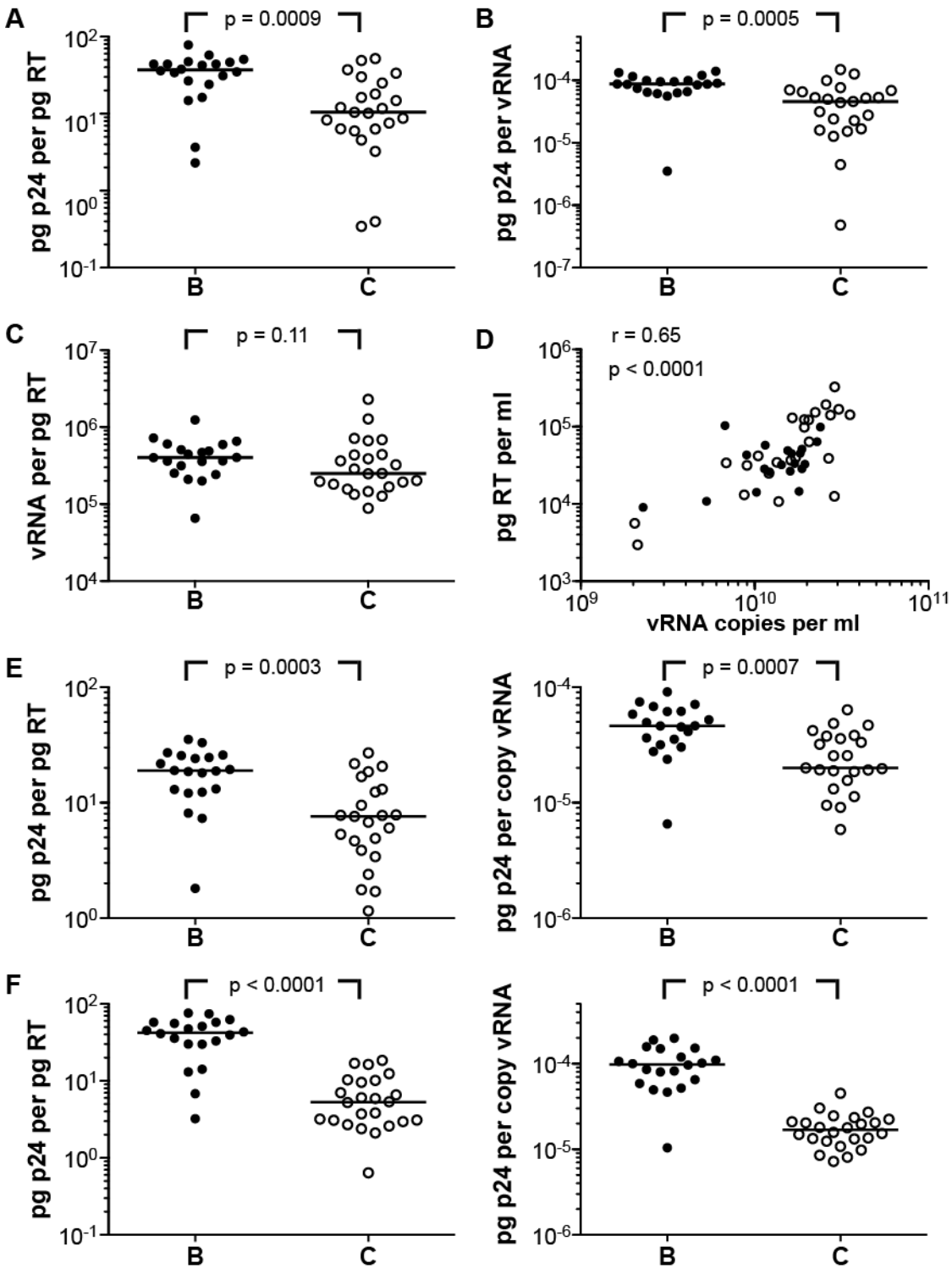
A
p = 0.0009
pg p24 per pg RT
B
C
B
p = 0.0005
pg p24 per vRNA
B
C
C
p = 0.11
vRNA per pg RT
B
C
D
r = 0.65
p < 0.0001
pg RT per ml
vRNA copies per ml
E
p = 0.0003
pg p24 per pg RT
B
C
p = 0.0007
pg p24 per copy vRNA
B
C
F
p < 0.0001
pg p24 per pg RT
B
C
p < 0.0001
pg p24 per copy vRNA
B
C

Figure 5-3. Virus quantification by p24 capture, RT activity and RNA content. For each virus stock, p24 antigen content (measured in picogram), RT activity (measured in picograms), and viral RNA (vRNA) copy number were determined. Individual panels compare these values for subtype B (solid circles) and subtype C (open circles) viruses, respectively. p24 antigen content was measured by alphaLISA (panels A and B; results are shown for four independent experiments), Alliance ELISA (panel E; results are shown for two independent experiments) and a method described by Grivel et al. (panel F; results are shown for two independent experiments). RT activity was measured using the colorimetric Roche Reverse Transcriptase Assay (results from three independent experiments are shown). Viral RNA copies were measured by the Roche COBAS AmpliPrep/COBAS Taqman HIV-1 v. 2.0 test at different viral dilutions (results from one experiment are shown). Values for subtype B and C viruses were compared using a Mann-Whitney test (*p*-values are indicated). Panel D depicts the relationship between vRNA copies per ml (*x*-axis) and pg RT activity per ml (*y*-axis) for each virus stock, with Spearman's correlation coefficient and *p*-value indicated.

Transmitted founder viruses exhibit enhanced infectivity. Plasma virus collected during ramp-up stages of acute SIVmac infection has been shown to be significantly more infectious than virus collected from later plasma samples (217). To examine whether this was also true for HIV-1, we used a single round infection assay to determine whether TF virions were more infectious on a per-particle basis than CC virions. Serial dilutions of CD4+ T cell derived viral stocks were used to infect TZM-bl cells (which express luciferase under the control of an HIV-1 promoter) and the resulting relative light units (RLUs) were expressed as a function of the input RT activity. The results showed that TF viruses as a group were 1.7-fold more infectious than CC viruses (Fig. 5-4*A*), although this difference was only marginally significant (p=0.049 by perm test; p=0.062 by GLM). Similar results were obtained when subtype B and C viruses were considered separately (there was no subtype dependence of infectivity by GLM, Fig. 5-4*B*). To enhance virus infectivity, we repeated these experiments in the presence of diethylaminoethyl (DEAE) dextran, which is known to increase virion attachment to target cells (186, 278). As expected, DEAE dextran increased the per particle infectivity of all viruses by up to three orders of magnitude (Fig. 5-4*C*), with a significantly greater effect on subtype C than subtype B virions (p=0.015 by GLM; Fig. 5-4*D*). However, in the presence of DEAE dextran the marginally significant difference between TF and CC viruses shifted to non-significance (p=0.068 by perm test; 0.083 by GLM). Taken together, these data indicate that TF viruses are on average twice as infectious as viruses that persist during chronic infection. However, when normal barriers to cell-free infection were mitigated by DEAE dextran, this difference was no longer significant, although a trend was still evident.

Transmitted founder virions have a higher Env content. Previous computational analyses of TF and CC *env* gene sequences revealed genetic signatures in TF viruses that increased Env expression and particle incorporation when tested in the context of pseudoviruses (10). We thus examined whether TF virions packaged more Env per particle than CC virions. To detect both subtype B and C Env proteins with comparable efficiency, we developed a new enzyme-linked immunosorbent assay (ELISA) that utilized antibodies previously shown to bind genetically highly

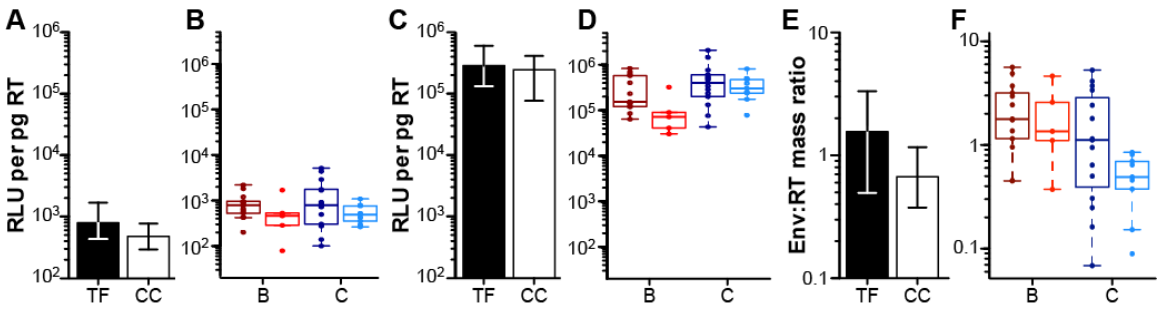

Figure 5-4. Virion infectivity and Env content. (*A-D*) Infectivity values for TF and CC viruses (*x*-axis) are expressed as relative light units (RLU) per picogram (pg) of viral RT activity (*y*-axis). (*A*) Bars indicate the median infectivity of TF (filled) and CC (open) viruses, with interquartile ranges indicated. TF were 1.7-fold more infectious than CC viruses (p=0.049). (*B*) Infectivity values are shown for each virus. Subtype B and C viruses are shown in red and blue, with TF viruses indicated in dark red and CC viruses in light blue, respectively. Values indicate averages from four independent experiments. (*C, D*) Infectivity values are shown for TF and CC viruses as in panels *A* and *B*, except infections were performed in the presence of DEAE dextran. Values indicate averages from three independent experiments. (*E, F*) Env content of TF and CC virions (x-axis) is expressed as the mass ratio of Env and RT content (*y*-axis). (*E*) Bars indicate the median values of Env content for TF (filled) and CC (open) viruses, with interquartile ranges indicated. TF viruses contained 1.9 times more Env per unit of RT activity than CC viruses (p=0.048). (*F*) Env content is shown for each virus and color-coded as in *B* and *D*. Values indicate averages from two independent experiments.

diverse envelope (gp120) proteins. To capture Env, we used CD4-218.3-E51, a chimeric antibody that contains the first (D1) and second (D2) domains of human CD4 linked to the CD4-induced (CD4i) monoclonal E51 (370). To detect bound Env, we selected affinity-purified anti-gp120-specific polyclonal antibodies that were isolated from human plasma (Advanced Bioscience Laboratories, Inc.). Using this ELISA, we found that TF viruses contained 1.9 times more Env per unit of RT activity than CC viruses (Fig. 5-4*E*), although these differences were only marginally significant (p=0.048 by perm test; p=0.057 by GLM). Subtype B viruses appeared to package 2.4-fold more Env per particle than subtype C viruses (Fig. 5-4*F*). However, this was largely due to a binding preference of the capture antibody, which recognized subtype B Env glycoproteins twice more efficiently than subtype C Env glycoproteins. Nonetheless, this subtype bias did not affect the differential between TF and CC viruses, which was seen for both subtypes B and C, and was controlled for in the statistical analyses (Fig. 5-4*F*). As expected, there also was a significant correlation between Env content and particle infectivity (r=0.33; p=0.036).

Transmitted founder viruses bind dendritic cells more efficiently. DCs have been proposed to play an important role in HIV-1 transmission, since they are located in the mucosa (105, 160, 169), capture viruses using lectins (123, 356) and glycosphingolipid receptors (289), and efficiently transmit infectious particles to CD4+ T cells (19, 50, 106). To examine whether TF and CC viruses differ in their ability to bind DCs, we pulsed immature monocyte-derived DCs (moDCs) with equal amounts of virus (normalized by RT activity), washed the cells extensively to remove cell-free virions, and then lysed the cells to quantify the amount of cell-associated virus. Using cells from three different donors (Fig. 5-5*A*), we found that moDCs captured TF viruses 1.6-times more efficiently than CC viruses (p=0.040 by perm. test; p=0.060 by GLM). This increase was observed for both subtype B and C TF viruses (Fig. 5-5*B*), although subtype B viruses were captured 3.4-times more efficiently than subtype C viruses (p=4.6 x 10^{-6} by GLM; Fig. 5-5*B*).

Because in the above experiment we had normalized virus input by RT activity, but had measured virion capture using the more sensitive p24 assay, we considered the possibility that the subtype-specific differences were an artifact of the p24 antigen capture assay. To explore

this, we repeated the binding experiment with cells from three additional donors, but this time normalizing virus input by p24 content (Fig. 5-5*C* and *D*). Despite adding an estimated 5-fold excess of subtype C virions, TF viruses were again captured 1.8-times more efficiently than CC viruses (p=0.030 by perm test; p=0.014 by GLM). Moreover, there was still a subtype specific difference, with subtype B viruses being captured 1.9-times more efficiently than subtype C viruses (p=0.0029 by GLM). As a control, we treated an aliquot of the pulsed moDCs with 0.25% trypsin-EDTA, and showed that this removed all detectable cell-associated virus, confirming that most of the DC-associated virus was surface-exposed (279). We also cultured virus-exposed moDCs for nine days and showed that moDCs were not productively infected. Finally, we asked whether the percentage of captured virus for each strain correlated between different donors. This was indeed the case, regardless of whether virus input was normalized by RT activity or p24 content, thus validating the DC binding assay (Fig. 5-6*A*).

Although the combined data from all six donors indicated that DCs captured TF viruses 1.7 fold more efficiently as CC viruses (p=0.035 by perm test; p=0.005 by GLM), there was considerable donor variability, with moDCs from donors A and F failing to yield significant binding differences (Fig. 5-5*B* and *D*). To examine potential reasons, we compared surface expression levels of DC-SIGN (dendritic cell-specific intracellular adhesion molecule-3-grabbing non-integrin) and macrophage mannose receptor by flow cytometry. Interestingly, moDCs of donors A and F expressed lower levels of these molecules (Fig. 5-6*B* and *C*), suggesting that the number of Env-specific binding sites on their cells was limited. For the remaining four donors, moDC virus capture tended to correlate with particle Env content (Fig. 5-6*D*). These data suggest that virion Env content represents an important determinant in moDCs binding, although expression of lectins and other factors clearly also play a role (142).

To examine the efficiency of virus transfer from moDC to CD4+ T cells, we pulsed moDCs with equivalent amounts of TF and CC viruses, co-cultured these cells with autologous CD4+ T cells, and then measured RT activity in culture supernatants as an indicator of virus replication. Analysis of cells from two different donors showed that TF viruses replicated to

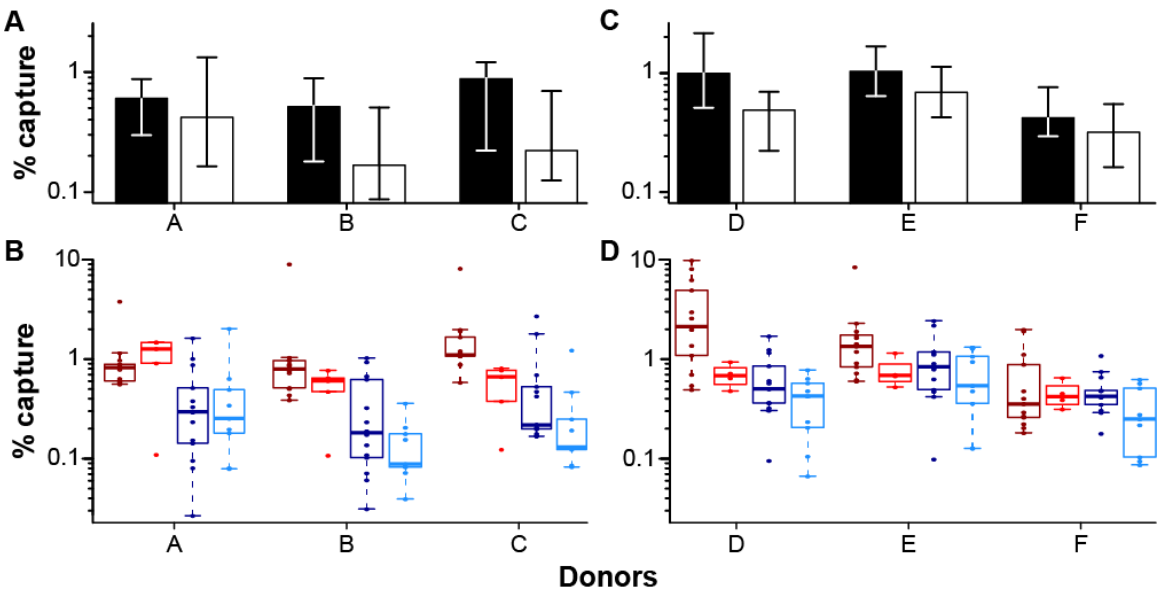

Figure 5-5. Monocyte derived dendritic cell binding. The percent of captured TF and CC virus is plotted (*y*-axis) for moDC cell preparations from six different donors (*A*-*F*) (*x*-axis). (*A, B*) Virus input was normalized by RT activity. (*C, D*) Virus input was normalized by p24 content. (*A, C*) Bars indicate median values of moDC capture for TF (filled) and CC (open) viruses, with interquartile ranges indicated. TF viruses were captured 1.7 fold more efficiently than CC viruses (p=0.035). (*B, D*) Values are plotted for each virus individually (color coding for TF and CC viruses from subtypes B and C as in Fig. 5-4). Subtype B viruses were captured 3.4-times more efficiently than subtype C viruses (p=4.6 x 10^{-6} by GLM).

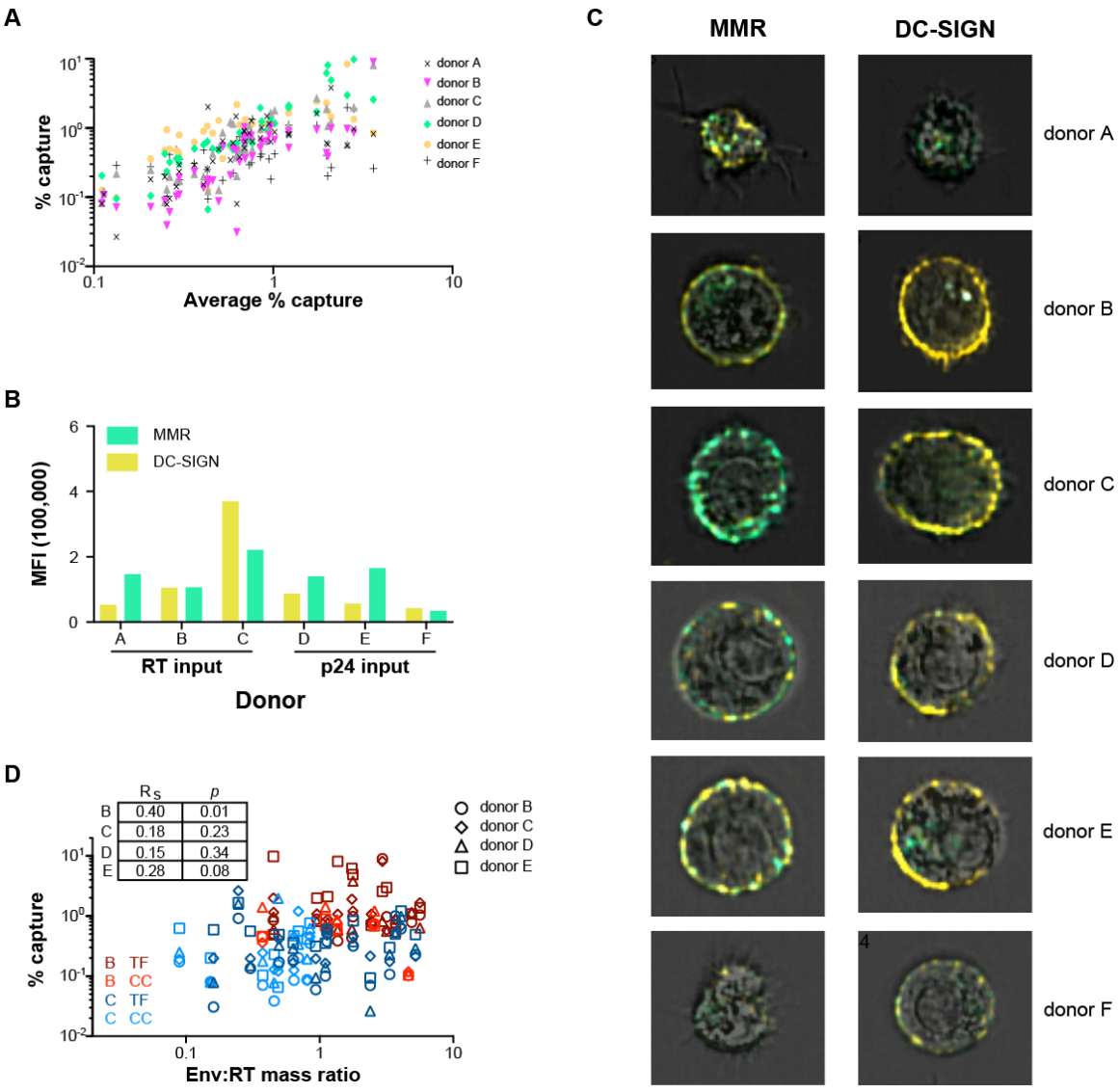
A
% capture
Average % capture
donor A
donor B
donor C
donor D
donor E
donor F
B
MFI (100,000)
MMR
DC-SIGN
RT input
p24 input
Donor
C
MMR
DC-SIGN
donor A
donor B
donor C
donor D
donor E
donor F
D
Rs
p
B 0.40 0.01
C 0.18 0.23
D 0.15 0.34
E 0.28 0.08
B TF
B CC
C TF
C CC
% capture
Env:RT mass ratio
donor B
donor C
donor D
donor E

Figure 5-6. Virus capture by moDCs is variable across donors and correlates only weakly with particle Env content. (*A*) The percent virus captured for each virus (y-axis) by cells from different donors (indicated) is shown in relation to the average percent virus captured of that virus in all donors (*x*-axis). Virus capture by cells from donors A and F were the least well correlated (Spearman correlation coefficient R_s = 0.72 and 0.40, respectively; other donors R_s > 0.8). (*B*) The mean fluorescent intensity of DC-SIGN (dendritic cell-specific intracellular adhesion molecule-3-grapping non-integrin) and MMR (macrophage mannose receptor) staining (yellow and green bars, respectively), is shown for different donors (A-F) and virus input (RT activity or p24 content). Cells from donors A and F expressed less DC-SIGN and MMR than other moDC donors. (*C*) Images of representative moDCs expressing DC-SIGN (yellow) and MMR (green) for each donor. (*D*) The percent moDC capture of a given virus (*y*-axis) is shown in relation to its Env content (*x*-axis). This relationship was significant for cells from donor B, with a trend observed for the other donors. (R_s and *p*-values are shown for each donor). Subtype B TF and CC viruses are shown in dark and light red, respectively; subtype C TF and CC viruses are shown in dark and light blue, respectively. Different moDC donors are shown by different symbols as indicated.

slightly higher titers than CC viruses (one representative donor is shown in Fig. 5-7). Although these differences were not significant in the permutation test (p=0.104), significant differences in TF and CC virus titers were observed in the GLM analysis (p=0.025). To explore the reason for this apparent discordance, we ran the permutation test on subtype B and C viruses separately (Fig. 5-7*B*), and found that subtype B TF viruses (p=0.004), but not subtype C TF viruses (p=0.23), grew to significantly higher titers than their respective chronic controls. Averaging across all days, this differences was 11.2-fold for subtype B, but only 1.4-fold for subtype C. Since subtype B virions bound moDCs 3.5-fold more efficiently than subtype C viruses (Fig. 5-5*B* and *D*), we interpret these findings to indicate that virions that bind moDCs more efficiently are also transferred to CD4+ T cells more efficiently.

Transmitted founder viruses are relatively more resistant to IFN-α. CD4+ T cells represent the predominant target cells in gut-associated lymphoid tissues and the first cell type to become productively infected following transmission (227). To determine the growth potential of TF and CC viruses in this cell type, we infected activated CD4+ T cells from three healthy donors with equivalent amounts of virus, and monitored viral growth by measuring RT activity in culture supernatants (Fig. 5-8*A, C, E;* grey lines). Although TF viruses replicated to slightly higher titers, especially at the earliest time point post infection, this was not statistically significant (p=0.16 by perm test; p=0.186 by GLM). Thus, in activated CD4+ T cells, TF and CC viruses replicated with comparable efficiency.

IFN-α is produced early in infection by plasmacytoid DCs (337), which are among the first cells to be recruited to the mucosal site of virus entry (209). This cytokine stimulates expression of hundreds of host genes (interferon stimulated genes; ISGs) (87), many of which have anti-HIV-1 activity (324). IFN-α has also been shown to limit Env incorporation into virus particles that are released from infected CD4+ T cells (150). To determine the sensitivity of TF and CC viruses to the antiviral activity of this cytokine, we analyzed their replication kinetics in CD4+ T cells in the presence of 500 U/ml of IFN-α. Determining RT activity in culture supernatants as a measure of

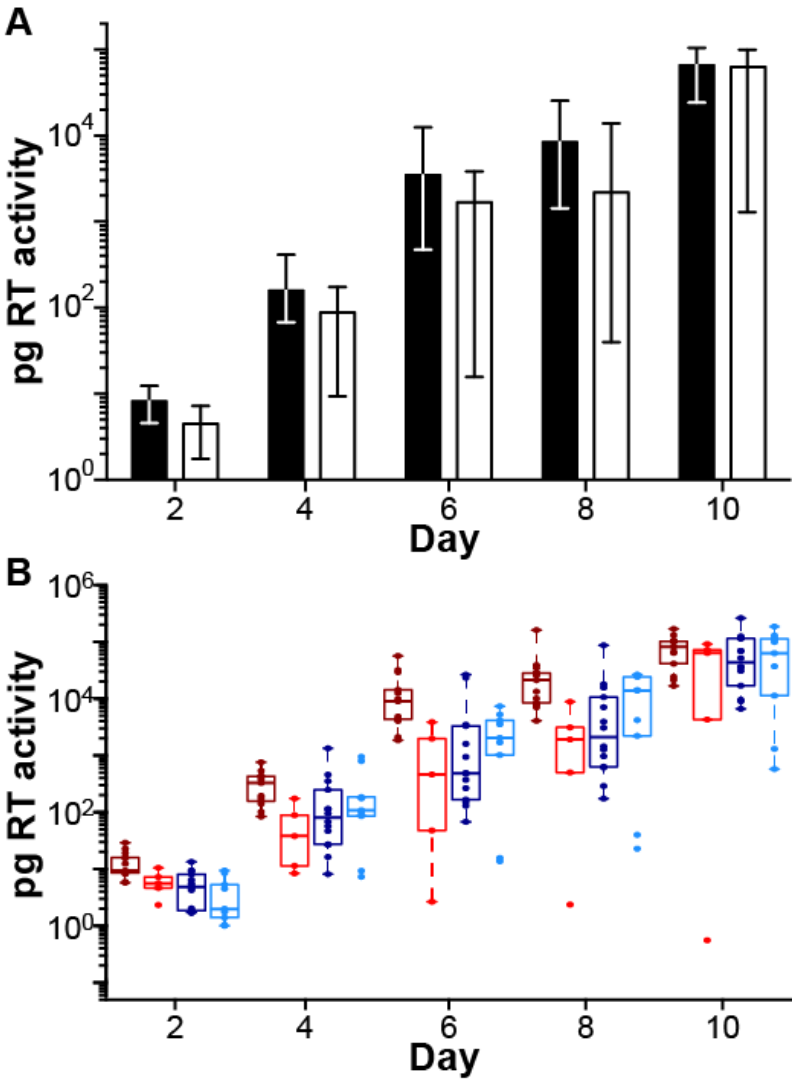

Figure 5-7. Dendritic cell mediated *trans*-infection. (*A*) Virus replication expressed as picograms (pg) of RT activity per ml of culture supernatant (*y*-axis) is shown after cocultivation of virus pulsed moDC with CD4+ T cells for one representative donor over time (*x*-axis). Bars indicate median values of viral replication for TF (filled) and CC (open) viruses, with interquartile ranges indicated (there were no significant differences between TF and CC viruses). (*B*) Values are plotted for each virus individually (color coding for TF and CC viruses from subtypes B and C as in Fig. 5-4). Averaging across all days, subtype B TF viruses grew to 11.2-fold higher titers than subtype B CC viruses (p=0.004), while subtype C TF grew only 1.4-fold more efficiently than subtype C CC viruses (p=0.23).

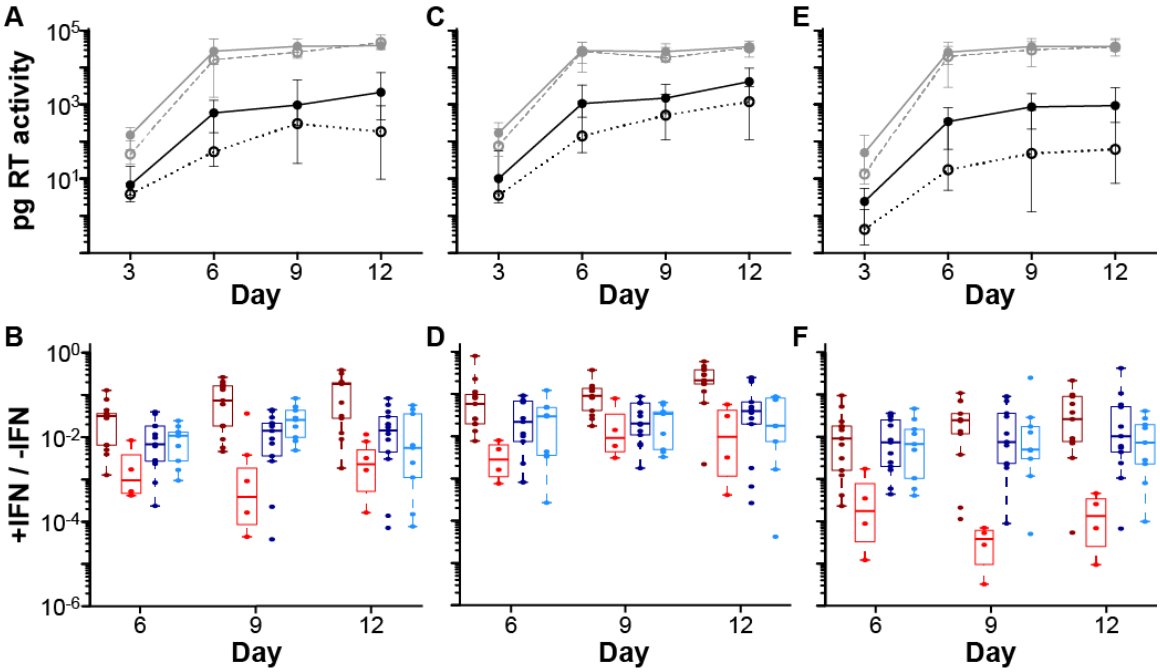

Figure 5-8. Virus replication in CD4+ T cells in the presence and absence of IFN-α. (*A, C, E*) The replication kinetics of TF (solid lines) and CC (broken lines) viruses are shown in CD4+ T cells from three donors, in the absence (grey lines) and presence (black lines) of 500 U of IFN-α. RT activity indicated as picogram (pg) per ml of culture supernatant (*y*-axis) was measured every three days (*x*-axis). Data points indicate median values of virus production, with interquartile ranges indicated. In the presence of IFN-α, TF viruses grew to 24-fold higher titers than CC viruses (p=0.012). (*B, D, F*) The ratio of virus production in the presence and absence of IFN-α is plotted for each virus (*y*-axis) at different timepoints (days) post infection (*x*-axis) (color coding for TF and CC viruses from subtypes B and C as in Fig. 5-4). Subtype B TF viruses grew to 62-fold higher titers than subtype B CC viruses (p=0.000013), while subtype C TF viruses grew only 1.7-fold more efficiently than subtype C CC viruses (p=0.53).

viral replication, we found significant differences in the growth rate of TF and CC viruses (Fig. 5-8*A, C, E,* black lines). However, this effect was highly subtype specific (Fig. 5-9). Estimating the magnitude of the IFN-α impact on TF versus CC virus replication, we found that subtype B TF viruses grew to 62-fold higher titers than subtype B CC viruses (p=0.000013 by GLM). In contrast, subtype C TF viruses grew only 1.7-fold more efficiently than their respective CC viruses, which was not significant (p=0.53 by GLM). Importantly, this difference was not due to a lack of IFN-α resistance of the subtype C TF viruses, but an increased IFN-α resistance of the respective chronic controls (Fig. 5-8*B, D, F)*. Inclusion of gender and risk group information into the statistical analyses suggested that the observed subtype differences were not the result of an uneven representation of covariates, since neither gender nor risk group were statistically significantly associated with IFN-α resistance. However, due to the small number of viruses in each of these groups, the study was not sufficiently powered to examine the impact of gender and risk group, and a contribution of these factors can therefore not be excluded (Fig. 5-9).

As a different way to analyze these data, we also calculated for each virus strain the ratio of virus production in the presence and absence of IFN-α (Fig. 5-8*B, D, F*). Comparing across all donors, we again found that TF viruses were significantly more resistant to inhibition by IFN-α than chronic viruses (p=0.027 by perm test). However, when considering the two clades separately, this was significant only for subtype B (p=0.0004 by one-sided Wilcoxon test), and not for subtype C (p=0.84). Viruses that were highly resistant in one donor were also highly resistant in the other donors (Fig. 5-10), indicating that their IFN-α phenotype was consistent between donors.

To determine whether the higher titers of TF viruses were due to increased particle release or differences in viral spread, we used flow cytometry to measure the percent of infected cells in IFN-α-treated cultures from two donors (Fig. 5-11). In the presence of IFN-α, TF viruses infected a larger number of cells than CC viruses, although the overall effect was only marginally significant (p=0.049 by perm test). However, GLM analysis again detected a significant

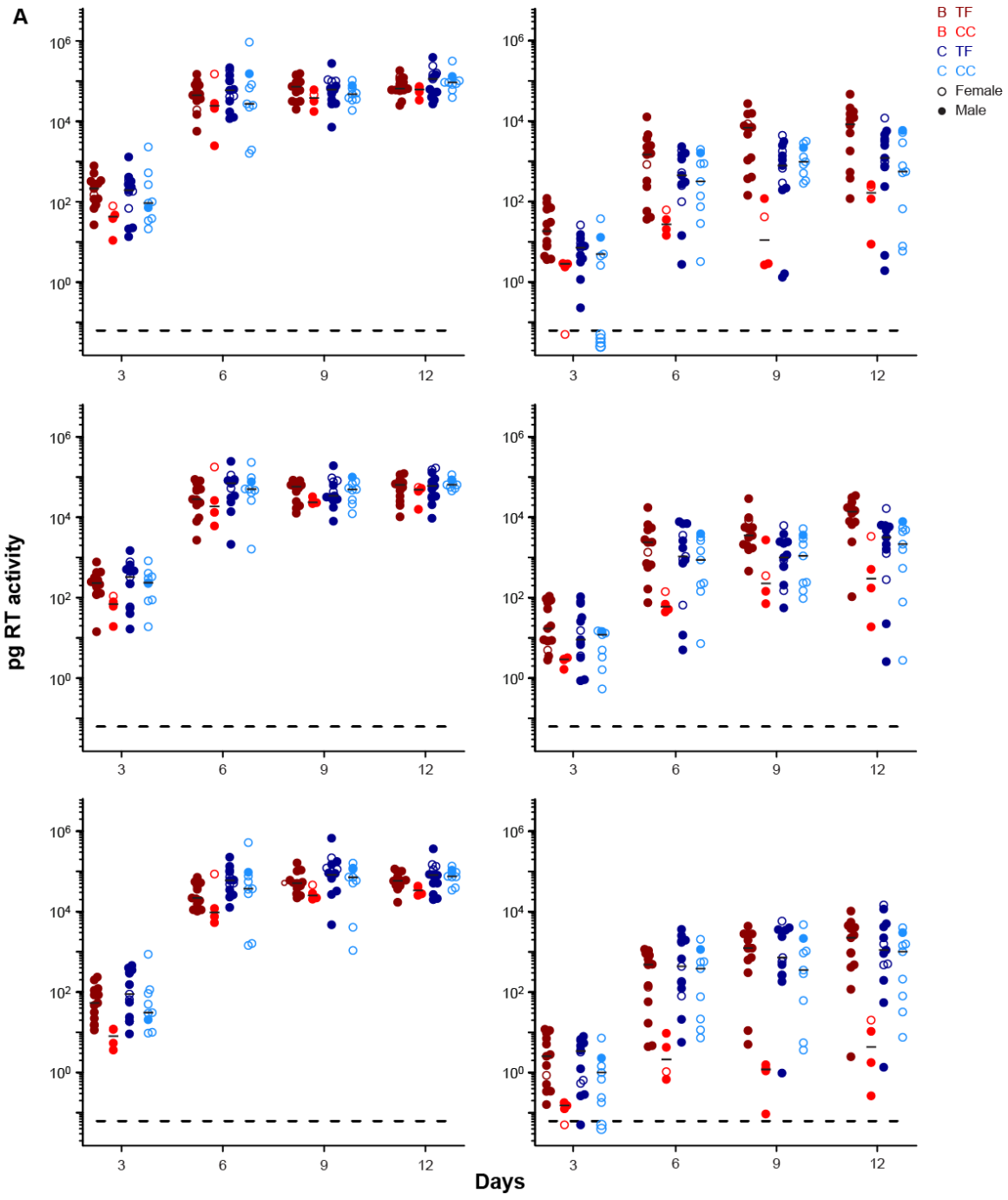
A
B TF
B CC
C TF
C CC
Female
Male
pg RT activity
Days

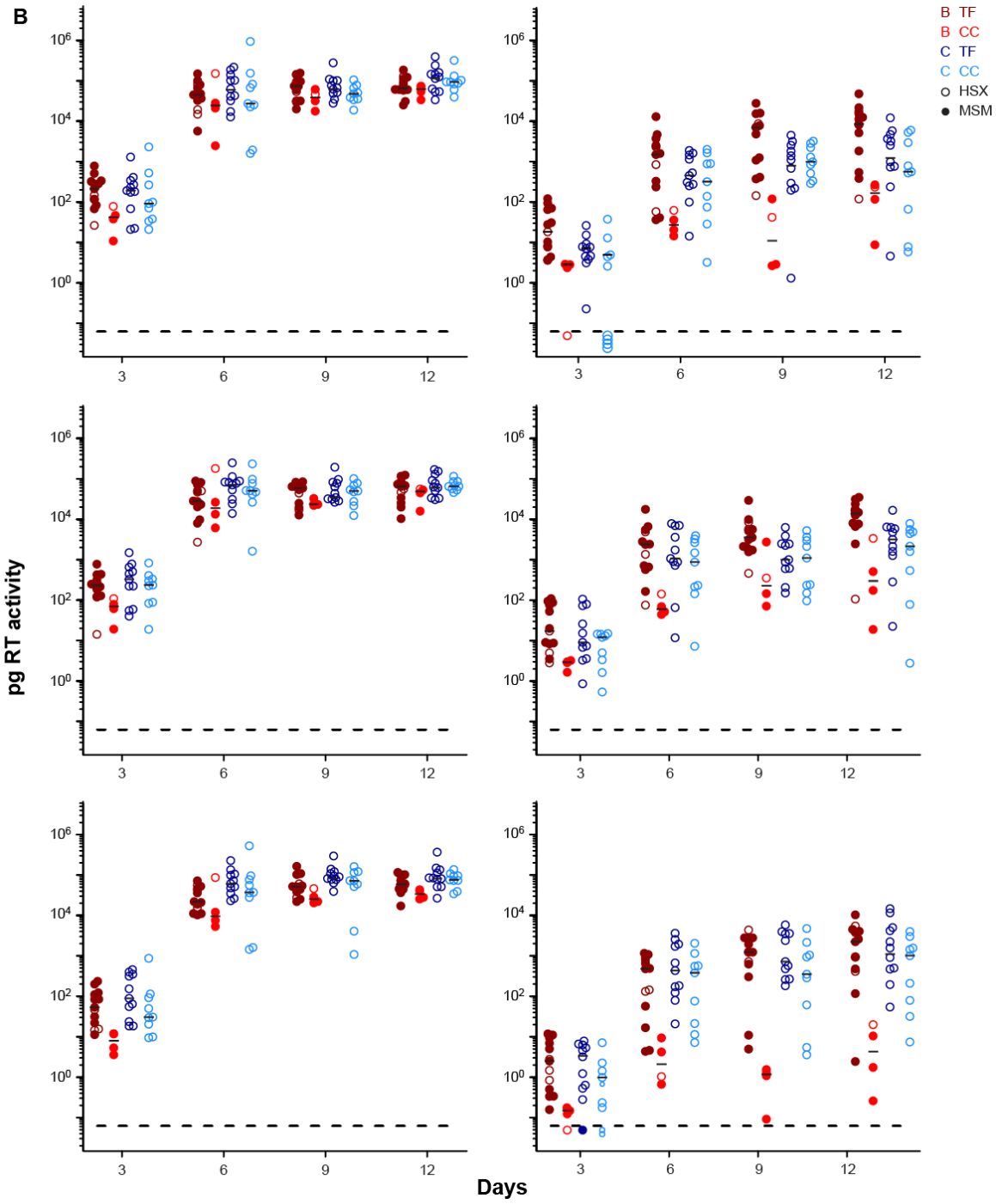
B
B TF
B CC
C TF
C CC
HSX
MSM
pg RT activity
Days
10^6
10^4
10^2
10^0
3
6
9
12

Figure 5-9. Virus replication in CD4+ T cells in the absence and presence of IFN-α. Activated CD4+ T cells from three healthy donors (rows 1-3) were infected with equivalent amount of virus and cultured in the absence (left column) and in the presence (right column) of 500 U of IFN-α. Virus replication was monitored by RT activity in culture supernatants (expressed as picogram per ml of culture supernatant) at four different time points (days) post infection (*x*-axis). Values are shown for each virus. Subtype B and C viruses are shown in red and blue, with TF viruses indicated in dark red and CC viruses in light blue, respectively. Values indicate average RT activity from duplicate measurements. (*A*) open circles denote IMCs from female patients, filled circles from male patients. (*B*) open circles denote IMCs from heterosexual transmissions (HSX), filled circles from homosexual transmissions (MSM). Circles beneath the broken line indicate that no virus was detectable. There was no significant interaction between subtype and gender (p=0.162 by GML), and gender was not a significant fixed effect when included as an independent variable (p=0.8), or when subtype was excluded from the model (p=0.4). All MSM samples were from the B clade, so subtype-risk interactions could not be explored.

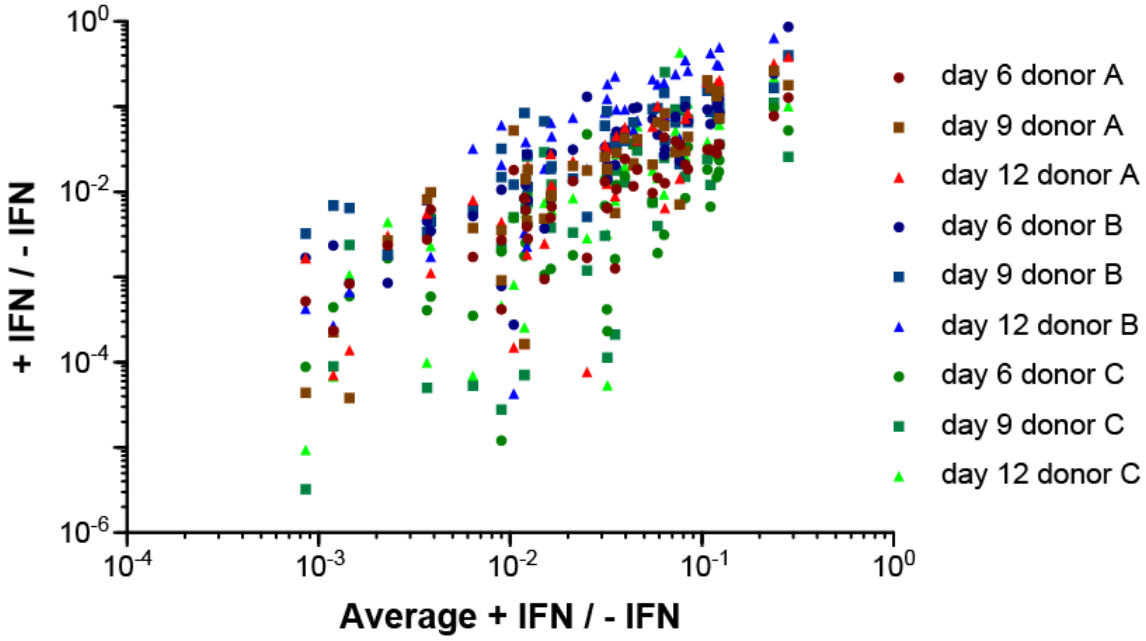

Figure 5-10. IFN-α resistance is consistent across donors and time-points. The ratio of virus production in the presence and absence of IFN-α for each virus (*y*-axis) is shown in relation to the average ratio of virus production in the presence and absence of IFN-α for the same virus (*x*-axis). Although there is donor-to-donor variability in the magnitude of the IFN-α effect, the observed levels of sensitivity or resistance are consistent across all donors.

interaction between subtype and TF/CC status (p=0.041), indicating that the differences were primarily due to subtype B viruses. Since the ratio of virus production in the presence and absence of IFN-α correllated well with the percent of Gag positive cells (*p*<0.0001; Fig. 5-11*B* and *C*), it is likely that IFN-α resistance represents an enhanced ability to spread between CD4+ T cells. Interestingly, this phenotype correlated only weakly with particle infectivity and Env content (not shown). Thus, Env content is not the main driver of the relative IFN-α resistance of TF viruses.

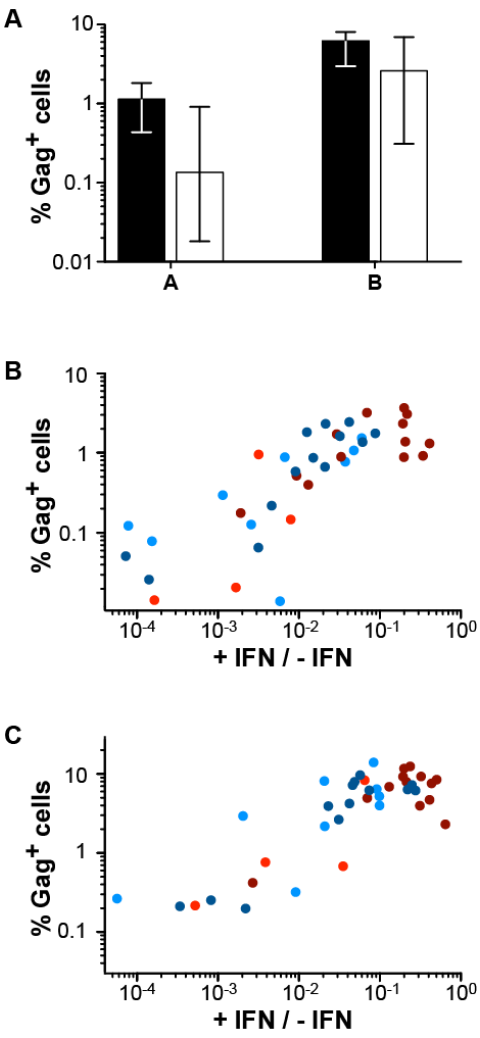

Figure 5-11. IFN-α resistance affects cell-to-cell virus spread. (*A*) CD4+ T cells from two donors (A and B as shown in Fig. 4) were infected with TF (filled bars) and CC (open bars) viruses in the presence of 500 U of IFN-α and analyzed for Gag positive cells by flow cytometry 12 days post infection. Bars indicate the median percent of Gag positive cells (*y*-axis), with interquartile ranges indicated. TF viruses infected a higher percentage of cells by day 12 than CC viruses (p=0.049). (*B, C*) The ratio of virus production in the presence and absence of IFN-α is shown for each virus at day 12 (*x*-axis) is shown in relation to the percent of Gag positive cells infected by this virus (*y*-axis). Viruses that are resistant to IFN-α infect a higher percentage of cells than viruses that are sensitive to IFN-α (R_s=0.80 and 0.63 for *B* and *C*, respectively; both p<0.0001).

Materials and Methods

Study subjects

Plasma samples were obtained from subjects enrolled in acute and established HIV-1 infection cohorts (cohort 001). A summary of available epidemiological data, clinical information, and infection status is shown in Table S1. Acutely infected individuals were staged as described (112). Whole blood was collected in acid citrate dextrose, and plasma was separated and stored at −70°C. All subjects provided written informed consent for the collection of samples and subsequent analysis. The study was approved by the Institutional Review Boards of the University of Pennsylvania and Duke University.

Single genome amplification (SGA)

SGA was performed as described previously (204, 270, 312, 313). Briefly, plasma viral RNA was extracted, reverse transcribed using superscript III reverse transcriptase (Invitrogen), and the resulting cDNA was diluted in 96 well plates such that each well contained on average less than one cDNA template. 3' and 5' genome halves were amplified by nested PCR using primers and conditions as described (204, 270, 312, 313). Amplicons were sequenced directly and any sequence containing double peaks in the chromatogram was excluded from further analysis. The resulting sequences are thus representative of viral genomes present in the plasma, and devoid of PCR artifacts and cloning biases.

IMC construction

Full-length TF and clonally expanded CC genome sequences were inferred as described (13, 204, 257, 270, 313). To clone TF genomes, overlapping half-genome and LTR fragments were amplified from PBMC genomic DNA, cloned into plasmid vectors, and combined within a plasmid vector (pBR322, pUC`9, or pCR-XL-TOPO) as a complete proviral genome (313). To clone CC genomes, consensus sequences of viral expansion rakes were chemically synthesized (Blue Heron Biotech or GenScript) as 3 to 4 fragments and used to construct a complete provirus

(270). This approach was also used for TF viruses derived from patients who were infected by multiple viruses, except for ZM247Fv1 and ZM247Fv2 that have been described elsewhere (313).

Virus stock preparation

Virus stocks were generated by transfecting 30% confluent 293T cells (in a 10 cm dish) with 6 µg of IMC DNA. Virus was harvested 72 hours post-transfection and passed through a 0.45 micron polyvinylidene fluoride filter. Viral infectious units for each stock were determined using TZM-bl cells as described previously (366). To generate physiologically relevant viral stocks, CD4+ T cells were positively selected (Miltenyi Biotec) from buffy coats of nine healthy donors (Research Blood Components), and cryopreserved using CS10 freezing media (CryoStor). Cell aliquots were thawed quickly in a 37°C water bath, resuspended at a density of $1x10^6$ cells per ml, allowed to recover overnight in RPMI 1640 media containing 10% FBS and 30 IU/ml IL-2 (CD4+ T cell media) in a 37°C incubator with 5% CO_2, and then stimulated by adding Staphylococcal Enterotoxin B at a concentration of 50 ng/ml for 48 hours. Cells were then pooled and $1x10^7$ cells were inoculated with $1x10^5$ infectious units of each 293T derived virus stock overnight in 1 ml of CD4+ T cell media. Cells were washed and resuspended at $1x10^6$ cells per ml in CD4+ T cell media. An additional 10 ml of media was added at day three after infection. On day five after infection, all media was exchanged and cells were resuspended in 30 ml of CD4+ T cell media. At day 11 post infection, microvesicles were depleted as described elsewhere (264) with the following modifications: biotinylated anti-CD45 antibody (clone 2D1, R&D systems) was added to streptavidin-coated magnetic beads (M-270 beads, Invitrogen) for one hour at room temperature at a concentration of 10 µg mAb per mg bead, washed three times in PBS then stored at 4°C. Beads were added to clarified supernatant to a final concentration of 100 µg/ml for one hour at room temperature and then magnetically captured using a 50 ml conical tube magnet (StemCell Technology) at 4°C for 20 minutes. Supernatant was passed through a 0.45 micron polyvinylidene fluoride filter and virus was pelleted through a 20% sucrose cushion at 100,000 g, resuspended in PBS, and stored in aliquots at -80°C.

The p24 antigen content in virus stocks was quantified using commercially available PerkinElmer high sensitivity alphaLISA and Alliance ELISA p24 assays as well as an assay developed by Grivel and colleagues (33). Viral RNA was quantified using the Roche COBAS AmpliPrep/COBAS Taqman HIV-1 v. 2.0 test. Reverse transcriptase activity was determined using the Roche colorimetric reverse transcriptase assay.

Since the alphaLISA p24 assay was approximately two orders of magnitude more sensitive than the RT activity assay, we sought to convert p24 antigen concentrations measured by this assay to RT activity in order to use this assay when RT determinations were below the limits of detection. Thus, we calculated the ratio of p24 to RT activity for each virus in four independently prepared high-titer virus stocks. Since these ratios were highly consistent, we used the average ratio for each virus strain to convert p24 to RT activity.

Coreceptor tropism

Coreceptor tropism was assessed by pre-incubating TZM-bl cells with 1.2 μM AMD3100 and/or 10μM TAK779 before infection with $1x10^3$ infectious units of 293T cell supernatant. Viruses were considered dual-tropic if inhibited at least 5% by AMD3100 and no more than 95% by TAK779.

Analysis of per-particle infectivity

$1x10^4$ TZM-bl cells were seeded per well in a 96 well plate in 100 μl DMEM containing 10% FBS. After 24 hours, media was removed from each well, and cells were infected with 50 μl of virus serially diluted in DMEM containing 1% FBS with or without 10 μg/ml DEAE-Dextran. Two hours later, 50 μl of DMEM containing 20% FBS was added. 36 hours after infection, luciferase production was assayed using Brite-Glo luciferase substrate (Promega) and a Biotek H4 reader. As a control, a third-generation fusion inhibitor (T2635) was added at a saturating concentration (1 μg/ml) 12 hours after virus addition to one of the duplicate wells (102). Relative light units (RLUs) generated per volume of each virus stock were calculated using all virus

dilutions in the linear range of the assay ($2x10^3$-$6x10^5$ RLUs). The infectivity per particle was then calculated as the RLU generated per pg of RT activity present in each virus stock.

Particle Env content

A sandwich ELISA was developed to measure virion Env content. 200 pg of the monoclonal E51-218.3-CD4 was added in 100 µl of 0.2 M sodium carbonate/bicarbonate (pH 10) solution to each well of 96 well ELISA plates (Nunc MaxiSorp) and incubated overnight. E51-218.3-CD4 is a chimeric antibody that contains the first (D1) and second (D2) domains of human CD4 linked to the CD4-induced (CD4i) monoclonal E51. Its architecture is similar to that of other chimeric antibodies (370), except that the peptide that links the CD4 and E51 moieties was modified for stability. Wells were washed twice with 200 µl of PBS with magnesium and calcium containing 0.2% Tween 20 (PBS-T), blocked with 200 µl of 5% non-fat milk in PBS-T for 2 hours at room temperature, and washed three times with 200 µl of PBS-T. Plates were stored at 4°C for up to one month. Virus was diluted in PBS-T with 1% Triton X-100 detergent to disrupt virions, added to wells in three 10-fold serial dilutions (100 µl) and incubated at 37°C for two hours. Commercially available gp120 standards were similarly diluted and added to wells in serial 2-fold dilutions starting at 100 ng/ml. Wells were washed 5x with PBS-T and then incubated with 100 µl of horseradish peroxidase-conjugated, affinity-purified human anti-gp120 (Advanced Bioscience Laboratories) for one hour at 37^oC. Wells were washed five times with PBS-T, incubated with o-phenylenediamine dihydrochloride substrate followed by 2 N sulfuric acid, and absorbance was read at 490 nm with a 630 nm reference. After 15 minutes of development, the assay had a dynamic range from approximately 100 pg gp120/ml to 50 ng/ml. Multiple dilutions were used to determine the Env content for each virus stock, which was then normalized by the RT activity.

Dendritic cell capture and *trans*-infection assays

Monocyte derived dendritic cells (moDCs) were differentiated from peripheral blood monocytes purified by CD14 immunomagnetic selection of PBMC isolated from buffy coats of

healthy donors. Monocytes were further enriched by removing cells that did not adhere to polystyrene after 1 hour incubation at 37°C in RMPI 1640 with 5% NHS, and 1% HEPES buffer. Adherent cells were cultured in the same media supplemented with 100 IU/ml GM-CSF and 200 IU/ml IL-4 (refreshed every two days) for seven days after which they became non-adherent. On day six, cells were analyzed by flow cytometry. $1.0x10^6$ cells were treated with Fc-receptor blocking reagent (Miltenyi Biotec) according to manufacturer's instructions, stained with lineage cocktail 1 [which contains antibodies to CD3, CD14, CD16, CD19, CD20 and CD56) (FITC), CD11b (PE), CD11c (PE/Cy5) and CD14 (Pacific Blue)] or separately with CD209 (FITC), CD206 (PE), CCR5 (PE-CF594) and DAPI, and analyzed using an Amnis ImageStream machine. The phenotype of moDCs was $lin1^-$, $CD206^+$, $CD209^+$, and $CD11c^+$. CD14 staining was less intense on fresh monocytes, but remained detectable on day six. On day seven, $1x10^5$ moDCs were seeded into a deepwell 96 well plate at a concentration of $1x10^6$ cells per ml then pulsed with 30 pg RT activity of each virus stock (diluted in 5 µl of RPMI) for 3 hours. To calculate the amount of p24 added to each well, 15 µl of well-mixed cells and media were removed, and p24 was measured. Next, cells were washed three times with 1 ml of pre-warmed Hank's balanced salt solution with calcium and magnesium to remove cell-free virus. Cells were then lysed in PBS containing 0.5% Triton X-100 and the percent capture was calculated as the cell-associated p24 divided by p24 present prior to wash. For one TF virus (CH040), 300 pg and 3 pg RT activity was also added to determine the linear range of the assay. In both cases, the percent capture was not statistically different than when 30 pg were added. As an additional control, 30 pg of CH040 was added to wells with no moDCs to determine possible background due to incomplete removal of media between washes. No p24 was detectable in these wells. For a small number of viruses (3-5), no p24 was detectable after washing. Thus, we used the limit of p24 detection to calculate the percent capture. Because we observed that adding as much as 10 times more virus in this assay did not affect the percent capture, we repeated this assay in three additional donors adding 600 pg of viral p24 antigen of each virus. When input was normalized by p24, only one virus in one donor was captured at a level below the assay's limit of detection.

To test for productive infection of moDCs, $3.3x10^4$ moDCs were cultured in 200 µl of RMPI 1640 with 5% normal human serum, and 1% HEPES buffer with 100 IU/ml GM-CSF and 200 IU/ml IL-4 for nine days in 96 well plates. Media was replaced at day six. To test if bound virus was accessible to trypsin, $3.3x10^4$ moDCs were incubated in 0.25% trypsin-EDTA for 15 minutes at 37°C prior to the final wash in HBSS, then lysed as above.

To measure moDC transfer to CD4+ T cells, buffy coats were split, with half of the cells processed to isolate monocytes as above and the other half depleted of non CD4+ T cells (RosetteSep, StemCell Technologies). MoDCs were generated as above and CD4+ T cells were stimulated for 48 hours with 50 ng/ml SEB then cultured at $1x10^6$ cells per ml in CD4+ T cell media. On day seven, $1x10^5$ DCs were pulsed for three hours with 50 pg RT of each virus then washed as above and co-cultured with $5x10^5$ CD4+ T cells in 1 ml of CD4+ T cell media in 48 well plates. To measure virus replication, 200 µl of media were sampled with replacement every two days. At day 6, 800 µl of media was exchanged.

Virus replication in the presence and absence of IFN-α

CD4+ T cells were isolated from buffy coats by depleting non-CD4+ T cells and then stimulated with 50 ng/ml SEB for 48 hours in CD4+ T cell media at a concentration of $1x10^6$ cells per ml. The cocktail used for depletion contains anti-CD123 antibodies, and thus also depletes plasmacytoid dendritic cells. Cells were washed, resuspended at $1x10^7$ cells per ml, with $2x10^6$ cells incubated overnight with an equivalent amount of each virus (30 pg RT activity). Next, cells were washed twice with 1 ml of PBS and split into two equal parts, one of which was cultured in CD4+ T cell media alone and the other supplemented with 500 U/ml IFN-α (A2; PBL Laboratories) in 1 ml in 48 well plates. 200 µl of media were sampled with replacement every three days. At day six, 800 µl was exchanged with fresh media containing 500 U/ml IFN-α.

On day 12, cells were analyzed by flow cytometry. Cells were washed 1x in PBS then incubated with 1 µl of a 1:1000 dilution of live/dead green stain (Invitrogen) in DMSO. Cells were incubated for 30 minutes at 4°C with anti-CD4 antibody (OKT4 APC/Cy7, BioLegend), washed

and permeabilized using Cytofix/Cytoperm kit (BD) according to manufacturer's instructions, and then incubated with anti-Gag antibody (KC-57 RD-1, Beckman-Coulter) for one hour at 4°C. Cells were fixed in 1% paraformaldehyde and analyzed on an Amnis ImageStream instrument. Gag positive cells were expressed as a percentage of all living cells. All samples were collected and analyzed under code, and four mock-infected cultures were used to define baseline anti-Gag staining. Cell viability at day 12 in mock-infected cultures was comparable in the presence and absence of IFN-α.

Statistical analyses

We used two statistical strategies to determine whether TF and CC viruses have distinct phenotypic characteristics. A non-parametric rank-based permutation test was used to determine whether values from TF viruses were significantly different from those derived from CC viruses. This test was designed to account for clade and donor differences, and the p-value reflected the likelihood of observing differences between TF and CC viruses by chance alone. The test took into account that (i) viruses were derived from two clades (B and C), (ii) repeat experiments were performed using different donor cells; and (iii) in some experiments responses were evaluated at different times. Specifically, the TF ranking for each experiment was determined, and if an experiment was repeated, its ranks were summed across the replicate experiments (for example, if 3 repeat experiments were done in 3 different donor cells, and a TF IMC scored the highest in two experiments, second in the third, the sum of the ranks for that IMC was 1+1+2 = 4). TF and CC labels were then randomly reassigned 10,000 times, and the sum of the various ranks from the randomized data tallied. The fraction of occurrences of a given rank-sum value observed in 10,000 randomized data sets provides an estimate for the probability of observing that rank-sum value in the actual data by chance alone. Thus, the fraction of occurrences in the randomized data of rank-sum values equal to or less than that observed rank-sum in the actual data provides a p-value that the observed rank-sum is statistically significant. Each IMC was randomized independently, including cases in which multiple IMCs were derived from the same subject, because these IMCs were genetically and phenotypically distinctive. The independence of the

IMCs was supported by subsequent GLM analyses (see below). The code for this permutation test was written in-house for this project using perl.

The general linearized model (GLM) consisted of fitting a log-normal generalized mixed-effect model to the data; all analyses related to the model were performed using R (http://www.r-project.org/). The advantage of using this model was that it allowed us to estimate the impact of, and assess the relationships between, different parameters. Using this approach, we modeled the response variables in each experiment versus subtype (B or C) and transmitted (TF) or chronic (CC) status, considering the cell donor and the IMC as random effects to account for the different levels of donor and IMC responses. We compared nested models, simplifying from more complex models to simpler ones (with less variables) in a step-wise manner using the Akaike Information Criterion (AIC), and we only kept variables that reached a significance level of 0.05 or lower. This allowed us to test for possible interactions between variables, for example, when the response variable had a different TF vs. CC effect between clades. To test whether the various IMCs were independent when derived from the same subject, we also introduced a variable “patient”. The patient variable was never statistically supported in our models, suggesting the IMC were behaving independently, even when derived from the same individual. The GLM was implemented using the glmer function (http://lme4.r-forge.r-project.org/), and the anova function (52) was used to compare models using the AIC. We used a Shapiro-Wilcoxon test (306) to show that the data were consistent with a log-normal distribution.

Discussion

A primary goal of AIDS vaccine development is to prevent acquisition of HIV-1 at mucosal surfaces. In this context, it is critical to determine whether newly transmitted HIV-1 strains share properties that provide novel targets for effective immunization. For this purpose, the analysis of full-length TF genomes is ideal, since their corresponding IMCs contain the complete genetic information of viruses that successfully transmit infection. Moreover, genetic linkage is maintained to preserve potentially important regulatory and structural protein interactions (176, 204, 257, 313). Characterizing a large set of TF and CC IMCs from two major HIV-1 group M subtypes B and C, we found that TF viruses were slightly more infectious on a per particle basis, packaged slightly more Env and bound to moDCs more efficiently than chronic control viruses. We also found that TF viruses were more resistant to the antiviral effects of IFN-α, although this was statistically significant only for subtype B TF viruses. These biological differences could act in concert to enhance cell-free infection and virus replication in the face of an early innate immune response.

Analyzing particle composition and infectivity, we found that TF virions were on average twice as infectious and contained twice as much Env as CC virions. These phenotypic differences are consistent with data from a recent genetic study (126), which identified sequence signatures in the signal peptide of TF Env sequences. When tested in the context of pseudoviruses, these signatures increased steady state Env expression and particle incorporation (10). Assuming 35 enzymatically-active RT dimers per virion, we estimate that the median TF virion contains 18 Env trimer spikes, while the median CC virion contains seven– a value essentially identical to previous estimates (55). Since only one or a few functional Env trimers are believed to be necessary for cell fusion and infection (218, 382), it would appear that TF viruses carry an “excess” of envelope glycoprotein. However, such “excess” may be of advantage during the earliest stages of HIV-1 infection, since viruses with a higher Env content can be expected to also contain more functional trimers. Particle-associated Env may also play a role beyond the mere fusion and cell entry function (15). For example, excess Env could ensure

more stable attachment of virions to target cells and/or could be involved in receptor and/or co-receptor mediated signaling (15). In addition, excess Env may compensate for shedding or inactivation by semen (221) and cervicovaginal mucous (262). Thus, it seems likely that the increased Env content and associated enhanced infectivity of TF viruses serve to increase their transmission fitness. Conversely, the lower Env content of CC viruses may be more advantageous once infection is established and may even be selected for by Env-specific neutralizing antibodies.

We also found that TF viruses bind more efficiently to moDCs than their chronic counterparts. Although moDCs are only a proxy for classical mucosal DC subsets, previous studies have shown that tissue- and *in vitro*- derived DCs have similar virus capture capabilities (134, 144, 168). Thus, it is likely that the improved interaction of TF viruses with tissue culture derived moDCs is also a reflection of their *in vivo* biological properties. The differential binding of TF viruses was statistically significant across different donors and across both clades, and thus seems to represent a general feature of TF viruses. There are at least two steps in the transmission process where this phenotype may confer an advantage. First, more efficient binding to tissue resident DCs may increase the likelihood of a successful transfer to CD4+ T cells. Second, more efficient binding to emigrating DCs may promote the seeding of regional lymph nodes (341). In this context, it is of interest that adaptive changes that conferred mucosal transmissibility to a commonly used SHIV strain (SF162P3) increased the binding capacity of its Env glycoprotein to DC-SIGN (162). Our data are thus consistent with the view that DCs are among the first cells to interact with HIV-1 after exposure and that this interaction is important for transmission, although DCs themselves are not productively infected.

One unexpected finding was that TF viruses replicated and spread in CD4+ T cells in the presence of IFN-α more efficiently than did CC viruses. Although this effect was most pronounced for subtype B TF viruses, a trend was also observed for subtype C TF viruses. This finding raises the question whether IFN-α responses in the mucosa are protective against HIV-1 infection. On first glance, the answer to this question seems to be no. Previous studies in macaques

concluded that the initial innate immune response is ineffective at containing SIVmac infection and may even enhance early viral replication (209). Moreover, mucosal pre-treatment with toll-like receptor (TLR) agonists induced IFN-α, but did not protect animals from SIVmac challenge (77). However, these studies were not only assessing the effects of IFN-α, but were also causing immune activation by inducing pro-inflammatory cytokines and chemokines. In fact, it has been shown more recently that systemic administration of pegylated IFN-α alone delayed SIVmac infection in treated compared to untreated macaques following a high-dose vaginal challenge (Danny Douek, personal communication). It thus appears that early interferon responses can be protective against HIV-1 infection. The fact that IFN-α levels (157) as well as interferon regulatory factor polymorphisms (18) have been associated with protection in highly exposed but uninfected individuals is consistent with this hypothesis. Thus, the induction of an effective early "anti-viral state" appears to contribute to the population bottleneck associated with mucosal HIV-1 transmission.

We hypothesized that virions containing more Env would be more resistant to IFN-α, because *in vitro* experiments had shown that this cytokine can decrease cell-free virus transmission (361), particle release (383) and particle infectivity (150, 392). However, we failed to see a significant correlation between IFN-α resistance and Env content or virion infectivity. Thus, higher baseline Env incorporation cannot explain the IFN-α resistant phenotype of TF viruses. Nonetheless, the ability of TF viruses to replicate in the presence of IFN-α indicates that resistance conferring determinants must exist. There are several candidates, such as the accessory proteins Vpu and Vif, which are known to counteract the interferon stimulated genes tetherin and APOBEC3G, respectively (252, 333), as well as the Tat protein, which has been reported to modulate the IFN-induced RNAse L antiviral pathway (325) and to down-regulate the ISG protein kinase R (304). Structural proteins, such as Gag, may also contribute to IFN-α resistance by exhibiting differential sensitivity to the tripartite motif (TRIM) family of proteins (24, 296, 385). Finally, IFN-α resistance may not only be protein-mediated, since variation the number

of transcription factor binding sites in the LTR could also influence IFN-α sensitivity (16, 170). Notably, there is a relationship between IFN-α resistance and efficiency of transmission in other viruses, including Venezuelan Equine Encephalitis virus (342) and Bovine Viral Diarrhea Virus (53, 233), suggesting that increased IFN-α resistance may be a common property of transmitted founder viruses.

If IFN-α resistance is a pre-requisite for efficient HIV-1 transmission, one would expect this viral property to be conserved across all clades. The lack of significance between subtype C TF and CC viruses seems to argue against this; however, Figure 4 shows that this is not due to a loss of IFN-α resistance of subtype C TF viruses. Instead, the 62-fold difference observed for subtype B viruses reflects a much greater IFN-α sensitivity of the respective chronic viruses. Although our panel of TF and CC IMCs is larger than any previously tested set, there are epidemiological differences between the patient cohorts from which they were derived. For example, all but one of the chronic subtype B IMCs were derived from men who had sex with men, while seven of eight chronic subtype C IMCs were derived from women (Table S1). This gender bias, although not statistically significant, may have contributed to the increased IFN-α resistance of chronic subtype C viruses, since pDCs of women have been reported to generate more IFN-α in response to HIV-1 than pDCs of men (230). In addition, all subtype C viruses were derived from individuals living in Africa, while all subtype B viruses were derived from patients residing the US (Table S1). Thus, environmental factors, such as concurrent infections that increase general inflammation levels, may have contributed to the much higher IFN-α resistance of the African CC viruses. Moreover, all subtype C infected subjects with established infection had lower CD4 counts (Table S1) and thus possibly more advanced disease, which could have also influenced the level of IFN-α resistance of their viruses (101, 192). Finally, if loss of IFN-α resistance is the result of pressure from host adaptive responses, then duration of infection, which was unknown for all subtype C infected subjects, may have been an important variable. Borrow and colleagues have recently demonstrated that subtype B viruses isolated from subjects

later in infection are more sensitive to IFN-α than the viruses isolated shortly after transmission (Fenton-May et al, manuscript in preparation). Thus, it seems clear that to decipher the differences in IFN-α resistance observed here, future studies will need to consider patient demographics, subtype, route of transmission and duration of infection in addition to TF and CC virus status.

One of the motivations to characterize the phenotypic properties of TF viruses is the possibility that virus traits might be uncovered that could represent useful vaccine targets. In this context, the increased Env content of TF viruses may increase their sensitivity to neutralization by allowing antibodies to bind bivalently and crosslink more densely-packed Env spikes (184). Similarly, the identification of key ISGs that contribute significantly to viral control during the most vulnerable stages of HIV-1 infection may provide a new vaccination strategy, either by vaccine vector mediated type I IFN production and/or by the induction of T cells that express the critical antiviral ISGs.

The molecular identification and biological analysis of TF viral genomes is a powerful enabling tool for characterizing the transmission requirements and subsequent evolution of HIV-1, SIV and other viruses (176, 204, 205, 257, 297, 313). In the present study, we used TF analyses to characterize the biological properties of full-length HIV-1 genomes captured at the moment of transmission. Although we identified significant phenotypic differences, none of these completely differentiated TF from CC viruses and the magnitude of the differences in these properties was generally modest. This is not surprising since TF viruses, by necessity, represent a subset of a much larger and more diverse set of viruses that replicates persistently throughout chronic infection. We speculate that the viral population bottleneck associated with mucosal transmission is mediated largely by physical barriers associated with the genitourinary and gastrointestinal tracts but also by specific virus-host cell interactions necessary for virus infection and replication. Each of which may pose hurdles to virus acquisition. Thus, even slight advantages of TF viruses at one or more of these biophysical checkpoints could result in a transmission fitness advantage. Defining the viral determinants that underlie this fitness may provide further insights into the

biology of mucosal HIV-1 transmission that can enhance vaccine immunogen design.

Acknowledgements

We thank John Moore and Frank Kirchhoff for helpful discussions; the University of Pennsylvania's Center for AIDS Research (CFAR) Human Immunology, Flow Cytometry, and Viral and Molecular Core facilities for reagents and protocols; Patricia Crystal for artwork and manuscript preparation. This work was supported by grants from the National Institutes of Health (R01 AI45378 and R01 AI04088), the Center for HIV/AIDS Vaccine Immunology (U19 AI067854), the Center for HIV/AIDS Vaccine Immunology and Immunogen Discovery (UM1 AI100645), and the Bill and Melinda Gates Foundation (grant #37874). N.F.P., C.B.W., and S.S.I. were supported by a training grant (T32 AI07632).

CHAPTER 6

Summary and Future Directions

Nicholas F. Parrish

Department of Medicine and Microbiology, Perlman School of Medicine at the University of Pennsylvania

Introduction

Transmitted/founder (T/F) human immunodeficiency viruses have all the biological properties required for transmission. Therefore, targeting the key properties of these viruses should be a high priority when designing interventions to prevent transmission. Chapters two and three describe the intrinsic envelope glycoprotein (Env) function of T/F and chronic control (CC) viruses from subtypes B and C, with a focus on receptor and coreceptor interactions. Chapter four reports a virus that established primary infection despite extremely inefficient use of CCR5 when tested *in vitro*. Chapter five characterizes T/F and CC viruses biochemically and in binding and replication experiments using primary cells. Together this work builds a foundation for future studies of T/F virus biology. Three differences between T/F and CC viruses deserve focused follow-up studies: a poorly understood feature of many CC Envs typified by low-level resistance to maraviroc, the high Env content of T/F viruses, and the relative resistance of T/F viruses to interferon alpha (IFN-α). Here I propose a number of experiments that could be used as starting points for such follow-up.

Future Directions

Intrinsic Env entry functions. Chapters two and three described experiments using, for the most part, Env complementation assays to determine the entry functions of subtype B and C T/F and CC viruses. While the most obvious difference between these two studies is the subtype of virus investigated, several other important differences should be noted. First, the approach used to generate control Envs was different between the two; subtype B control *envs* were chosen at random from the many *envs* detected after single-genome amplification (SGA) from the plasma of chronically infected individuals. The only selective criterion was that the Env mediated entry into TZM-bl reporter cells; some 30% of *envs* sequenced from the plasma by SGA do not encode Envs capable of this basic function (180). In contrast, we required that all subtype C control *envs* have evidence of *in vivo* clonal amplification, arguing strongly for their *in vivo* functionality. Although we do not yet know the precise mechanisms responsible for clonal amplification (362), this provides the highest level of assurance available that the control Envs tested are functional and relevant to ongoing chronic infection, rather than evolutionary dead-ends integrated and thereby archived in long-lived CD4+ T cells. Thus the control Envs used for subtype C represent a more stringent comparison than the control Envs used for subtype B. In contrast, all 24 of the T/F Envs for subtype B came from infections initiated by a single T/F variant, whereas six of 20 subtype C T/F viruses were from multiple-variant transmissions. This is despite the majority of subtype B Envs being transmitted to men who have sex with men, which has higher risk of multiple-variant transmission (204) than heterosexual contact, the known risk factor for the subjects infected with the subtype C T/F variants we tested. Multiple-variant transmission is also associated with intravenous drug use (21) and inflammatory genital diseases (145), which are associated with a substantially increased epidemiological risk of transmission (305). Thus it is possible that for some of the subtype C T/F Envs the barriers to mucosal transmission were less intact than those for subtype B.

The most apparent biological difference between the panels of subtype B and C T/F and CC Envs was in their sensitivity to CD4 binding site (CD4bs) antibodies and pooled polyclonal

antibodies from human immunodeficiency virus type 1 (HIV-1) infected individuals (HIVIG) (Figures 2-6 and 3-7). T/F Envs from subtype B Envs were significantly more sensitive to VRC01 and b12 than CC Envs, whereas a non-significant trend in this direction was seen for subtype C. The reagents used to address this hypothesis were arguably more appropriate for subtype B than for subtype C; b12 poorly neutralized all subtype C Envs relative to VRC01 and the HIVIG preparation used for subtype C was selected from a small number of subjects containing very broadly neutralizing antibodies. Thus at this point we are unable to definitively address the following possibilities to account for this difference: 1) there is a subtype-specific biological difference in this property, with subtype B T/F and CC Envs having different neutralization sensitivity, 2) there is a real difference that would be observed if a larger or more representative (e.g. more T/F Envs from single-variant transmissions) panel of subtype C Envs was used 3) There would be no difference in this property, even for subtype B, if clonally-expanded, *in vivo* functional subtype B Envs were used as controls. Fortunately, this ambiguity does not influence the important message of our finding for vaccine design: CD4bs antibodies potently inhibit T/F Envs (perhaps even more so than chronic Envs), and virus resistance to these antibodies may be associated with a functional “cost” in terms of CD4 use efficiency (Figure 3-8). Thus this class of antibodies would be ideal to elicit by vaccination, which is less cleaar for the PGT class of antibodies, reported to be less potent against T/F Envs than CC Envs (246).

Similarities between the phenotype of T/F Envs from subtypes B and C allow us to generalize several conclusions about T/F Env entry function relative to control Envs. First, neither subtype C or subtype B T/F Envs efficiently mediate entry into cells that express low levels of CD4. Examples of such cells include macrophages (73) and dendritic cells (271). Tropism for these cell types is dependent on efficient entry (322), thus our data suggests that T/F viruses are not macrophage or dendritic cell tropic, consistent with reports by others (204, 257, 313). In contrast, T/F Envs do mediate efficient entry into primary CD4+ T cells, especially effector memory CD4+ T cells. The CD4+ T cell subset was preferentially infected by T/F Env pseudoviruses from subtypes B and C, potentially due to higher expression of the coreceptor

CCR5 (316). While all T/F Envs tested to date are capable of using CCR5 as a coreceptor and there are no examples of T/F Envs that use CXCR4 exclusively, T/F Envs appear to have a similar efficiency of CCR5 use as CC Envs. This was determined by measuring the inhibitory effect of blocking CCR5 with the small molecule maraviroc (MVC); similar concentrations of MVC were required to inhibit 50 percent of infection (IC_{50}) by both T/F and CC Env pseudoviruses on NP2/CD4/CCR5 cells. However, if the maximal inhibition (MI) by saturating MVC is examined rather than the IC_{50}, MVC showed a trend towards more complete inhibition of entry by T/F than CC Envs in both subtypes B and C (268). When data from both B and C panels was combined, this difference was statistically significant. Indeed, when both panels were tested again on a cell line expressing higher levels of CCR5 (affinofile cells), the difference in MI by MVC between T/F and CC Envs became readily apparent (268). Thus T/F Envs are more completely inhibited by MVC than CC Envs, though the mechanisms underlying this phenotypic difference are not yet clear; it is unlikely that any of these viruses have ever been exposed to MVC, thus the low-level MVC resistance of many CC Envs is an epiphenomenon.

One focus of chapter three is the hypothesis that the integrin pair α4β7 promotes entry and infection by subtype C T/F Envs more than for CC Envs. This hypothesis is consistent with known genetic signatures pertaining to glycosylation of the variable loops and seems to provide a mechanism by which viruses could specifically target highly permissive CD4+ T cells in the gut (62, 250). However, we found no evidence that blocking the Env/α4β7 interaction decreased infection of primary T/F or CC viruses although it did have some effect on the lab strain SF162. Unpublished structural data suggests that the gp120 residues thought to be critical for binding α4β7 mediate protomer-protomer interactions and are thereby internally sequestered and prevented from binding α4β7 (Joe Sodroski, personal communication). It is therefore very unlikely that α4β7 interacts with Env prior to CD4 engagement as originally conceived (63). Practically speaking, unless compelling data using physiologically relevant viruses is presented to support that claim that α4β7 is an important host protein for HIV-1 transmission, future experiments are unnecessary. However, if there is a role for α4β7 after CD4 engagement,

investigators might develop tools that allow this interaction to be studied in experimental systems that are more easily manipulated and permit testing of many viruses. For example, pseudoviruses could be generated in cells (e.g. 293S GnTI-) lacking N-acetylglucosaminyltransferase I activity to generate a glyocosylation pattern more reflective of primary cells (38) and monoclonal antibodies that induce an “active” conformation of α4β7 with high affinity for its ligands (48) could be used to study the Env/α4β7 interaction using cell lines.

Future work is needed to define the differences in intrinsic entry functions of T/F Envs in comparison to those of CC Envs more generally and in higher resolution. First, only subtype B and C have been examined in detail. Ongoing work suggests that while subtype A T/F viruses are CD4+ T cell-tropic and not macrophage tropic, subtype D T/F viruses are often macrophage tropic (13). Future investigators aiming to identify general phenotypic properties of T/F Envs should endeavor to compile panels of T/F Envs of multiple subtypes using the same stringent selection criteria. Based on our experience, differences in intrinsic Env function are likely to be subtle. Thus panels of at least 50 T/F and 50 CC Envs should be tested simultaneously. This problem is well illustrated by the following: in the subtype B panels there was a significant difference in T/F and CC Env sensitivity to VRC01 and HIVIG, in subtype C there was a trend in the same direction, and pooling all data revealed a significant difference between T/F and CC. However, given the differences in selection criteria between these two panels and *post hoc* statistical analysis, this difference is difficult to interpret.

Future studies should focus on the mechanism of the difference in MVC inhibition by T/F and CC Envs, specifically that T/F viruses are less completely inhibited by MVC than CC Envs (269). Some biologically plausible hypotheses include: 1) T/F Envs have a conserved, constrained means of interacting with CCR5 that is more sensitive to inhibition by MVC because the Env/CCR5 interaction must mediate cellular signaling (369) in order for a virus to be efficiently transmitted, but this signaling is not required during chronic infection. This could be tested by calcium flux experiments or other experiments to probe differences in intracellular signaling of T/F and CC gp120 and viruses. 2) The MVC sensitivity of T/F Envs is a surrogate of resistance or

sensitivity to inhibition by one or more of the various CCR5-interacting beta-chemokines that could be present at high levels during primary infection, including CCL3, CCL4, CCL5, or CCL3L1. This would be straightforward to test, although purchasing enough of these recombinant proteins from commercial sources for a comprehensive analysis might be cost-prohibitive. 3) CCR5 is known to exist in different antigenic conformations, which are expressed at different levels on different cell types (31, 199). Perhaps the initial target cells during mucosal transmission are more constrained in their expression of CCR5 isoforms. Exclusive use of the isoforms expressed by these cells for entry could be associated with complete inhibition by MVC. Characterizing CCR5 expression on primary cells from mucosal tissues and cell lines using well-defined monoclonal antibodies with known CCR5 isoform recognition preferences would thus refine this hypothesis and help define the CCR5 isoforms/epitopes involved in this phenomenon. One clue regarding this phenomenon comes from the observation that Envs incompletely inhibited by MVC also tend to require more of the fusion inhibitor T20 to reach 50% inhibition (R_s=0.59, p=0.00007). However, these data are available only for only subtype B panel at this time, so the generality of this correlation should be examined. This might suggest a general explanation for the observed MVC resistance of CC Envs relating to the kinetics of Env conformational change.

The use of CCR5 in a constrained, MVC-sensitive manner is a key generalizable feature of T/F Envs. Indeed, it was observed for the virus described in chapter four (ZP6248) which used CCR5 *in vitro* very inefficiently. ZP6248 is informative despite being an extreme outlier because it helps delineate the properties necessary and sufficient for transmission. Pseudoviruses expressing the Env of this virus entered NP2 cells expressing CCR5 approximately two orders of magnitude less than the next lowest T/F pseudovirus (Figure 4-6), and only 5-fold more efficiently than the X4-using Env NL4-3 (Table 4-1). In contrast, this Env mediated entry into NP2 cells expressing the alternative coreceptor GPR15 more efficiently than any other T/F or CC Env tested. Thus efficient use of CCR5, at least as tested *in vitro*, is not an absolute requirement for transmission although it is observed in the vast majority of T/F viruses. One speculation is that

ZP6248 actually did use CCR5 *in vivo*, although in a form that is not recapitulated *in vitro* or present at high levels in peripheral CD4+ T cells. Thus the coreceptor use of ZP6248 should be revisited once there is a better understanding of the MVC-inhibition phenomenon, as the two may be related. Another possibility is that this virus used GPR15 to establish primary infection. In any case, this observation highlights the phenotypic diversity of T/F HIV-1 and should motivate future studies with the goal of quantifying the selective advantage R5-use confers for HIV-1 transmission (51, 299). However, all current data suggests that MVC-containing microbicides should be very effective against the population of viruses most relevant to mucosal transmission, ignoring concerns about pharmacokinetics or adherence. Furthermore, structurally defining the Env domains involved in the constrained, MVC-sensitive CCR5 use of T/F viruses could guide immunogen design.

Function of infectious molecular clones (IMCs). The atypical coreceptor use of the Env described in chapter four prompted us to generate an IMC representing the entire genome of the T/F virus. This was done to ensure that the phenotype of the Env pseudovirus was representative of the complete T/F virus, which was indeed the case for this virus. Previously, we characterized two T/F *env* expression cassettes that did not functionally complement an *env*-deficient HIV-1 provirus backbone (191). Because the inference of the T/F *env* sequence was unambiguous, the Envs encoded by these cassettes must have mediated entry sufficient for transmission. Indeed, complete IMCs of the viruses in question were fully functional in a variety of experimental systems. We then defined the source of the pseudovirus assay artifact: a post-transcriptional block in steady-state Env production in the pseudovirus system that was specific to *env* cassettes with a certain reading frame configuration upstream of *env* (191). Thus due to differences in Env protein production, and therefore incorporation into particles, pseudoviruses generated using these *env* cassettes were not representative of the complete T/F virus from which the *envs* were derived. Such a phenomenon may explain the seeming discordance of Figure 2-4 and Figures 5-5 and 5-7, although differences in virus input normalization likely also play a role.

The entry function of T/F Envs described in chapters two through four was determined primarily using trans-complementation assays and thus does not address whether viral genes other than *env* or differences in Env requiring production and incorporation in its native context play a role in transmission. Therefore we characterized subtype B and C T/F and CC IMCs as reported in chapter five. The first hypothesis we tested was based on the most significant genotypic difference between T/F and chronic *env* sequences – conservation of a histidine at residue 12 of the signal peptide in T/F viruses (126). This residue was shown to lead to increased Env expression and incorporation (11). Furthermore, a number of other T/F signatures were found in the signal peptide or cytoplasmic tail of gp41, locations considered more likely to influence Env content than Env receptor binding functions (although the cytoplasmic tail of gp41 is important for both (60)). Thus we hypothesized that increased Env incorporation represented a biological difference between T/F and CC viruses that could be accomplished thorough a number of individually weak genotypic signatures. Our data support this hypothesis, with T/F viruses on average containing about twice as much Env as CC viruses.

Future studies of the consequences of increased Env content on virus neutralization and sensitivity of virus-producing cells to antibody (Ab) dependent cell-mediated cytotoxicity (ADCC) are warranted. For example, it has been hypothesized that HIV-1 avoids Ab neutralization by containing relatively few Env spikes, such that a single Ab can only interact with one spike at a time (184). Thus if Env density is increased on T/F viruses to a level that allows bivalent Ab binding, there may be a paradoxical increase in neutralization sensitivity to Abs that are capable of cross-linking spikes. This could be tested either by engineering an epitope tag into the fourth variable region of gp120 of a panel of viruses with different Env content (295) or generating pseudovirus with a spectrum of Env content by changing the ratio of transfected *env* to backbone DNA. If this theory is borne out, targeting regions of Env structurally positioned to allow cross-spike binding by Ab might be ideal. It is also of interest to determine if cells infected by viruses with high Env content are more readily targeted for ADCC than cells infected by viruses with low Env content. Since virus assembly takes place at the plasma membrane (173), Env must be

present here, at least momentarily, prior to virus budding; in many cases viruses with high Env content have been shown to have high cell surface Env expression (219, 320, 386, 387). Thus there may be more target molecules for Env-binding antibodies present on the surface of cells producing viruses with high Env content. Cell surface IgG binding correlates directly with ADCC (338), thus increased cell surface Env binding would likely lead to increased killing of infected cells. This would also provide a biologically plausible mechanism for differences in Env content between the acute and chronic phases of infection, as ADCC-mediating antibodies gradually increase during early chronic infection and then generally remain at high levels (11, 132, 261).

Functional Env content can likely be modulated in a number of ways, including matrix-gp41 interaction (60), endocytosis mediated by the gp41 cytoplasmic tail (317), CD4 downregulation efficiency (8), and Env stability (4), but which of these are employed by T/F viruses to achieve high Env content is not known. If there were to be a conserved interaction important for high Env incorporation, it could make an attractive drug target. There are many potential starting points: Previous investigators have concluded that Env incorporation is the major determinant of Env content (56), but this could be confirmed using relevant T/F and CC viral strains. The influence of all of the signature genotypes identified by Korber and colleagues (126) on Env content could be determined in the context of IMCs. Furthermore, the role of Env potential asparagine-linked glycan (PNLG) count, consistently observed to be slightly lower in T/F viruses, on Env processing, retention in the Golgi complex, steady state expression, or content in virions should be explored and the impact of T/F *env* codon usage on inhibition by the restriction factor schlafen 11 examined (206).

Characterizing the downstream biological consequences of increased Env content might help build a more complete model of the cell-host interactions important for mucosal transmission. We show that infectivity and dendritic cell binding correlated weakly with Env content, but more experiments would be needed to determine if Env content directly affects these properties. Cells infected by HIV-1 with high Env content activated NFkB, increased proviral transcription, and higher virus production (15). This suggests that increased Env may play a role

in signaling. Furthermore, the stability of viruses with high Env content at physiological temperatures and pH, as well as in complex biological solutions such as semen or cervicovaginal mucous, should be determined.

The relative resistance of T/F viruses to interferon alpha (IFN-α) is another area for future focus. Our interpretation that T/F viruses are selected on the basis of their ability to overcome innate immune responses during mucosal transmission challenges the concept that these earliest responses to HIV-1 infection are ineffective or even harmful. The most direct support for the notion of a harmful innate response comes from the observation that mucosal administration of toll-like receptor agonists did not prevent transmission after high-dose SIV challenge despite inducing IFN-α (364). The challenge dose used in these experiments was sufficient to infect 15/16 animals after two mucosal exposures, in contrast to the 100-1000 mucosal exposures often occurring prior to HIV-1 infection. Thus these experiments should be repeated with a lower challenge dose. Indeed, direct administration of IFN-α prior to repeated low-dose challenge was protective, and a lower number of T/F variant were observed in animals that were eventually infected (Daniel C. Douek, personal communication). The dynamics of IFN-α in different stages of HIV-1 infection should also be re-examined because increased infectiousness has been observed during late-stage disease (161), which may relate to the elevated IFN-α and correspondingly IFN-α resistant viruses present at this stage (101, 192).

The mechanism of IFN-α resistance by T/F viruses should be defined in order to translate this finding into a useful intervention. Some but not much of the IFN-α resistance of T/F viruses may be related to their increased Env content. The existence of an IFN-α-induced activity that specifically limits Env incorporation can be inferred from early work (89, 150). One molecule with such an activity is the secretory glycoprotein 90K, encoded by *LGALS3BP* (127), thus its influence on T/F and CC virus production should be explored. One candidate for a viral protein mediating IFN-α resistance is the viral protein U (Vpu). Vpu has been shown to deplete interferon regulatory factor 3 (92), which otherwise activates transcription of IFN-a and interferon stimulated

genes in the context of virus infection (91). In addition to hypothesis-based approaches to identify viral proteins involved in IFN-α resistance, knockouts of all accessory genes in representative T/F and CC IMCs should be tested for IFN-α resistance and the step in the viral life cycle that IFN-α has disparate effects on T/F and CC viruses should be defined. If viral proteins necessary for IFN-α resistance are identified, the functional motifs involved should be targeted by vaccination. Our data suggests that high IFN-α resistance is less critical in chronic infection. Thus immunizing chronically infected individuals against these proteins might lead to virus mutation at motifs important for IFN-α resistance. Evolutionarily, this can be thought of as applying a selective pressure that can be readily escaped from with little within-host fitness cost, yet escape bears a large cost in terms of inter-host fitness, i.e. transmission (202). However, IFN-α resistance is not necessarily a protein-mediated effect; the influence of nucleotide sequence variation in the long-terminal repeat (LTR), including variants with more or fewer functional NFkB binding sites (16, 170, 229), on IFN-α resistance should be explored. Finally, we tested the replication of T/F and CC IMCs in very highly stimulated CD4+ T cells. The ability of T/F and CC viruses to infect minimally activated CD4+ T cells should also be tested (340), especially considering the evidence that these are the initial target cells in SIV-infected animals.

Our favored interpretation of the phenotypic differences between T/F and CC viruses described here is that they are due to selective transmission of viruses with certain biological properties. Formally, there are several other interpretations, including phenotypic compartmentalization of viruses with T/F-like properties in genital secretions or biased selection of T/F lineages that have experienced less pressure from host adaptive immune systems than CC lineages due to acute-to-acute transmission chains. Perhaps only a subset of chronically infected individuals harbor virus that is competent for ongoing transmission, and while mucosal barriers only allow transmission of viruses from such patients, all variants present in an inoculum from such individuals have an equal likelihood of being transmitted. These possibilities might best be definitively addressed by performing studies similar to those here using viruses from transmission pairs and from subjects sampled longitudinally from acute infection. This should become

exponentially more facile with advances in DNA sequencing, chemical synthesis, and *in vitro* manipulation (232). Additionally, experimental infection of humanized mice with T/F and CC HIV-1 variants could directly determine if T/F viruses are more readily transmitted. Repeat low-dose challenge of macaques with SIV variants with known phenotypes (e.g. high vs low Env content or IFN-α resistance) could be used to challenge macaques to determine if transmission is selective on the basis of these phenotypes.

Developing new mathematical models of viral population dynamics incorporating these results may be helpful to understand mucosal HIV-1 transmission. For example, serial bottleneck events present a risk of fitness loss due to genetic drift and irreversible accumulation of deleterious mutations known as "Muller's ratchet" (111). While generally applicable only to organisms that do not recombine, Muller's ratchet may apply to HIV-1 in the case of serial single-variant transmissions. Such an effect has been demonstrated for other RNA viruses with high mutation rates (98). Passage of HIV-1 *in vitro* has been associated with severe fitness loss after as few as seven passages (388). Selective transmission of "fit" viruses may prevent such an effect, even if only one variant is transmitted. Models that could estimate the impact of intermittent multiple-variant transmissions or superinfection on the fitness of a viral lineage might be especially informative. Finally, it would be helpful to understand the effect of interventions that decrease the number of transmitted variants in the absence of sterilizing protection, as this may be the most tractable goal in the high-risk populations in which HIV-1 incidence continues to increase (5).

In summary, our results provide a foundation to understand the biology of T/F viruses. Due to the fact that T/F viruses are drawn from the larger population of CC viruses, there is no "black and white" dichotomy in the traits of T/F and CC viruses. However, T/F viruses are a non-random subset of CC viruses, quantitatively different in a number of phenotypes including coreceptor tropism, Env content, and IFN-α resistance. Future work is needed because our current knowledge of these differences is phenomenological rather than mechanistic. While the results described here can be used to refine conceptual models of mucosal HIV-1 transmission,

higher resolution information about the phenotypic differences between T/F and CC viruses is needed to translate this knowledge into useful interventions.

BIBLIOGRAPHY

1. 2012. Priority: Expanding Basic Discovery Research, Etiology and Pathogenesis. National Institutes of Health.
2. 2008. Report on the global AIDS epidemic Joint United Nations Programme on HIV/AIDS (UNAIDS).
3. Abrahams, M. R., J. A. Anderson, E. E. Giorgi, C. Seoighe, K. Mlisana, L. H. Ping, G. S. Athreya, F. K. Treurnicht, B. F. Keele, N. Wood, J. F. Salazar-Gonzalez, T. Bhattacharya, H. Chu, I. Hoffman, S. Galvin, C. Mapanje, P. Kazembe, R. Thebus, S. Fiscus, W. Hide, M. S. Cohen, S. A. Karim, B. F. Haynes, G. M. Shaw, B. H. Hahn, B. T. Korber, R. Swanstrom, and C. Williamson. 2009. Quantitating the multiplicity of infection with human immunodeficiency virus type 1 subtype C reveals a non-poisson distribution of transmitted variants. J Virol 83:3556-3567.
4. Agrawal, N., D. P. Leaman, E. Rowcliffe, H. Kinkead, R. Nohria, J. Akagi, K. Bauer, S. X. Du, R. G. Whalen, D. R. Burton, and M. B. Zwick. 2011. Functional stability of unliganded envelope glycoprotein spikes among isolates of human immunodeficiency virus type 1 (HIV-1). PLoS One 6:e21339.
5. Alexander, M., R. Lynch, J. Mulenga, S. Allen, C. A. Derdeyn, and E. Hunter. 2010. Donor and recipient envs from heterosexual human immunodeficiency virus subtype C transmission pairs require high receptor levels for entry. J Virol 84:4100-4104.
6. Anderson, J. A., L. H. Ping, O. Dibben, C. B. Jabara, L. Arney, L. Kincer, Y. Tang, M. Hobbs, I. Hoffman, P. Kazembe, C. D. Jones, P. Borrow, S. Fiscus, M. S. Cohen, and R. Swanstrom. 2010. HIV-1 Populations in Semen Arise through Multiple Mechanisms. PLoS Pathog 6:e1001053.
7. Ansari, A. A., K. A. Reimann, A. E. Mayne, Y. Takahashi, S. T. Stephenson, R. Wang, X. Wang, J. Li, A. A. Price, D. M. Little, M. Zaidi, R. Lyles, and F. Villinger. 2011. Blocking of alpha4beta7 gut-homing integrin during acute infection leads to decreased plasma and gastrointestinal tissue viral loads in simian immunodeficiency virus-infected rhesus macaques. J Immunol 186:1044-1059.
8. Arganaraz, E. R., M. Schindler, F. Kirchhoff, M. J. Cortes, and J. Lama. 2003. Enhanced CD4 down-modulation by late stage HIV-1 nef alleles is associated with increased Env incorporation and viral replication. J Biol Chem 278:33912-33919.
9. Arthos, J., C. Cicala, E. Martinelli, K. Macleod, D. Van Ryk, D. Wei, Z. Xiao, T. D. Veenstra, T. P. Conrad, R. A. Lempicki, S. McLaughlin, M. Pascuccio, R. Gopaul, J. McNally, C. C. Cruz, N. Censoplano, E. Chung, K. N. Reitano, S. Kottilil, D. J. Goode, and A. S. Fauci. 2008. HIV-1 envelope protein binds to and signals through integrin

alpha4beta7, the gut mucosal homing receptor for peripheral T cells. Nat Immunol 9:301-309.

10. Asmal, M., I. Hellmann, W. Liu, B. F. Keele, A. S. Perelson, T. Bhattacharya, S. Gnanakaran, M. Daniels, B. F. Haynes, B. T. Korber, B. H. Hahn, G. M. Shaw, and N. L. Letvin. 2011. A signature in HIV-1 envelope leader peptide associated with transition from acute to chronic infection impacts envelope processing and infectivity. PLoS One 6:e23673.
11. Asmal, M., Y. Sun, S. Lane, W. Yeh, S. D. Schmidt, J. R. Mascola, and N. L. Letvin. 2011. Antibody-dependent cell-mediated viral inhibition emerges after simian immunodeficiency virus SIVmac251 infection of rhesus monkeys coincident with gp140-binding antibodies and is effective against neutralization-resistant viruses. J Virol 85:5465-5475.
12. Atashili, J., C. Poole, P. M. Ndumbe, A. A. Adimora, and J. S. Smith. 2008. Bacterial vaginosis and HIV acquisition: a meta-analysis of published studies. AIDS 22:1493-1501.
13. Baalwa, J., S. Wang, N. F. Parrish, J. M. Decker, B. F. Keele, G. H. Learn, L. Yue, E. Ruzagira, D. Ssemwanga, A. Kamali, P. N. Amornkul, M. A. Price, J. C. Kappes, E. Karita, P. Kaleebu, E. Sanders, J. Gilmour, S. Allen, E. Hunter, D. C. Montefiori, B. F. Haynes, E. Cormier, B. H. Hahn, and G. M. Shaw. 2012. Molecular identification, cloning and characterization of transmitted/founder HIV-1 subtype A, D and A/D infectious molecular clones. Virology.
14. Baba, M., H. Miyake, X. Wang, M. Okamoto, and K. Takashima. 2007. Isolation and characterization of human immunodeficiency virus type 1 resistant to the small-molecule CCR5 antagonist TAK-652. Antimicrob Agents Chemother 51:707-715.
15. Bachrach, E., H. Dreja, Y. L. Lin, C. Mettling, V. Pinet, P. Corbeau, and M. Piechaczyk. 2005. Effects of virion surface gp120 density on infection by HIV-1 and viral production by infected cells. Virology 332:418-429.
16. Bachu, M., S. Yalla, M. Asokan, A. Verma, U. Neogi, S. Sharma, R. V. Murali, A. B. Mukthey, R. Bhatt, S. Chatterjee, R. E. Rajan, N. Cheedarla, V. S. Yadavalli, A. Mahadevan, S. K. Shankar, N. Rajagopalan, A. Shet, S. Saravanan, P. Balakrishnan, S. Solomon, M. Vajpayee, K. S. Satish, T. K. Kundu, K. T. Jeang, and U. Ranga. 2012. Multiple NF-kappaB sites in HIV-1 subtype C LTR confer superior magnitude of transcription and thereby the enhanced viral predominance. J Biol Chem.
17. Baldauf, H. M., X. Pan, E. Erikson, S. Schmidt, W. Daddacha, M. Burggraf, K. Schenkova, I. Ambiel, G. Wabnitz, T. Gramberg, S. Panitz, E. Flory, N. R. Landau, S. Sertel, F. Rutsch, F. Lasitschka, B. Kim, R. Konig, O. T. Fackler, and O. T. Keppler. 2012. SAMHD1 restricts HIV-1 infection in resting CD4(+) T cells. Nat Med 18:1682-1689.

18. Ball, T. B., H. Ji, J. Kimani, P. McLaren, C. Marlin, A. V. Hill, and F. A. Plummer. 2007. Polymorphisms in IRF-1 associated with resistance to HIV-1 infection in highly exposed uninfected Kenyan sex workers. AIDS 21:1091-1101.
19. Ballweber, L., B. Robinson, A. Kreger, M. Fialkow, G. Lentz, M. J. McElrath, and F. Hladik. 2011. Vaginal langerhans cells nonproductively transporting HIV-1 mediate infection of T cells. J Virol 85:13443-13447.
20. Balotta, C., P. Bagnarelli, M. Violin, A. L. Ridolfo, D. Zhou, A. Berlusconi, S. Corvasce, M. Corbellino, M. Clementi, M. Clerici, M. Moroni, and M. Galli. 1997. Homozygous delta 32 deletion of the CCR-5 chemokine receptor gene in an HIV-1-infected patient. AIDS 11:F67-71.
21. Bar, K. J., H. Li, A. Chamberland, C. Tremblay, J. P. Routy, T. Grayson, C. Sun, S. Wang, G. H. Learn, C. J. Morgan, J. E. Schumacher, B. F. Haynes, B. F. Keele, B. H. Hahn, and G. M. Shaw. 2010. Wide variation in the multiplicity of HIV-1 infection among injection drug users. J Virol 84:6241-6247.
22. Bar, K. J., C. Y. Tsao, S. S. Iyer, J. M. Decker, Y. Yang, M. Bonsignori, X. Chen, K. K. Hwang, D. C. Montefiori, H. X. Liao, P. Hraber, W. Fischer, H. Li, S. Wang, S. Sterrett, B. F. Keele, V. V. Ganusov, A. S. Perelson, B. T. Korber, I. Georgiev, J. S. McLellan, J. W. Pavlicek, F. Gao, B. F. Haynes, B. H. Hahn, P. D. Kwong, and G. M. Shaw. 2012. Early low-titer neutralizing antibodies impede HIV-1 replication and select for virus escape. PLoS Pathog 8:e1002721.
23. Barbas, C. F., 3rd, E. Bjorling, F. Chiodi, N. Dunlop, D. Cababa, T. M. Jones, S. L. Zebedee, M. A. Persson, P. L. Nara, E. Norrby, and et al. 1992. Recombinant human Fab fragments neutralize human type 1 immunodeficiency virus in vitro. Proc Natl Acad Sci U S A 89:9339-9343.
24. Barr, S. D., J. R. Smiley, and F. D. Bushman. 2008. The interferon response inhibits HIV particle production by induction of TRIM22. PLoS Pathog 4:e1000007.
25. Bednarczyk, J. L., and B. W. McIntyre. 1990. A monoclonal antibody to VLA-4 alpha-chain (CDw49d) induces homotypic lymphocyte aggregation. Journal of immunology 144:777-784.
26. Bednarczyk, J. L., T. K. Teague, J. N. Wygant, L. S. Davis, P. E. Lipsky, and B. W. McIntyre. 1992. Regulation of T cell proliferation by anti-CD49d and anti-CD29 monoclonal antibodies. Journal of leukocyte biology 52:456-462.
27. Begaud, E., G. Feindirongai, P. Versmisse, J. Ipero, J. Leal, Y. Germani, J. Morvan, H. Fleury, M. Muller-Trutwin, F. Barre-Sinoussi, and G. Pancino. 2003. Broad spectrum of coreceptor usage and rapid disease progression in HIV-1-infected individuals from Central African Republic. AIDS Res Hum Retroviruses 19:551-560.

28. Berger, E. A., P. M. Murphy, and J. M. Farber. 1999. Chemokine receptors as HIV-1 coreceptors: roles in viral entry, tropism, and disease. Annu Rev Immunol 17:657-700.
29. Berlier, W., M. Cremel, H. Hamzeh, R. Levy, F. Lucht, T. Bourlet, B. Pozzetto, and O. Delezay. 2006. Seminal plasma promotes the attraction of Langerhans cells via the secretion of CCL20 by vaginal epithelial cells: involvement in the sexual transmission of HIV. Hum Reprod 21:1135-1142.
30. Berro, R., P. J. Klasse, D. Lascano, A. Flegler, K. A. Nagashima, R. W. Sanders, T. P. Sakmar, T. J. Hope, and J. P. Moore. 2011. Multiple CCR5 conformations on the cell surface are used differentially by human immunodeficiency viruses resistant or sensitive to CCR5 inhibitors. J Virol.
31. Berro, R., P. J. Klasse, D. Lascano, A. Flegler, K. A. Nagashima, R. W. Sanders, T. P. Sakmar, T. J. Hope, and J. P. Moore. 2011. Multiple CCR5 conformations on the cell surface are used differentially by human immunodeficiency viruses resistant or sensitive to CCR5 inhibitors. J Virol 85:8227-8240.
32. Berro, R., R. W. Sanders, M. Lu, P. J. Klasse, and J. P. Moore. 2009. Two HIV-1 variants resistant to small molecule CCR5 inhibitors differ in how they use CCR5 for entry. PLoS Pathog 5:e1000548.
33. Biancotto, A., B. Brichacek, S. S. Chen, W. Fitzgerald, A. Lisco, C. Vanpouille, L. Margolis, and J. C. Grivel. 2009. A highly sensitive and dynamic immunofluorescent cytometric bead assay for the detection of HIV-1 p24. J Virol Methods 157:98-101.
34. Biswas, P., G. Tambussi, and A. Lazzarin. 2007. Access denied? The status of co-receptor inhibition to counter HIV entry. Expert Opin Pharmacother 8:923-933.
35. Bleul, C. C., L. Wu, J. A. Hoxie, T. A. Springer, and C. R. Mackay. 1997. The HIV coreceptors CXCR4 and CCR5 are differentially expressed and regulated on human T lymphocytes. Proc Natl Acad Sci U S A 94:1925-1930.
36. Boeras, D. I., P. T. Hraber, M. Hurlston, T. Evans-Strickfaden, T. Bhattacharya, E. E. Giorgi, J. Mulenga, E. Karita, B. T. Korber, S. Allen, C. E. Hart, C. A. Derdeyn, and E. Hunter. 2011. Role of donor genital tract HIV-1 diversity in the transmission bottleneck. Proc Natl Acad Sci U S A 108:E1156-1163.
37. Bomsel, M. 1997. Transcytosis of infectious human immunodeficiency virus across a tight human epithelial cell line barrier. Nat Med 3:42-47.
38. Bonomelli, C., K. J. Doores, D. C. Dunlop, V. Thaney, R. A. Dwek, D. R. Burton, M. Crispin, and C. N. Scanlan. 2011. The glycan shield of HIV is predominantly oligomannose independently of production system or viral clade. PLoS One 6:e23521.
39. Borrok, M. J., and L. L. Kiessling. 2007. Non-carbohydrate inhibitors of the lectin DC-SIGN. J Am Chem Soc 129:12780-12785.

40. Borrow, P., H. Lewicki, X. Wei, M. S. Horwitz, N. Peffer, H. Meyers, J. A. Nelson, J. E. Gairin, B. H. Hahn, M. B. Oldstone, and G. M. Shaw. 1997. Antiviral pressure exerted by HIV-1-specific cytotoxic T lymphocytes (CTLs) during primary infection demonstrated by rapid selection of CTL escape virus. Nat Med 3:205-211.
41. Brenchley, J. M., T. W. Schacker, L. E. Ruff, D. A. Price, J. H. Taylor, G. J. Beilman, P. L. Nguyen, A. Khoruts, M. Larson, A. T. Haase, and D. C. Douek. 2004. CD4+ T cell depletion during all stages of HIV disease occurs predominantly in the gastrointestinal tract. J Exp Med 200:749-759.
42. Brenner, B. G., M. Roger, J. P. Routy, D. Moisi, M. Ntemgwa, C. Matte, J. G. Baril, R. Thomas, D. Rouleau, J. Bruneau, R. Leblanc, M. Legault, C. Tremblay, H. Charest, and M. A. Wainberg. 2007. High rates of forward transmission events after acute/early HIV-1 infection. J Infect Dis 195:951-959.
43. Bridger, G. J., R. T. Skerlj, D. Thornton, S. Padmanabhan, S. A. Martellucci, G. W. Henson, M. J. Abrams, N. Yamamoto, K. De Vreese, R. Pauwels, and et al. 1995. Synthesis and structure-activity relationships of phenylenebis(methylene)-linked bis-tetraazamacrocycles that inhibit HIV replication. Effects of macrocyclic ring size and substituents on the aromatic linker. J Med Chem 38:366-378.
44. Brighty, D. W., M. Rosenberg, I. S. Chen, and M. Ivey-Hoyle. 1991. Envelope proteins from clinical isolates of human immunodeficiency virus type 1 that are refractory to neutralization by soluble CD4 possess high affinity for the CD4 receptor. Proc Natl Acad Sci U S A 88:7802-7805.
45. Bunnik, E. M., Z. Euler, M. R. Welkers, B. D. Boeser-Nunnink, M. L. Grijsen, J. M. Prins, and H. Schuitemaker. 2010. Adaptation of HIV-1 envelope gp120 to humoral immunity at a population level. Nat Med 16:995-997.
46. Burton, D. R., C. F. Barbas, 3rd, M. A. Persson, S. Koenig, R. M. Chanock, and R. A. Lerner. 1991. A large array of human monoclonal antibodies to type 1 human immunodeficiency virus from combinatorial libraries of asymptomatic seropositive individuals. Proc Natl Acad Sci U S A 88:10134-10137.
47. Burton, D. R., J. Pyati, R. Koduri, S. J. Sharp, G. B. Thornton, P. W. Parren, L. S. Sawyer, R. M. Hendry, N. Dunlop, P. L. Nara, and et al. 1994. Efficient neutralization of primary isolates of HIV-1 by a recombinant human monoclonal antibody. Science 266:1024-1027.
48. Byron, A., J. D. Humphries, J. A. Askari, S. E. Craig, A. P. Mould, and M. J. Humphries. 2009. Anti-integrin monoclonal antibodies. J Cell Sci 122:4009-4011.
49. Cai, F., H. Chen, C. B. Hicks, J. A. Bartlett, J. Zhu, and F. Gao. 2007. Detection of minor drug-resistant populations by parallel allele-specific sequencing. Nat. Methods 4:123-125.

50. Cameron, P. U., P. S. Freudenthal, J. M. Barker, S. Gezelter, K. Inaba, and R. M. Steinman. 1992. Dendritic cells exposed to human immunodeficiency virus type-1 transmit a vigorous cytopathic infection to CD4+ T cells. Science 257:383-387.
51. Chalmet, K., K. Dauwe, L. Foquet, F. Baatz, C. Seguin-Devaux, B. Van Der Gucht, D. Vogelaers, L. Vandekerckhove, J. Plum, and C. Verhofstede. 2012. Presence of CXCR4-using HIV-1 in patients with recently diagnosed infection: correlates and evidence for transmission. J Infect Dis 205:174-184.
52. Chambers, J. M., and T. J. Hastie. 1992. Statistical Models in S. Wadsworth & Brooks/Cole.
53. Charleston, B., M. D. Fray, S. Baigent, B. V. Carr, and W. I. Morrison. 2001. Establishment of persistent infection with non-cytopathic bovine viral diarrhoea virus in cattle is associated with a failure to induce type I interferon. J Gen Virol 82:1893-1897.
54. Chen, Z., D. Kwon, Z. Jin, S. Monard, P. Telfer, M. S. Jones, C. Y. Lu, R. F. Aguilar, D. D. Ho, and P. A. Marx. 1998. Natural infection of a homozygous delta24 CCR5 red-capped mangabey with an R2b-tropic simian immunodeficiency virus. J Exp Med 188:2057-2065.
55. Chertova, E., J. W. Bess, B. J. Crise, R. C. Sowder, T. M. Schaden, J. M. Hilburn, J. A. Hoxie, R. E. Benveniste, J. D. Lifson, L. E. Henderson, and L. O. Arthur. 2002. Envelope glycoprotein incorporation, not shedding of surface envelope glycoprotein (gp120/SU), is the primary determinant of SU content of purified human immunodeficiency virus type 1 and simian immunodeficiency virus. Journal of Virology 76:5315-5325.
56. Chertova, E., J. W. Bess, Jr., B. J. Crise, I. R. Sowder, T. M. Schaden, J. M. Hilburn, J. A. Hoxie, R. E. Benveniste, J. D. Lifson, L. E. Henderson, and L. O. Arthur. 2002. Envelope glycoprotein incorporation, not shedding of surface envelope glycoprotein (gp120/SU), Is the primary determinant of SU content of purified human immunodeficiency virus type 1 and simian immunodeficiency virus. J Virol 76:5315-5325.
57. Chesebro, B., and K. Wehrly. 1988. Development of a sensitive quantitative focal assay for human immunodeficiency virus infectivity. J Virol 62:3779-3788.
58. Choe, H., M. Farzan, M. Konkel, K. Martin, Y. Sun, L. Marcon, M. Cayabyab, M. Berman, M. E. Dorf, N. Gerard, C. Gerard, and J. Sodroski. 1998. The orphan seven-transmembrane receptor apj supports the entry of primary T-cell-line-tropic and dualtropic human immunodeficiency virus type 1. J Virol 72:6113-6118.
59. Chohan, B., D. Lang, M. Sagar, B. Korber, L. Lavreys, B. Richardson, and J. Overbaugh. 2005. Selection for human immunodeficiency virus type 1 envelope glycosylation variants with shorter V1-V2 loop sequences occurs during transmission of certain genetic subtypes and may impact viral RNA levels. J Virol 79:6528-6531.

60. Chojnacki, J., T. Staudt, B. Glass, P. Bingen, J. Engelhardt, M. Anders, J. Schneider, B. Muller, S. W. Hell, and H. G. Krausslich. 2012. Maturation-dependent HIV-1 surface protein redistribution revealed by fluorescence nanoscopy. Science 338:524-528.
61. Chung, A. W., G. Isitman, M. Navis, M. Kramski, R. J. Center, S. J. Kent, and I. Stratov. 2011. Immune escape from HIV-specific antibody-dependent cellular cytotoxicity (ADCC) pressure. Proc Natl Acad Sci U S A 108:7505-7510.
62. Cicala, C., J. Arthos, and A. S. Fauci. 2011. HIV-1 envelope, integrins and co-receptor use in mucosal transmission of HIV. J Transl Med 9 Suppl 1:S2.
63. Cicala, C., E. Martinelli, J. P. McNally, D. J. Goode, R. Gopaul, J. Hiatt, K. Jelicic, S. Kottilil, K. Macleod, A. O'Shea, N. Patel, D. Van Ryk, D. Wei, M. Pascuccio, L. Yi, L. McKinnon, P. Izulla, J. Kimani, R. Kaul, A. S. Fauci, and J. Arthos. 2009. The integrin alpha4beta7 forms a complex with cell-surface CD4 and defines a T-cell subset that is highly susceptible to infection by HIV-1. Proc Natl Acad Sci U S A 106:20877-20882.
64. Cichutek, K., H. Merget, S. Norley, R. Linde, W. Kreuz, M. Gahr, and R. Kurth. 1992. Development of a quasispecies of human immunodeficiency virus type 1 in vivo. Proc Natl Acad Sci U S A 89:7365-7369.
65. Cilliers, T., J. Nhlapo, M. Coetzer, D. Orlovic, T. Ketas, W. C. Olson, J. P. Moore, A. Trkola, and L. Morris. 2003. The CCR5 and CXCR4 coreceptors are both used by human immunodeficiency virus type 1 primary isolates from subtype C. J Virol 77:4449-4456.
66. Cilliers, T., S. Willey, W. M. Sullivan, T. Patience, P. Pugach, M. Coetzer, M. Papathanasopoulos, J. P. Moore, A. Trkola, P. Clapham, and L. Morris. 2005. Use of alternate coreceptors on primary cells by two HIV-1 isolates. Virology 339:136-144.
67. Clayton, F., D. P. Kotler, S. K. Kuwada, T. Morgan, C. Stepan, J. Kuang, J. Le, and J. Fantini. 2001. Gp120-induced Bob/GPR15 activation: a possible cause of human immunodeficiency virus enteropathy. Am J Pathol 159:1933-1939.
68. Cleghorn, F. R., N. Jack, J. K. Carr, J. Edwards, B. Mahabir, A. Sill, C. B. McDanal, S. M. Connolly, D. Goodman, R. Q. Bennetts, T. R. O'Brien, K. J. Weinhold, C. Bartholomew, W. A. Blattner, and M. L. Greenberg. 2000. A distinctive clade B HIV type 1 is heterosexually transmitted in Trinidad and Tobago. Proc Natl Acad Sci U S A 97:10532-10537.
69. Cocchi, F., A. L. DeVico, A. Garzino-Demo, S. K. Arya, R. C. Gallo, and P. Lusso. 1995. Identification of RANTES, MIP-1 alpha, and MIP-1 beta as the major HIV-suppressive factors produced by CD8+ T cells. Science 270:1811-1815.
70. Cohen, M. S. 2007, posting date. CHAVI 001: Acute HIV-1 Infection Prospective Cohort Study. Center for HIV/AIDS Vaccine Immunology (CHAVI) 2.0. [Online.]
71. Cohen, M. S., G. M. Shaw, A. J. McMichael, and B. F. Haynes. 2011. Acute HIV-1 Infection. N Engl J Med 364:1943-1954.

72. Collins-Fairclough, A. M., M. Charurat, Y. Nadai, M. Pando, M. M. Avila, W. A. Blattner, and J. K. Carr. 2011. Significantly longer envelope V2 loops are characteristic of heterosexually transmitted subtype B HIV-1 in Trinidad. PLoS One 6:e19995.
73. Collman, R., B. Godfrey, J. Cutilli, A. Rhodes, N. F. Hassan, R. Sweet, S. D. Douglas, H. Friedman, N. Nathanson, and F. Gonzalez-Scarano. 1990. Macrophage-tropic strains of human immunodeficiency virus type 1 utilize the CD4 receptor. J Virol 64:4468-4476.
74. Collman, R., N. F. Hassan, R. Walker, B. Godfrey, J. Cutilli, J. C. Hastings, H. Friedman, S. D. Douglas, and N. Nathanson. 1989. Infection of monocyte-derived macrophages with human immunodeficiency virus type 1 (HIV-1). Monocyte-tropic and lymphocyte-tropic strains of HIV-1 show distinctive patterns of replication in a panel of cell types. J Exp Med 170:1149-1163.
75. Connor, R. I., K. E. Sheridan, D. Ceradini, S. Choe, and N. R. Landau. 1997. Change in coreceptor use correlates with disease progression in HIV-1--infected individuals. J Exp Med 185:621-628.
76. Coombs, R. W., C. E. Speck, J. P. Hughes, W. Lee, R. Sampoleo, S. O. Ross, J. Dragavon, G. Peterson, T. M. Hooton, A. C. Collier, L. Corey, L. Koutsky, and J. N. Krieger. 1998. Association between culturable human immunodeficiency virus type 1 (HIV-1) in semen and HIV-1 RNA levels in semen and blood: evidence for compartmentalization of HIV-1 between semen and blood. J Infect Dis 177:320-330.
77. Cormier, E. G., and T. Dragic. 2002. The crown and stem of the V3 loop play distinct roles in human immunodeficiency virus type 1 envelope glycoprotein interactions with the CCR5 coreceptor. J Virol 76:8953-8957.
78. Cormier, E. G., D. N. Tran, L. Yukhayeva, W. C. Olson, and T. Dragic. 2001. Mapping the determinants of the CCR5 amino-terminal sulfopeptide interaction with soluble human immunodeficiency virus type 1 gp120-CD4 complexes. J Virol 75:5541-5549.
79. Curlin, M. E., R. Zioni, S. E. Hawes, Y. Liu, W. Deng, G. S. Gottlieb, T. Zhu, and J. I. Mullins. 2010. HIV-1 envelope subregion length variation during disease progression. PLoS Pathog 6:e1001228.
80. Dalgleish, A. G., P. C. Beverley, P. R. Clapham, D. H. Crawford, M. F. Greaves, and R. A. Weiss. 1984. The CD4 (T4) antigen is an essential component of the receptor for the AIDS retrovirus. Nature 312:763-767.
81. De Clercq, E., N. Yamamoto, R. Pauwels, J. Balzarini, M. Witvrouw, K. De Vreese, Z. Debyser, B. Rosenwirth, P. Peichl, R. Datema, and et al. 1994. Highly potent and selective inhibition of human immunodeficiency virus by the bicyclam derivative JM3100. Antimicrob Agents Chemother 38:668-674.
82. De Cock, K. M., H. W. Jaffe, and J. W. Curran. 2012. The evolving epidemiology of HIV/AIDS. AIDS 26:1205-1213.

83. de Mendoza, C., C. Rodriguez, F. Garcia, J. M. Eiros, L. Ruiz, E. Caballero, A. Aguilera, P. Leiva, J. Colomina, F. Gutierrez, J. del Romero, J. Aguero, and V. Soriano. 2007. Prevalence of X4 tropic viruses in patients recently infected with HIV-1 and lack of association with transmission of drug resistance. J Antimicrob Chemother 59:698-704.
84. Decker, J. M., F. Bibollet-Ruche, X. Wei, S. Wang, D. N. Levy, W. Wang, E. Delaporte, M. Peeters, C. A. Derdeyn, S. Allen, E. Hunter, M. S. Saag, J. A. Hoxie, B. H. Hahn, P. D. Kwong, J. E. Robinson, and G. M. Shaw. 2005. Antigenic conservation and immunogenicity of the HIV coreceptor binding site. J Exp Med 201:1407-1419.
85. Delwart, E., M. Magierowska, M. Royz, B. Foley, L. Peddada, R. Smith, C. Heldebrant, A. Conrad, and M. Busch. 2002. Homogeneous quasispecies in 16 out of 17 individuals during very early HIV-1 primary infection. AIDS 16:189-195.
86. Deng, H. K., D. Unutmaz, V. N. KewalRamani, and D. R. Littman. 1997. Expression cloning of new receptors used by simian and human immunodeficiency viruses. Nature 388:296-300.
87. Der, S. D., A. Zhou, B. R. Williams, and R. H. Silverman. 1998. Identification of genes differentially regulated by interferon alpha, beta, or gamma using oligonucleotide arrays. Proc Natl Acad Sci U S A 95:15623-15628.
88. Derdeyn, C. A., J. M. Decker, F. Bibollet-Ruche, J. L. Mokili, M. Muldoon, S. A. Denham, M. L. Heil, F. Kasolo, R. Musonda, B. H. Hahn, G. M. Shaw, B. T. Korber, S. Allen, and E. Hunter. 2004. Envelope-constrained neutralization-sensitive HIV-1 after heterosexual transmission. Science 303:2019-2022.
89. Dianzani, F., C. Castilletti, M. Gentile, H. R. Gelderblom, F. Frezza, and M. R. Capobianchi. 1998. Effects of IFN alpha on late stages of HIV-1 replication cycle. Biochimie 80:745-754.
90. Dickover, R., E. Garratty, K. Yusim, C. Miller, B. Korber, and Y. Bryson. 2006. Role of maternal autologous neutralizing antibody in selective perinatal transmission of human immunodeficiency virus type 1 escape variants. J Virol 80:6525-6533.
91. Doehle, B. P., K. Chang, L. Fleming, J. McNevin, F. Hladik, M. J. McElrath, and M. Gale, Jr. 2012. Vpu-deficient HIV strains stimulate innate immune signaling responses in target cells. J Virol 86:8499-8506.
92. Doehle, B. P., K. Chang, A. Rustagi, J. McNevin, M. J. McElrath, and M. Gale, Jr. 2012. Vpu mediates depletion of interferon regulatory factor 3 during HIV infection by a lysosome-dependent mechanism. J Virol 86:8367-8374.
93. Doores, K. J., and D. R. Burton. Variable loop glycan dependency of the broad and potent HIV-1-neutralizing antibodies PG9 and PG16. J Virol 84:10510-10521.
94. Doranz, B. J., Z. H. Lu, J. Rucker, T. Y. Zhang, M. Sharron, Y. H. Cen, Z. X. Wang, H. H. Guo, J. G. Du, M. A. Accavitti, R. W. Doms, and S. C. Peiper. 1997. Two distinct CCR5

domains can mediate coreceptor usage by human immunodeficiency virus type 1. J Virol 71:6305-6314.

95. Doranz, B. J., J. Rucker, Y. Yi, R. J. Smyth, M. Samson, S. C. Peiper, M. Parmentier, R. G. Collman, and R. W. Doms. 1996. A dual-tropic primary HIV-1 isolate that uses fusin and the beta-chemokine receptors CKR-5, CKR-3, and CKR-2b as fusion cofactors. Cell 85:1149-1158.

96. Dragic, T., V. Litwin, G. P. Allaway, S. R. Martin, Y. Huang, K. A. Nagashima, C. Cayanan, P. J. Maddon, R. A. Koup, J. P. Moore, and W. A. Paxton. 1996. HIV-1 entry into CD4+ cells is mediated by the chemokine receptor CC-CKR-5. Nature 381:667-673.

97. Dragic, T., A. Trkola, D. A. Thompson, E. G. Cormier, F. A. Kajumo, E. Maxwell, S. W. Lin, W. Ying, S. O. Smith, T. P. Sakmar, and J. P. Moore. 2000. A binding pocket for a small molecule inhibitor of HIV-1 entry within the transmembrane helices of CCR5. Proc Natl Acad Sci U S A 97:5639-5644.

98. Duarte, E., D. Clarke, A. Moya, E. Domingo, and J. Holland. 1992. Rapid fitness losses in mammalian RNA virus clones due to Muller's ratchet. Proc Natl Acad Sci U S A 89:6015-6019.

99. Eckstein, D. A., M. L. Penn, Y. D. Korin, D. D. Scripture-Adams, J. A. Zack, J. F. Kreisberg, M. Roederer, M. P. Sherman, P. S. Chin, and M. A. Goldsmith. 2001. HIV-1 actively replicates in naive CD4(+) T cells residing within human lymphoid tissues. Immunity 15:671-682.

100. Edinger, A. L., T. L. Hoffman, M. Sharron, B. Lee, Y. Yi, W. Choe, D. L. Kolson, B. Mitrovic, Y. Zhou, D. Faulds, R. G. Collman, J. Hesselgesser, R. Horuk, and R. W. Doms. 1998. An orphan seven-transmembrane domain receptor expressed widely in the brain functions as a coreceptor for human immunodeficiency virus type 1 and simian immunodeficiency virus. J Virol 72:7934-7940.

101. Edlin, B. R., M. H. St Clair, P. M. Pitha, S. M. Whaling, D. M. King, J. D. Bitran, and R. A. Weinstein. 1992. In-vitro resistance to zidovudine and alpha-interferon in HIV-1 isolates from patients: correlations with treatment duration and response. Ann Intern Med 117:457-460.

102. Eggink, D., C. E. Baldwin, Y. Deng, J. P. Langedijk, M. Lu, R. W. Sanders, and B. Berkhout. 2008. Selection of T1249-resistant human immunodeficiency virus type 1 variants. J Virol 82:6678-6688.

103. Emmelkamp, J. M., and J. K. Rockstroh. 2007. CCR5 antagonists: comparison of efficacy, side effects, pharmacokinetics and interactions--review of the literature. Eur J Med Res 12:409-417.

104. Etemad, B., A. Fellows, B. Kwambana, A. Kamat, Y. Feng, S. Lee, and M. Sagar. 2009. Human immunodeficiency virus type 1 V1-to-V5 envelope variants from the chronic

phase of infection use CCR5 and fuse more efficiently than those from early after infection. J Virol 83:9694-9708.

105. Fahrbach, K. M., S. M. Barry, M. R. Anderson, and T. J. Hope. 2010. Enhanced cellular responses and environmental sampling within inner foreskin explants: implications for the foreskin's role in HIV transmission. Mucosal Immunol 3:410-418.

106. Fahrbach, K. M., S. M. Barry, S. Ayehunie, S. Lamore, M. Klausner, and T. J. Hope. 2007. Activated CD34-derived Langerhans cells mediate transinfection with human immunodeficiency virus. J Virol 81:6858-6868.

107. Farstad, I. N., T. S. Halstensen, D. Kvale, O. Fausa, and P. Brandtzaeg. 1997. Topographic distribution of homing receptors on B and T cells in human gut-associated lymphoid tissue: relation of L-selectin and integrin alpha 4 beta 7 to naive and memory phenotypes. Am J Pathol 150:187-199.

108. Farstad, I. N., T. S. Halstensen, B. Lien, P. J. Kilshaw, A. I. Lazarovits, and P. Brandtzaeg. 1996. Distribution of beta 7 integrins in human intestinal mucosa and organized gut-associated lymphoid tissue. Immunology 89:227-237.

109. Farzan, M., H. Choe, K. Martin, L. Marcon, W. Hofmann, G. Karlsson, Y. Sun, P. Barrett, N. Marchand, N. Sullivan, N. Gerard, C. Gerard, and J. Sodroski. 1997. Two orphan seven-transmembrane segment receptors which are expressed in CD4-positive cells support simian immunodeficiency virus infection. J Exp Med 186:405-411.

110. Faulkner, D. V., and J. Jurka. 1988. Multiple aligned sequence editor (MASE). Trends Biochem Sci 13:321-322.

111. Felsenstein, J. 1974. The evolutionary advantage of recombination. Genetics 78:737-756.

112. Fiebig, E. W., D. J. Wright, B. D. Rawal, P. E. Garrett, R. T. Schumacher, L. Peddada, C. Heldebrant, R. Smith, A. Conrad, S. H. Kleinman, and M. P. Busch. 2003. Dynamics of HIV viremia and antibody seroconversion in plasma donors: implications for diagnosis and staging of primary HIV infection. AIDS 17:1871-1879.

113. Finzi, D., M. Hermankova, T. Pierson, L. M. Carruth, C. Buck, R. E. Chaisson, T. C. Quinn, K. Chadwick, J. Margolick, R. Brookmeyer, J. Gallant, M. Markowitz, D. D. Ho, D. D. Richman, and R. F. Siliciano. 1997. Identification of a reservoir for HIV-1 in patients on highly active antiretroviral therapy. Science 278:1295-1300.

114. Fischer, W., V. V. Ganusov, E. E. Giorgi, P. T. Hraber, B. F. Keele, T. Leitner, C. S. Han, C. D. Gleasner, L. Green, C. C. Lo, A. Nag, T. C. Wallstrom, S. Wang, A. J. McMichael, B. F. Haynes, B. H. Hahn, A. S. Perelson, P. Borrow, G. M. Shaw, T. Bhattacharya, and B. T. Korber. 2010. Transmission of single HIV-1 genomes and dynamics of early immune escape revealed by ultra-deep sequencing. PLoS One 5:e12303.

115. Fouda, G. G., N. L. Yates, J. Pollara, X. Shen, G. R. Overman, T. Mahlokozera, A. B. Wilks, H. H. Kang, J. F. Salazar-Gonzalez, M. G. Salazar, L. Kalilani, S. R. Meshnick, B. H. Hahn, G. M. Shaw, R. V. Lovingood, T. N. Denny, B. Haynes, N. L. Letvin, G. Ferrari, D. C. Montefiori, G. D. Tomaras, and S. R. Permar. 2011. HIV-specific functional antibody responses in breast milk mirror those in plasma and are primarily mediated by IgG antibodies. J Virol 85:9555-9567.

116. Freel, S. A., R. A. Picking, G. Ferrari, H. Ding, C. Ochsenbauer, J. C. Kappes, J. L. Kirchherr, K. A. Soderberg, K. J. Weinhold, C. K. Cunningham, T. N. Denny, J. A. Crump, M. S. Cohen, A. J. McMichael, B. F. Haynes, and G. D. Tomaras. 2012. Initial HIV-1 antigen-specific CD8+ T cells in acute HIV-1 infection inhibit transmitted/founder virus replication. J Virol 86:6835-6846.

117. Frost, S. D., Y. Liu, S. L. Pond, C. Chappey, T. Wrin, C. J. Petropoulos, S. J. Little, and D. D. Richman. 2005. Characterization of human immunodeficiency virus type 1 (HIV-1) envelope variation and neutralizing antibody responses during transmission of HIV-1 subtype B. J Virol 79:6523-6527.

118. Gaines, H., M. A. von Sydow, L. V. von Stedingk, G. Biberfeld, B. Bottiger, L. O. Hansson, P. Lundbergh, A. B. Sonnerborg, J. Wasserman, and O. O. Strannegaard. 1990. Immunological changes in primary HIV-1 infection. AIDS 4:995-999.

119. Ganesh, L., K. Leung, K. Lore, R. Levin, A. Panet, O. Schwartz, R. A. Koup, and G. J. Nabel. 2004. Infection of specific dendritic cells by CCR5-tropic human immunodeficiency virus type 1 promotes cell-mediated transmission of virus resistant to broadly neutralizing antibodies. J Virol 78:11980-11987.

120. Ganguly, D., G. Chamilos, R. Lande, J. Gregorio, S. Meller, V. Facchinetti, B. Homey, F. J. Barrat, T. Zal, and M. Gilliet. 2009. Self-RNA-antimicrobial peptide complexes activate human dendritic cells through TLR7 and TLR8. J Exp Med 206:1983-1994.

121. Gao, F., E. Bailes, D. L. Robertson, Y. Chen, C. M. Rodenburg, S. F. Michael, L. B. Cummins, L. O. Arthur, M. Peeters, G. M. Shaw, P. M. Sharp, and B. H. Hahn. 1999. Origin of HIV-1 in the chimpanzee Pan troglodytes troglodytes. Nature 397:436-441.

122. Gaschen, B., J. Taylor, K. Yusim, B. Foley, F. Gao, D. Lang, V. Novitsky, B. Haynes, B. H. Hahn, T. Bhattacharya, and B. Korber. 2002. Diversity considerations in HIV-1 vaccine selection. Science 296:2354-2360.

123. Geijtenbeek, T. B., D. S. Kwon, R. Torensma, S. J. van Vliet, G. C. van Duijnhoven, J. Middel, I. L. Cornelissen, H. S. Nottet, V. N. KewalRamani, D. R. Littman, C. G. Figdor, and Y. van Kooyk. 2000. DC-SIGN, a dendritic cell-specific HIV-1-binding protein that enhances trans-infection of T cells. Cell 100:587-597.

124. Giorgi, J. V., L. E. Hultin, J. A. McKeating, T. D. Johnson, B. Owens, L. P. Jacobson, R. Shih, J. Lewis, D. J. Wiley, J. P. Phair, S. M. Wolinsky, and R. Detels. 1999. Shorter

survival in advanced human immunodeficiency virus type 1 infection is more closely associated with T lymphocyte activation than with plasma virus burden or virus chemokine coreceptor usage. J Infect Dis 179:859-870.

125. Gnanadurai, C. W., I. Pandrea, N. F. Parrish, M. H. Kraus, G. H. Learn, M. G. Salazar, U. Sauermann, K. Topfer, R. Gautam, J. Munch, C. Stahl-Hennig, C. Apetrei, B. H. Hahn, and F. Kirchhoff. 2010. Genetic identity and biological phenotype of a transmitted/founder virus representative of nonpathogenic simian immunodeficiency virus infection in African green monkeys. J Virol 84:12245-12254.

126. Gnanakaran, S., T. Bhattacharya, M. Daniels, B. F. Keele, P. T. Hraber, A. S. Lapedes, T. Shen, B. Gaschen, M. Krishnamoorthy, H. Li, J. M. Decker, J. F. Salazar-Gonzalez, S. Wang, C. Jiang, F. Gao, R. Swanstrom, J. A. Anderson, L. H. Ping, M. S. Cohen, M. Markowitz, P. A. Goepfert, M. S. Saag, J. J. Eron, C. B. Hicks, W. A. Blattner, G. D. Tomaras, M. Asmal, N. L. Letvin, P. B. Gilbert, A. C. Decamp, C. A. Magaret, W. R. Schief, Y. E. Ban, M. Zhang, K. A. Soderberg, J. G. Sodroski, B. F. Haynes, G. M. Shaw, B. H. Hahn, and B. Korber. 2011. Recurrent signature patterns in HIV-1 B clade envelope glycoproteins associated with either early or chronic infections. PLoS Pathog 7:e1002209.

127. Goffinet, C. 2012. Presented at the Retroviruses, Cold Spring Harbor, New York.

128. Goodenow, M. M., and R. G. Collman. 2006. HIV-1 coreceptor preference is distinct from target cell tropism: a dual-parameter nomenclature to define viral phenotypes. J Leukoc Biol 80:965-972.

129. Goonetilleke, N., M. K. Liu, J. F. Salazar-Gonzalez, G. Ferrari, E. Giorgi, V. V. Ganusov, B. F. Keele, G. H. Learn, E. L. Turnbull, M. G. Salazar, K. J. Weinhold, S. Moore, N. Letvin, B. F. Haynes, M. S. Cohen, P. Hraber, T. Bhattacharya, P. Borrow, A. S. Perelson, B. H. Hahn, G. M. Shaw, B. T. Korber, and A. J. McMichael. 2009. The first T cell response to transmitted/founder virus contributes to the control of acute viremia in HIV-1 infection. J Exp Med 206:1253-1272.

130. Gordon, S. N., B. Cervasi, P. Odorizzi, R. Silverman, F. Aberra, G. Ginsberg, J. D. Estes, M. Paiardini, I. Frank, and G. Silvestri. 2010. Disruption of intestinal CD4+ T cell homeostasis is a key marker of systemic CD4+ T cell activation in HIV-infected individuals. J Immunol 185:5169-5179.

131. Gorry, P. R., C. Zhang, S. Wu, K. Kunstman, E. Trachtenberg, J. Phair, S. Wolinsky, and D. Gabuzda. 2002. Persistence of dual-tropic HIV-1 in an individual homozygous for the CCR5 Delta 32 allele. Lancet 359:1832-1834.

132. Goudsmit, J., K. Ljunggren, L. Smit, M. Jondal, and E. M. Fenyo. 1988. Biological significance of the antibody response to HIV antigens expressed on the cell surface. Arch Virol 103:189-206.

133. Granelli-Piperno, A., E. Delgado, V. Finkel, W. Paxton, and R. M. Steinman. 1998. Immature dendritic cells selectively replicate macrophagetropic (M-tropic) human immunodeficiency virus type 1, while mature cells efficiently transmit both M- and T-tropic virus to T cells. J Virol 72:2733-2737.
134. Granelli-Piperno, A., B. Moser, M. Pope, D. Chen, Y. Wei, F. Isdell, U. O'Doherty, W. Paxton, R. Koup, S. Mojsov, N. Bhardwaj, I. Clark-Lewis, M. Baggiolini, and R. M. Steinman. 1996. Efficient interaction of HIV-1 with purified dendritic cells via multiple chemokine coreceptors. J Exp Med 184:2433-2438.
135. Gray, E. S., M. C. Madiga, T. Hermanus, P. L. Moore, C. K. Wibmer, N. L. Tumba, L. Werner, K. Mlisana, S. Sibeko, C. Williamson, S. S. Abdool Karim, and L. Morris. 2011. The neutralization breadth of HIV-1 develops incrementally over four years and is associated with CD4+ T cell decline and high viral load during acute infection. J Virol 85:4828-4840.
136. Gray, R. H., M. J. Wawer, R. Brookmeyer, N. K. Sewankambo, D. Serwadda, F. Wabwire-Mangen, T. Lutalo, X. Li, T. vanCott, and T. C. Quinn. 2001. Probability of HIV-1 transmission per coital act in monogamous, heterosexual, HIV-1-discordant couples in Rakai, Uganda. Lancet 357:1149-1153.
137. Grivel, J. C., R. J. Shattock, and L. B. Margolis. 2011. Selective transmission of R5 HIV-1 variants: where is the gatekeeper? J Transl Med 9 Suppl 1:S6.
138. Groot, F., T. M. van Capel, J. Schuitemaker, B. Berkhout, and E. C. de Jong. 2006. Differential susceptibility of naive, central memory and effector memory T cells to dendritic cell-mediated HIV-1 transmission. Retrovirology 3:52.
139. Guadalupe, M., E. Reay, S. Sankaran, T. Prindiville, J. Flamm, A. McNeil, and S. Dandekar. 2003. Severe CD4+ T-cell depletion in gut lymphoid tissue during primary human immunodeficiency virus type 1 infection and substantial delay in restoration following highly active antiretroviral therapy. J Virol 77:11708-11717.
140. Guindon, S., J. F. Dufayard, V. Lefort, M. Anisimova, W. Hordijk, and O. Gascuel. 2010. New algorithms and methods to estimate maximum-likelihood phylogenies: assessing the performance of PhyML 3.0. Syst Biol 59:307-321.
141. Guindon, S., and O. Gascuel. 2003. A simple, fast, and accurate algorithm to estimate large phylogenies by maximum likelihood. Syst Biol 52:696-704.
142. Gummuluru, S., M. Rogel, L. Stamatatos, and M. Emerman. 2003. Binding of human immunodeficiency virus type 1 to immature dendritic cells can occur independently of DC-SIGN and mannose binding C-type lectin receptors via a cholesterol-dependent pathway. J Virol 77:12865-12874.
143. Gupta, K., and P. J. Klasse. 2006. How do viral and host factors modulate the sexual transmission of HIV? Can transmission be blocked? PLoS Med 3:e79.

144. Gurney, K. B., J. Elliott, H. Nassanian, C. Song, E. Soilleux, I. McGowan, P. A. Anton, and B. Lee. 2005. Binding and transfer of human immunodeficiency virus by DC-SIGN+ cells in human rectal mucosa. J Virol 79:5762-5773.
145. Haaland, R. E., P. A. Hawkins, J. Salazar-Gonzalez, A. Johnson, A. Tichacek, E. Karita, O. Manigart, J. Mulenga, B. F. Keele, G. M. Shaw, B. H. Hahn, S. A. Allen, C. A. Derdeyn, and E. Hunter. 2009. Inflammatory genital infections mitigate a severe genetic bottleneck in heterosexual transmission of subtype A and C HIV-1. PLoS Pathog 5:e1000274.
146. Haase, A. T. 2011. Early events in sexual transmission of HIV and SIV and opportunities for interventions. Annu Rev Med 62:127-139.
147. Haase, A. T. 2010. Targeting early infection to prevent HIV-1 mucosal transmission. Nature 464:217-223.
148. Haim, H., Z. Si, N. Madani, L. Wang, J. R. Courter, A. Princiotto, A. Kassa, M. DeGrace, K. McGee-Estrada, M. Mefford, D. Gabuzda, A. B. Smith, 3rd, and J. Sodroski. 2009. Soluble CD4 and CD4-mimetic compounds inhibit HIV-1 infection by induction of a short-lived activated state. PLoS Pathog 5:e1000360.
149. Hallenberger, S., V. Bosch, H. Angliker, E. Shaw, H. D. Klenk, and W. Garten. 1992. Inhibition of furin-mediated cleavage activation of HIV-1 glycoprotein gp160. Nature 360:358-361.
150. Hansen, B. D., P. L. Nara, R. K. Maheshwari, G. S. Sidhu, J. G. Bernbaum, D. Hoekzema, M. S. Meltzer, and H. E. Gendelman. 1992. Loss of infectivity by progeny virus from alpha interferon-treated human immunodeficiency virus type 1-infected T cells is associated with defective assembly of envelope gp120. J Virol 66:7543-7548.
151. Harrison, J. E., J. B. Lynch, L. J. Sierra, L. A. Blackburn, N. Ray, R. G. Collman, and R. W. Doms. 2008. Baseline resistance of primary human immunodeficiency virus type 1 strains to the CXCR4 inhibitor AMD3100. J Virol 82:11695-11704.
152. Hedskog, C., M. Mild, and J. Albert. 2012. Transmission of the X4 phenotype of HIV-1: is there evidence against the "random transmission" hypothesis? J Infect Dis 205:163-165.
153. Heise, C., C. J. Miller, A. Lackner, and S. Dandekar. 1994. Primary acute simian immunodeficiency virus infection of intestinal lymphoid tissue is associated with gastrointestinal dysfunction. J Infect Dis 169:1116-1120.
154. Hemelaar, J., E. Gouws, P. D. Ghys, and S. Osmanov. 2011. Global trends in molecular epidemiology of HIV-1 during 2000-2007. AIDS 25:679-689.
155. Henderson, D. A. 2011. The eradication of smallpox - An overview of the past, present, and future. Vaccine.
156. Hendrix, C. W., C. Flexner, R. T. MacFarland, C. Giandomenico, E. J. Fuchs, E. Redpath, G. Bridger, and G. W. Henson. 2000. Pharmacokinetics and safety of AMD-

3100, a novel antagonist of the CXCR-4 chemokine receptor, in human volunteers. Antimicrob Agents Chemother 44:1667-1673.

157. Hirbod, T., J. Nilsson, S. Andersson, C. Uberti-Foppa, D. Ferrari, M. Manghi, J. Andersson, L. Lopalco, and K. Broliden. 2006. Upregulation of interferon-alpha and RANTES in the cervix of HIV-1-seronegative women with high-risk behavior. J Acquir Immune Defic Syndr 43:137-143.

158. Hladik, F., and T. J. Hope. 2009. HIV infection of the genital mucosa in women. Curr HIV/AIDS Rep 6:20-28.

159. Hladik, F., and M. J. McElrath. 2008. Setting the stage: host invasion by HIV. Nat Rev Immunol 8:447-457.

160. Hladik, F., P. Sakchalathorn, L. Ballweber, G. Lentz, M. Fialkow, D. Eschenbach, and M. J. McElrath. 2007. Initial events in establishing vaginal entry and infection by human immunodeficiency virus type-1. Immunity 26:257-270.

161. Hollingsworth, T. D., R. M. Anderson, and C. Fraser. 2008. HIV-1 transmission, by stage of infection. J Infect Dis 198:687-693.

162. Hsu, M., J. M. Harouse, A. Gettie, C. Buckner, J. Blanchard, and C. Cheng-Mayer. 2003. Increased mucosal transmission but not enhanced pathogenicity of the CCR5-tropic, simian AIDS-inducing simian/human immunodeficiency virus SHIV(SF162P3) maps to envelope gp120. J Virol 77:989-998.

163. Hu, J., M. B. Gardner, and C. J. Miller. 2000. Simian immunodeficiency virus rapidly penetrates the cervicovaginal mucosa after intravaginal inoculation and infects intraepithelial dendritic cells. J Virol 74:6087-6095.

164. Huang, C. C., M. Tang, M. Y. Zhang, S. Majeed, E. Montabana, R. L. Stanfield, D. S. Dimitrov, B. Korber, J. Sodroski, I. A. Wilson, R. Wyatt, and P. D. Kwong. 2005. Structure of a V3-containing HIV-1 gp120 core. Science 310:1025-1028.

165. Huang, K. H., D. Bonsall, A. Katzourakis, E. C. Thomson, S. J. Fidler, J. Main, D. Muir, J. N. Weber, A. J. Frater, R. E. Phillips, O. G. Pybus, P. J. Goulder, M. O. McClure, G. S. Cooke, and P. Klenerman. 2010. B-cell depletion reveals a role for antibodies in the control of chronic HIV-1 infection. Nat Commun 1:102.

166. Hughes, J. P., J. M. Baeten, J. R. Lingappa, A. S. Magaret, A. Wald, G. de Bruyn, J. Kiarie, M. Inambao, W. Kilembe, C. Farquhar, and C. Celum. 2012. Determinants of per-coital-act HIV-1 infectivity among African HIV-1-serodiscordant couples. J Infect Dis 205:358-365.

167. Isaacman-Beck, J., E. A. Hermann, Y. Yi, S. J. Ratcliffe, J. Mulenga, S. Allen, E. Hunter, C. A. Derdeyn, and R. G. Collman. 2009. Heterosexual transmission of human immunodeficiency virus type 1 subtype C: Macrophage tropism, alternative coreceptor use, and the molecular anatomy of CCR5 utilization. J Virol 83:8208-8220.

168. Izquierdo-Useros, N., J. Blanco, I. Erkizia, M. T. Fernandez-Figueras, F. E. Borras, M. Naranjo-Gomez, M. Bofill, L. Ruiz, B. Clotet, and J. Martinez-Picado. 2007. Maturation of blood-derived dendritic cells enhances human immunodeficiency virus type 1 capture and transmission. J Virol 81:7559-7570.

169. Jameson, B., F. Baribaud, S. Pohlmann, D. Ghavimi, F. Mortari, R. W. Doms, and A. Iwasaki. 2002. Expression of DC-SIGN by dendritic cells of intestinal and genital mucosae in humans and rhesus macaques. J Virol 76:1866-1875.

170. Jeeninga, R. E., M. Hoogenkamp, M. Armand-Ugon, M. de Baar, K. Verhoef, and B. Berkhout. 2000. Functional differences between the long terminal repeat transcriptional promoters of human immunodeficiency virus type 1 subtypes A through G. J Virol 74:3740-3751.

171. Jiang, C., N. F. Parrish, C. B. Wilen, H. Li, Y. Chen, J. W. Pavlicek, A. Berg, X. Lu, H. Song, J. C. Tilton, J. M. Pfaff, E. A. Henning, J. M. Decker, M. A. Moody, M. S. Drinker, R. Schutte, S. Freel, G. D. Tomaras, R. Nedellec, D. E. Mosier, B. F. Haynes, G. M. Shaw, B. H. Hahn, R. W. Doms, and F. Gao. 2011. Primary infection by a human immunodeficiency virus with atypical coreceptor tropism. J Virol 85:10669-10681.

172. Johnston, S. H., M. A. Lobritz, S. Nguyen, K. Lassen, S. Delair, F. Posta, Y. J. Bryson, E. J. Arts, T. Chou, and B. Lee. 2009. A quantitative affinity-profiling system that reveals distinct CD4/CCR5 usage patterns among human immunodeficiency virus type 1 and simian immunodeficiency virus strains. J Virol 83:11016-11026.

173. Jouvenet, N., S. J. Neil, C. Bess, M. C. Johnson, C. A. Virgen, S. M. Simon, and P. D. Bieniasz. 2006. Plasma membrane is the site of productive HIV-1 particle assembly. PLoS Biol 4:e435.

174. Kaizu, M., A. M. Weiler, K. L. Weisgrau, K. A. Vielhuber, G. May, S. M. Piaskowski, J. Furlott, N. J. Maness, T. C. Friedrich, J. T. Loffredo, A. Usborne, and E. G. Rakasz. 2006. Repeated intravaginal inoculation with cell-associated simian immunodeficiency virus results in persistent infection of nonhuman primates. J Infect Dis 194:912-916.

175. Kalams, S. A., S. P. Buchbinder, E. S. Rosenberg, J. M. Billingsley, D. S. Colbert, N. G. Jones, A. K. Shea, A. K. Trocha, and B. D. Walker. 1999. Association between virus-specific cytotoxic T-lymphocyte and helper responses in human immunodeficiency virus type 1 infection. J Virol 73:6715-6720.

176. Keele, B. F., E. E. Giorgi, J. F. Salazar-Gonzalez, J. M. Decker, K. T. Pham, M. G. Salazar, C. Sun, T. Grayson, S. Wang, H. Li, X. Wei, C. Jiang, J. L. Kirchherr, F. Gao, J. A. Anderson, L. H. Ping, R. Swanstrom, G. D. Tomaras, W. A. Blattner, P. A. Goepfert, J. M. Kilby, M. S. Saag, E. L. Delwart, M. P. Busch, M. S. Cohen, D. C. Montefiori, B. F. Haynes, B. Gaschen, G. S. Athreya, H. Y. Lee, N. Wood, C. Seoighe, A. S. Perelson, T. Bhattacharya, B. T. Korber, B. H. Hahn, and G. M. Shaw. 2008. Identification and

characterization of transmitted and early founder virus envelopes in primary HIV-1 infection. Proc Natl Acad Sci U S A 105:7552-7557.

177. Keele, B. F., H. Li, G. H. Learn, P. Hraber, E. E. Giorgi, T. Grayson, C. Sun, Y. Chen, W. W. Yeh, N. L. Letvin, J. R. Mascola, G. J. Nabel, B. F. Haynes, T. Bhattacharya, A. S. Perelson, B. T. Korber, B. H. Hahn, and G. M. Shaw. 2009. Low-dose rectal inoculation of rhesus macaques by SIVsmE660 or SIVmac251 recapitulates human mucosal infection by HIV-1. J Exp Med 206:1117-1134.

178. Kemal, K. S., B. Foley, H. Burger, K. Anastos, H. Minkoff, C. Kitchen, S. M. Philpott, W. Gao, E. Robison, S. Holman, C. Dehner, S. Beck, W. A. Meyer, 3rd, A. Landay, A. Kovacs, J. Bremer, and B. Weiser. 2003. HIV-1 in genital tract and plasma of women: compartmentalization of viral sequences, coreceptor usage, and glycosylation. Proc Natl Acad Sci U S A 100:12972-12977.

179. Kimura, M. 1980. A simple method for estimating evolutionary rates of base substitutions through comparative studies of nucleotide sequences. J Mol Evol 16:111-120.

180. Kirchherr, J. L., J. Hamilton, X. Lu, S. Gnanakaran, M. Muldoon, M. Daniels, W. Kasongo, V. Chalwe, C. Mulenga, L. Mwananyanda, R. M. Musonda, X. Yuan, D. C. Montefiori, B. T. Korber, B. F. Haynes, and F. Gao. 2011. Identification of amino acid substitutions associated with neutralization phenotype in the human immunodeficiency virus type-1 subtype C gp120. Virology 409:163-174.

181. Kirchherr, J. L., X. Lu, W. Kasongo, V. Chalwe, L. Mwananyanda, R. M. Musonda, S. M. Xia, R. M. Scearce, H. X. Liao, D. C. Montefiori, B. F. Haynes, and F. Gao. 2007. High throughput functional analysis of HIV-1 env genes without cloning. J Virol Methods 143:104-111.

182. Kittinunvorakoon, C., M. K. Morris, K. Neeyapun, B. Jetsawang, G. C. Buehring, and C. V. Hanson. 2009. Mother to child transmission of HIV-1 in a Thai population: role of virus characteristics and maternal humoral immune response. J Med Virol 81:768-778.

183. Klatzmann, D., F. Barre-Sinoussi, M. T. Nugeyre, C. Danquet, E. Vilmer, C. Griscelli, F. Brun-Veziret, C. Rouzioux, J. C. Gluckman, J. C. Chermann, and et al. 1984. Selective tropism of lymphadenopathy associated virus (LAV) for helper-inducer T lymphocytes. Science 225:59-63.

184. Klein, J. S., and P. J. Bjorkman. 2010. Few and far between: how HIV may be evading antibody avidity. PLoS Pathog 6:e1000908.

185. Kondru, R., J. Zhang, C. Ji, T. Mirzadegan, D. Rotstein, S. Sankuratri, and M. Dioszegi. 2008. Molecular interactions of CCR5 with major classes of small-molecule anti-HIV CCR5 antagonists. Mol Pharmacol 73:789-800.

186. Konopka, K., L. Stamatatos, C. E. Larsen, B. R. Davis, and N. Duzgunes. 1991. Enhancement of human immunodeficiency virus type 1 infection by cationic liposomes: the role of CD4, serum and liposome-cell interactions. J Gen Virol 72 (Pt 11):2685-2696.
187. Kosmrlj, A., E. L. Read, Y. Qi, T. M. Allen, M. Altfeld, S. G. Deeks, F. Pereyra, M. Carrington, B. D. Walker, and A. K. Chakraborty. 2010. Effects of thymic selection of the T-cell repertoire on HLA class I-associated control of HIV infection. Nature 465:350-354.
188. Koyanagi, Y., S. Miles, R. T. Mitsuyasu, J. E. Merrill, H. V. Vinters, and I. S. Chen. 1987. Dual infection of the central nervous system by AIDS viruses with distinct cellular tropisms. Science 236:819-822.
189. Kraft, C. S., D. Basu, P. A. Hawkins, P. T. Hraber, E. Chomba, J. Mulenga, W. Kilembe, N. H. Khu, C. A. Derdeyn, S. A. Allen, O. Manigart, and E. Hunter. 2012. Timing and source of subtype-C HIV-1 superinfection in the newly infected partner of Zambian couples with disparate viruses. Retrovirology 9:22.
190. Kramer, H. B., K. J. Lavender, L. Qin, A. R. Stacey, M. K. Liu, K. di Gleria, A. Simmons, N. Gasper-Smith, B. F. Haynes, A. J. McMichael, P. Borrow, and B. M. Kessler. 2010. Elevation of intact and proteolytic fragments of acute phase proteins constitutes the earliest systemic antiviral response in HIV-1 infection. PLoS Pathog 6:e1000893.
191. Kraus, M. H., N. F. Parrish, K. S. Shaw, J. M. Decker, B. F. Keele, J. F. Salazar-Gonzalez, T. Grayson, D. T. McPherson, L. H. Ping, J. A. Anderson, R. Swanstrom, C. Williamson, G. M. Shaw, and B. H. Hahn. 2010. A rev1-vpu polymorphism unique to HIV-1 subtype A and C strains impairs envelope glycoprotein expression from rev-vpu-env cassettes and reduces virion infectivity in pseudotyping assays. Virology 397:346-357.
192. Kunzi, M. S., H. Farzadegan, J. B. Margolick, D. Vlahov, and P. M. Pitha. 1995. Identification of human immunodeficiency virus primary isolates resistant to interferon-alpha and correlation of prevalence to disease progression. J Infect Dis 171:822-828.
193. Kwong, P. D., R. Wyatt, J. Robinson, R. W. Sweet, J. Sodroski, and W. A. Hendrickson. 1998. Structure of an HIV gp120 envelope glycoprotein in complex with the CD4 receptor and a neutralizing human antibody. Nature 393:648-659.
194. Laakso, M. M., F. H. Lee, B. Haggarty, C. Agrawal, K. M. Nolan, M. Biscone, J. Romano, A. P. Jordan, G. J. Leslie, E. G. Meissner, L. Su, J. A. Hoxie, and R. W. Doms. 2007. V3 loop truncations in HIV-1 envelope impart resistance to coreceptor inhibitors and enhanced sensitivity to neutralizing antibodies. PLoS Pathog 3:e117.
195. Laga, M., A. Manoka, M. Kivuvu, B. Malele, M. Tuliza, N. Nzila, J. Goeman, F. Behets, V. Batter, M. Alary, and et al. 1993. Non-ulcerative sexually transmitted diseases as risk factors for HIV-1 transmission in women: results from a cohort study. AIDS 7:95-102.

196. Laguette, N., B. Sobhian, N. Casartelli, M. Ringeard, C. Chable-Bessia, E. Segeral, A. Yatim, S. Emiliani, O. Schwartz, and M. Benkirane. 2011. SAMHD1 is the dendritic- and myeloid-cell-specific HIV-1 restriction factor counteracted by Vpx. Nature 474:654-657.
197. Lathey, J. L., D. Brambilla, M. M. Goodenow, M. Nokta, S. Rasheed, E. B. Siwak, J. W. Bremer, D. D. Huang, Y. Yi, P. S. Reichelderfer, and R. G. Collman. 2000. Co-receptor usage was more predictive than NSI/SI phenotype for HIV replication in macrophages: is NSI/SI phenotyping sufficient? J Leukoc Biol 68:324-330.
198. Lazarovits, A. I., R. A. Moscicki, J. T. Kurnick, D. Camerini, A. K. Bhan, L. G. Baird, M. Erikson, and R. B. Colvin. 1984. Lymphocyte activation antigens. I. A monoclonal antibody, anti-Act I, defines a new late lymphocyte activation antigen. J Immunol 133:1857-1862.
199. Lee, B., M. Sharron, C. Blanpain, B. J. Doranz, J. Vakili, P. Setoh, E. Berg, G. Liu, H. R. Guy, S. R. Durell, M. Parmentier, C. N. Chang, K. Price, M. Tsang, and R. W. Doms. 1999. Epitope mapping of CCR5 reveals multiple conformational states and distinct but overlapping structures involved in chemokine and coreceptor function. J Biol Chem 274:9617-9626.
200. Lee, B., M. Sharron, L. J. Montaner, D. Weissman, and R. W. Doms. 1999. Quantification of CD4, CCR5, and CXCR4 levels on lymphocyte subsets, dendritic cells, and differentially conditioned monocyte-derived macrophages. Proc Natl Acad Sci U S A 96:5215-5220.
201. Lee, H. Y., E. E. Giorgi, B. F. Keele, B. Gaschen, G. S. Athreya, J. F. Salazar-Gonzalez, K. T. Pham, P. A. Goepfert, J. M. Kilby, M. S. Saag, E. L. Delwart, M. P. Busch, B. H. Hahn, G. M. Shaw, B. T. Korber, T. Bhattacharya, and A. S. Perelson. 2009. Modeling sequence evolution in acute HIV-1 infection. J Theor Biol 261:341-360.
202. Levin, B. R., and J. J. Bull. 1994. Short-sighted evolution and the virulence of pathogenic microorganisms. Trends Microbiol 2:76-81.
203. Li, B., J. M. Decker, R. W. Johnson, F. Bibollet-Ruche, X. Wei, J. Mulenga, S. Allen, E. Hunter, B. H. Hahn, G. M. Shaw, J. L. Blackwell, and C. A. Derdeyn. 2006. Evidence for potent autologous neutralizing antibody titers and compact envelopes in early infection with subtype C human immunodeficiency virus type 1. J Virol 80:5211-5218.
204. Li, H., K. J. Bar, S. Wang, J. M. Decker, Y. Chen, C. Sun, J. F. Salazar-Gonzalez, M. G. Salazar, G. H. Learn, C. J. Morgan, J. E. Schumacher, P. Hraber, E. E. Giorgi, T. Bhattacharya, B. T. Korber, A. S. Perelson, J. J. Eron, M. S. Cohen, C. B. Hicks, B. F. Haynes, M. Markowitz, B. F. Keele, B. H. Hahn, and G. M. Shaw. 2010. High Multiplicity Infection by HIV-1 in Men Who Have Sex with Men. PLoS Pathog 6:e1000890.
205. Li, H., M. B. Stoddard, S. Y. Wang, L. M. Blair, E. E. Giorgi, E. H. Parrish, G. H. Learn, P. Hraber, P. A. Goepfert, M. S. Saag, T. N. Denny, B. F. Haynes, B. H. Hahn, R. M.

Ribeiro, A. S. Perelson, B. T. Korber, T. Bhattacharya, and G. M. Shaw. 2012. Elucidation of Hepatitis C Virus Transmission and Early Diversification by Single Genome Sequencing. Plos Pathogens 8.

206. Li, M., E. Kao, X. Gao, H. Sandig, K. Limmer, M. Pavon-Eternod, T. E. Jones, S. Landry, T. Pan, M. D. Weitzman, and M. David. 2012. Codon-usage-based inhibition of HIV protein synthesis by human schlafen 11. Nature 491:125-128.

207. Li, M., J. F. Salazar-Gonzalez, C. A. Derdeyn, L. Morris, C. Williamson, J. E. Robinson, J. M. Decker, Y. Li, M. G. Salazar, V. R. Polonis, K. Mlisana, S. A. Karim, K. Hong, K. M. Greene, M. Bilska, J. Zhou, S. Allen, E. Chomba, J. Mulenga, C. Vwalika, F. Gao, M. Zhang, B. T. Korber, E. Hunter, B. H. Hahn, and D. C. Montefiori. 2006. Genetic and neutralization properties of subtype C human immunodeficiency virus type 1 molecular env clones from acute and early heterosexually acquired infections in Southern Africa. J Virol 80:11776-11790.

208. Li, Q., L. Duan, J. D. Estes, Z. M. Ma, T. Rourke, Y. Wang, C. Reilly, J. Carlis, C. J. Miller, and A. T. Haase. 2005. Peak SIV replication in resting memory CD4+ T cells depletes gut lamina propria CD4+ T cells. Nature 434:1148-1152.

209. Li, Q., J. D. Estes, P. M. Schlievert, L. Duan, A. J. Brosnahan, P. J. Southern, C. S. Reilly, M. L. Peterson, N. Schultz-Darken, K. G. Brunner, K. R. Nephew, S. Pambuccian, J. D. Lifson, J. V. Carlis, and A. T. Haase. 2009. Glycerol monolaurate prevents mucosal SIV transmission. Nature 458:1034-1038.

210. Liao, H. X., X. Chen, S. Munshaw, R. Zhang, D. J. Marshall, N. Vandergrift, J. F. Whitesides, X. Lu, J. S. Yu, K. K. Hwang, F. Gao, M. Markowitz, S. L. Heath, K. J. Bar, P. A. Goepfert, D. C. Montefiori, G. C. Shaw, S. M. Alam, D. M. Margolis, T. N. Denny, S. D. Boyd, E. Marshal, M. Egholm, B. B. Simen, B. Hanczaruk, A. Z. Fire, G. Voss, G. Kelsoe, G. D. Tomaras, M. A. Moody, T. B. Kepler, and B. F. Haynes. 2011. Initial antibodies binding to HIV-1 gp41 in acutely infected subjects are polyreactive and highly mutated. J Exp Med 208:2237-2249.

211. Liu, J., M. D. Miller, R. M. Danovich, N. Vandergrift, F. Cai, C. B. Hicks, D. J. Hazuda, and F. Gao. 2011. Analysis of low frequency mutations associated with drug-resistance to raltegravir before antiretroviral treatment. Antimicrob Agents Chemother.

212. Liu, R., W. A. Paxton, S. Choe, D. Ceradini, S. R. Martin, R. Horuk, M. E. MacDonald, H. Stuhlmann, R. A. Koup, and N. R. Landau. 1996. Homozygous defect in HIV-1 coreceptor accounts for resistance of some multiply-exposed individuals to HIV-1 infection. Cell 86:367-377.

213. Liu, Y., M. E. Curlin, K. Diem, H. Zhao, A. K. Ghosh, H. Zhu, A. S. Woodward, J. Maenza, C. E. Stevens, J. Stekler, A. C. Collier, I. Genowati, W. Deng, R. Zioni, L. Corey, T. Zhu,

and J. I. Mullins. 2008. Env length and N-linked glycosylation following transmission of human immunodeficiency virus Type 1 subtype B viruses. Virology 374:229-233.

214. Lu, X., B. Hora, F. Cai, and F. Gao. 2010. Generation of random mutant libraries with multiple primers in a single reaction. J Virol Methods 167:146-151.

215. Lue, J., M. Hsu, D. Yang, P. Marx, Z. Chen, and C. Cheng-Mayer. 2002. Addition of a single gp120 glycan confers increased binding to dendritic cell-specific ICAM-3-grabbing nonintegrin and neutralization escape to human immunodeficiency virus type 1. J Virol 76:10299-10306.

216. Lynch, R. M., L. Tran, M. K. Louder, S. D. Schmidt, M. Cohen, R. Dersimonian, Z. Euler, E. S. Gray, S. Abdool Karim, J. Kirchherr, D. C. Montefiori, S. Sibeko, K. Soderberg, G. Tomaras, Z. Y. Yang, G. J. Nabel, H. Schuitemaker, L. Morris, B. F. Haynes, and J. R. Mascola. 2012. The development of CD4 binding site antibodies during HIV-1 infection. J Virol 86:7588-7595.

217. Ma, Z. M., M. Stone, M. Piatak, Jr., B. Schweighardt, N. L. Haigwood, D. Montefiori, J. D. Lifson, M. P. Busch, and C. J. Miller. 2009. High specific infectivity of plasma virus from the pre-ramp-up and ramp-up stages of acute simian immunodeficiency virus infection. J Virol 83:3288-3297.

218. Magnus, C., P. Rusert, S. Bonhoeffer, A. Trkola, and R. R. Regoes. 2009. Estimating the stoichiometry of human immunodeficiency virus entry. J Virol 83:1523-1531.

219. Manrique, J. M., C. C. Celma, E. Hunter, J. L. Affranchino, and S. A. Gonzalez. 2003. Positive and negative modulation of virus infectivity and envelope glycoprotein incorporation into virions by amino acid substitutions at the N terminus of the simian immunodeficiency virus matrix protein. J Virol 77:10881-10888.

220. Margolis, L., and R. Shattock. 2006. Selective transmission of CCR5-utilizing HIV-1: the 'gatekeeper' problem resolved? Nat Rev Microbiol 4:312-317.

221. Martellini, J. A., A. L. Cole, N. Venkataraman, G. A. Quinn, P. Svoboda, B. K. Gangrade, J. Pohl, O. E. Sorensen, and A. M. Cole. 2009. Cationic polypeptides contribute to the anti-HIV-1 activity of human seminal plasma. FASEB J 23:3609-3618.

222. Matano, T., R. Shibata, C. Siemon, M. Connors, H. C. Lane, and M. A. Martin. 1998. Administration of an anti-CD8 monoclonal antibody interferes with the clearance of chimeric simian/human immunodeficiency virus during primary infections of rhesus macaques. J Virol 72:164-169.

223. McKinnon, L. R., B. Nyanga, D. Chege, P. Izulla, M. Kimani, S. Huibner, L. Gelmon, K. E. Block, C. Cicala, A. O. Anzala, J. Arthos, J. Kimani, and R. Kaul. 2011. Characterization of a human cervical CD4+ T cell subset coexpressing multiple markers of HIV susceptibility. J Immunol 187:6032-6042.

224. McLaren, P. J., T. B. Ball, C. Wachihi, W. Jaoko, D. J. Kelvin, A. Danesh, J. Kimani, F. A. Plummer, and K. R. Fowke. 2010. HIV-exposed seronegative commercial sex workers show a quiescent phenotype in the CD4+ T cell compartment and reduced expression of HIV-dependent host factors. J Infect Dis 202 Suppl 3:S339-344.
225. McMichael, A. J., P. Borrow, G. D. Tomaras, N. Goonetilleke, and B. F. Haynes. 2010. The immune response during acute HIV-1 infection: clues for vaccine development. Nat Rev Immunol 10:11-23.
226. McNearney, T., Z. Hornickova, R. Markham, A. Birdwell, M. Arens, A. Saah, and L. Ratner. 1992. Relationship of human immunodeficiency virus type 1 sequence heterogeneity to stage of disease. Proc Natl Acad Sci U S A 89:10247-10251.
227. Mehandru, S., M. A. Poles, K. Tenner-Racz, A. Horowitz, A. Hurley, C. Hogan, D. Boden, P. Racz, and M. Markowitz. 2004. Primary HIV-1 infection is associated with preferential depletion of CD4+ T lymphocytes from effector sites in the gastrointestinal tract. J Exp Med 200:761-770.
228. Mehandru, S., K. Tenner-Racz, P. Racz, and M. Markowitz. 2005. The gastrointestinal tract is critical to the pathogenesis of acute HIV-1 infection. J Allergy Clin Immunol 116:419-422.
229. Mehta, R., R. Ramakrishnan, K. Doktor, V. Sundaravaradan, and N. Ahmad. 2008. Genetic characterization of HIV type 1 long terminal repeat following vertical transmission. AIDS Res Hum Retroviruses 24:437-445.
230. Meier, A., J. J. Chang, E. S. Chan, R. B. Pollard, H. K. Sidhu, S. Kulkarni, T. F. Wen, R. J. Lindsay, L. Orellana, D. Mildvan, S. Bazner, H. Streeck, G. Alter, J. D. Lifson, M. Carrington, R. J. Bosch, G. K. Robbins, and M. Altfeld. 2009. Sex differences in the Toll-like receptor-mediated response of plasmacytoid dendritic cells to HIV-1. Nat Med 15:955-959.
231. Meissner, E. G., K. M. Duus, F. Gao, X. F. Yu, and L. Su. 2004. Characterization of a thymus-tropic HIV-1 isolate from a rapid progressor: role of the envelope. Virology 328:74-88.
232. Merryman, C., and D. G. Gibson. 2012. Methods and applications for assembling large DNA constructs. Metab Eng 14:196-204.
233. Meyers, G., A. Ege, C. Fetzer, M. von Freyburg, K. Elbers, V. Carr, H. Prentice, B. Charleston, and E. M. Schurmann. 2007. Bovine viral diarrhea virus: prevention of persistent fetal infection by a combination of two mutations affecting Erns RNase and Npro protease. J Virol 81:3327-3338.
234. Michael, N. L., J. A. Nelson, V. N. KewalRamani, G. Chang, S. J. O'Brien, J. R. Mascola, B. Volsky, M. Louder, G. C. White, 2nd, D. R. Littman, R. Swanstrom, and T. R. O'Brien. 1998. Exclusive and persistent use of the entry coreceptor CXCR4 by human

immunodeficiency virus type 1 from a subject homozygous for CCR5 delta32. J Virol 72:6040-6047.

235. Migeotte, I., D. Communi, and M. Parmentier. 2006. Formyl peptide receptors: a promiscuous subfamily of G protein-coupled receptors controlling immune responses. Cytokine Growth Factor Rev 17:501-519.

236. Miller, C. J. 1998. Localization of Simian immunodeficiency virus-infected cells in the genital tract of male and female Rhesus macaques. J Reprod Immunol 41:331-339.

237. Miller, C. J., N. J. Alexander, P. Vogel, J. Anderson, and P. A. Marx. 1992. Mechanism of genital transmission of SIV: a hypothesis based on transmission studies and the location of SIV in the genital tract of chronically infected female rhesus macaques. J Med Primatol 21:64-68.

238. Miller, C. J., Q. Li, K. Abel, E. Y. Kim, Z. M. Ma, S. Wietgrefe, L. La Franco-Scheuch, L. Compton, L. Duan, M. D. Shore, M. Zupancic, M. Busch, J. Carlis, S. Wolinsky, and A. T. Haase. 2005. Propagation and dissemination of infection after vaginal transmission of simian immunodeficiency virus. J Virol 79:9217-9227.

239. Miller, C. J., M. Marthas, J. Greenier, D. Lu, P. J. Dailey, and Y. Lu. 1998. In vivo replication capacity rather than in vitro macrophage tropism predicts efficiency of vaginal transmission of simian immunodeficiency virus or simian/human immunodeficiency virus in rhesus macaques. J Virol 72:3248-3258.

240. Miller, C. J., J. R. McGhee, and M. B. Gardner. 1993. Mucosal immunity, HIV transmission, and AIDS. Lab Invest 68:129-145.

241. Miyauchi, K., Y. Kim, O. Latinovic, V. Morozov, and G. B. Melikyan. 2009. HIV enters cells via endocytosis and dynamin-dependent fusion with endosomes. Cell 137:433-444.

242. Miyauchi, K., M. M. Kozlov, and G. B. Melikyan. 2009. Early steps of HIV-1 fusion define the sensitivity to inhibitory peptides that block 6-helix bundle formation. PLoS Pathog 5:e1000585.

243. Mo, H., S. Monard, H. Pollack, J. Ip, G. Rochford, L. Wu, J. Hoxie, W. Borkowsky, D. D. Ho, and J. P. Moore. 1998. Expression patterns of the HIV type 1 coreceptors CCR5 and CXCR4 on CD4+ T cells and monocytes from cord and adult blood. AIDS Res Hum Retroviruses 14:607-617.

244. Modlin, J. F. 2012. Inactivated polio vaccine and global polio eradication. Lancet Infect Dis 12:93-94.

245. Moir, S., and A. S. Fauci. 2009. B cells in HIV infection and disease. Nat Rev Immunol 9:235-245.

246. Moore, P. L., E. S. Gray, C. K. Wibmer, J. N. Bhiman, M. Nonyane, D. J. Sheward, T. Hermanus, S. Bajimaya, N. L. Tumba, M. R. Abrahams, B. E. Lambson, N. Ranchobe, L. Ping, N. Ngandu, Q. A. Karim, S. S. Karim, R. I. Swanstrom, M. S. Seaman, C.

Williamson, and L. Morris. 2012. Evolution of an HIV glycan-dependent broadly neutralizing antibody epitope through immune escape. Nat Med 18:1688-1692.

247. Moore, P. L., N. Ranchobe, B. E. Lambson, E. S. Gray, E. Cave, M. R. Abrahams, G. Bandawe, K. Mlisana, S. S. Abdool Karim, C. Williamson, and L. Morris. 2009. Limited neutralizing antibody specificities drive neutralization escape in early HIV-1 subtype C infection. PLoS Pathog 5:e1000598.

248. Moss, G. B., D. Clemetson, L. D'Costa, F. A. Plummer, J. O. Ndinya-Achola, M. Reilly, K. K. Holmes, P. Piot, G. M. Maitha, S. L. Hillier, and et al. 1991. Association of cervical ectopy with heterosexual transmission of human immunodeficiency virus: results of a study of couples in Nairobi, Kenya. J Infect Dis 164:588-591.

249. Naarding, M. A., I. S. Ludwig, F. Groot, B. Berkhout, T. B. Geijtenbeek, G. Pollakis, and W. A. Paxton. 2005. Lewis X component in human milk binds DC-SIGN and inhibits HIV-1 transfer to CD4+ T lymphocytes. J Clin Invest 115:3256-3264.

250. Nawaz, F., C. Cicala, D. Van Ryk, K. E. Block, K. Jelicic, J. P. McNally, O. Ogundare, M. Pascuccio, N. Patel, D. Wei, A. S. Fauci, and J. Arthos. 2011. The genotype of early-transmitting HIV gp120s promotes alpha (4) beta(7)-reactivity, revealing alpha (4) beta(7) +/CD4+ T cells as key targets in mucosal transmission. PLoS Pathog 7:e1001301.

251. Nedellec, R., M. Coetzer, N. Shimizu, H. Hoshino, V. R. Polonis, L. Morris, U. E. Martensson, J. Binley, J. Overbaugh, and D. E. Mosier. 2009. Virus entry via the alternative coreceptors CCR3 and FPRL1 differs by human immunodeficiency virus type 1 subtype. J Virol 83:8353-8363.

252. Neil, S. J., T. Zang, and P. D. Bieniasz. 2008. Tetherin inhibits retrovirus release and is antagonized by HIV-1 Vpu. Nature 451:425-430.

253. Nishimura, Y., C. R. Brown, J. J. Mattapallil, T. Igarashi, A. Buckler-White, B. A. Lafont, V. M. Hirsch, M. Roederer, and M. A. Martin. 2005. Resting naive CD4+ T cells are massively infected and eliminated by X4-tropic simian-human immunodeficiency viruses in macaques. Proc Natl Acad Sci U S A 102:8000-8005.

254. Norvell, M. K., G. I. Benrubi, and R. J. Thompson. 1984. Investigation of microtrauma after sexual intercourse. J Reprod Med 29:269-271.

255. O'Brien, T. R., C. Winkler, M. Dean, J. A. Nelson, M. Carrington, N. L. Michael, and G. C. White, 2nd. 1997. HIV-1 infection in a man homozygous for CCR5 delta 32. Lancet 349:1219.

256. O'Doherty, U., W. J. Swiggard, and M. H. Malim. 2000. Human immunodeficiency virus type 1 spinoculation enhances infection through virus binding. J Virol 74:10074-10080.

257. Ochsenbauer, C., T. G. Edmonds, H. Ding, B. F. Keele, J. Decker, M. G. Salazar, J. F. Salazar-Gonzalez, R. Shattock, B. F. Haynes, G. M. Shaw, B. H. Hahn, and J. C. Kappes. 2012. Generation of Transmitted/Founder HIV-1 Infectious Molecular Clones

and Characterization of Their Replication Capacity in CD4 T Lymphocytes and Monocyte-Derived Macrophages. J Virol 86:2715-2728.

258. Ochsenbauer, C., T. G. Edmonds, H. Ding, B. F. Keele, J. Decker, M. G. Salazar, J. F. Salazar-Gonzalez, R. Shattock, B. F. Haynes, G. M. Shaw, B. H. Hahn, and J. C. Kappes. 2011. Generation of Transmitted/Founder HIV-1 Infectious Molecular Clones and Characterization of their Replication Capacity in CD4 T-Lymphocytes and Monocyte-derived Macrophages. J Virol.

259. Ogert, R. A., L. Wojcik, C. Buontempo, L. Ba, P. Buontempo, R. Ralston, J. Strizki, and J. A. Howe. 2008. Mapping resistance to the CCR5 co-receptor antagonist vicriviroc using heterologous chimeric HIV-1 envelope genes reveals key determinants in the C2-V5 domain of gp120. Virology 373:387-399.

260. Oh, D. Y., H. Jessen, C. Kucherer, K. Neumann, N. Oh, G. Poggensee, B. Bartmeyer, A. Jessen, A. Pruss, R. R. Schumann, and O. Hamouda. 2008. CCR5Delta32 genotypes in a German HIV-1 seroconverter cohort and report of HIV-1 infection in a CCR5Delta32 homozygous individual. PLoS One 3:e2747.

261. Ojo-Amaize, E., P. G. Nishanian, D. F. Heitjan, A. Rezai, I. Esmail, E. Korns, R. Detels, J. Fahey, and J. V. Giorgi. 1989. Serum and effector-cell antibody-dependent cellular cytotoxicity (ADCC) activity remains high during human immunodeficiency virus (HIV) disease progression. J Clin Immunol 9:454-461.

262. Ongradi, J., L. Ceccherini-Nelli, M. Pistello, S. Specter, and M. Bendinelli. 1990. Acid sensitivity of cell-free and cell-associated HIV-1: clinical implications. AIDS Res Hum Retroviruses 6:1433-1436.

263. Ostrowski, M. A., T. W. Chun, S. J. Justement, I. Motola, M. A. Spinelli, J. Adelsberger, L. A. Ehler, S. B. Mizell, C. W. Hallahan, and A. S. Fauci. 1999. Both memory and CD45RA+/CD62L+ naive CD4(+) T cells are infected in human immunodeficiency virus type 1-infected individuals. J Virol 73:6430-6435.

264. Ott, D. E. 2009. Purification of HIV-1 virions by subtilisin digestion or CD45 immunoaffinity depletion for biochemical studies. Methods Mol Biol 485:15-25.

265. Padian, N. S., S. I. McCoy, S. S. Karim, N. Hasen, J. Kim, M. Bartos, E. Katabira, S. M. Bertozzi, B. Schwartlander, and M. S. Cohen. 2011. HIV prevention transformed: the new prevention research agenda. Lancet 378:269-278.

266. Pandrea, I., N. F. Parrish, K. Raehtz, T. Gaufin, H. J. Barbian, D. Ma, J. Kristoff, R. Gautam, F. Zhong, G. S. Haret-Richter, A. Trichel, G. M. Shaw, B. H. Hahn, and C. Apetrei. 2012. Mucosal simian immunodeficiency virus transmission in African green monkeys: susceptibility to infection is proportional to target cell availability at mucosal sites. J Virol 86:4158-4168.

267. Pang, S., Y. Shlesinger, E. S. Daar, T. Moudgil, D. D. Ho, and I. S. Chen. 1992. Rapid generation of sequence variation during primary HIV-1 infection. AIDS 6:453-460.

268. Parker, Z. F., S. S. Iyer, C. B. Wilen, N. F. Parrish, K. C. Chikere, F. H. Lee, C. A. Didigu, R. Berro, P. J. Klasse, B. Lee, J. P. Moore, G. M. Shaw, B. H. Hahn, and R. W. Doms. 2012. Transmitted/Founder and Chronic HIV-1 Envelope Proteins are Distinguished by Differential Utilization of CCR5. J Virol.

269. Parker, Z. I., S. S.; Wilen, C. B.; Parrish, N. F.; Chikere, K.; Lee, F. H.; Didigu, C.; Berro, R.; Klasse, P. J.; Lee, B. H.; Moore, J. P.; Shaw, G. M.; Hahn, B. H.; Doms, R. W. 2013. Transmitted/Founder and Chronic HIV-1 Envelope Proteins are Distinguished by Differential Utilization of CCR5. Journal of Virology.

270. Parrish, N. F., C. B. Wilen, L. B. Banks, S. S. Iyer, J. M. Pfaff, J. F. Salazar-Gonzalez, M. G. Salazar, J. M. Decker, E. H. Parrish, A. Berg, J. Hopper, B. Hora, A. Kumar, T. Mahlokozera, S. Yuan, C. Coleman, M. Vermeulen, H. Ding, C. Ochsenbauer, J. C. Tilton, S. R. Permar, J. C. Kappes, M. R. Betts, M. P. Busch, F. Gao, D. Montefiori, B. F. Haynes, G. M. Shaw, B. H. Hahn, and R. W. Doms. 2012. Transmitted/founder and chronic subtype C HIV-1 use CD4 and CCR5 receptors with equal efficiency and are not inhibited by blocking the integrin alpha4beta7. PLoS Pathog 8:e1002686.

271. Patterson, S., J. Gross, N. English, A. Stackpoole, P. Bedford, and S. C. Knight. 1995. CD4 expression on dendritic cells and their infection by human immunodeficiency virus. J Gen Virol 76 (Pt 5):1155-1163.

272. Pauls, E., E. Ballana, G. Moncunill, M. Bofill, B. Clotet, C. Ramo-Tello, and J. A. Este. 2009. Evaluation of the anti-HIV activity of natalizumab, an antibody against integrin alpha4. AIDS 23:266-268.

273. Pereyra, F., X. Jia, P. J. McLaren, A. Telenti, P. I. de Bakker, B. D. Walker, S. Ripke, C. J. Brumme, S. L. Pulit, M. Carrington, C. M. Kadie, J. M. Carlson, D. Heckerman, R. R. Graham, R. M. Plenge, S. G. Deeks, L. Gianniny, G. Crawford, J. Sullivan, E. Gonzalez, L. Davies, A. Camargo, J. M. Moore, N. Beattie, S. Gupta, A. Crenshaw, N. P. Burtt, C. Guiducci, N. Gupta, X. Gao, Y. Qi, Y. Yuki, A. Piechocka-Trocha, E. Cutrell, R. Rosenberg, K. L. Moss, P. Lemay, J. O'Leary, T. Schaefer, P. Verma, I. Toth, B. Block, B. Baker, A. Rothchild, J. Lian, J. Proudfoot, D. M. Alvino, S. Vine, M. M. Addo, T. M. Allen, M. Altfeld, M. R. Henn, S. Le Gall, H. Streeck, D. W. Haas, D. R. Kuritzkes, G. K. Robbins, R. W. Shafer, R. M. Gulick, C. M. Shikuma, R. Haubrich, S. Riddler, P. E. Sax, E. S. Daar, H. J. Ribaudo, B. Agan, S. Agarwal, R. L. Ahern, B. L. Allen, S. Altidor, E. L. Altschuler, S. Ambardar, K. Anastos, B. Anderson, V. Anderson, U. Andrady, D. Antoniskis, D. Bangsberg, D. Barbaro, W. Barrie, J. Bartczak, S. Barton, P. Basden, N. Basgoz, S. Bazner, N. C. Bellos, A. M. Benson, J. Berger, N. F. Bernard, A. M. Bernard,

C. Birch, S. J. Bodner, R. K. Bolan, E. T. Boudreaux, M. Bradley, J. F. Braun, J. E. Brndjar, S. J. Brown, K. Brown, S. T. Brown, et al. 2010. The major genetic determinants of HIV-1 control affect HLA class I peptide presentation. Science 330:1551-1557.

274. Pfaff, J. M., C. B. Wilen, J. E. Harrison, J. F. Demarest, B. Lee, R. W. Doms, and J. C. Tilton. 2010. HIV-1 resistance to CCR5 antagonists associated with highly efficient use of CCR5 and altered tropism on primary CD4+ T cells. J Virol 84:6505-6514.

275. Piantadosi, A., B. Chohan, V. Chohan, R. S. McClelland, and J. Overbaugh. 2007. Chronic HIV-1 infection frequently fails to protect against superinfection. PLoS Pathog 3:e177.

276. Piguet, V., and R. M. Steinman. 2007. The interaction of HIV with dendritic cells: outcomes and pathways. Trends Immunol 28:503-510.

277. Pillai, S. K., B. Good, S. K. Pond, J. K. Wong, M. C. Strain, D. D. Richman, and D. M. Smith. 2005. Semen-specific genetic characteristics of human immunodeficiency virus type 1 env. J Virol 79:1734-1742.

278. Platt, E. J., S. L. Kozak, J. P. Durnin, T. J. Hope, and D. Kabat. 2010. Rapid dissociation of HIV-1 from cultured cells severely limits infectivity assays, causes the inactivation ascribed to entry inhibitors, and masks the inherently high level of infectivity of virions. J Virol 84:3106-3110.

279. Pohlmann, S., F. Baribaud, B. Lee, G. J. Leslie, M. D. Sanchez, K. Hiebenthal-Millow, J. Munch, F. Kirchhoff, and R. W. Doms. 2001. DC-SIGN interactions with human immunodeficiency virus type 1 and 2 and simian immunodeficiency virus. J Virol 75:4664-4672.

280. Pohlmann, S., M. Krumbiegel, and F. Kirchhoff. 1999. Coreceptor usage of BOB/GPR15 and Bonzo/STRL33 by primary isolates of human immunodeficiency virus type 1. J Gen Virol 80 (Pt 5):1241-1251.

281. Pohlmann, S., E. J. Soilleux, F. Baribaud, G. J. Leslie, L. S. Morris, J. Trowsdale, B. Lee, N. Coleman, and R. W. Doms. 2001. DC-SIGNR, a DC-SIGN homologue expressed in endothelial cells, binds to human and simian immunodeficiency viruses and activates infection in trans. Proc Natl Acad Sci U S A 98:2670-2675.

282. Poles, M. A., J. Elliott, P. Taing, P. A. Anton, and I. S. Chen. 2001. A preponderance of CCR5(+) CXCR4(+) mononuclear cells enhances gastrointestinal mucosal susceptibility to human immunodeficiency virus type 1 infection. J Virol 75:8390-8399.

283. Pope, M., M. G. Betjes, N. Romani, H. Hirmand, P. U. Cameron, L. Hoffman, S. Gezelter, G. Schuler, and R. M. Steinman. 1994. Conjugates of dendritic cells and memory T lymphocytes from skin facilitate productive infection with HIV-1. Cell 78:389-398.

284. Pope, M., M. G. Betjes, N. Romani, H. Hirmand, L. Hoffman, S. Gezelter, G. Schuler, P. U. Cameron, and R. M. Steinman. 1995. Dendritic cell-T cell conjugates that migrate from

normal human skin are an explosive site of infection for HIV-1. Adv Exp Med Biol 378:457-460.

285. Poss, M., H. L. Martin, J. K. Kreiss, L. Granville, B. Chohan, P. Nyange, K. Mandaliya, and J. Overbaugh. 1995. Diversity in virus populations from genital secretions and peripheral blood from women recently infected with human immunodeficiency virus type 1. J Virol 69:8118-8122.

286. Powers, K. A., A. C. Ghani, W. C. Miller, I. F. Hoffman, A. E. Pettifor, G. Kamanga, F. E. Martinson, and M. S. Cohen. 2011. The role of acute and early HIV infection in the spread of HIV and implications for transmission prevention strategies in Lilongwe, Malawi: a modelling study. Lancet 378:256-268.

287. Powers, K. A., C. Poole, A. E. Pettifor, and M. S. Cohen. 2008. Rethinking the heterosexual infectivity of HIV-1: a systematic review and meta-analysis. Lancet Infect Dis 8:553-563.

288. Puffer, B. A., L. A. Altamura, T. C. Pierson, and R. W. Doms. 2004. Determinants within gp120 and gp41 contribute to CD4 independence of SIV Envs. Virology 327:16-25.

289. Puryear, W. B., X. Yu, N. P. Ramirez, B. M. Reinhard, and S. Gummuluru. 2012. HIV-1 incorporation of host-cell-derived glycosphingolipid GM3 allows for capture by mature dendritic cells. Proc Natl Acad Sci U S A 109:7475-7480.

290. Quakkelaar, E. D., F. P. van Alphen, B. D. Boeser-Nunnink, A. C. van Nuenen, R. Pantophlet, and H. Schuitemaker. 2007. Susceptibility of recently transmitted subtype B human immunodeficiency virus type 1 variants to broadly neutralizing antibodies. J Virol 81:8533-8542.

291. Quinonez, R., I. Sinha, I. R. Singh, and R. E. Sutton. 2003. Genetic footprinting of the HIV co-receptor CCR5: delineation of surface expression and viral entry determinants. Virology 307:98-115.

292. Redd, A. D., A. N. Collinson-Streng, N. Chatziandreou, C. E. Mullis, O. Laeyendecker, C. Martens, S. Ricklefs, N. Kiwanuka, P. H. Nyein, T. Lutalo, M. K. Grabowski, X. Kong, J. Manucci, N. Sewankambo, M. J. Wawer, R. H. Gray, S. F. Porcella, A. S. Fauci, M. Sagar, D. Serwadda, and T. C. Quinn. 2012. Previously Transmitted HIV-1 Strains Are Preferentially Selected During Subsequent Sexual Transmissions. J Infect Dis 206:1433-1442.

293. Redd, A. D., C. E. Mullis, D. Serwadda, X. Kong, C. Martens, S. M. Ricklefs, A. A. Tobian, C. Xiao, M. K. Grabowski, F. Nalugoda, G. Kigozi, O. Laeyendecker, J. Kagaayi, N. Sewankambo, R. H. Gray, S. F. Porcella, M. J. Wawer, and T. C. Quinn. 2012. The rates of HIV superinfection and primary HIV incidence in a general population in Rakai, Uganda. J Infect Dis 206:267-274.

294. Reeves, J. D., S. A. Gallo, N. Ahmad, J. L. Miamidian, P. E. Harvey, M. Sharron, S. Pohlmann, J. N. Sfakianos, C. A. Derdeyn, R. Blumenthal, E. Hunter, and R. W. Doms. 2002. Sensitivity of HIV-1 to entry inhibitors correlates with envelope/coreceptor affinity, receptor density, and fusion kinetics. Proc Natl Acad Sci U S A 99:16249-16254.

295. Ren, X., J. Sodroski, and X. Yang. 2005. An unrelated monoclonal antibody neutralizes human immunodeficiency virus type 1 by binding to an artificial epitope engineered in a functionally neutral region of the viral envelope glycoproteins. J Virol 79:5616-5624.

296. Reynolds, M. R., J. B. Sacha, A. M. Weiler, G. J. Borchardt, C. E. Glidden, N. C. Sheppard, F. A. Norante, P. A. Castrovinci, J. J. Harris, H. T. Robertson, T. C. Friedrich, A. B. McDermott, N. A. Wilson, D. B. Allison, W. C. Koff, W. E. Johnson, and D. I. Watkins. 2011. The TRIM5{alpha} genotype of rhesus macaques affects acquisition of simian immunodeficiency virus SIVsmE660 infection after repeated limiting-dose intrarectal challenge. J Virol 85:9637-9640.

297. Ribeiro, R. M., H. Li, S. Y. Wang, M. B. Stoddard, G. H. Learn, B. T. Korber, T. Bhattacharya, J. Guedj, E. H. Parrish, B. H. Hahn, G. M. Shaw, and A. S. Perelson. 2012. Quantifying the Diversification of Hepatitis C Virus (HCV) during Primary Infection: Estimates of the In Vivo Mutation Rate. Plos Pathogens 8.

298. Riddick, N. E., E. A. Hermann, L. M. Loftin, S. T. Elliott, W. C. Wey, B. Cervasi, J. Taaffe, J. C. Engram, B. Li, J. G. Else, Y. Li, B. H. Hahn, C. A. Derdeyn, D. L. Sodora, C. Apetrei, M. Paiardini, G. Silvestri, and R. G. Collman. 2010. A novel CCR5 mutation common in sooty mangabeys reveals SIVsmm infection of CCR5-null natural hosts and efficient alternative coreceptor use in vivo. PLoS Pathog 6:e1001064.

299. Rieder, P., B. Joos, A. U. Scherrer, H. Kuster, D. Braun, C. Grube, B. Niederost, C. Leemann, S. Gianella, K. J. Metzner, J. Boni, R. Weber, and H. F. Gunthard. 2011. Characterization of human immunodeficiency virus type 1 (HIV-1) diversity and tropism in 145 patients with primary HIV-1 infection. Clin Infect Dis 53:1271-1279.

300. Rizzuto, C., and J. Sodroski. 2000. Fine definition of a conserved CCR5-binding region on the human immunodeficiency virus type 1 glycoprotein 120. AIDS Res Hum Retroviruses 16:741-749.

301. Rizzuto, C. D., R. Wyatt, N. Hernandez-Ramos, Y. Sun, P. D. Kwong, W. A. Hendrickson, and J. Sodroski. 1998. A conserved HIV gp120 glycoprotein structure involved in chemokine receptor binding. Science 280:1949-1953.

302. Roben, P., J. P. Moore, M. Thali, J. Sodroski, C. F. Barbas, 3rd, and D. R. Burton. 1994. Recognition properties of a panel of human recombinant Fab fragments to the CD4 binding site of gp120 that show differing abilities to neutralize human immunodeficiency virus type 1. J Virol 68:4821-4828.

303. Roos, M. T., J. M. Lange, R. E. de Goede, R. A. Coutinho, P. T. Schellekens, F. Miedema, and M. Tersmette. 1992. Viral phenotype and immune response in primary human immunodeficiency virus type 1 infection. J Infect Dis 165:427-432.
304. Roy, S., M. G. Katze, N. T. Parkin, I. Edery, A. G. Hovanessian, and N. Sonenberg. 1990. Control of the interferon-induced 68-kilodalton protein kinase by the HIV-1 tat gene product. Science 247:1216-1219.
305. Royce, R. A., A. Sena, W. Cates, Jr., and M. S. Cohen. 1997. Sexual transmission of HIV. N Engl J Med 336:1072-1078.
306. Royston, J. P. 1982. The W Test for Normality. Applied Statistics-Journal of the Royal Statistical Society Series C 31:176-180.
307. Rusert, P., H. Kuster, B. Joos, B. Misselwitz, C. Gujer, C. Leemann, M. Fischer, G. Stiegler, H. Katinger, W. C. Olson, R. Weber, L. Aceto, H. F. Gunthard, and A. Trkola. 2005. Virus isolates during acute and chronic human immunodeficiency virus type 1 infection show distinct patterns of sensitivity to entry inhibitors. J Virol 79:8454-8469.
308. Russell, E. S., J. J. Kwiek, J. Keys, K. Barton, V. Mwapasa, D. C. Montefiori, S. R. Meshnick, and R. Swanstrom. 2011. The genetic bottleneck in vertical transmission of subtype C HIV-1 is not driven by selection of especially neutralization-resistant virus from the maternal viral population. J Virol 85:8253-8262.
309. Sagar, M., O. Laeyendecker, S. Lee, J. Gamiel, M. J. Wawer, R. H. Gray, D. Serwadda, N. K. Sewankambo, J. C. Shepherd, J. Toma, W. Huang, and T. C. Quinn. 2009. Selection of HIV variants with signature genotypic characteristics during heterosexual transmission. J Infect Dis 199:580-589.
310. Sagar, M., X. Wu, S. Lee, and J. Overbaugh. 2006. Human immunodeficiency virus type 1 V1-V2 envelope loop sequences expand and add glycosylation sites over the course of infection, and these modifications affect antibody neutralization sensitivity. J Virol 80:9586-9598.
311. Saitou, N., and M. Nei. 1987. The neighbor-joining method: a new method for reconstructing phylogenetic trees. Mol Biol Evol 4:406-425.
312. Salazar-Gonzalez, J. F., E. Bailes, K. T. Pham, M. G. Salazar, M. B. Guffey, B. F. Keele, C. A. Derdeyn, P. Farmer, E. Hunter, S. Allen, O. Manigart, J. Mulenga, J. A. Anderson, R. Swanstrom, B. F. Haynes, G. S. Athreya, B. T. Korber, P. M. Sharp, G. M. Shaw, and B. H. Hahn. 2008. Deciphering human immunodeficiency virus type 1 transmission and early envelope diversification by single-genome amplification and sequencing. J Virol 82:3952-3970.
313. Salazar-Gonzalez, J. F., M. G. Salazar, B. F. Keele, G. H. Learn, E. E. Giorgi, H. Li, J. M. Decker, S. Wang, J. Baalwa, M. H. Kraus, N. F. Parrish, K. S. Shaw, M. B. Guffey, K. J. Bar, K. L. Davis, C. Ochsenbauer-Jambor, J. C. Kappes, M. S. Saag, M. S. Cohen, J.

Mulenga, C. A. Derdeyn, S. Allen, E. Hunter, M. Markowitz, P. Hraber, A. S. Perelson, T. Bhattacharya, B. F. Haynes, B. T. Korber, B. H. Hahn, and G. M. Shaw. 2009. Genetic identity, biological phenotype, and evolutionary pathways of transmitted/founder viruses in acute and early HIV-1 infection. J Exp Med 206:1273-1289.

314. Salazar-Gonzalez, J. F., M. G. Salazar, G. H. Learn, G. G. Fouda, H. H. Kang, T. Mahlokozera, A. B. Wilks, R. V. Lovingood, A. Stacey, L. Kalilani, S. R. Meshnick, P. Borrow, D. C. Montefiori, T. N. Denny, N. L. Letvin, G. M. Shaw, B. H. Hahn, and S. R. Permar. 2011. Origin and evolution of HIV-1 in breast milk determined by single-genome amplification and sequencing. J Virol 85:2751-2763.

315. Sallusto, F., J. Geginat, and A. Lanzavecchia. 2004. Central memory and effector memory T cell subsets: function, generation, and maintenance. Annu Rev Immunol 22:745-763.

316. Sallusto, F., D. Lenig, R. Forster, M. Lipp, and A. Lanzavecchia. 1999. Two subsets of memory T lymphocytes with distinct homing potentials and effector functions. Nature 401:708-712.

317. Sauter, M. M., A. Pelchen-Matthews, R. Bron, M. Marsh, C. C. LaBranche, P. J. Vance, J. Romano, B. S. Haggarty, T. K. Hart, W. M. Lee, and J. A. Hoxie. 1996. An internalization signal in the simian immunodeficiency virus transmembrane protein cytoplasmic domain modulates expression of envelope glycoproteins on the cell surface. J Cell Biol 132:795-811.

318. Scarlatti, G., E. Tresoldi, A. Bjorndal, R. Fredriksson, C. Colognesi, H. K. Deng, M. S. Malnati, A. Plebani, A. G. Siccardi, D. R. Littman, E. M. Fenyo, and P. Lusso. 1997. In vivo evolution of HIV-1 co-receptor usage and sensitivity to chemokine-mediated suppression. Nat Med 3:1259-1265.

319. Schacker, T., S. Little, E. Connick, K. Gebhard, Z. Q. Zhang, J. Krieger, J. Pryor, D. Havlir, J. K. Wong, R. T. Schooley, D. Richman, L. Corey, and A. T. Haase. 2001. Productive infection of T cells in lymphoid tissues during primary and early human immunodeficiency virus infection. J Infect Dis 183:555-562.

320. Schiavoni, I., S. Trapp, A. C. Santarcangelo, V. Piacentini, K. Pugliese, A. Baur, and M. Federico. 2004. HIV-1 Nef enhances both membrane expression and virion incorporation of Env products. A model for the Nef-dependent increase of HIV-1 infectivity. J Biol Chem 279:22996-23006.

321. Schmitz, J. E., M. J. Kuroda, S. Santra, V. G. Sasseville, M. A. Simon, M. A. Lifton, P. Racz, K. Tenner-Racz, M. Dalesandro, B. J. Scallon, J. Ghrayeb, M. A. Forman, D. C. Montefiori, E. P. Rieber, N. L. Letvin, and K. A. Reimann. 1999. Control of viremia in simian immunodeficiency virus infection by CD8+ lymphocytes. Science 283:857-860.

322. Schnell, G., S. Joseph, S. Spudich, R. W. Price, and R. Swanstrom. 2011. HIV-1 replication in the central nervous system occurs in two distinct cell types. PLoS Pathog 7:e1002286.
323. Schnittman, S. M., H. C. Lane, J. Greenhouse, J. S. Justement, M. Baseler, and A. S. Fauci. 1990. Preferential infection of CD4+ memory T cells by human immunodeficiency virus type 1: evidence for a role in the selective T-cell functional defects observed in infected individuals. Proc Natl Acad Sci U S A 87:6058-6062.
324. Schoggins, J. W., S. J. Wilson, M. Panis, M. Y. Murphy, C. T. Jones, P. Bieniasz, and C. M. Rice. 2011. A diverse range of gene products are effectors of the type I interferon antiviral response. Nature 472:481-485.
325. Schroder, H. C., D. Ugarkovic, R. Wenger, P. Reuter, T. Okamoto, and W. E. Muller. 1990. Binding of Tat protein to TAR region of human immunodeficiency virus type 1 blocks TAR-mediated activation of (2'-5')oligoadenylate synthetase. AIDS Res Hum Retroviruses 6:659-672.
326. Schuitemaker, H., M. Koot, N. A. Kootstra, M. W. Dercksen, R. E. de Goede, R. P. van Steenwijk, J. M. Lange, J. K. Schattenkerk, F. Miedema, and M. Tersmette. 1992. Biological phenotype of human immunodeficiency virus type 1 clones at different stages of infection: progression of disease is associated with a shift from monocytotropic to T-cell-tropic virus population. J Virol 66:1354-1360.
327. Seaman, M. S., H. Janes, N. Hawkins, L. E. Grandpre, C. Devoy, A. Giri, R. T. Coffey, L. Harris, B. Wood, M. G. Daniels, T. Bhattacharya, A. Lapedes, V. R. Polonis, F. E. McCutchan, P. B. Gilbert, S. G. Self, B. T. Korber, D. C. Montefiori, and J. R. Mascola. 2010. Tiered categorization of a diverse panel of HIV-1 Env pseudoviruses for assessment of neutralizing antibodies. J Virol 84:1439-1452.
328. Seibert, C., W. Ying, S. Gavrilov, F. Tsamis, S. E. Kuhmann, A. Palani, J. R. Tagat, J. W. Clader, S. W. McCombie, B. M. Baroudy, S. O. Smith, T. Dragic, J. P. Moore, and T. P. Sakmar. 2006. Interaction of small molecule inhibitors of HIV-1 entry with CCR5. Virology 349:41-54.
329. Sharp, P. M., and B. H. Hahn. 2011. Origins of HIV and the AIDS Pandemic. Cold Spring Harb Perspect Med 1:a006841.
330. Sharron, M., S. Pohlmann, K. Price, E. Lolis, M. Tsang, F. Kirchhoff, R. W. Doms, and B. Lee. 2000. Expression and coreceptor activity of STRL33/Bonzo on primary peripheral blood lymphocytes. Blood 96:41-49.
331. Shaw, G. M., and E. Hunter. 2012. HIV transmission. Cold Spring Harb Perspect Med 2.
332. Shaw, G. M., Hunter, E. 2011. HIV Transmission, p. 135-151. *In* F. D. Bushman, Nabel, G.J., Swanstrom R (ed.), HIV: From Biology to Prevention and Treatment. Cold Spring Harbor Laboratory Press, Cold Spring Harbor, New York.

333. Sheehy, A. M., N. C. Gaddis, J. D. Choi, and M. H. Malim. 2002. Isolation of a human gene that inhibits HIV-1 infection and is suppressed by the viral Vif protein. Nature 418:646-650.
334. Sheppard, H. W., C. Celum, N. L. Michael, S. O'Brien, M. Dean, M. Carrington, D. Dondero, and S. P. Buchbinder. 2002. HIV-1 infection in individuals with the CCR5-Delta32/Delta32 genotype: acquisition of syncytium-inducing virus at seroconversion. J Acquir Immune Defic Syndr 29:307-313.
335. Shimizu, N., A. Tanaka, A. Oue, T. Mori, T. Ohtsuki, C. Apichartpiyakul, H. Uchiumi, Y. Nojima, and H. Hoshino. 2009. Broad usage spectrum of G protein-coupled receptors as coreceptors by primary isolates of HIV. AIDS 23:761-769.
336. Shioda, T., J. A. Levy, and C. Cheng-Mayer. 1991. Macrophage and T cell-line tropisms of HIV-1 are determined by specific regions of the envelope gp120 gene. Nature 349:167-169.
337. Siegal, F. P., N. Kadowaki, M. Shodell, P. A. Fitzgerald-Bocarsly, K. Shah, S. Ho, S. Antonenko, and Y. J. Liu. 1999. The nature of the principal type 1 interferon-producing cells in human blood. Science 284:1835-1837.
338. Smalls-Mantey, A., N. Doria-Rose, R. Klein, A. Patamawenu, S. A. Migueles, S. Y. Ko, C. W. Hallahan, H. Wong, B. Liu, L. You, J. Scheid, J. C. Kappes, C. Ochsenbauer, G. J. Nabel, J. R. Mascola, and M. Connors. 2012. Antibody-dependent cellular cytotoxicity against primary HIV-infected CD4+ T cells is directly associated with the magnitude of surface IgG binding. J Virol 86:8672-8680.
339. Soda, Y., N. Shimizu, A. Jinno, H. Y. Liu, K. Kanbe, T. Kitamura, and H. Hoshino. 1999. Establishment of a new system for determination of coreceptor usages of HIV based on the human glioma NP-2 cell line. Biochem Biophys Res Commun 258:313-321.
340. Spina, C. A., T. J. Kwoh, M. Y. Chowers, J. C. Guatelli, and D. D. Richman. 1994. The importance of nef in the induction of human immunodeficiency virus type 1 replication from primary quiescent CD4 lymphocytes. J Exp Med 179:115-123.
341. Spira, A. I., P. A. Marx, B. K. Patterson, J. Mahoney, R. A. Koup, S. M. Wolinsky, and D. D. Ho. 1996. Cellular targets of infection and route of viral dissemination after an intravaginal inoculation of simian immunodeficiency virus into rhesus macaques. J Exp Med 183:215-225.
342. Spotts, D. R., R. M. Reich, M. A. Kalkhan, R. M. Kinney, and J. T. Roehrig. 1998. Resistance to alpha/beta interferons correlates with the epizootic and virulence potential of Venezuelan equine encephalitis viruses and is determined by the 5' noncoding region and glycoproteins. J Virol 72:10286-10291.
343. Stacey, A. R., P. J. Norris, L. Qin, E. A. Haygreen, E. Taylor, J. Heitman, M. Lebedeva, A. DeCamp, D. Li, D. Grove, S. G. Self, and P. Borrow. 2009. Induction of a striking

systemic cytokine cascade prior to peak viremia in acute human immunodeficiency virus type 1 infection, in contrast to more modest and delayed responses in acute hepatitis B and C virus infections. J Virol 83:3719-3733.

344. Stephenson, J. 2007. Researchers buoyed by novel HIV drugs: will expand drug arsenal against resistant virus. JAMA 297:1535-1536.

345. Stevenson, M., T. L. Stanwick, M. P. Dempsey, and C. A. Lamonica. 1990. HIV-1 replication is controlled at the level of T cell activation and proviral integration. EMBO J 9:1551-1560.

346. Stone, M., B. F. Keele, Z. M. Ma, E. Bailes, J. Dutra, B. H. Hahn, G. M. Shaw, and C. J. Miller. 2010. A limited number of SIVenv variants are transmitted to rhesus macaques vaginally inoculated with SIVmac251. J Virol 84:7083-7095.

347. Takehisa, J., M. H. Kraus, A. Ayouba, E. Bailes, F. Van Heuverswyn, J. M. Decker, Y. Li, R. S. Rudicell, G. H. Learn, C. Neel, E. M. Ngole, G. M. Shaw, M. Peeters, P. M. Sharp, and B. H. Hahn. 2009. Origin and biology of simian immunodeficiency virus in wild-living western gorillas. J Virol 83:1635-1648.

348. Theodorou, I., L. Meyer, M. Magierowska, C. Katlama, and C. Rouzioux. 1997. HIV-1 infection in an individual homozygous for CCR5 delta 32. Seroco Study Group. Lancet 349:1219-1220.

349. Thompson, J. D., D. G. Higgins, and T. J. Gibson. 1994. CLUSTAL W: improving the sensitivity of progressive multiple sequence alignment through sequence weighting, position-specific gap penalties and weight matrix choice. Nucleic Acids Res 22:4673-4680.

350. Tilton, J. C., H. Amrine-Madsen, J. L. Miamidian, K. M. Kitrinos, J. Pfaff, J. F. Demarest, N. Ray, J. L. Jeffrey, C. C. Labranche, and R. W. Doms. 2010. HIV type 1 from a patient with baseline resistance to CCR5 antagonists uses drug-bound receptor for entry. AIDS Res Hum Retroviruses 26:13-24.

351. Tilton, J. C., C. B. Wilen, C. A. Didigu, R. Sinha, J. E. Harrison, C. Agrawal-Gamse, E. A. Henning, F. D. Bushman, J. N. Martin, S. G. Deeks, and R. W. Doms. 2010. A maraviroc-resistant HIV-1 with narrow cross-resistance to other CCR5 antagonists depends on both N-terminal and extracellular loop domains of drug-bound CCR5. J Virol 84:10863-10876.

352. Tilton, J. C., C. B. Wilen, C. A. Didigu, R. Sinha, J. E. Harrison, C. Agrawal-Gamse, E. A. Henning, F. D. Bushman, J. N. Martin, S. G. Deeks, and R. W. Doms. A maraviroc-resistant HIV-1 with narrow cross-resistance to other CCR5 antagonists depends on both N-terminal and extracellular loop domains of drug-bound CCR5. J Virol 84:10863-10876.

353. Tomaras, G. D., N. L. Yates, P. Liu, L. Qin, G. G. Fouda, L. L. Chavez, A. C. Decamp, R. J. Parks, V. C. Ashley, J. T. Lucas, M. Cohen, J. Eron, C. B. Hicks, H. X. Liao, S. G. Self, G. Landucci, D. N. Forthal, K. J. Weinhold, B. F. Keele, B. H. Hahn, M. L. Greenberg, L.

Morris, S. S. Karim, W. A. Blattner, D. C. Montefiori, G. M. Shaw, A. S. Perelson, and B. F. Haynes. 2008. Initial B-cell responses to transmitted human immunodeficiency virus type 1: virion-binding immunoglobulin M (IgM) and IgG antibodies followed by plasma anti-gp41 antibodies with ineffective control of initial viremia. J Virol 82:12449-12463.

354. Trkola, A., T. J. Ketas, K. A. Nagashima, L. Zhao, T. Cilliers, L. Morris, J. P. Moore, P. J. Maddon, and W. C. Olson. 2001. Potent, broad-spectrum inhibition of human immunodeficiency virus type 1 by the CCR5 monoclonal antibody PRO 140. J Virol 75:579-588.

355. Tsibris, A. M., M. Sagar, R. M. Gulick, Z. Su, M. Hughes, W. Greaves, M. Subramanian, C. Flexner, F. Giguel, K. E. Leopold, E. Coakley, and D. R. Kuritzkes. 2008. In vivo emergence of vicriviroc resistance in a human immunodeficiency virus type 1 subtype C-infected subject. J Virol 82:8210-8214.

356. Turville, S. G., P. U. Cameron, A. Handley, G. Lin, S. Pohlmann, R. W. Doms, and A. L. Cunningham. 2002. Diversity of receptors binding HIV on dendritic cell subsets. Nat Immunol 3:975-983.

357. Unutmaz, D., V. N. KewalRamani, and D. R. Littman. 1998. G protein-coupled receptors in HIV and SIV entry: new perspectives on lentivirus-host interactions and on the utility of animal models. Semin Immunol 10:225-236.

358. van Montfort, T., A. A. Nabatov, T. B. Geijtenbeek, G. Pollakis, and W. A. Paxton. 2007. Efficient capture of antibody neutralized HIV-1 by cells expressing DC-SIGN and transfer to CD4+ T lymphocytes. J Immunol 178:3177-3185.

359. van't Wout, A. B., N. A. Kootstra, G. A. Mulder-Kampinga, N. Albrecht-van Lent, H. J. Scherpbier, J. Veenstra, K. Boer, R. A. Coutinho, F. Miedema, and H. Schuitemaker. 1994. Macrophage-tropic variants initiate human immunodeficiency virus type 1 infection after sexual, parenteral, and vertical transmission. J Clin Invest 94:2060-2067.

360. Veazey, R. S., M. DeMaria, L. V. Chalifoux, D. E. Shvetz, D. R. Pauley, H. L. Knight, M. Rosenzweig, R. P. Johnson, R. C. Desrosiers, and A. A. Lackner. 1998. Gastrointestinal tract as a major site of CD4+ T cell depletion and viral replication in SIV infection. Science 280:427-431.

361. Vendrame, D., M. Sourisseau, V. Perrin, O. Schwartz, and F. Mammano. 2009. Partial inhibition of human immunodeficiency virus replication by type I interferons: impact of cell-to-cell viral transfer. J Virol 83:10527-10537.

362. Wagner, T. A., J. L. McKernan, N. H. Tobin, K. A. Tapia, J. I. Mullins, and L. M. Frenkel. 2012. An Increasing Proportion of Monotypic HIV-1 DNA Sequences During Antiretroviral Treatment Suggests Proliferation of HIV-Infected Cells. J Virol.

363. Walker, L. M., S. K. Phogat, P. Y. Chan-Hui, D. Wagner, P. Phung, J. L. Goss, T. Wrin, M. D. Simek, S. Fling, J. L. Mitcham, J. K. Lehrman, F. H. Priddy, O. A. Olsen, S. M.

Frey, P. W. Hammond, S. Kaminsky, T. Zamb, M. Moyle, W. C. Koff, P. Poignard, and D. R. Burton. 2009. Broad and potent neutralizing antibodies from an African donor reveal a new HIV-1 vaccine target. Science 326:285-289.

364. Wang, Y., K. Abel, K. Lantz, A. M. Krieg, M. B. McChesney, and C. J. Miller. 2005. The Toll-like receptor 7 (TLR7) agonist, imiquimod, and the TLR9 agonist, CpG ODN, induce antiviral cytokines and chemokines but do not prevent vaginal transmission of simian immunodeficiency virus when applied intravaginally to rhesus macaques. J Virol 79:14355-14370.

365. Wawer, M. J., R. H. Gray, N. K. Sewankambo, D. Serwadda, X. Li, O. Laeyendecker, N. Kiwanuka, G. Kigozi, M. Kiddugavu, T. Lutalo, F. Nalugoda, F. Wabwire-Mangen, M. P. Meehan, and T. C. Quinn. 2005. Rates of HIV-1 transmission per coital act, by stage of HIV-1 infection, in Rakai, Uganda. J Infect Dis 191:1403-1409.

366. Wei, X., J. M. Decker, H. Liu, Z. Zhang, R. B. Arani, J. M. Kilby, M. S. Saag, X. Wu, G. M. Shaw, and J. C. Kappes. 2002. Emergence of resistant human immunodeficiency virus type 1 in patients receiving fusion inhibitor (T-20) monotherapy. Antimicrob Agents Chemother 46:1896-1905.

367. Wei, X., J. M. Decker, S. Wang, H. Hui, J. C. Kappes, X. Wu, J. F. Salazar-Gonzalez, M. G. Salazar, J. M. Kilby, M. S. Saag, N. L. Komarova, M. A. Nowak, B. H. Hahn, P. D. Kwong, and G. M. Shaw. 2003. Antibody neutralization and escape by HIV-1. Nature 422:307-312.

368. Wei, X., S. K. Ghosh, M. E. Taylor, V. A. Johnson, E. A. Emini, P. Deutsch, J. D. Lifson, S. Bonhoeffer, M. A. Nowak, B. H. Hahn, and et al. 1995. Viral dynamics in human immunodeficiency virus type 1 infection. Nature 373:117-122.

369. Weissman, D., R. L. Rabin, J. Arthos, A. Rubbert, M. Dybul, R. Swofford, S. Venkatesan, J. M. Farber, and A. S. Fauci. 1997. Macrophage-tropic HIV and SIV envelope proteins induce a signal through the CCR5 chemokine receptor. Nature 389:981-985.

370. West, A. P., Jr., R. P. Galimidi, C. P. Foglesong, P. N. Gnanapragasam, J. S. Klein, and P. J. Bjorkman. 2010. Evaluation of CD4-CD4i antibody architectures yields potent, broadly cross-reactive anti-human immunodeficiency virus reagents. J Virol 84:261-269.

371. Westby, M., C. Smith-Burchnell, J. Mori, M. Lewis, M. Mosley, M. Stockdale, P. Dorr, G. Ciaramella, and M. Perros. 2007. Reduced maximal inhibition in phenotypic susceptibility assays indicates that viral strains resistant to the CCR5 antagonist maraviroc utilize inhibitor-bound receptor for entry. J Virol 81:2359-2371.

372. Wilen, C. B., N. F. Parrish, J. M. Pfaff, J. M. Decker, E. A. Henning, H. Haim, J. E. Petersen, J. A. Wojcechowskyj, J. Sodroski, B. F. Haynes, D. C. Montefiori, J. C. Tilton, G. M. Shaw, B. H. Hahn, and R. W. Doms. 2011. Phenotypic and immunologic

comparison of clade B transmitted/founder and chronic HIV-1 envelope glycoproteins. J Virol 85:8514-8527.

373. Wilen, C. B., J. C. Tilton, and R. W. Doms. 2012. HIV: cell binding and entry. Cold Spring Harb Perspect Med 2.

374. Wolfs, T. F., G. Zwart, M. Bakker, and J. Goudsmit. 1992. HIV-1 genomic RNA diversification following sexual and parenteral virus transmission. Virology 189:103-110.

375. Wolinsky, S. M., C. M. Wike, B. T. Korber, C. Hutto, W. P. Parks, L. L. Rosenblum, K. J. Kunstman, M. R. Furtado, and J. L. Munoz. 1992. Selective transmission of human immunodeficiency virus type-1 variants from mothers to infants. Science 255:1134-1137.

376. Wu, L., and V. N. KewalRamani. 2006. Dendritic-cell interactions with HIV: infection and viral dissemination. Nat Rev Immunol 6:859-868.

377. Wu, L., W. A. Paxton, N. Kassam, N. Ruffing, J. B. Rottman, N. Sullivan, H. Choe, J. Sodroski, W. Newman, R. A. Koup, and C. R. Mackay. 1997. CCR5 levels and expression pattern correlate with infectability by macrophage-tropic HIV-1, in vitro. J Exp Med 185:1681-1691.

378. Wu, X., A. B. Parast, B. A. Richardson, R. Nduati, G. John-Stewart, D. Mbori-Ngacha, S. M. Rainwater, and J. Overbaugh. 2006. Neutralization escape variants of human immunodeficiency virus type 1 are transmitted from mother to infant. J Virol 80:835-844.

379. Wu, X., Z. Y. Yang, Y. Li, C. M. Hogerkorp, W. R. Schief, M. S. Seaman, T. Zhou, S. D. Schmidt, L. Wu, L. Xu, N. S. Longo, K. McKee, S. O'Dell, M. K. Louder, D. L. Wycuff, Y. Feng, M. Nason, N. Doria-Rose, M. Connors, P. D. Kwong, M. Roederer, R. T. Wyatt, G. J. Nabel, and J. R. Mascola. 2010. Rational design of envelope identifies broadly neutralizing human monoclonal antibodies to HIV-1. Science 329:856-861.

380. Xiang, S. H., M. Farzan, Z. Si, N. Madani, L. Wang, E. Rosenberg, J. Robinson, and J. Sodroski. 2005. Functional mimicry of a human immunodeficiency virus type 1 coreceptor by a neutralizing monoclonal antibody. J Virol 79:6068-6077.

381. Xiao, L., D. L. Rudolph, S. M. Owen, T. J. Spira, and R. B. Lal. 1998. Adaptation to promiscuous usage of CC and CXC-chemokine coreceptors in vivo correlates with HIV-1 disease progression. AIDS 12:F137-143.

382. Yang, X., S. Kurteva, X. Ren, S. Lee, and J. Sodroski. 2005. Stoichiometry of envelope glycoprotein trimers in the entry of human immunodeficiency virus type 1. J Virol 79:12132-12147.

383. Yasuda, Y., S. Miyake, S. Kato, M. Kita, T. Kishida, T. Kimura, and K. Ikuta. 1990. Interferon-alpha treatment leads to accumulation of virus particles on the surface of cells persistently infected with the human immunodeficiency virus type 1. J Acquir Immune Defic Syndr 3:1046-1051.

384. Yeh, W. W., I. Rahman, P. Hraber, R. T. Coffey, D. Nevidomskyte, A. Giri, M. Asmal, S. Miljkovic, M. Daniels, J. B. Whitney, B. F. Keele, B. H. Hahn, B. T. Korber, G. M. Shaw, M. S. Seaman, and N. L. Letvin. 2010. Autologous neutralizing antibodies to the transmitted/founder viruses emerge late after simian immunodeficiency virus SIVmac251 infection of rhesus monkeys. J Virol 84:6018-6032.

385. Yeh, W. W., S. S. Rao, S. Y. Lim, J. Zhang, P. T. Hraber, L. M. Brassard, C. Luedemann, J. P. Todd, A. Dodson, L. Shen, A. P. Buzby, J. B. Whitney, B. T. Korber, G. J. Nabel, J. R. Mascola, and N. L. Letvin. 2011. The TRIM5 gene modulates penile mucosal acquisition of simian immunodeficiency virus in rhesus monkeys. J Virol 85:10389-10398.

386. Yuste, E., W. Johnson, G. N. Pavlakis, and R. C. Desrosiers. 2005. Virion envelope content, infectivity, and neutralization sensitivity of simian immunodeficiency virus. J Virol 79:12455-12463.

387. Yuste, E., J. D. Reeves, R. W. Doms, and R. C. Desrosiers. 2004. Modulation of Env content in virions of simian immunodeficiency virus: correlation with cell surface expression and virion infectivity. J Virol 78:6775-6785.

388. Yuste, E., S. Sanchez-Palomino, C. Casado, E. Domingo, and C. Lopez-Galindez. 1999. Drastic fitness loss in human immunodeficiency virus type 1 upon serial bottleneck events. J Virol 73:2745-2751.

389. Zaitseva, M., A. Blauvelt, S. Lee, C. K. Lapham, V. Klaus-Kovtun, H. Mostowski, J. Manischewitz, and H. Golding. 1997. Expression and function of CCR5 and CXCR4 on human Langerhans cells and macrophages: implications for HIV primary infection. Nat Med 3:1369-1375.

390. Zhang, H., M. Rola, J. T. West, D. C. Tully, P. Kubis, J. He, C. Kankasa, and C. Wood. 2010. Functional properties of the HIV-1 subtype C envelope glycoprotein associated with mother-to-child transmission. Virology 400:164-174.

391. Zhang, H., Y. Zhou, C. Alcock, T. Kiefer, D. Monie, J. Siliciano, Q. Li, P. Pham, J. Cofrancesco, D. Persaud, and R. F. Siliciano. 2004. Novel single-cell-level phenotypic assay for residual drug susceptibility and reduced replication capacity of drug-resistant human immunodeficiency virus type 1. J Virol 78:1718-1729.

392. Zhang, J., and C. Liang. 2010. BST-2 diminishes HIV-1 infectivity. J Virol 84:12336-12343.

393. Zhang, L. Q., P. MacKenzie, A. Cleland, E. C. Holmes, A. J. Brown, and P. Simmonds. 1993. Selection for specific sequences in the external envelope protein of human immunodeficiency virus type 1 upon primary infection. J Virol 67:3345-3356.

394. Zhang, M., B. Gaschen, W. Blay, B. Foley, N. Haigwood, C. Kuiken, and B. Korber. 2004. Tracking global patterns of N-linked glycosylation site variation in highly variable viral

glycoproteins: HIV, SIV, and HCV envelopes and influenza hemagglutinin. Glycobiology 14:1229-1246.

395. Zhang, Z., T. Schuler, M. Zupancic, S. Wietgrefe, K. A. Staskus, K. A. Reimann, T. A. Reinhart, M. Rogan, W. Cavert, C. J. Miller, R. S. Veazey, D. Notermans, S. Little, S. A. Danner, D. D. Richman, D. Havlir, J. Wong, H. L. Jordan, T. W. Schacker, P. Racz, K. Tenner-Racz, N. L. Letvin, S. Wolinsky, and A. T. Haase. 1999. Sexual transmission and propagation of SIV and HIV in resting and activated CD4+ T cells. Science 286:1353-1357.

396. Zhang, Z. Q., S. W. Wietgrefe, Q. Li, M. D. Shore, L. Duan, C. Reilly, J. D. Lifson, and A. T. Haase. 2004. Roles of substrate availability and infection of resting and activated CD4+ T cells in transmission and acute simian immunodeficiency virus infection. Proc Natl Acad Sci U S A 101:5640-5645.

397. Zhou, T., I. Georgiev, X. Wu, Z. Y. Yang, K. Dai, A. Finzi, Y. D. Kwon, J. F. Scheid, W. Shi, L. Xu, Y. Yang, J. Zhu, M. C. Nussenzweig, J. Sodroski, L. Shapiro, G. J. Nabel, J. R. Mascola, and P. D. Kwong. Structural basis for broad and potent neutralization of HIV-1 by antibody VRC01. Science 329:811-817.

398. Zhu, J., F. Hladik, A. Woodward, A. Klock, T. Peng, C. Johnston, M. Remington, A. Magaret, D. M. Koelle, A. Wald, and L. Corey. 2009. Persistence of HIV-1 receptor-positive cells after HSV-2 reactivation is a potential mechanism for increased HIV-1 acquisition. Nat Med 15:886-892.

399. Zhu, T., H. Mo, N. Wang, D. S. Nam, Y. Cao, R. A. Koup, and D. D. Ho. 1993. Genotypic and phenotypic characterization of HIV-1 patients with primary infection. Science 261:1179-1181.

400. Zhu, T., N. Wang, A. Carr, D. S. Nam, R. Moor-Jankowski, D. A. Cooper, and D. D. Ho. 1996. Genetic characterization of human immunodeficiency virus type 1 in blood and genital secretions: evidence for viral compartmentalization and selection during sexual transmission. J Virol 70:3098-3107.